Authors are requested to submit three copies of manuscripts and illustrations to the Editorial Department, Institute of Radio Engineers, 1 East 79 St., New York 21, N. Y.

PROCEEDINGS OF THE IRE®

Published Monthly by

The Institute of Radio Engineers, Inc.

VOLUME 45 — *July, 1957* — NUMBER 7

CONTENTS

ADVERTISING SECTION

THE COVER—The photograph of an rf pentode, flanked by the graphical symbols of a reflex klystron (in red) and a six-anode vapor rectifier are suggestive of the wide variety of devices developed in the electron tube field which have quite different physical features and operating characteristics. The wide diversity of these devices and their applications has led to the evolution of a large number of technical terms related to tubes and their operation. Over 600 of these terms and their definitions, which form a substantial portion of the technical language of the electronic engineer, appear in the IRE Standard which starts on page 983.

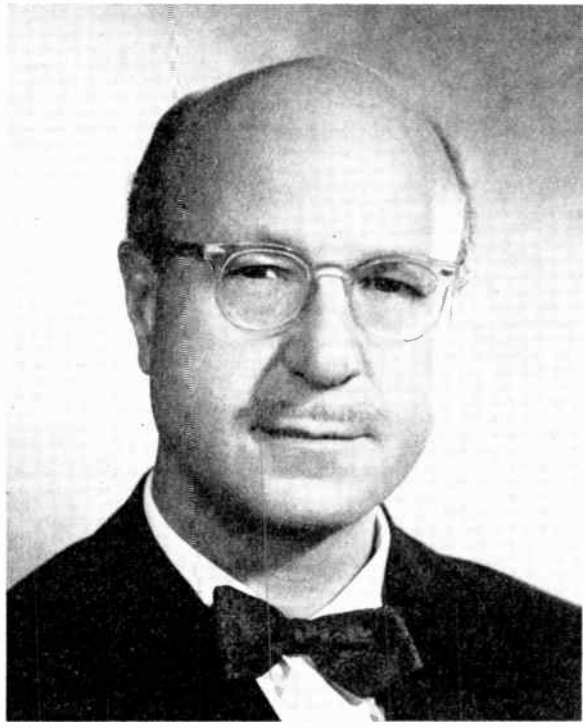

Daniel E. Noble

DIRECTOR, 1957–1959

Daniel E. Noble was born in Naugatuck, Conn., October 4, 1901. He received his early education in Naugatuck, and was awarded his Bachelor of Science degree by the educational institution which is now the University of Connecticut. His Connecticut training was supplemented by graduate work at the Massachusetts Institute of Technology, and by summer work at Harvard. Over a period of seventeen years, he combined the teaching of mathematics and electrical engineering at the University of Connecticut with consulting work and radio and electronic experimentation. In 1936, he became interested in frequency modulation and built a 100-megacycle, 100-watt fm system which was used to relay campus-originated programs through the Hartford broadcast stations, WDRC and WTIC, approximately twenty-five miles away. He later utilized phase modulation to design and develop the first two-way mobile radio state police voice communication system for the Connecticut State Police.

Dr. Noble joined Motorola Inc. as Director of Research in September, 1940. Since then, in addition to other duties, he has been continuously in charge of their development of communications and industrial electronic equipment. He became a vice-president and director of Motorola in 1947, and executive vice-president in 1956.

As a Motorola executive vice-president, he is responsible for the administration of three divisions of the company, with laboratories and production facilities in Chicago, Phoenix, Arizona, and Riverside, California. He directs all company activities concerned with research, development, production and sale of communications, industrial, semiconductor and military electronics products.

He has participated, either as member or as chairman, in many radio and scientific committee activities, including RTPB and NTSC. He is, at present, the chairman of the American Ordnance Association Committee on Missile Guidance & Control, and a member of the Signal Corps R&D Advisory Council and the Army Scientific Advisory Council. He holds radio amateur license W9GGJ, and he still holds a valid first-class commercial radio ticket. He was awarded the honorary degree of Doctor of Science by Arizona State College on May 28, 1957.

Poles and Zeros

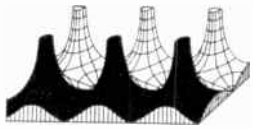

Houston. For some years it has been the custom of the Board of Directors to hold one of its meetings each year outside New York, on the theory that a face-to-face confrontation of Directors and regional affairs might have mutually beneficial effects. This year, the occasion for the extra-HQ meeting was the Ninth Southwestern IRE Regional Conference and Show at Houston, Texas, which was held coincidentally with the National Simulation Conference, April 11–13. Despite a number of counter attractions, including the conferences themselves, the heady decor and swimming pool of the Shamrock-Hilton Hotel, said Directors immured themselves for two days, transacting ordinary business on one day and devoting the other to a "committee of the whole" meeting on the educational trends and problems of our profession. As the French say, both meetings marched well. So much was accomplished, in fact, that the Board agreed henceforth to permit two meetings out of five to be held each year at regional centers, and to take advantage of the opportunity thus presented for extended consideration of IRE affairs.

Among the actions taken were: *Item.* The details of a pension plan for IRE employees were approved and put into effect, retroactive to August, 1956. This step, essential to attracting and holding outstanding talent in our Headquarters operations, had received extended study by Directors Pratt and Baker to assure that the provisions of the Pension Trust not only fully protected the post-retirement status of the employees but also fitted into the financial operations of the Institute on a sound basis. *Item.* A joint action with the AIEE was concluded which, while perhaps of minor effect on the Institute as a whole, was a welcome augury of similar cooperative steps to come. This provides for membership in both societies by the Student Chairman of a Joint IRE-AIEE Branch, but requiring the payment of dues to only one society during his incumbency. *Item.* Student Branches were authorized in all educational institutions whose students qualify for Student Membership. This "right of assembly" statute corrected an inconsistency of long standing. *Item.* A new classification of Student Membership, Student Associate, for technical institutes approved by the Executive Committee, and Student Associate Branch facilities were established.

Item. The Board voted to seek membership for the IRE in the Engineers' Council for Professional Development (ECPD). This was by far the most far-reaching step taken at Houston, and it is hoped that the application for membership, since tendered by President Henderson, will receive favorable action by the Council. ECPD has several functions, foremost among which is the regular examination of the courses of study, laboratories and teaching facilities upon invitation extended by engineering colleges and technical institutes. Courses found by the examining teams to meet the ECPD standards are officially accredited for a period of five years and are re-examined at five year intervals. Failure to qualify is a serious matter in academic circles, and the ECPD thus provides vital impetus to improving the quality of engineering instruction. Since the future of our profession depends entirely on the quality of its future members, we can hardly imagine a more important force with which the IRE could align itself.

Exerting effective pressure for better engineering education requires a clear concept of what in fact constitutes better engineering education. The concept at present is rapidly changing, and it is this state of flux with which the educators on the IRE Board are deeply concerned. As recently as twenty-five years ago, the curricula of even our foremost institutions put heavy emphasis on manual skills and other non-cerebral attainments. In those days if you hoped to graduate as an electrical engineer you went through several months of learning to file metal by hand and to operate a lathe. The progress of technology since that time has forced such courses out of most curricula, because there is no longer time to learn do-it-yourself lore while learning to compete in the higher echelons of modern science and engineering. But many courses of study, and indeed many of the accrediting standards, still put much store on "handbook knowledge," *i.e.* the use of derived equations without clear knowledge of the underlying fundamentals.

Dean F. E. Terman first brought the dangers of this educational philosophy to the attention of the IRE in the *Student Quarterly* in "Electrical Engineers are Going Back to Science!" (reprinted in the PROCEEDINGS, June, 1956). This article was, in fact, the first step in the chain of discussion, carried forward thereafter principally by Professors Brainerd and Ryder of the IRE Board, which led to the present desire of the Institute to take a more active part in the accreditation of engineering schools, through participation in the work of the ECPD.

All in all, the Houston meeting was one to remember long after the image of the mermaids of the Shamrock Water Ballet (a not inconsiderable event which the Directors took some pains to finish their business in time for) is lost in the mists of time.

Addition. We are happy to announce the appointment of Mr. Paul Lucey as Assistant Editor of the *IRE Student Quarterly*. He will assist SQ Editor Hunter and Managing Editor Gannett not only in producing the Quarterly but also in maintaining contact with IRE student activities in the field. Mr. Lucey has had considerable experience in dealing with student groups and has presented demonstrations of American technology at World Trade Fairs in India and Pakistan. We are glad to welcome him to the staff.—D.G.F.

Scanning the Issue

The Effect of Nuclear Radiation on Selected Semiconductor Devices (Keister and Stewart, p. 931)—The situations in which semiconductor devices may be exposed to nuclear radiation are increasing very rapidly. For example, considerable attention is now being given to transistorizing various types of electronic equipment used in nuclear instrumentation and control work. General communications equipment, too, can be subject to the possibility of exposure, not only in military applications but, to cite one instance, in nuclear-powered aircraft. When the nearly perfect crystal structure of a semiconductor material is exposed to radiation, the bombarding gamma rays and neutrons cause a dislocation or transmutation of some of the atoms. These structural imperfections alter substantially the behavior of the carriers within the material. Radiation also has an important effect on the surface properties near a *p-n* junction. This paper investigates the relative sensitivity of germanium and silicon transistors to nuclear radiation, and the type and extent of damage that results. It brings to light some of the main problems that exist in the use of semiconductors in a radiation environment and provides valuable evidence as to the areas where further research is needed.

A Traveling-Wave Frequency Multiplier (Bates and Ginzton, p. 938)—Frequency multiplication in the microwave region is usually accomplished by using either a crystal rectifier or klystron frequency multiplier as a harmonic generator. These methods suffer from certain limitations which restrict their usefulness. Crystal rectifiers are relatively inefficient and can handle only small amounts of power, while klystrons have a limited tuning range that precludes their use except at a few discrete frequencies. Two months ago it was reported in these pages that ferrites, also, could be used as frequency doublers, with greater efficiency and better power-handling capabilities than crystals. Still another advance is now reported, utilizing an interesting variation of the traveling-wave tube. The tube employs two helices in cascade. By simply adjusting the voltage of the second helix, a particular harmonic of the input frequency may be selected and amplified. The experimental model built by the authors was found to operate over a wide range of input frequencies (100 to 1000 mc) to produce useful output power in the 2 to 4 kmc range, thus utilizing harmonics as high as the fortieth.

Very Narrow Base Diode (Rediker and Sawyer, p. 944)—A technique of controlled selective bath etching has been developed to produce semiconductor diodes with extremely thin base widths, on the order of one to ten millionths of an inch. The narrowness of the base permits the minority carriers to be removed more rapidly which, in turn, allows the diode to be switched more rapidly from the forward low-impedance state to the reverse high-impedance state. In addition, the narrow base exhibits a low bulk resistance, so that the entire range of forward currents can be obtained at low forward voltages. This combination of high-frequency capability and low forward-voltage drop makes this diode especially useful in computer circuits. The device may also prove useful as a variable capacitor in uhf applications, and as a mixer.

Application of the Smith Chart to General Impedance Transformations (Dawirs, p. 954)—The Smith Chart is a basic and very useful tool for making impedance calculations for transmission line networks. Its use has, by and large, been restricted to lossless networks, the characteristic impedances of which are real numbers. This paper presents an interesting and very useful extension to cases involving complex characteristic impedances, thus making the Smith Chart adaptable to any linear, passive, bilateral two terminal-pair network. Readers will find the ratio of usefulness to length of this article particularly high.

Behavior of Noise Figure in Junction Transistors (Nielsen, p. 956)—At frequencies above 1 kilocycle, noise in transistors can usually be assumed to arise chiefly from diffusion and recombination fluctuations in the base region and from ordinary thermal noise in the base resistance. In an earlier paper, a method was developed for representing these noise sources, for the purpose of circuit analysis, by equivalent noise generators attached to the equivalent circuit of a transistor. In this paper the author presents a simplified version of this equivalent circuit, and from that develops equations for determining the conditions for minimum noise figure and the effect of transistor and circuit parameters on the noise figure. The result is a paper on a subject about which very little appears in the literature, that gives the circuit designer a workable set of formulas and data which are both practical and directly applicable to circuit design.

Improvement of Binary Transmission by Null-Zone Reception (Bloom, *et al.*, p. 963)—During the past few years considerable attention has been given to various pulse code modulation schemes and methods of improving the speed and reliability with which they can transmit information in the presence of noise. When the noise level becomes appreciable, the reliability of receiving the message correctly becomes especially important. Binary systems offer greater reliability than higher order systems since the receiver has only to distinguish correctly which of two possible pulse levels is being transmitted. In the customary binary systems, the receiver after making this decision on each transmitted pulse prints out one of two symbols. This paper considers schemes in which the receiver prints out one of three symbols (single-null zone reception) or one of four symbols (double-null zone reception). These extra symbols permit the receiver to indicate uncertainty as to which of the two pulses is being transmitted instead of forcing it to make a choice that may be incorrect, resulting in a significant improvement in the information rate of binary transmission.

Back Scattering from Water and Land at Centimeter and Millimeter Wavelengths (Grant and Yaplee, p. 976)—This paper presents valuable experimental data on high-angle back scattering from water and land at frequencies where there is little published information. The study brings in the effects of wind velocity over the water surface, the angle of incidence, and frequency. The data collected by the authors will be of considerable interest to people concerned with radar and navigation problems and, to some extent, communications.

IRE Standards on Electron Tubes: Definitions of Terms (p. 983)—During the past seven years IRE technical committees have produced nine Standards dealing with electron tube terminology, bringing up to date old terms and introducing new ones as the art progressed. The Electron Tube Committee has now combined all nine of these Standards into one convenient package, revising many of the previous definitions and adding a large number of new terms in the process. This Standard is one of the largest the IRE has ever produced—a valuable dictionary of over 600 basic terms comprising a goodly share of the radio engineering language.

The Effect of Nuclear Radiation on Selected Semiconductor Devices*

G. L. KEISTER† AND H. V. STEWART†

Summary—Selected samples of both germanium and silicon devices have been exposed to a nuclear radiation environment.

This environment consisted of either a fission-produced gamma spectrum or a combined neutron and gamma spectrum as obtained in the graphite region of the Materials Testing Reactor in Scoville, Idaho. Several parameters of the devices were measured before, during, and after irradiation. Noise and photovoltaic voltages were observed during exposure to a gamma flux of 2×10^6 Roentgens/hour (R/hr). In some devices, transient changes occurred in those parameters sensitive to surface conditions. After continued exposure of from 5×10^5 to 5×10^8 Roentgens or 5×10^{10} to 5×10^{13} neutrons per square cm, permanent damage occurred in the device characteristics. No real distinction could be made between silicon or germanium devices so far as noise, photovoltaic, or transient effects are concerned.

However, there is a marked difference between silicon and germanium devices with respect to permanent damage.

Silicon devices are more susceptible to damage in parameters dependent upon the minority carrier lifetime such as the current gain, the forward resistance of high efficiency diodes, and the valley voltage of unijunction transistors. Germanium devices are also susceptible to the conversion of n material to p type and this results in the reduction of the punch-through voltage of p-n-p germanium transistors.

For both silicon and germanium transistors it was found that the thinner base transistors were the more resistant to reduction in current gain.

Introduction

WITH THE ADVENT of nuclear energy in airplane propulsion and other industrial applications, electronic devices are being exposed to a new environment.

This environment of nuclear radiation consists mainly of neutrons and gamma rays from both radioactive materials and operating reactors.

The extremely desirable electrical and mechanical characteristics of the transistor make it an attractive component for use in ground or airborne electronic equipment which may become exposed to nuclear radiation. The fact that the operation of this semiconductor device depends on a highly uniform crystal structure suggests that it is extremely sensitive to nuclear radiation damage.

To determine the extent, type, and relative sensitivity of transistors to nuclear radiation, programs in radiation damage were initiated in April, 1956. It has been reported by several investigators[1–5] that germanium and silicon are sensitive to nuclear bombardment. Most measurements have been concentrated on the majority carrier density properties of these materials; that is, measurements of resistivity and Hall coefficients. These changes in resistivity are attributed to imperfections produced in the crystal structure of the semiconductor. The imperfection can be caused either by displacement of the atoms in the crystal structure by fast neutrons, recoil nuclei, and gamma rays, or by transmutation of the atoms caused mainly by slow neutrons. These imperfections trap the carriers and thus affect the resistivity and Hall coefficient. Trapping of the carrier also affects the bulk minority carrier lifetime.[6–8] No direct information is available on the effect of radiation on the surface properties of the semiconductor material, in particular near a p-n junction. Surface properties of semiconductors have proven to be extremely important in the fabrication of acceptable semiconductor devices, and the lack of this information makes it difficult to predict the effects of nuclear radiation on these devices. At the time of this investigation, little work had been done to determine the effects of nuclear radiation on transistors and diodes.

The information that was available was on static-type tests in which the electrical characteristics of the transistor were measured before and after the irradiation to determine permanent damage effects. Nothing or very little had been done in measuring changes in device characteristics while they were undergoing irradiation.

* Original manuscript received by the IRE, February 26, 1957; revised manuscript received, April 29, 1957. This work was undertaken in partial support of an Air Force contract between The Air Res. and Dev. Center, Wright-Patterson AFB, Ohio, and Boeing Airplane Co.

† Boeing Airplane Co., Seattle 24, Wash.

[1] Solid State Division Quart. Prog. Rep. for period ending February 10, 1953, Oak Ridge Natl. Lab. Rep. ORNL-1506, Oak Ridge, Tenn.; June, 1953.

[2] J. W. Cleland, J. H. Crawford, Jr., and D. K. Holmes, "Effect of gamma radiation on germanium," *Phys. Rev.*, vol. 102, pp. 722–724; May 1, 1956.

[3] J. W. Cleland, J. H. Crawford, Jr., K. Lark-Horovitz, J. C. Pigg, and F. W. Young, Jr., "The effect of fast neutron bombardment on the electrical properties of germanium," *Phys. Rev.*, vol. 83, pp. 312–319; July 15, 1951.

[4] J. W. Cleland, J. H. Crawford, Jr., and J. C. Pigg, "Fast-neutron bombardment of n-type germanium," *Phys. Rev.*, vol. 98, pp. 1742–1750; June 15, 1955.

[5] K. Lark-Horovitz, "Nucleon Bombarded Semiconductors," in "Reading Conference on Semiconducting Materials," Thorton Butterworth, Ltd., London, Eng., pp. 47–69; 1951.

[6] P. Rappaport, "Minority carrier lifetime in semiconductors as sensitive indicator of radiation damage," *Phys. Rev.*, vol. 94, pp. 1409–1410; June 1, 1954.

[7] J. J. Loferski and P. Rappaport, "Electron voltaic study of electron bombardment damage in Ge and Si," *Phys. Rev.*, vol. 98, pp. 1861–1863; June 15, 1955.

[8] P. Rappaport, J. J. Loferski, and E. G. Linder, "The electron voltaic effect in Ge and Si p-n junctions," *RCA Rev.*, vol. 17, pp. 101–128; March, 1956. See pp. 120–122.

The work described here includes tests performed while the device was being irradiated. Parameters were chosen to reveal the most about the type of damage inflicted, but were consistent with the experimental difficulties in the actual performance of the test. By performing both static and dynamic tests on several types of germanium and silicon devices, it is felt that the major problems of the effects of nuclear radiation on semiconductor devices have been established.

Description of Test Method and Facilities

The tests were performed at the Atomic Energy Commission (AEC) installations at Scoville, Idaho. Included at these installations are the Materials Testing Reactor (MTR) and the MTR Gamma Facility. The nuclear reactor is a heterogeneous source of thermal and fast neutrons, and gamma radiation. The Gamma Facility utilizes the spent fuel elements from the MTR and produces a full fission product, gamma spectrum. The gamma flux was approximately 2×10^6 R/hr. Static and dynamic tests were made under gamma radiation only so that the observed results could be used to separate effects observed due to gamma and neutron irradiations within the pile. Ports on top of the MTR provided access into the graphite region by means of spiraled, vertical holes approximately one inch in diameter. Most of the testing was performed at a position 18 feet from the top of the reactor in a fast neutron flux of approximately 5×10^9 neutrons per square centimeter per second (nv), when the reactor was operating at a power level of 40 megawatts. The total neutron dose was measured in neutrons per square centimeter (nvt)[9] and varied depending upon the individual unit tested.

Due to the limited size of the access hole, transistors were tested one at a time. Because of the possibility that gamma heating in the transistor could cause an increase in the temperature of the junction resulting in a false indication of radiation damage, forced air cooling was provided and the ambient temperature monitored by means of a thermocouple for each irradiation. A 25-mil cadmium foil shield was used to reduce the number of slow neutrons in the majority of tests.

The transistor parameters to be measured were chosen so that the operating region of the transistor would be defined. This region is defined by the collector leakage current, the current gain, and the breakdown or punch-through voltage. The variation of these parameters was recorded by two means. At first, a test set was constructed that automatically recorded four parameters of the transistor every 45 seconds. These parameters were I_{co}, the collector leakage current at 6 volts; β, the grounded emitter current gain with the transistor bias at V_{bc} equal to 6 v, and I_e equal to one ma for low-powered transistors and 10 ma for high-powered transistors; the collector breakdown voltage, defined at I_e equal to 0.5 ma for low-powered transistors and 2 ma for high-powered transistors; and the voltage difference between the breakdown and punch-through voltage. Later, a characteristic curve plotter[10] was used to plot the grounded emitter output characteristics. The curve plotter revealed more information about the damage than the test set and has been used exclusively in the last phases of the tests. Since radiation-induced noise could be a limiting factor in some transistor applications, a cursory noise test was performed in which a transistor amplifier was irradiated to determine whether or not the nuclear radiation would affect the noise figure of the transistor. Measurements of the floating potential of grown junction transistors were also made.

Prior to testing the transistors, extensive tests were performed to determine if the effect of radiation on the exposed sections of test equipment (*i.e.*, the cables) could induce erroneous voltages into the equipment. It has been reported that voltages can be induced in cables subjected to nuclear radiation.[11] The test equipment was designed exclusively of low impedance circuitry and, because of this, no difficulty was experienced with induced voltages in the cables. However, measuring the same cable with a high impedance electrostatic voltmeter revealed voltages in the order of 20 v. To measure the effect of gamma heating upon the transistor junction, a test was performed in which a thermocouple was placed within the case on the junction of a transistor and the difference in ambient and junction temperature measured. The difference was less than 10°C for a gamma flux of 2×10^6 R/hr.

Results of Test

As was found by other investigators,[5] the gamma radiation produced excess carriers in the semiconductors which resulted in a photovoltaic voltage being induced in a p-n junction. This voltage was observed for both transistor and diode p-n junctions and was the of order of 10 to 50 millivolts for a gamma flux of 2×10^6 R/hr. As might be expected, the devices having longer minority carrier lifetimes exhibited the higher voltages. The voltage was also dependent upon the loading of the measurement circuit.

In the cursory noise test, a grounded emitter transistor amplifier was subjected to gamma radiation and the output noise measured. It was found that an increase in the noise level of approximately 25 db was observed when the transistor was placed in a gamma flux of 2×10^6 R/hr. Fig. 1 shows the output of the amplifier

[9] The unit nvt used in nuclear dosimetry is an abbreviation for the number of *n*eutrons per cubic centimeter multiplied by their *v*elocity in cm per second and the *t*ime in second.

[10] This was suggested by K. E. Palm of RCA, Camden, N. J., who was observing the tests.

[11] J. C. Pigg, C. D. Bopp, O. Sisman, and C. C. Robinson, "The Effect of Reactor Irradiation on Electrical Insulation," Paper 55-694, AIEE Fall General Meeting, Chicago, Ill.; October 3–7, 1955.

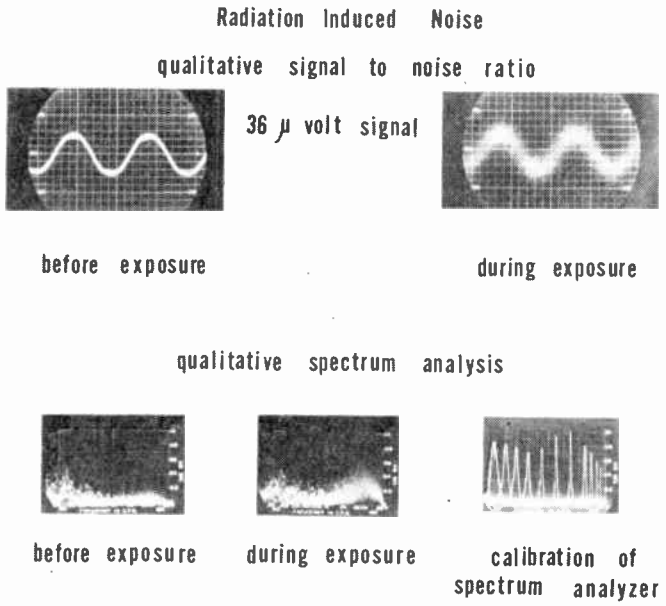

Fig. 1—Radiation induced noise in a GE2N43 caused by a gamma ray flux of 2×10^6 R/hr. The 5-kc sine wave output was produced by a 36-microvolt signal in the amplifier input. Noise spectrum of GE2N43 before and during Co^{60} irradiation, plotted as a linear mv scale vs log frequency from 40 cps to 20 kc.

for a 36-microvolt input signal before and during irradiation. It can be seen from this figure that radiation-induced noise may be a considerable problem for applications involving low signal levels. Using the Boeing Co^{60} gamma facility and a sonic analyzer, a picture of the noise spectrum was obtained. This is also shown in Fig. 1. In both cases the radiation induced noise disappeared immediately upon removal from the flux.

One of the most significant results of the test was the transient changes observed in the collector characteristics when the transistors were exposed to gamma radiation. The most sensitive parameters to this type of radiation were I_{co}, β, and the floating potential. The transient effects in these parameters are differentiated from the rate effects (*i.e.*, photovoltaic effect and noise) in that the transient changes occur on a time scale of seconds to minutes as compared to the immediate effect induced by the flux rate. The magnitude of both the transient and rate effects are a direct function of the flux intensity. Fig. 2 shows the three general types of variations experienced in the measurement of I_{co} vs irradiation time. In some cases [Fig. 2(b)] I_{co} continued to increase with time until the transistor was removed from the flux. Other transistors exhibited saturation [Fig. 2(a)] or maxima [Fig. 2(c)] in their collector leakage current. Fig. 3, which is a plot of the floating potential and I_{co} vs irradiation time, indicates that the floating potential varies in the same manner as I_{co}. As will be discussed later, this is an indication of the phenomena responsible for the effect. The changes in the collector characteristics are graphically demonstrated in Fig. 4, which is a series of photographs taken

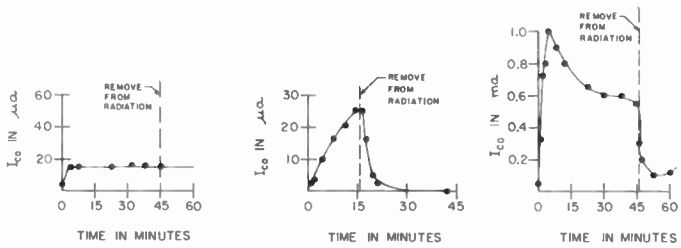

Fig. 2—Representative curves of collector leakage current variation vs irradiation time in gamma flux of 2×10^6 R/hr. (a) 2N139 Ge *p-n-p*. (b) 904 Si *n-p-n*. (c) 2N57 Ge *p-n-p*.

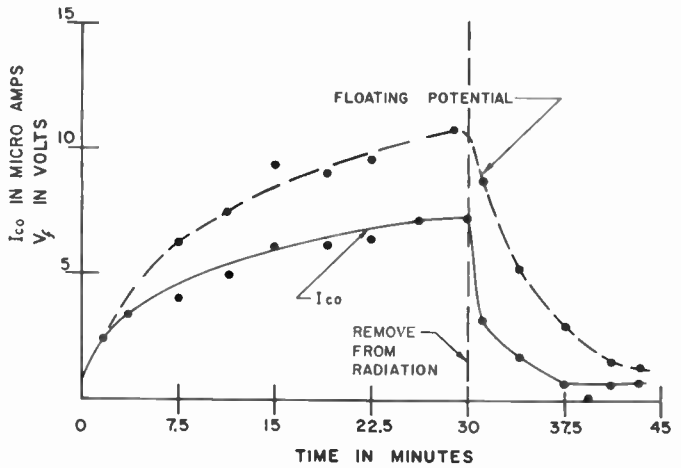

Fig. 3—Correlation between floating potential and collector leakage current of 2N27 Ge *n-p-n* grown junction transistor.

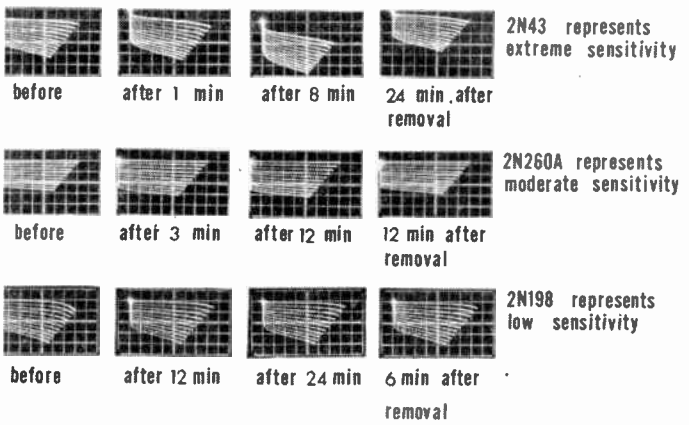

Fig. 4—Curve plotter photographs in which I_c is plotted against V_c for constant I_b. These photographs are representative of the type and extent of the transient damage experienced by transistors exposed to a gamma flux of approximately 2×10^6 R/hr.

of representative transistors before, during, and after radiation. It is seen in this figure that transient changes occur during irradiation in collector leakage current, current gain, and collector resistance. These parameters returned to what were almost the original values within seconds to minutes after being removed from the flux. Several transistors exhibited this type of change in varying degrees. Fig. 4 shows representative examples of

TABLE I

SENSITIVITY OF TRANSISTORS TO GAMMA* INDUCED TRANSIENT DAMAGE

Degree of Sensitivity	Transistor Type	Kind	Material	Manufacture Method	Manufacturer	Case Filling	Parameter Most Sensitive
Extreme	2N43	*p-n-p*	Ge	Alloyed	GE	Grease	I_{co}, β V_b
	904, 905	*n-p-n*	Si	Grown	TI	Gas	I_{co}
	XH5	*p-n-p*	Ge	Alloyed	MH	Gas	I_{co}, β
Moderate	926	*n-p-n*	Si	Grown Diffused	TI	Gas	I_{co}
	501	*p-n-p*	Ge	Grown Diffused	TI	Grease	I_{co}
	2N27	*n-p-n*	Ge	Grown	WE	Varnish	β
	SB-100	*p-n-p*	Ge	Surface Barrier	Philco	Grease	β
	2N139	*p-n-p*	Ge	Alloyed	RCA	Grease	I_{co}
	2N43	*p-n-p*	Ge	Alloyed	Transitron	Gas	β
	2N99	*n-p-n*	Ge	Grown	GP	Red Paint on Junction	I_{co}
	2N260A	*p-n-p*	Si	Alloyed	Clevite	Grease	β
	2N167	*n-p-n*	Ge	Rate Grown	GE	?	I_{co}
Low	2N198	*p-n-p*	Ge	Alloyed	Transitron	Gas	—
	CK790	*p-n-p*	Si	Alloyed	Raytheon	Grease	—
	2N34	*p-n-p*	Ge	Alloyed	Sylvania	Gas	—
	2N35	*n-p-n*	Ge	Alloyed	Sylvania	Gas	—
	2N109	*p-n-p*	Ge	Alloyed	RCA	Grease	—
	156	*n-p-n*	Ge	Alloyed	RCA	—	—
	951, 952, 953	*n-p-n*	Si	Grown	TI	Glit	—
	L6101	*n-p-n*	Si	Surface Alloy	Philco	Grease	—

* Gamma flux approximately 2×10^8 R/hr (spent fuel source).

extreme, moderate, and low sensitivity to this type radiation. Table I lists the transistors according to their sensitivity to gamma radiation. Also listed in Table I are the case fillings of the transistors as determined by opening the case after the test. It is seen from this that no direct correlation exists between general types of case filling and the sensitivity to gamma radiation. From a casual examination of Table I, it is difficult to see any reason for the wide range of sensitivity which has been observed.

Permanent damage observations while the transistors were being irradiated were complicated by the transient changes in the characteristics. It is difficult to distinguish in some cases between transient and permanent damage until the transistor is removed from the radiation flux. Due to the longer times required for permanent damage induced by gamma radiation, these tests were performed statically. Due to the large neutron flux used in the pile irradiation, permanent damage accumulated much more rapidly, and dynamic tests were performed. This permanent damage consisted of a reduction in the current gain of all samples exposed and in some cases, an increase in the leakage current and a reduction of the punch-through voltage of the transistor was observed. Fig. 5 shows the reduction in current gain of all the transistors tested vs integrated gamma or neutron flux. It is seen that the general characteristics of the curves are similar for all types of transistors. The most interesting observation from these curves is that the high-frequency, thin-based transistors are the most resistant to nuclear radiation, and the germanium transistors, more resistant than equivalent silicon types. Fig. 6 shows the variation in the collector characteristics as the transistor is exposed to pile radiation. The most noticeable changes in the characteristics other than the transient leakage current due to the gamma radiation are a drastic reduction in the current gain and the uniform reduction in the punch-through voltage.

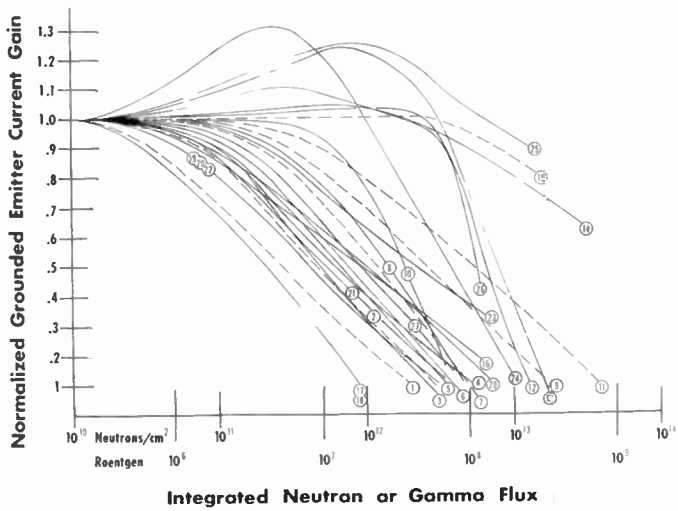

TRANSISTOR TYPES

1. 2N260A	8. 2N35	15. 501	22. 2N198
2. CK790	9. 926	16. 2N198	23. 2N198
3. XH5	10. 953	17. CK790	24. L6101
4. 904	11. 2N43 Transitron	18. CK790	25. 501
5. XH5	12. 2N139	19. 926	26. 501
6. 953	13. 2N139	20. 2N43 Transitron	27. 2N260A
7. 2N43 GE	14. SB100	21. 2N99	28. 2N167

Fig. 5—The permanent change in the normalized grounded emitter current gain is plotted vs integrated fast neutron or gamma flux. - - - - Permanent gamma damage. ——— Permanent neutron damage.

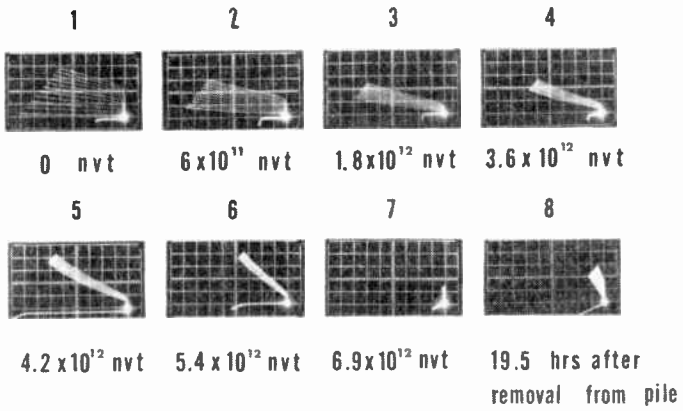

Fig. 6—Curve plotter photographs in which I_e is plotted against V_e for constant values of I_b. These photographs are representative of the reduction in current gain and in the punch-through voltage experienced in pile exposure.

As will be described later, the general reduction of the current gain of the transistor is caused by the reduction in the minority carrier lifetime of the semiconductor. Two devices which are very sensitive to the minority carrier lifetime are the high efficiency diode and the unijunction transistor. Due to the expected sensitivity of these devices, they were exposed in the gamma facility to determine their radiation susceptibility. Fig. 7 shows the variations observed in the forward characteristic of high efficiency silicon diodes, and Fig. 8 shows the changes in the input characteristics of a unijunction transistor. An attempt was made to anneal the damage to the high efficiency diode by heating it to a temperature of 200° C for 8 hours. No annealing was observed.

Discussion of Results

The observation of the photo effect in the *p-n* junction was an expected result and has been observed by others.[5] This voltage is due to the production of minority carriers by the nuclear radiation in a similar manner as minority carriers are generated in photovoltaic cells. It was found that the photo effect does not noticeably affect the use of transistors in fluxes of the order of 10^6 R/hr.

The noise observed in the cursory noise test could be due to one or both of the following phenomena. The reverse bias collector junction of the transistor could be acting as a nuclear counter in that large numbers of minority carriers generated at the junction could cause pulses of current which would show up as noise in the associated circuitry.[12] Secondly, the large number of ions present on the transistor surface could be the source of noise due to the recombination of carriers at the semiconductor surface.

[12] W. H. Fonger, J. J. Loferski, and P. Rappaport, "Electron bombardment induced noise in *p-n* junctions" *Bull. Am. Phys. Soc.*, vol. 1, p. 135; March 15, 1956.

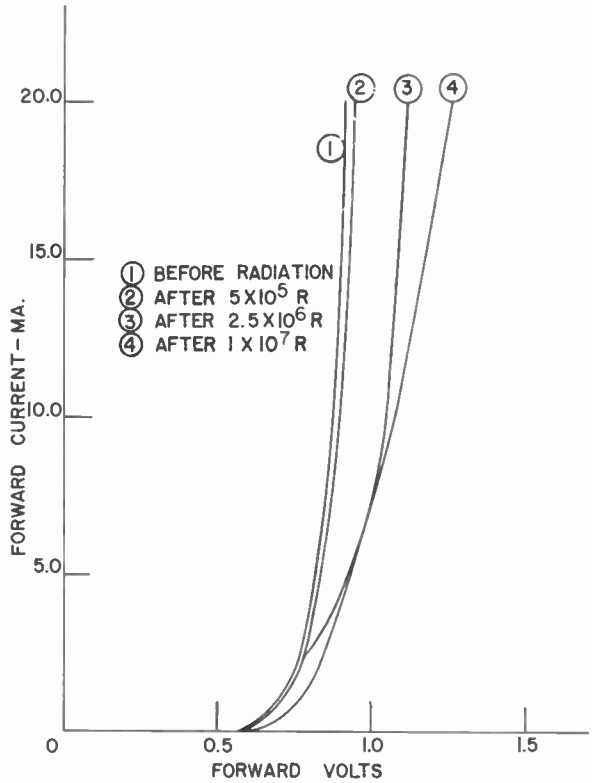

Fig. 7—Permanent changes in the forward characteristic of a high efficiency HG6006 diode due to a reduction in the minority carrier lifetime of the silicon.

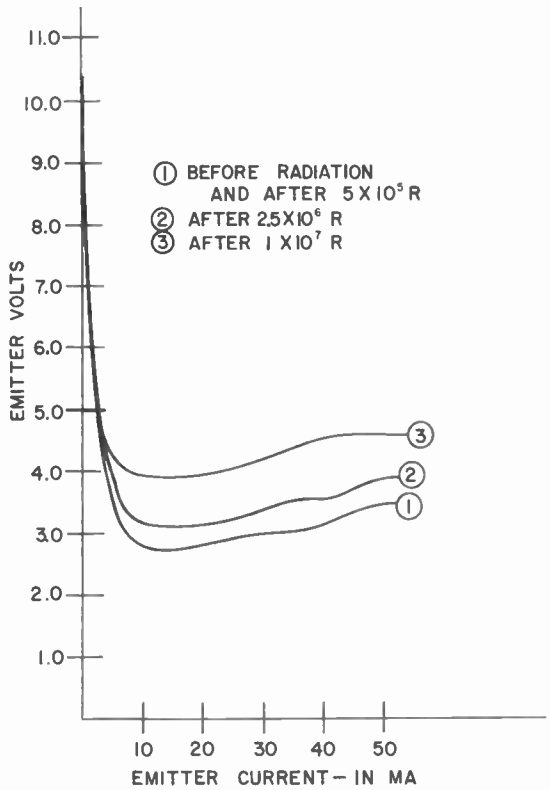

Fig. 8—Permanent changes in the input characteristics of a unijunction transistor (*i.e.*, double base diode) due to a reduction in the minority carrier lifetime of the silicon base material.

Transient changes in the leakage current and current gain of the transistors exposed to gamma radiation were observed for the first time during these tests. The apparent lack of correlation of this effect between transistor types leads to the suspicion that the intense ionization produced by the gamma radiation caused changes in the surface properties of the semiconductor. The following facts are presented as evidence that the observed transient changes are associated with changes in the surface properties of the semiconductor:

1) The general shape of the collector characteristics indicates that the changes are due to surface leakage.
2) The variation in floating potential of grown junction transistors indicates the formation of conduction channels between collector and emitter.
3) The general shape of the curves in Fig. 2 could be explained by the slow movement of ions on the insulating oxide layer at the surface of the semiconductor.
4) The reason for the difference in sensitivity of various manufacturers' transistors could be the difference in surface preparation and case filling materials.
5) Measurements of minority carrier lifetime by the after pulse method shows that the carrier lifetime changes in about the same way as the floating potential and I_{co} for those devices most sensitive to gamma radiation.[13]

Texas Instrument types 905 and 951 are essentially identical in manufacture except for the silicone rubber in the 951. It is indicated in Table I that the silicone rubber reduces the radiation sensitivity of the silicon grown junction transistor. It has also been observed[14] that the GE2N43 has a low sensitivity to gammar radiation when the silicone grease is removed from the can. In addition to these two seemingly contradictory statements of fact, the distribution of transistors in Table I indicates that the transient change in the transistor characteristics could be a fairly complicated function of the various manufacturing processes. The sensitivity of transistors to radiation may be an indication of the stability of the surfaces and could be used as a rapid test of stabilizing manufacturing techniques. No such correlation has been observed, and this is offered only as a suggestion.

The permanent damage to the germanium semiconductor devices is the result of two changes in the electrical properties of the semiconductor. First, the deterioration of the minority carrier lifetime and, secondly, the conversion of n-type material to p-type. Silicon devices are subject to changes in the minority carrier lifetime, but the resistivity tends toward the intrinsic value. The deterioration of the minority carrier lifetime is indicated by the reduction of the current gain as a function of base thickness of the transistor, the reduction of the forward resistance in high efficiency diodes, and the increase in the valley voltage of unijunction transistors. The conversion of the n-type base material of p-n-p alloyed junction transistors to p-type material manifests itself by a reduction in the punch-through voltage. The reduction in the punch-through is a linear function of the integrated flux as is shown in Fig. 9. The rate of conversion is dependent upon the initial doping or resistivity of the base material. The greater the doping the longer it takes for conversion. If transistors could be made such that the base resistivity were well controlled, it is conceivable that they could be used as radiation dosimeters. Although n-p-n germanium transistors will not experience a reduction in punch-through, conversion of the n regions will destroy the p-n junction and make them useless.

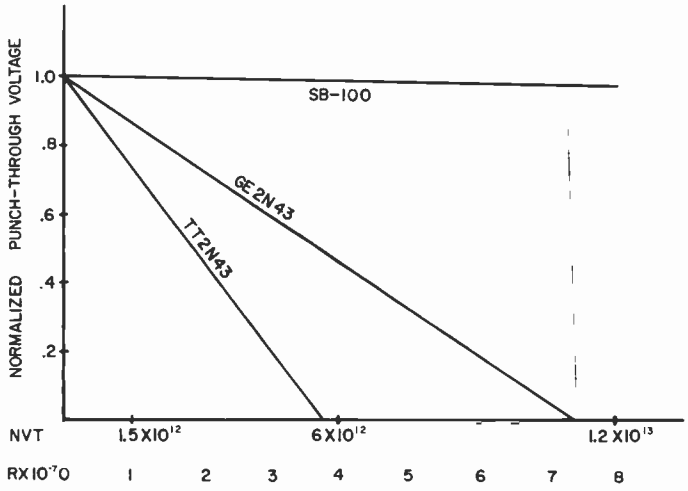

Fig. 9—The punch-through voltage of this p-n-p transistor is plotted vs integrated fast neutron flux or integrated gamma dose. The slope of the linear relationship is dependent upon the doping of the base material.

Silicon does not experience a preferential conversion to n- or p-type material.[5] Thus silicon transistors do not exhibit variations in the punch-through voltage.

Fig. 10 is a comparison of all semiconductor devices tested. They are listed according to their susceptibility to permanent damage caused by nuclear radiation. It is seen from this figure that the destruction of a semiconductor device by radiation is dependent upon the type of device. If the device requires a long minority carrier lifetime, it will withstand only the minimum of radiation. If it is not dependent upon the minority carrier lifetime, it may be orders of magnitude less susceptible to radiation.

[13] V. Hugo Schmidt, private communication.
[14] A. B. Grafinger and C. D. Birkhahn, "Gamma Ray Effects on Germanium Transistors," General Electric Tech. Info. Ser. No. 56SD76.

Due to the uncertainty in dosimetry as well as the wide variations in semiconductor manufacturing methods, it is impossible at present to give accurate quantitative answers to the question, "At what integrated neutron flux will a particular type transistor have its grounded emitter current gain reduced by a factor of 2?" The shaded areas in Fig. 10 indicate that permanent changes in the device characteristics will be noted in the lightly shaded region. As the shaded area becomes darker it indicates that the changes in the device characteristics will be sufficient to noticeably affect their operation in the more sensitive circuit applications.

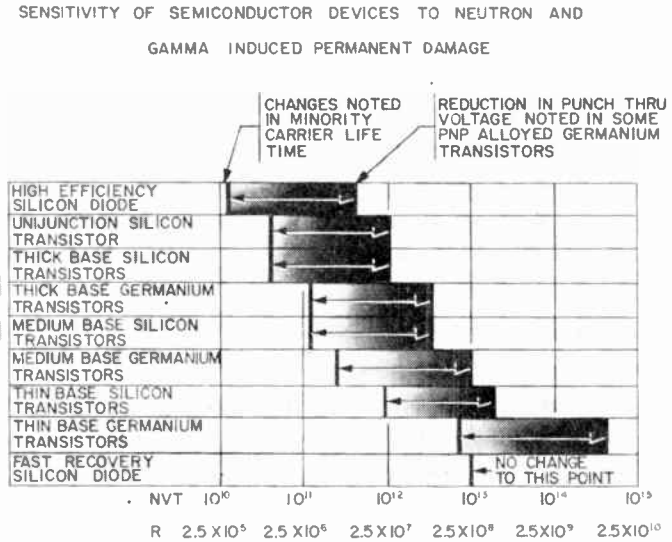

Fig. 10—A comparison of the sensitivity of semiconductor devices to neutron and gamma induced permanent damage. The degradation is associated with the grounded emitter current gain for the junction transistor, the valley voltage for the unijunction transistor, and the forward resistance for the silicon diode.

Conclusion

As is seen in the discussion of the results, the radiation environment offers a new challenge to both the device users and manufacturers. By properly fabricating semiconductor devices, they can be made orders of magnitude more resistant to nuclear radiation than presently available devices. The user of semiconductor devices must be aware of this broad range of susceptibility and, where necessary, use those devices which are more resistant to this new environment.

The difficulty of determining the exact limitations of semiconductor devices to nuclear radiation is compounded by several factors. The first of these is the large variety of semiconductor devices having similar electrical specifications, but being made by drastically different manufacturing methods. Because of this, transistors cannot be selected according to their electrical specifications for use in a nuclear radiation environment. More attention must be paid to the method of manufacture and to a new specification indicating the device's susceptibility to radiation. The second main problem is that of dosimetry. Although many tests are being performed to determine the answer to the problem of semiconductor sensitivity to nuclear radiation, too little attention is being paid to the type of radiation, the spectrum of the radiation, and the total integrated flux. The third problem area, which is more the problem of the applications engineer, is the uncertainty in the expected nuclear environment in which the semiconductor device must live.

This paper points out some of the main problems that exist in the use of semiconductors in the radiation environment, but much work remains to be done. It is suggested that more basic work on the effect of nuclear radiation on minority carrier lifetime, surface conditions of the semiconductor, and conversion of the basic semiconductor materials would help greatly in understanding these problems. If the transistor manufacturer were given information of this type, he would be in a better position to construct or develop a radiation resistant transistor; that is, a transistor perhaps orders of magnitude more resistant to nuclear radiation than those available on the open market today.

Acknowledgment

The authors wish to express their appreciation to Bill Cooley, Warren Leyde, and Kermit Thompson, all of Boeing Airplane Company, for designing various equipment used during these tests. To our technician, Gilbert K. Bruce, we express our thanks for his cooperation and initiative. We especially appreciate the help and support given this program by K. E. Palm, RCA, Camden, N. J., whose contributions at the reactor site proved invaluable. And to the many transistor manufacturers who provided us with selected transistor types, we are deeply indebted.

A Traveling-Wave Frequency Multiplier*

D. J. BATES† AND E. L. GINZTON†, FELLOW, IRE

Summary—A traveling-wave tube designed to operate as a frequency multiplier (twfm) is described, together with experimental results. The tube employs two helices in cascade, the output helix being a dispersive forward-wave helix operating at *S* band. A wide range of input frequencies can be used, and the dispersive character of the output helix permits the selection of a particular harmonic by voltage tuning of the helix.

The experimental tube was designed to operate with an input frequency range of 0.5 to 1.0 kmc and an output range of 2 to 4 kmc, although it was found to have a useful input frequency range from 0.1 to 1.0 kmc. It was found that multiplication ratios up to 10 or 15 are feasible with substantial gain, and with output power corresponding to normal operation of the second helix as an amplifier. Using an input frequency as low as 0.1 kmc, well below the design value, harmonic output in the order of a few milliwatts has been obtained at harmonics as high as the fortieth. For beam powers of 2 to 4 watts and for input frequencies down to 0.25 kmc, the harmonic power varied from 20 to 100 mw, depending upon the output frequency and multiplication ratio.

The gross features of the gain characteristics of the twfm using a cascade gain analysis are shown.

Introduction

IN NUMEROUS microwave applications, it is necessary to employ harmonic generators utilizing frequency multiplying elements. The two most common microwave harmonic generators employed in the past have been the crystal rectifier and the klystron frequency multiplier. The large conversion loss and low output power of the former, and the difficulty of tuning the cavities of the latter, have resulted in numerous practical difficulties. In particular, the usual limited tuning range of available klystrons precludes their use except at a few discrete frequencies, strongly restricting their application in a number of practical systems. In some systems it is desirable to change either the input or the output frequency rapidly. For these reasons it seemed worthwhile to explore the possibility of employing a frequency multiplier utilizing traveling-wave circuits and, in particular, two different structures in cascade. In a device of this type, the broad-band characteristics of a traveling-wave tube can be easily retained. By employing a dispersive-type second helix, it is possible to obtain selective amplification of the desired harmonic and a substantial reduction of the undesired harmonic signals. This paper describes an essentially experimental study of a tube which was designed to explore the possibilities of this type of device and to study its gross characteristics.

* Original manuscript received by the IRE, March 14, 1957; revised manuscript received, May 1, 1957. The research reported in this paper was supported in part by the U. S. Army Signal Corps, Air Force, and Navy (Office of Naval Research). Additional project support in reduction to practice was obtained through a subcontract from the Microwave Laboratory of The General Electric Co., Palo Alto, Calif.

† Microwave Lab., Stanford Univ., Stanford, Calif.

For laboratory convenience, the design parameters of the proposed tube were arbitrarily selected to allow operation at any input frequency between 0.5 and 1 kmc, and to obtain harmonic frequencies in the band from 2 to 4 kmc. For the purpose of the proposed tests, the power level was considered unimportant, but to simplify the laboratory measurements, an output power level of about 10 mw was selected.

A number of composite traveling-wave structures were studied, and a particular one employing two forward-wave helices in cascade was selected. It was decided to utilize components of existing traveling-wave tubes as much as possible in order to eliminate the problem of designing two complete traveling-wave tubes, to reduce the labor in construction, and to compare the performance of the multiplier with an ordinary amplifier. Fortunately, it was possible to obtain nearly all of the parts needed for the twfm from a commercial laboratory.[1] The low-frequency (or buncher) helix is a forward-wave single helix intended for use in a nondispersive tube in the region of 0.5 to 1 kmc. Experimentally, the buncher was found to have a useful frequency range from 0.1 to 1.0 kmc. The high-frequency output helix (or harmonic amplifier) is a standard forward-wave single helix operating in the dispersive region in the frequency range of 2 to 4 kmc. The dispersive helix, as noted above, was chosen to permit the selective amplification of a particular harmonic.

Tube Design

A photograph and a schematic drawing of the first experimental tube are shown in Figs. 1 and 2, respectively. Referring to Fig. 2, the electron beam enters the buncher helix at the left and bunching is produced by interaction with the circuit fields at the fundamental frequency. (In the design shown, the buncher voltage is in the neighborhood of 150 volts.) The bunched beam is accelerated to the voltage of the second helix and then enters this helix. The various harmonic components of the rf current induce circuit fields on the harmonic amplifier helix, and a particular harmonic is preferentially amplified by adjusting the voltage of this helix with respect to the cathode. A method of operation of the frequency multiplier will be described where no adjustments other than this voltage are necessary to provide near-optimum output at nearly any desired harmonic within the output-frequency band. Both helices are terminated by loss on the ends opposite the couplers, and additional decoupling loss is added to the

[1] Huggins Labs., Inc., Menlo Park, Calif. The voltage tunable dispersive amplifier was originally studied at Stanford University by L. A. Roberts and others.

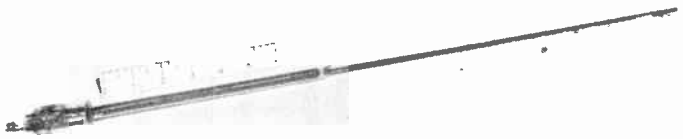

Fig. 1—Experimental severed-helix traveling-wave frequency multiplier. The buncher helix is on the left and harmonic amplifier on the right. The pin near the center is for external connection to the harmonic helix.

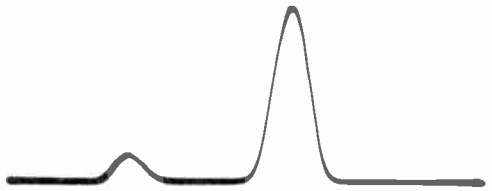

Fig. 3—Oscillograph of the harmonic power as the buncher helix is swept in voltage. Input frequency is 0.75 kmc; harmonic frequency is 3 kmc. Length of horizontal trace is 175 volts, centered at 125 volts.

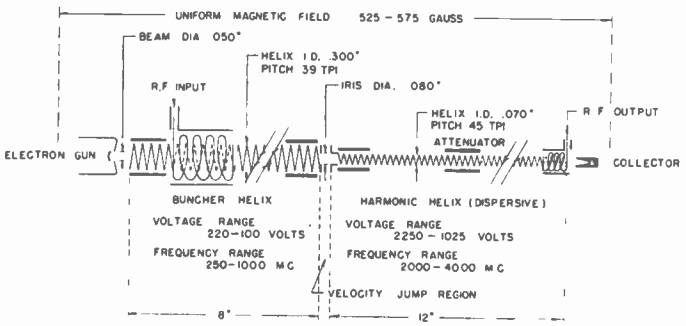

Fig. 2—Schematic diagram of the twfm showing essential design data.

second helix to prevent oscillation. Movable coupled-helix couplers are used, permitting the effective length of the buncher to be varied for experimental purposes. The attenuators used are of the lossy coupled-helix type and can be positioned wherever desired along the tube. The electron gun, which produces a larger diameter beam than is used by the manufacturer in the small-diameter harmonic-amplifier helix, was borrowed from another traveling-wave tube built at Stanford. The principal design parameters for the twfm are shown in Fig. 2.

Experimental Studies

Several types of tests were conducted to investigate the general characteristics of the twfm and the dependence of the harmonic output upon some of the operating parameters.

In most of the tests, the dc buncher voltage was modulated by a 60-cycle sinusoidal voltage to permit dynamic observation of the harmonic output power as a function of the buncher voltage. Fig. 3 shows a typical oscillograph of the output power as a function of the buncher voltage for a particular harmonic. In this case, there are two voltages, approximately 95 and 150 volts (at an input frequency of 0.75 kmc), at which peaks of harmonic output occur for moderate input levels. For higher input levels, there are, in addition, a number of lower voltages at which output peaks also occur. In all cases, unless otherwise stated, only the output of the higher voltage bunching peaks (the one on the right in Fig. 3) is measured. The significance of the different output peaks will be discussed later.

The tests reported below, unless otherwise noted, correspond to rf input levels which are not greater than the saturation level for the buncher helix. When the actual data was taken the 60-cycle modulation of the buncher voltage was removed, and the buncher voltage and harmonic-amplifier voltage were adjusted to maximize *the power output in a particular harmonic.*

The curves and derived data presented are not the optimum which were obtained because when these data were taken, oscillations in the harmonic amplifier limited the beam current which could be used. Substantially better results were obtained in later tests when additional loss was added to the harmonic amplifier section, which allowed the use of a higher beam current. The output characteristics of the two sections were measured by operating the sections separately as amplifiers. From these data, an estimate of the dependence of the output power on the harmonic number and on other factors was obtained.

General Results

Figs. 4, 5, and 6 show the results of frequency multiplication tests for moderate signal levels at a fixed output frequency of 3 kmc. When the data for these graphs were taken, the cathode current was 1 ma with transmission to the collector varying from 75 to 90 per cent, depending upon the relative potentials on the two helices. The length of the buncher helix was $5\frac{3}{8}$ inches for all tests except those for which buncher length was the variable parameter.

In Figs. 4 and 5, the various curves represent data which were obtained for different harmonics by varying the input frequency with a fixed output frequency of 3 kmc. (Some of the curves are shown dashed for clarity, but these represent the same type of data as the solid curves.) In Fig. 5, it can be seen that the conversion gain is not a constant as it is in the linear region of a twa; instead, the conversion gain depends upon the input power level. Fig. 6 shows the maximum conversion gain and the maximum harmonic-power output plotted as a function of the order of harmonic. The output power and, hence, the maximum gain, is limited by saturation in the output helix for harmonics up to about the seventh, at this particular output frequency. This factor limited the maximum conversion gain for the lower harmonics; in addition, there is a large reduction in conversion gain for both the lower and the upper harmonics due to reduced gain of the buncher at the corresponding input frequencies. Both the maximum conversion gain and the maximum output power are

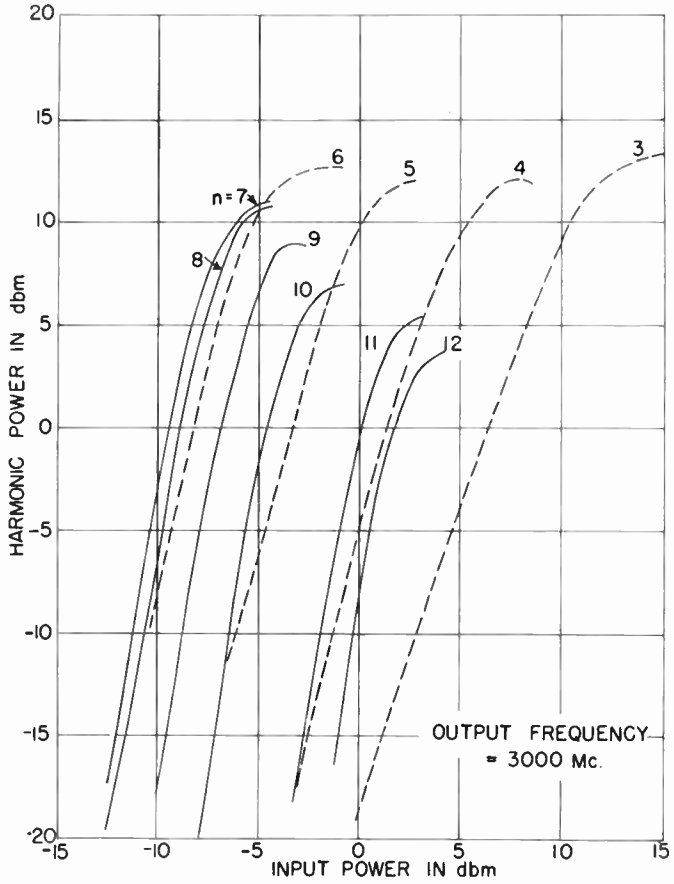

Fig. 4—Harmonic power output vs input power at fixed output frequency of 3 kmc for moderate input level. The order of harmonic is varied by changing the input frequency.

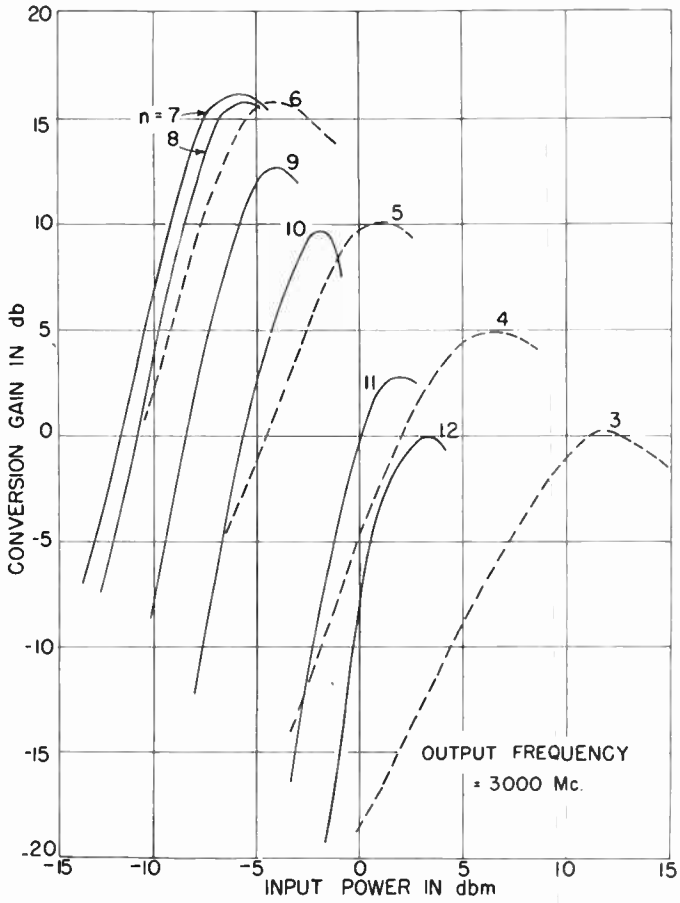

Fig. 5—Conversion gain as a function of input power for fixed output frequency of 3 kmc.

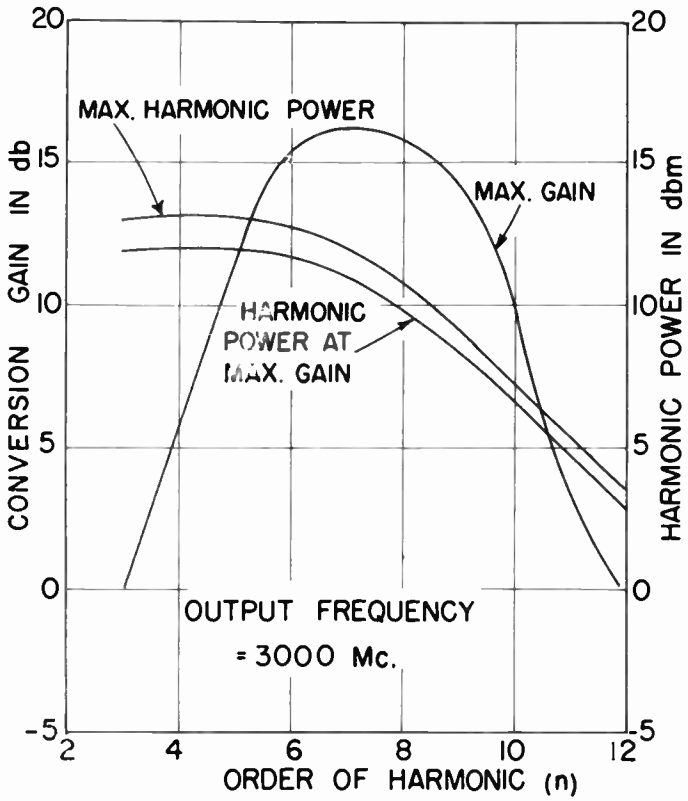

Fig. 6—Maximum harmonic power and conversion gain for various harmonics at fixed output frequency of 3 kmc.

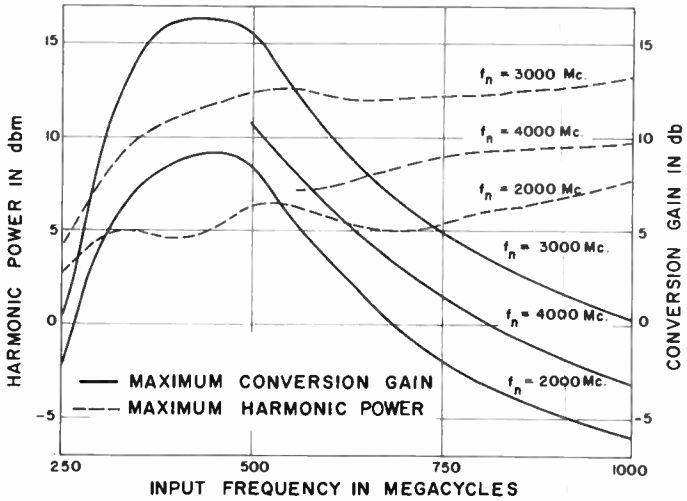

Fig. 7—Maximum harmonic power and maximum conversion gain as a function of input frequency for three different values of harmonic frequency.

shown as functions of the input frequency for three values of output frequency in Fig. 7. These curves indicate the approximate manner in which the gain varies in both the input and output sections. A conversion-gain curve for constant output frequency shows the approximate gain characteristics of the buncher section, while the relative displacement of the conversion-gain curves indicates the variation of gain in the output helix. If the

gain of the output helix were constant, the conversion-gain curve for an output frequency of 2 kmc should be higher than the others. If the gain of the input helix were constant, a single conversion-gain curve should increase as the input frequency increases due to the expected decrease of harmonic current as the order of harmonic increases. The output helix gain is approximately 5 db at the lowest frequency, increasing to about 30 db at the highest frequency, while the variation in the actual buncher gain is about 15 db greater than the variation indicated by the conversion-gain curves. The gains of the two sections are listed for a number of frequencies in Table I, which is discussed later.

TABLE I

n	f_1	f_n	G_0	G_n	G_c	L_n*
2	1000	2000	−16.4	5.0	−11.4	5.2
3	667	2000	−5.0	5.0	0	−0.5
	1000	3000	−16.4	26.5	10.1	−9.9
4	500	2000	3.7	5.0	8.7	0.3
	667	2667	−5.0	22.0	17.0	−8.8
	750	3000	8.0	26.5	18.5	13.5
5	400	2000	10.0	5.0	15.0	−6.2
	500	2500	3.7	19.0	22.7	−7.9
	555	2775	0.4	23.6	24.0	−9.4
	600	3000	−2.0	26.5	24.5	−14.3
	667	3333	−5.0	29.6	24.6	−16.3
6	333	2000	11.0	5.0	16.0	−10.0
	388	2333	10.5	15.8	26.3	−11.0
	445	2670	8.0	22.0	30.0	−11.8
	500	3000	3.7	26.5	30.2	−14.4
	555	3330	0.5	29.6	30.1	−16.5
	600	3600	−2.0	31.0	29.0	−21.0
7	286	2000	10.2	5.0	15.2	−12.4
	333	2333	11.0	15.8	26.8	−16.6
	428	3000	8.5	26.5	35.0	−18.8
	500	3500	3.7	30.4	34.1	−19.9
8	250	2000	5.6	5.0	10.6	−13.0
	333	2666	11.0	22.0	33.0	−20.0
	375	3000	11.0	26.5	37.5	−21.7
9	333	3000	11.0	26.5	37.5	−24.7
10	333	3330	11.0	29.6	40.6	−30.9

By properly selecting the input frequency and varying the current, it was possible to obtain at least 10 mw at any frequency across the 2- to 4-kmc band. By more careful adjustment of the loss on the output helix, which permitted the use of a higher beam current, it was possible to obtain more than 200 mw output at some frequencies, and at least 30 mw for any output frequency.

Some large signal data have been taken, and also data for considerably higher multiplication ratios. The two lower traces in Fig. 8 show typical patterns of the output power vs buncher voltage for buncher operation in the region beyond saturation. The variation of the harmonic power at the synchronous voltage is similar to the behavior of an ordinary twa beyond saturation, where the output power at synchronism decreases and the maximum output occurs at voltages different from synchronism. By using an input frequency as low as 0.1 kmc, total harmonic power on the order of 20 mw has been obtained for harmonics near the fortieth. Essentially saturation power was obtained for an input frequency of 0.1 kmc, with the harmonic amplifier tuned for maximum output at the thirtieth harmonic. Approximately four-tenths of the harmonic power was in the thirtieth harmonic, nearly all the remainder being in the two adjacent harmonics.

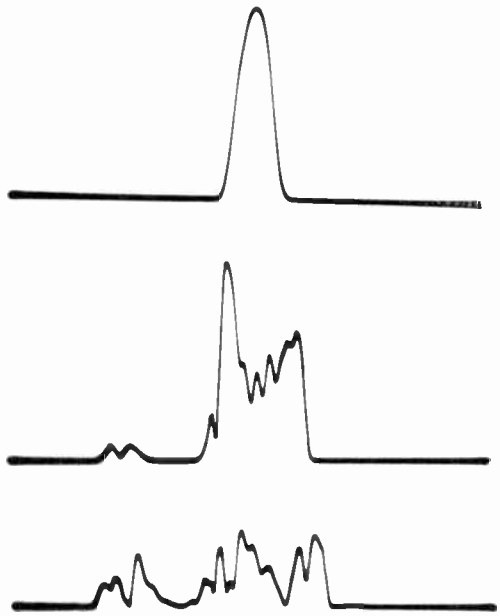

Fig. 8—Oscillograph of harmonic power as helix voltage is swept. The input signal level increases successively from the top trace downward; the top trace represents a moderate input level.

As the buncher length was decreased, the maximum conversion gain of the frequency multiplier decreased as expected, but the maximum harmonic power did not appreciably decrease. Fig. 9 shows the variation with buncher length of the maximum conversion gain and the maximum harmonic power for one particular set of input and output frequencies for the two bunching peaks shown in Fig. 3. For short buncher lengths (small CN) the gain of both bunching peaks is comparable. However, at large buncher lengths, the higher voltage peak predominates. It can be seen that no loss of efficiency results from the use of a short, low-gain buncher section, even though the conversion gain is considerably reduced.

Discussion

As indicated in Fig. 3, there are two widely-separated voltages at which strong interaction results in significant output; in addition, there is a series of lower voltages where greatly reduced output occurs. The peak of output power at the higher voltage occurs at a voltage nearly equal to that for maximum gain when the buncher is operated as an ordinary traveling-wave amplifier, but there is no gain at the lower voltage where a peak of output power is also observed. This is not a large signal or saturation effect; instead it is due

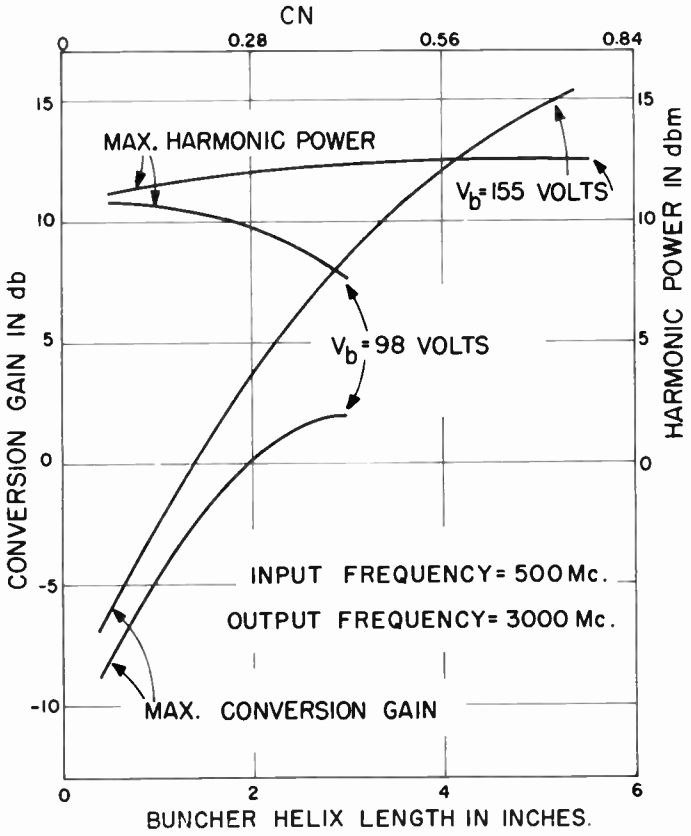

Fig. 9—Variation of maximum conversion gain and maximum harmonic power as a function of buncher length, for the two voltages where peaks of harmonic power occur. Buncher voltages are given where maximum output occurs.

to separate synchronization of the circuit wave with the two space-charge waves under abnormally high space-charge conditions. The higher voltage peak occurs for synchronization of the slow space-charge wave with the circuit wave traveling at very nearly the cold circuit velocity; the lower voltage peak occurs for synchronization between the fast space-charge wave and the circuit wave. As the space-charge factor ω_q/ω increases, the velocity of the circuit wave approaches the cold circuit velocity, and it can be shown that the relative voltage separation of the two peaks will approach $4\,\omega_q/\omega$, where ω_q is the reduced plasma angular frequency, and ω is the modulation angular frequency.[2] This predicted behavior has been adequately verified by experiment. Thus the higher voltage peak occurs for the ordinary traveling-wave amplifier mode of operation, while the lower voltage peak occurs for a mode of operation which produces the Kompfner-dip condition.[3]

In the former mode, which is characterized by the presence of an increasing circuit wave, there is a net transfer of rf power from the beam to the circuit. In the latter mode, the rf power, which is introduced on the circuit at the input, is completely transferred into the beam at the drift length corresponding to the Kompfner-dip length. For greater drift lengths, the rf power is transferred back to the circuit; if the tube is long enough this transferring of power will continue to alternate the power back and forth between the circuit and beam. The existence of the other lower voltage peaks has not been adequately explained, although the bunching is probably due to an interaction of the circuit wave and higher order space-charge waves. Only the amplitudes of the two higher voltage peaks are significant; of these, the fast space-charge wave interaction is relatively unimportant when *CN* is much greater than its value for the Kompfner-dip condition, except under large-signal conditions. The relative amplitudes of the two bunching peaks as a function of the drift length are shown in Fig. 9. No evidence was found of bunching due to either space-harmonic or time-harmonic fields on the buncher helix.

From the gain characteristics of the two separate helices, an estimate has been made of the decrease in gain to be expected as the harmonic number is increased. The values obtained are only approximate because of the effects of the variation in buncher gain, loss, saturation, velocity jump, and space charge. But these approximations can be used to provide an estimate of the behavior which might be expected from a severed-helix frequency multiplier.

In the linear region of operation of an ordinary traveling-wave amplifier, the output power is proportional to the input power, and thus the gain is constant. An expression derived for the small-signal harmonic output power shows that the harmonic power is proportional to the input power raised to an exponent equal to the harmonic number. The gain is therefore not constant, but depends upon the input signal level.

The small-signal conversion gain of a severed-helix twfm can be given by[2]

$$\mathcal{G}_{1n} = \mathcal{G}_0{}^n \mathcal{G}_n \mathcal{L}_n \mathcal{P}_0{}^{n-1} \tag{1}$$

where $\mathcal{G}_{1n}$ is the conversion gain of the twfm, n is the harmonic number, $\mathcal{G}_0$ is the gain of the buncher section, $\mathcal{G}_n$ is the gain of the harmonic amplifier section, $\mathcal{L}_n$ is a frequency conversion factor in units of watts raised to the $1-n$ exponent, and $\mathcal{P}_0$ is the input power in watts, (dimensionally, $\mathcal{L}_n$ and $\mathcal{P}_0{}^{n-1}$ are reciprocal quantities). The power loss resulting from the frequency conversion and also from the method of coupling the power from the input circuit to the output section is described by $\mathcal{L}_n$. Even when both sections are identical and there is no frequency conversion, there is some power loss ($\mathcal{L}_n$ is less than unity). Eq. (1) can be written more conveniently as

$$G_{1n} = nG_0 + G_n + L_n + (n-1)P_0 \tag{2}$$

where G_{1n} is the conversion gain in db, G_0 is the buncher gain in db, G_n is the harmonic amplifier gain in db, L_n is

[2] D. J. Bates, "A Traveling-Wave Frequency Multiplier," Microwave Lab. Rep. No. 381, Stanford Univ.; April, 1957.
[3] R. W. Gould, "A coupled mode description of the backward-wave oscillator and the Kompfner-dip condition," IRE TRANS., vol. ED-2, pp. 37–42; October, 1955.

the numerical value of $\mathfrak{L}_n$ in db, and P_0 is the numerical value of $\mathcal{P}_0$ in db.

Eq. (2) can be rewritten:

$$G_{1n} = L_n^* + G_c \tag{3}$$

where

$$L_n^* = L_n + (n-1)(P_0 + G_0) \tag{4}$$

and G_c is the cascade gain, or the sum of G_0 and G_n.

The actual gain characteristics of the twfm are given in terms of (3). Since the value of L_n^* depends upon the input power level, this level must be specified. The input power level has been chosen as that at which *the conversion gain is maximum*. At this power level, (1) is no longer valid, so that L_n^* is no longer given by (4); instead it is evaluated by the following equation:

$$L_n^* = (G_{1n})_{\max} - G_c. \tag{5}$$

Since $(G_{1n})_{\max}$ and G_c can be found experimentally, L_n^* can be determined.

The values of G_0 and G_n used to evaluate L_n^* were *the measured net gains* of the two traveling-wave amplifier sections. Although the expression for the harmonic amplifier gain could be replaced by $(BCN)_n$ [where the expression for the net gain is given by $(A+BCN)_n$], the actual gain of the harmonic amplifier section operating as a unit of the severed-helix amplifier is probably more nearly G_n. The symbols within the parenthesis are those defined by Pierce.[4]

It was found experimentally that, up to the fourth harmonic, the small-signal harmonic power varied as the input power raised to the exponent n. At harmonics higher than the fourth, there was a region of operation where the exponential variation of harmonic power was observed, but this exponent was less than n; this region should probably not be considered the small-signal region. Thus it can be seen that it is quite important to operate a twfm at large input levels in order to achieve the maximum conversion gain.

Some experimentally determined values of L_n^* are tabulated in Table I. Also shown are the gains of the individual sections of the twfm as well as the total cascade gain. Table I does not include all of the data which were taken and, in particular, does not include any data for an output frequency of 4 kmc because of its inconsistency. (The performance at this frequency was seriously affected by damage to the tube during processing.)

It should be noted that for an input frequency of 1 kmc and a multiplication ratio of two, the conversion-loss factor is greater than unity. This indicates either that the conversion gain of the twfm at the second harmonic is greater than the total cascade gain of the separate sections, or that the cascade gain has been underestimated. Although the former situation could actually exist, the latter is the more likely. In addition to assuming that the gain of the harmonic amplifier is the net gain of this section, as noted above, the gain of the velocity jump has been neglected in the cascade analysis. Therefore, it is probable that in every case the actual conversion-loss factor is less than the computed values of L_n^*.

From Table I it can be seen that the values of L_n^* are not the same for a fixed value of n; this variation is predominantly due to the variation in buncher gain as the input frequency is changed. To evaluate the variation of L_n^* as the harmonic number is increased, it is necessary to compare values of this quantity for a fixed input frequency; this comparison is shown in Table II. It can be noted that the quantity $L_n^* - L_{n-1}^*$ gives the decrease in conversion gain (or increase in conversion loss) as the harmonic number is increased. Thus it can be inferred that there is a minimum conversion loss of approximately 6 db as the harmonic number is increased by unity, although this loss depends upon the buncher gain as well as the effects of the other factors previously mentioned.

TABLE II

n	f_1	f_n	L_n^*	$L_n^* - L_{n-1}^*$
6	333	2000	−10	
7		2333	−16.6	−6.6
6		2667	−20	−3.4
9		3000	−24.7	−4.7
10		3330	−29.2	−4.5
4	500	2000	−2.7	
5		2500	−7.7	−5.0
6		3000	−14.4	−6.7
7		3500	−19.9	−5.5
3	667	2000	−0.5	
4		2667	−8.8	−8.3
5		3330	−16.3	−7.5
2	1000	2000	5.2	
3		3000	−9.9	−15.1

The effects of high space charge in the buncher were appreciable in the experimental twfm. The value of QC, the Pierce space-charge parameter,[3] varied from approximately 0.5 at 0.5 kmc to approximately 10 at 1.0 kmc, although QC was considerably smaller at the lower input frequencies. The high space charge resulted from the use of a small beam on the axis of the relatively large diameter buncher helix. Under low space-charge conditions, the two separate bunching peaks would not be observed. In addition to the unusual buncher characteristics, high space charge can significantly reduce the harmonic current, particularly at the higher harmonics. If optimum performance is desired in a twfm, it is important to have low QC, particularly for large multiplication ratios.

If a high-gain frequency multiplier is desired, or one having very high multiplication ratios, both structures should have high gain. The buncher should, in addition, have low QC and preferably high C. However, if gain

[4] J. R. Pierce, "Traveling-Wave Tubes," D. van Nostrand and Co., New York, N. Y.; 1950.

is not important, and it is desirable to have a frequency multiplier requiring a minimum of adjustment during operation, the buncher should be short ($CN=0.3$, or less).

Operation of a short buncher at large signal levels causes the output to be relatively insensitive to changes in both the buncher voltage and the input signal level. Thus a short buncher makes it possible to obtain nearly optimum output for a number of harmonics by simply changing the voltage of the output helix. In the case of a short buncher, the structure should have a high C, but even moderately high values of QC would be permissible.

Conclusion

The experimental studies show that the traveling-wave frequency multiplier can provide useful output at harmonics as high as the fortieth, and perhaps considerably higher. The saturation power output, even for high harmonics, approximates the power output that can be obtained for the same beam current in a normal traveling-wave amplifier. This indicates that the harmonic current content of the bunched beam at the buncher exit can be very high. The low efficiency commonly associated with a klystron frequency multiplier is not characteristic of the twfm.

A detailed quantitative investigation of the behavior of the traveling-wave frequency multiplier was not attempted.

Acknowledgment

The authors wish to thank Dr. L. A. Roberts of Huggins Laboratories for help in providing parts for the tube, and T. Wessel-Berg and Drs. Roberts, D. A. Dunn, H. Heffner, and M. Chodorow for helpful discussions.

Very Narrow Base Diode*

R. H. REDIKER†, ASSOCIATE MEMBER, IRE, AND D. E. SAWYER†, MEMBER IRE

Summary—**Techniques have been developed to fabricate semiconductor diodes with rectifying junction to ohmic contact distances of the order of microns. The current-voltage relationship of such a diode is a function of the degree of imperfection of the ohmic contact. If it were possible to make ideal ohmic contacts, the diode would exhibit extremely poor rectification. The rectification ratio of germanium diodes for practical ohmic contacts, however, is of the order of 10^5 to 10^6. The current-voltage relationship, the small-signal frequency response, and the switching characteristics of the very narrow base diode are analyzed using the appropriate boundary condition at the ohmic contact. The alloy junction current-voltage characteristics follow very closely the $(e^{qV/\alpha kT}-1)$ relationship with values of α between 1.02 and the theoretical value 1.00. Because of the narrow base width, the series bulk resistance for typical designs is between 0.3 and 3 ohms. Thus the entire range of forward currents can be obtained at low forward voltages. The diode is a high-frequency device both for small-signal applications and for switching applications, although the ultimate high-frequency capability is reduced because of the imperfection of the ohmic contact. In switching applications, the reverse recovery time may be limited as much by junction capacitance as by hole storage. A method of fabrication is described and small-signal applications at uhf are discussed. A computer diode design that switches at speeds up to 5 mc is described. This diode has the advantageous combination of low forward-voltage drop and high-frequency capability.**

I. Introduction

THE very narrow base germanium diodes with which this paper is concerned have base widths from 1 micron to 10 microns. The electrical characteristics of these diodes, which cannot be duplicated in any other presently available type of diode, are desirable in both computer and small-signal applications. A cross-sectional view of a typical narrow base diode is shown in Fig. 1. The diameter, d, of the active area of

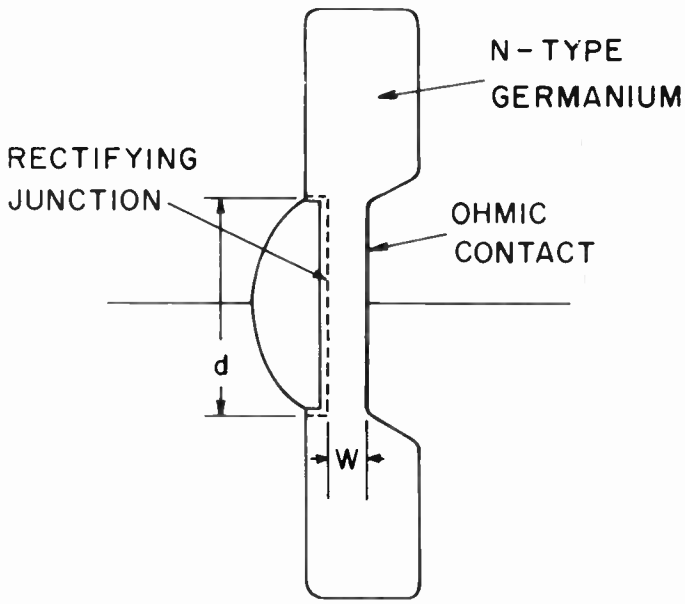

Fig. 1—Cross section of a very narrow base diode (not to scale).

the diodes may vary from 0.005 cm to more than 0.15 cm. For diodes in which d is larger than 0.030 cm, the rectifying junction is an indium alloy junction while

* Original manuscript received by the IRE, February 18, 1957. The research reported here was supported jointly by the U. S. Army, Navy, and Air Force under contract with Mass. Inst. Tech.

† Lincoln Lab., M.I.T., Lexington, Mass.

junctions of 0.005 cm diameter are made by bonding a gallium-gold wire.

Successful operation of very narrow base diodes is possible only because ohmic contacts are not ideal. The technique of fabricating ohmic contacts that have a given degree of imperfection and the technique of selective controlled etching the depression opposite the rectifying junction are described in Section V.

The advantageous combination of low forward-voltage drop and high-frequency capability makes this diode useful in many computer circuits. High-speed operation (switching rates above 1 mc and possibly above 10 mc) is a result of the small spacing between the rectifying junction and ohmic contact which minimizes hole-storage effects. Also, because of the narrow base width, the series bulk resistance of the diode is small. For the computer diode whose specifications are given in Section VI, the bulk resistance is less than 3 ohms and for special applications resistances below 0.05 ohm should be possible. Because of the low series bulk resistance, at forward currents up to several milliamperes most of the voltage applied to the diode appears across the rectifying junction. The diode current is related to the junction voltage, V_j, by the equation $I=I_0(e^{qV_j/akT}-1)$ where for the very narrow base alloy diode the value of a has varied between 1.02 and the theoretical value of unity. For conventional gold-bonded or point-contact junctions, the value of a is considerably larger than unity and for a given ratio of forward current to saturation current, the forward voltage for the very narrow base diode is significantly smaller than that for these conventional types of switching diodes. Thus for the very narrow base alloy diode, the entire range of forward currents can be obtained at low forward voltages. In the subsequent analysis, the quantity a, which for the narrow base alloy diode is close to unity, is omitted.

Because of the very small value possible for the product of the series bulk resistance and junction transition layer capacitance, the very narrow base diode can be used at reverse biases as a variable capacitor with calculated Q above 100 at 10^9 cps. The diffusion capacitance, which limits the frequency of operation in forward bias, is also small because of the very narrow base width. Very narrow base diodes, which have been fabricated with gold-bonded rectifying junctions to reduce capacitance, may have application as uhf mixers. Because the junction diameter of these diodes is about 25 times the base width, the planar junction theory developed in this paper should still apply.

When the reverse bias is increased so that the space-charge region punches through to the ohmic contact, the diode exhibits a low dynamic impedance. Switching time between the low-impedance punch-through region and the high-impedance reverse-bias region is capacitance limited and can be reduced below 10 millimicroseconds. Operation of the very narrow base diode in the punch-through region will not be described in this paper.

In this paper, the operation of the diode in the low-impedance forward and high-impedance reverse states will be investigated. The current-voltage relationship, the small-signal frequency response, and the switching characteristics will be analyzed. A method of fabrication will be described, and several applications of the diode will be discussed. In the analysis which follows, the base region has been assumed to be n-type, the minority carriers holes. The results can be applied to diodes with p-type base regions by a suitable change in notation. The analysis should be applicable to semiconductor diodes in general, in addition to the germanium diodes that have been fabricated.

II. Current-Voltage Relationship

A. The Planar Junction Current-Voltage Relationship

The operation of narrow base diodes is very sensitive to the properties of the ohmic contact. The ohmic contact may be characterized by the ratio, s, of the current density to the change in the charge density of minority carriers at the contact,

$$s=\frac{J}{q(p-p_n)}. \tag{1}$$

All symbols are defined at the end of this paper. The quantity s is the contact generation velocity and is analogous to the surface recombination velocity. An ohmic contact at which there is no change in carrier densities irrespective of the current will be denoted as an ideal ohmic contact. An ideal ohmic contact has an s value of infinity.

If one neglects the leakage resistance that shunts the junction, but includes the deviation from ideal behavior of the ohmic contact, the current in a planar junction diode can be determined from the diffusion equation and is given by

$$\frac{I}{A}=\frac{qDp_n}{L}\,\frac{D\sinh\frac{w}{L}+sL\cosh\frac{w}{L}}{D\cosh\frac{w}{L}+sL\sinh\frac{w}{L}}\,(e^{qV_j/kT}-1). \tag{2}$$

The minority carrier current in the heavily doped recrystallized "emitter" region is justifiably neglected in (2). For narrow base diodes where $w\ll L$, (2) reduces to

$$\frac{I}{A}=\frac{qDp_n}{w}\,\frac{1}{1+\frac{D}{sw}}\,(e^{qV_j/kT}-1), \tag{3}$$

or rearranging terms

$$\frac{I}{A}=qp_ns\,\frac{1}{1+\frac{sw}{D}}\,(e^{qV_j/kT}-1). \tag{3a}$$

For $L\gg w\gg D/s$, the term

$$\left(1+\frac{D}{sw}\right)^{-1}$$

in (3) is close to unity and the saturation current is an inverse function of the effective base width w. As the

diode reverse voltage is increased and the space-charge region becomes larger, the effective base width decreases and the reverse current increases and does not saturate. For this case, all the minority carriers generated at the ohmic contact are not collected at the rectifying junction at low reverse voltages, but as the voltage is increased and the effective base width becomes narrower, more and more of the carriers are collected.

If, on the other hand, $w \ll D/s$, the fraction in (3a) is close to unity, the reverse current is independent of w and does saturate. In this case, all the generated carriers at the ohmic contact are collected; there are no further carriers to collect irrespective of base width. If we take the value of s to be 5×10^4 cm/second, the quantity D/s for an n-type germanium base layer is 8.8×10^{-4} cm. The computer diode described in Section VI has a design base thickness of about 0.8×10^{-3} cm. For this diode, the fraction in (3a) varies from 0.52 to 1.00, as the reverse voltage is increased from zero volts towards punch through, and w decreases from 10^{-3} cm towards zero. This increase in saturation current by 92 per cent in 20 volts is perfectly consistent with back impedances about 1 megohm. If, on the other hand, the ohmic contact were ideal ($s=\infty$), the fraction in (3) would be unity, and the "saturation" current would vary as the reciprocal of the effective base width increasing from its low voltage value to infinity as the reverse voltage was increased. For this case, the reverse impedance of the very narrow base diode would be too low for it to have any practical application. Thus, the very narrow base diode is feasible only because ohmic contacts are not ideal. The value of s of 5×10^4 cm/second used above was determined by substituting the experimental value of the saturation current for various computer-type diodes into (3a).

B. Ohmic Bulk Resistance

The voltage across the diode is the sum of the junction voltage and the ohmic voltage drop across the bulk material. For a narrow base diode in forward bias, the bulk resistance to minority carriers determines the ohmic voltage drop. This bulk resistance can be ascertained from solution of the diffusion equations with appropriate boundary conditions and is given at low level injection by[1,2]

$$R = \left(\frac{\rho_0 w}{A}\right) b. \tag{4}$$

This resistance is the resistance which would be expected for majority carrier flow multiplied by b, the ratio of majority to minority carrier mobilities. The base width w which appears in (4) can be related by use of Poisson's equation to the resistivity and the punch-through voltage and is[3]

$$w = (2\mu_n\epsilon)^{1/2}(V_p\rho_0)^{1/2}. \tag{5}$$

For n-type germanium, in the system of units volts, ohms, and centimeters, $(2\mu_n\epsilon)^{1/2}=1.01\times10^{-4}$. Narrow base computer diodes designed to meet the specifications discussed in Section VI have had bulk resistances at low-injection level below 3 ohms, while other diodes that have been fabricated with lower resistivity germanium have had bulk resistances calculated from (4) of less than 0.05 ohm.

Eq. (4) gives the series bulk resistance at low-injection level. At large forward currents where the density of injected carriers is comparable to the net donor density in the base region, conductivity modulation reduces this bulk resistance even further. Because of its narrow base width, however, the narrow base diode requires a relatively small amount of carrier injection to produce the concentration gradient necessary for forward current flow. The ratio of the injected hole density in the base region to the current density is

$$\frac{p-p_n}{J} = \frac{1+\dfrac{sx}{D}}{qs} \tag{6}$$

where x is the distance from the ohmic contact. The other quantities are defined at the end of this paper. At 1 ma forward current, the maximum injected hole density for the computer diode of Section VI is less than $\frac{1}{5}$ the donor density. Thus for this diode, low level injection theory applies at forward currents of this magnitude.

It should be kept in mind that (4) gives the series bulk resistance to *minority* carrier current. Although this is the bulk resistance when the junction is forward biased, when the junction is reverse biased the series bulk resistance that becomes important at high frequency is the resistance to the majority carriers which cross the base region to charge the transition-region capacitance. For majority carriers, the bulk resistance is given by

$$R = \frac{\rho_0 w}{A}, \tag{7}$$

the conventional resistance-resistivity relationship for planar geometry.

III. Small-Signal Frequency Response

A. Junction Transition-Region Capacitance

The junction transition-region capacitance per unit area for an abrupt alloy planar junction is given by

[1] The derivation of (4) is included in Lincoln Lab. Tech. Rep. 137 (unpublished). This technical report also includes more complete design theory than reported here for narrow base diodes which meet different electrical specifications and more detailed information on diode manufacture.

[2] In this paper the base region is considered sufficiently doped so only the majority carriers need be taken into account in the calculation of the resistivity; *i.e.*, $\rho_0 = q\mu_n N_D$.

[3] Eq. (5) is derived with the assumption that the width of the space-charge region is much larger than the Debye length; *i.e.*, the space-charge region is completely depleted of mobile charge carriers.

$$\frac{C_T}{A} = \left[\frac{\epsilon}{2\mu_n \rho_0 (\overline{V}_j + V_0)}\right]^{1/2}. \tag{8}$$

$\overline{V}_j$ is the voltage applied to the junction and is considered positive in reverse bias, *i.e.*, $\overline{V}_j \equiv -V_j$. Eq. (8) has been derived with the assumption that the space-charge region is completely depleted of mobile charge carriers. If this assumption were valid, V_0 would have been equal in value to the internal contact potential of the junction. Although this assumption is not strictly correct, (8) may still be used if V_0 is considered for any given diode a "constant" of the equation.[4,5] In the derivation of (8) the resistivity of the recrystallized region has been assumed to be much smaller than that of the base region.

The equivalent circuit of a diode in its high-impedance state is shown in Fig. 2. This circuit is applicable from very low frequencies to ultra-high frequencies. Two quantities which may establish the upper-frequency limit of this circuit are the dielectric relaxation time $\epsilon\rho_0$ of the semiconductor and the diode lead inductance. The dielectric relaxation time is 1.4×10^{-12} seconds for 1 ohm-cm germanium and by proper packaging the diode lead inductance can be reduced so that it may be neglected at frequencies below 500 mc.

The product of the series bulk resistance and the junction capacitance is independent of the junction area. Combining (5), (7), and (8), this product is

$$RC_T = \epsilon\rho_0 \frac{V_p^{1/2} - \overline{V}_j^{1/2}}{(V_0 + \overline{V}_j)^{1/2}} \tag{9}$$

where the reduction of the effective base width by the junction transition layer has been included. The dielectric constant ϵ for germanium is 1.41×10^{-12} coulombs per volt-cm.

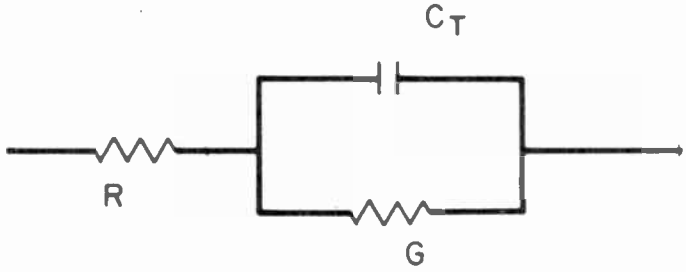

Fig. 2—Equivalent circuit of a diode in its high impedance state. G is the junction conductance and R is the series bulk resistance. C_T is the transition layer capacitance.

On the basis of (10), a diode that is fabricated from 0.5 ohm-cm material with a punch-through voltage of 15 volts and is operated about a reverse bias of 10 volts should have a Q larger than 4000 at 100 mc and larger than 800 at 500 mc. If lower resistivity material were used, even higher Q's should be obtainable. While for diodes fabricated to date the series resistance to *minority* carriers has been explained by (4), the series resistance to *majority* carriers at uhf has been higher than that calculated from (7). Hence, values of Q as high as predicted by (10) have not been obtained.

The additional series resistance has been attributed to the "ohmic" contact and work is in progress to improve this contact.

B. Junction Diffusion Capacitance

When a diode is operated in forward bias or at very low reverse bias, the diffusion capacitance cannot be ignored. If one neglects the transition-region capacitance and the junction leakage resistance, the small signal response of a planar junction can be determined from the diffusion equation and is given by

$$\frac{i}{A} = \frac{q\mu_p p_n e^{qV_j/kT}}{L}(1+j\omega\tau)^{1/2}\left[\frac{D(1+j\omega\tau)^{1/2}\sinh\frac{w}{L}(1+j\omega\tau)^{1/2} + sL\cosh\frac{w}{L}(1+j\omega\tau)^{1/2}}{D(1+j\omega\tau)^{1/2}\cosh\frac{w}{L}(1+j\omega\tau)^{1/2} + sL\sinh\frac{w}{L}(1+j\omega\tau)^{1/2}}\right] v_j e^{j\omega t}. \tag{11}$$

A diode operated in reverse bias can be used as a variable capacitor[6] (see Section VI). A figure of merit for this circuit element is the ratio of series reactance to series resistance. At high frequencies, where the shunt conductance (see Fig. 2) can be neglected, this ratio is

$$Q = \frac{1}{2\pi f R C_T} = \frac{1}{2\pi f \epsilon\rho_0}\frac{(\overline{V}_j + V_0)^{1/2}}{(V_p^{1/2} - \overline{V}_j^{1/2})}. \tag{10}$$

The imaginary part of the quantity multiplying the small-signal voltage on the right-hand side of (11) is the susceptance of the diffusion capacitance.

For narrow base diodes where $w \ll L$ and for frequencies where $\omega \ll (D/w^2)$, (11) reduces to

$$\frac{i}{A} = qp_n s e^{qV_j/kT}\frac{1}{1+\frac{sw}{D}}\left[1 + j\omega\frac{w}{s}\left(1+\frac{1}{3}\frac{\frac{s^2w^2}{D^2}}{1+\frac{sw}{D}}\right)\right]\frac{qv_j}{kT}e^{j\omega t}. \tag{12}$$

[4] D. R. Muss, "Capacitance measurements on alloyed indium-germanium junction diodes," *J. Appl. Phys.*, vol. 26, pp. 1514–1517; December, 1955.

[5] R. F. Schwarz and J. F. Walsh, "The properties of metal to semiconductor contacts," PROC. IRE, vol. 41, pp. 1715–1720; December, 1953.

[6] L. J. Giacoletto and J. O'Connell, "A variable-capacitance germanium junction diode for uhf," *RCA Rev.*, vol. 17, pp. 68–85; March, 1956.

At forward voltages above several kT/q the small-signal current can be expressed in terms of the direct current I by combining (3) and (12)

$$i = \frac{qI}{kT} v_j e^{j\omega t} \left[1 + j\omega \frac{w}{s} \left(1 + \frac{1}{3} \frac{\frac{s^2 w^2}{D^2}}{1 + \frac{sw}{D}} \right) \right]. \quad (12a)$$

In Fig. 3, the real and imaginary parts of the small-signal admittance $Y = i/v_j$ are plotted as a function of frequency for a diode with a 2-micron base width. The theoretical conductance and susceptance as determined from (11) are compared with the values obtained from the low-frequency approximation (12). As indicated in Fig. 3 for frequencies where the susceptance is less than the conductance, (12) can be used in place of (11).

If the ohmic contact were ideal ($s = \infty$), the reactive term in the parentheses in the right-hand side of (12) would be $j\omega(w^2/3D)$. For the narrow base diodes where $(sw/D)^2 \ll 1$, this term is $j\omega(w/s)$. Because of the imperfection of the ohmic contact, the diffusion capacitance determined by this reactive term is increased by the quantity $3D/sw$. As shown in Fig. 3, the frequency where the susceptance of a diode with a 2-micron base width is equal to its conductance is increased by a factor of four, when the s of the ohmic contact is increased by this same factor from 50,000 cm/second to 200,000 cm/second. Work is underway to further increase the value of s of the ohmic contact. However, if high reverse resistance is desirable, the value of s must not be increased to the point where $(sw/D) \gg 1$, because then as described in Section II, the diode back current will no longer saturate.

The small-signal admittance of the junction diode varies exponentially with the junction voltage V_j [see (11) or (12)]. At forward voltages where V_j is much larger than kT/q the capacitance associated with this admittance is much larger than the transition-layer capacitance discussed in Part A of this section. As V_j is reduced to zero, the diffusion capacitance decreases exponentially, and for reverse biases where V_j is again much larger in magnitude than kT/q, the diffusion capacitance is completely negligible. Because the diodes have such narrow base regions, the diffusion capacitance is usually small when compared to the transition-layer capacitance for all reverse biases down to kT/q.

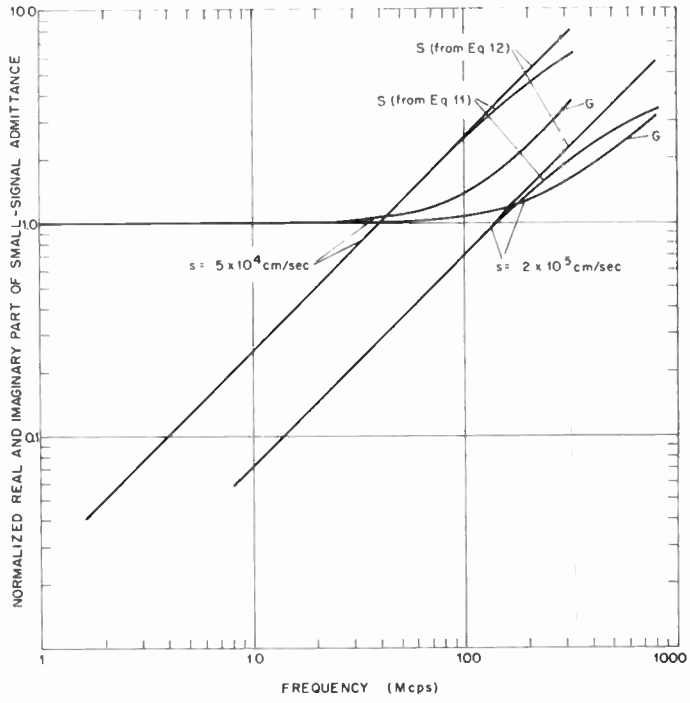

Fig. 3—The theoretical real and imaginary parts of the small-signal admittance of a narrow base diode with a 2-micron base width for two different values of ohmic contact generation velocity. The imaginary part of the admittance as determined from the approximation (12), is compared with that determined from the exact equation (11).

IV. Switching Speed for Computer Diodes

A. Effect of Hole Storage on Reverse Recovery Time

The switching speed of the narrow base diode is established by the time it takes to switch the diode from the forward low-impedance state to the reverse high-impedance state. Before the diode will exhibit the high impedance normally associated with its reverse bias state, the minority carriers (which we will assume are holes) stored in the diode when it is in the forward low-impedance state must be removed.

For a diode with an ideal ohmic contact, Lax and Neustadter[7] and Kingston[8] have shown that the hole-storage switching time is a decreasing function of the ratio of the maximum reverse current to the forward current the diode was conducting. This maximum reverse current is the applied reverse voltage divided by the loop impedance. The loop impedance includes the diode ohmic bulk resistance. As is seen from Fig. 4, which is adapted from Kingston, the switching time due to hole storage for the narrow base planar diode varies from 1.9 (w^2/D) to 3×10^{-3} (w^2/D) as I_r/I_f varies from 10^{-2} to 10^2.

B. Figure of Merit for Hole Storage

Although the hole-storage switching time varies with the circuit used, the ratio of the forward current to the charge of the holes stored during forward conduction depends only on the physical parameters of the diode. For a narrow base planar diode with an ideal ohmic con-

[7] B. Lax and S. F. Neustadter, "Transient response of p-n junction," *J. Appl. Phys.*, vol. 25, pp. 1148–1154; September, 1954.
[8] R. H. Kingston, "Switching time in junction diodes and junction transistors," Proc. IRE, vol. 42, pp. 829–834; May, 1954.

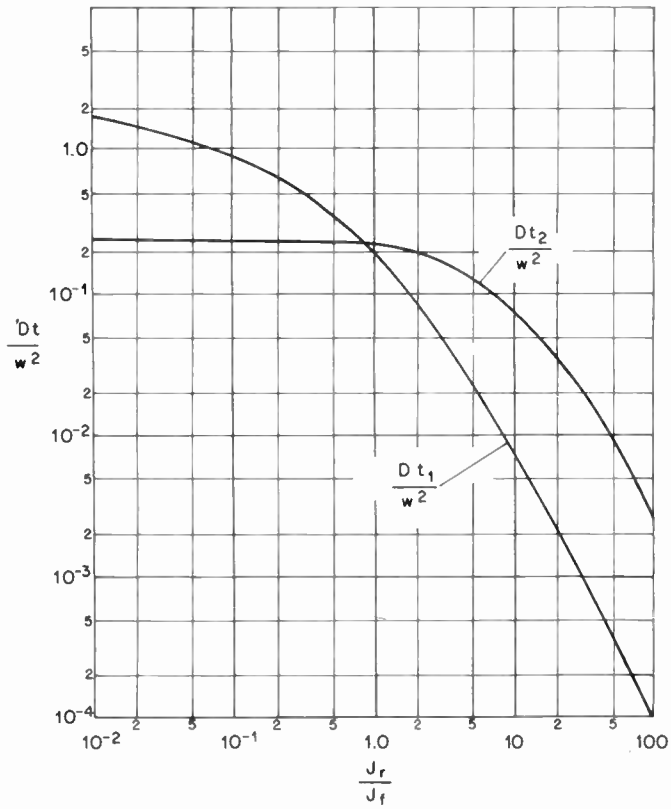

Fig. 4—Hole-storage switching time for the narrow base diode. t_1 is the duration of constant current phase and t_1+t_2 is the total switching time required for the junction voltage to reach 90 per cent of the applied reverse voltage.

tact, such as was considered by Kingston, the figure of merit is given by

$$I_f/Q_h = 2D/w^2. \tag{13}$$

Thus, the figure of merit is related to the reciprocal of the switching time.

If one includes the deviation from ideal behavior of the ohmic contact, the figure of merit for a planar alloy diode is given by

$$\frac{I_f}{Q_h} = \frac{1}{\tau}\,\frac{\sinh\frac{w}{L}+\frac{sL}{D}\cosh\frac{w}{L}}{\sinh\frac{w}{L}+\frac{sL}{D}\left(\cosh\frac{w}{L}-1\right)}. \tag{14}$$

For the narrow base diode, with $w \ll L$, (14) reduces to

$$\frac{I_f}{Q_h} = \frac{2D}{w^2}\,\frac{1}{1+\frac{2D}{sw}} \tag{15}$$

which for an ideal ohmic contact ($s=\infty$) reduces to (13). For limiting small base widths, $w \ll D/s$, the figure of merit becomes

$$\frac{I_f}{Q_h} = \frac{s}{w}. \tag{16}$$

The computer diode whose specifications are discussed in Section VI has been designed with a base width of 10^{-3} cm. The figure of merit for the hole storage for this diode calculated from (15) is 3.2×10^{-7} second. In this calculation, the s value of 50,000 cm/second which was experimentally determined from the current-voltage relationship was used.

C. Effect of Junction Capacitance on Reverse Recovery Time

Very narrow base diodes have been fabricated for which in normal switching operation the reverse recovery time is caused by junction transition-layer capacitance rather than hole storage. This has been shown experimentally by varying the forward current through the diode while the initial reverse current and the reverse bias voltage were kept constant. The switching time was found to be insensitive to the forward current except for unusually large values of the ratio of forward current to initial reverse current. As indicated by Fig. 4, if the switching time were due primarily to hole storage, it would have been a rapidly varying function of the forward current. The very narrow base diode is to our knowledge the first alloy diode where junction capacitance rather than hole storage may limit the switching speed for diode currents which are normally encountered in computer service.

For optimum design of the narrow base diode for fast-switching applications, the effects of both junction capacitance and hole storage must be minimized. As a first step in the design of this diode, we have attempted to minimize the sum of the charge of the holes stored during forward conduction (hole storage) and the charge in the space-charge region during reverse bias (the change in this charge with voltage is the junction capacitance).

The charge in the space-charge layer of an alloy junction with reverse bias $\overline{V}_j$ can be determined from Poisson's equation and is

$$Q_{sc} = A\left(\frac{2\epsilon\overline{V}_j}{\mu_n\rho_0}\right)^{1/2}. \tag{17}$$

The charge of the stored holes which are necessary to produce a forward current I_f for a narrow base diode is from (15)

$$Q_h = I_f\,\frac{w^2}{2D}\left(1+\frac{2D}{sw}\right). \tag{15a}$$

If we use (5) to express the base width in terms of the base resistivity and the punch-through voltage, (15a) becomes

$$Q_h = I\left[\frac{\mu_n\epsilon}{D}\,V_p\rho_0+\left(\frac{2\mu_n\epsilon}{s^2}\,V_p\rho_0\right)^{1/2}\right]. \tag{18}$$

If the operating voltage V_j and the punch-through voltage V_p (which can be considered the maximum voltage) are kept constant, as the resistivity is increased, the base width and Q_h increase, but the junction capacitance and Q_{sc} decrease. There is an optimum resistivity for which the sum of Q_h and Q_{sc} is a minimum.

In a typical computer application the reverse voltage applied to the diode may be 10 volts. If the punch-through voltage for a diode with an n-type base region is 20 volts and $s=5\times10^4$ cm/second, the resistivity for which the sum of Q_h and Q_{sc} is a minimum is the real root of the equation

$$\rho_0^{3/2} + 1.95\rho_0 - 19.5\frac{A}{I_f} = 0, \tag{19}$$

where I_f/A is in amperes per cm^2. For $I_f/A=1$ amp/cm^2, the optimum resistivity is 4.7 ohm-cm with a corresponding base width of 9.7×10^{-4} cm, while for $I_f/A=10$ amps/cm^2 the optimum resistivity is 0.69 ohm-cm with a corresponding base width of 3.7×10^{-4} cm. For these cases the charge stored in the space-charge region is larger than the charge of the holes stored during forward conduction: for the first $Q_h/Q_{sc}=0.72$ and for the second $Q_h/Q_{sc}=0.86$.

D. Forward Switching Transient

When a diode is switched from reverse bias to forward bias, the hole distribution in the base region associated with the equilibrium forward current must be reestablished. The effect on the switching transient of the storing of these holes depends on the forward current to which the diode is being switched.

If the forward current is small enough so that the junction resistance is large compared with the ohmic bulk resistance, the transient will be determined by the junction. In the approximation of (12) the junction is represented by a parallel RC network, the hole storage charge being approximated by the charge on the capacitor. The RC product for the computer diode described in Section VI is 2.4×10^{-8} seconds. Although (12) is not valid for frequencies above 1/RC, the RC product is an indication of the transient response time. For very narrow base diodes in normal computer service, the forward switching transient is due to the junction impedance. In most computer applications, the effects of this forward switching transient are much less important than the effects of the reverse transient.

At large forward currents where the ohmic bulk resistance is large compared with the junction resistance, a transient may occur because of changes in the bulk resistance. These changes will occur if the hole storage is large enough to modulate the bulk conductivity, in which case the bulk resistance of the diode is initially higher than its steady state value. The figure of merit for hole storage given in (15) can be used as a figure of merit for this forward switching transient. In this case, the reciprocal of this figure of merit is the time it takes the forward current to establish the stored minority carrier charge and modulate the bulk conductivity. For any switching source with internal resistance the diode voltage decreases with time during the conductivity modulation transient. On the other hand, for the same source if the transient is determined by junction impedance, the diode voltage increases with time during the transient.

Because of its small base width, the narrow base diode has low ohmic base resistance and in addition can carry currents of the order of milliamperes at low injection levels. Hence, the conductivity modulation transient, while common in many commercially available diodes, is negligible for the narrow base diode.

V. A Fabrication Technique

Controlled selective bath etching has proved to be a successful technique in the fabrication of very narrow base diodes.[9] The diodes are prepared by alloying an indium button into n-type germanium by conventional means. Simultaneously with the alloying, an antimony-gold plated kovar ring is bonded to the germanium to be used as an auxiliary ohmic contact during further fabrication. If smaller area rectifying contacts are desired, a gold-gallium bonded contact is used instead of the indium alloy contact. After the rectifying contact is "cleaned up" by conventional methods, the diode is inserted into the bath etcher as shown in Fig. 5. A plastic washer, coated with a silicone compound, protrudes below the bottom of the bath, and makes a watertight seal to the top surface of the germanium die. This seal prevents the bath electrolyte from reaching the kovar base tab, and is necessary for successful bath etching. When the diode is removed from the etcher, the silicone compound is removed from the germanium die. An electrolyte that has been used successfully in bath etching is an aqueous solution of 7.4 grams per liter indium trichloride and 2.1 grams per liter hydrochloric acid. Bath agitation is provided by feeding electrolyte at low pressure through a jet above the germanium surface.

When the switch of Fig. 5 is in position E, a depression is etched into the germanium opposite the indium button. The electrolyte is biased negative by a voltage source with respect to the germanium while the alloyed button is forward biased by the current source composed of R_1 and V_f. During etching the terminal characteristics of the bath assembly resemble those of a p-n-p transistor.[10,11] The alloyed button current may be designated the "emitter" current; the electrolyte current, the "col-

[9] Another technique to fabricate very narrow base diodes has been described by R. H. Rediker and J. Halpern, "Outdiffused junction diode," Second Annual Meeting of the PGED of the IRE; October, 1956.

[10] C. G. B. Garrett and W. H. Brattain, "Self-powered semiconductor amplifier," *Phys. Rev.*, vol. 95, pp. 1091–1092; August, 1954.

[11] W. H. Brattain and C. G. B. Garrett, "Experiments on the interface between germanium and an electrolyte," *Bell Sys. Tech. J.*, vol. 34, pp. 129–176; January, 1955.

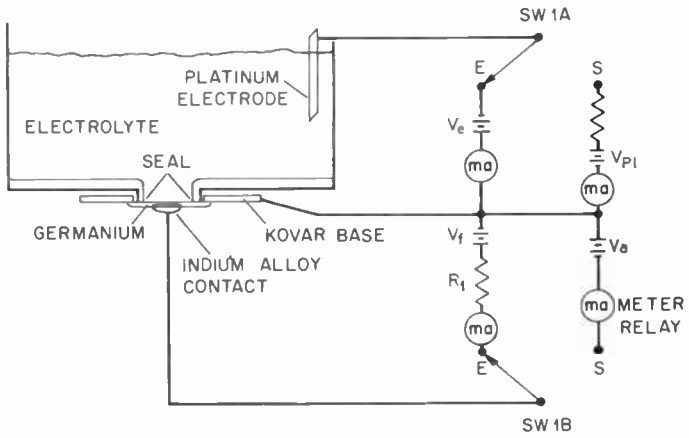

Fig. 5—Controlled selective bath etching. When switch is in position *E*, a depression is being etched into the germanium opposite the forward biased indium button. When switch is in position *S*, the indium button is reverse biased, a plate is being deposited on germanium, and the width of base layer opposite the button is being sensed. The switch alternately contacts the *E* and *S* positions.

lector" current; and the current through the kovar base, the base current. Collector current saturation slopes in the megohm range are obtained. It is found, as reported in the literature,[12] that the magnitude of the saturation current is in good agreement with that calculated from the area of germanium exposed to the bath electrolyte and the thermal generation rate of holes from the *n*-type base. The α of the bath assembly for collector voltages above that required for collector current saturation is larger than unity. Of course, α's smaller than unity can be obtained by reducing the collector voltage. The collector resistance in the so-called voltage saturation range is usually about 750 ohms.

Etching of the *n*-type germanium is limited by the flow of holes which are injected at the alloy rectifying contact. These holes diffuse across the *n*-type base and participate in the etching process at the germanium-electrolyte interface opposite the alloy junction. In addition to localizing the etched depression opposite the alloy junction, it is possible in bath etching to vary the distribution of the injected holes and hence the radius of curvature of the etched depression. For collector voltages which are large enough so that α is larger than unity, the direction of base-current flow is *into* the base contact. For this case a voltage drop occurs laterally in the base beneath the fusion area. The polarity of this voltage is such as to produce greater hole injection near the center of the emitter area than at the emitter periphery. As etching continues, the base becomes progressively thinner, and for a given constant emitter current the etching localizes even more at the center of the fusion. On the other hand, for collector voltages for which α is smaller than unity, the base-current flow is *out* of the base contact. The lateral base voltage now tends to bias off the central region of the emitter so that etching should occur at a faster rate at the periphery than at the center. The curvature of the etched depression expected from the above considerations is decreased somewhat because while the hole injection is reduced where the base region is more positive, the electrolyte-germanium voltage is increased. The etching rate however, is much more sensitive to hole injection than to the electrolyte-germanium voltage. Controlled selective bath etching, which incorporates hole injection into *n*-type germanium, not only yields well delineated etched surfaces of controlled curvature but also minimizes surface pitting. Unless a source of holes is provided by such means as injection or optical generation electrolytic methods of etching *n*-type germanium at any practical rate of germanium removal usually lead to excessive surface pitting.

In order to produce very narrow base diodes, the etching must be stopped when a predetermined base thickness remains opposite the alloy junction. When the switch in Fig. 5 is in position *S*, the thickness of the *n*-type germanium region remaining between the *p*-type recrystallized region under the alloy button and the surface of the depression is being sensed. The electrolyte is biased positive with respect to the germanium so that indium is plated onto the germanium surface. Also, a reverse voltage V_a is applied across the indium alloy junction. This voltage creates a space-charge region that penetrates from the alloy junction a distance w into the base. Using Poisson's equation, the equation which relates w to the base resistivity ρ_0 in ohm-cm and V_a in volts can be derived.[3]

$$w = 1.01 \times 10^{-4}\sqrt{V_a \rho_0} \text{ cm.} \tag{5a}$$

When etching has proceeded so that the space-charge region of the reverse biased diode reaches the *p*-type inversion layer under the plate being deposited, the reverse current of the diode increases. This increase in current operates a relay and stops further etching. By adjusting the sensing voltage V_a and the germanium resistivity, widths as low as a micron can be sensed.

Figs. 6 and 7 are metallographic sections of two bath-etched devices made with 5 ohm-cm *n*-type germanium. In Fig. 6, the alloy junction diameter is 0.030 inch and the *n*-type base thickness is approximately 5 microns and is quite flat. The rectifying junction of the diode whose section is shown in Fig. 7 was made by gold bonding a 0.002-inch-diameter gold-gallium wire to a germanium blank. The minimum base thickness of this diode is approximately 2 microns.

After the diode is bath etched, ohmic contact must be made to the thin base region. In order to maintain the base-width control inherent in bath etching, the penetration of the ohmic contact into the base region must be kept to a minimum. Ohmic contacts have been made by plating, by evaporation, by alloying, and by soldering. One successful method of making the ohmic contact to computer-type narrow base diodes is to plate a gold-antimony contact on the germanium surface

[12] A. Uhlir, Jr., "Electrolytic shaping of germanium and silicon," *Bell Sys. Tech. J.*, vol. 35, pp. 333–347; March, 1956.

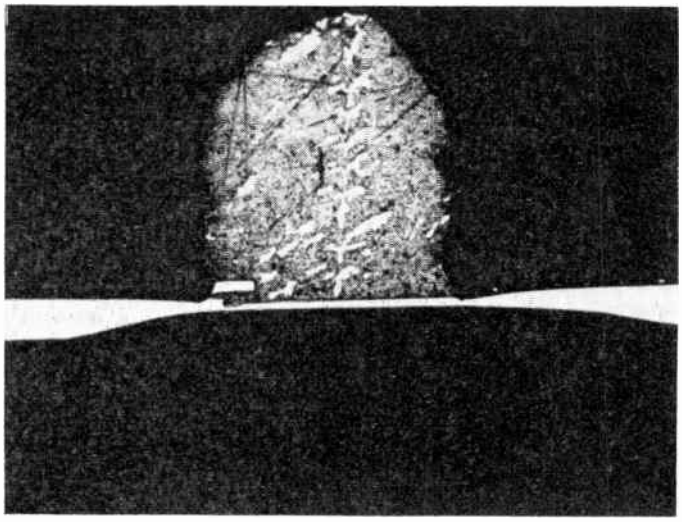

Fig. 6—Photomicrograph of the cross section of a bath-etched device. The alloy junction diameter is 0.030 inch and the n-type base thickness is approximately 5 microns and quite flat. The junction between the p-type recrystallized germanium and the n-type base is not shown.

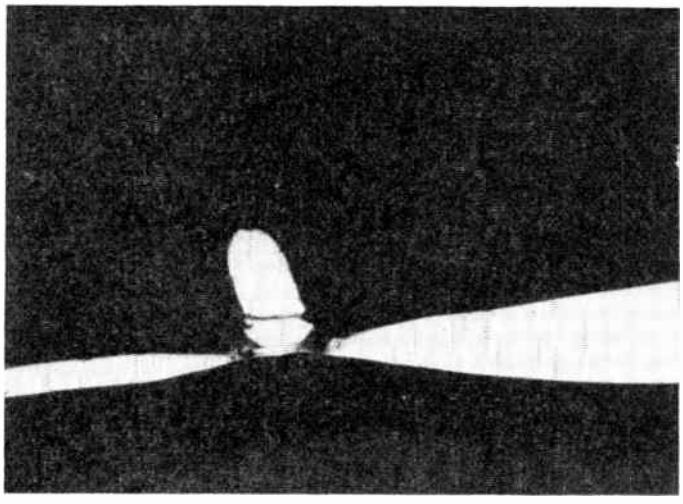

Fig. 7—Photomicrograph of the cross section of a bath-etched device with a gold bond as rectifying contact. The diameter of the gold wire is 0.002 inch and the minimum base thickness is 2 microns. The line in the germanium above the etched depression shows the junction of the p-type recrystallized region and the n-type base region.

which has first been abraded with a spray of an aqueous solution of either No. 1, No. 2, or No. 3 Alumina[13] from an artist's air brush. While this ohmic contact is very satisfactory for computer diodes, as mentioned in Section III, the seemingly large contact resistance ($\sim$5 ohms) to the flow of majority carriers at uhf has partially vitiated the advantages of the diode at uhf. Techniques are now being developed to make ohmic contacts which it is believed will not suffer this problem of contact resistance to majority carriers. In the laboratory models, the ohmic contact to the thin base region has been connected to the kovar ring contact with conducting paint.

[13] Distributed by Buehler Ltd., Evanston, Ill.

VI. Some Applications of the Very Narrow Base Diode

A. Computer Diode

A very narrow base diode has been designed for high-speed switching service and especially for computer applications where it is desirable to minimize the forward-voltage drop at currents of the order of one milliampere. Table I gives the important electrical specifications for the diode which has been called the Model II diode. This set of diode specifications is one of many to which very narrow base computer diodes can be designed. Because of its low forward drop, the Model II diode should be as useful in transistor computer circuits where voltage swings may be less than 5 volts, as conventional switching diodes are in vacuum-tube computer circuits where voltage swings are at least 20 volts. As a result of the relatively low-impedance level of most transistor computer circuitry, the reverse current of the Model II diode which is of the order of tens of microamperes is not deleterious. In addition to having characteristics desirable in transistorized computers, the Model II diode should be superior to conventional diodes in applications such as ladder networks in which many diodes are in series, and in applications where it is desired to clamp to within 0.1 volt of a given voltage.

TABLE I

Electrical Specifications for the Model II Very Narrow Base Diode

All Parameters Defined at $(25 \pm 1.5)°C$

Forward characteristics	$V=0.11$v $I>1$ ma $V=0.5$ v $I>100$ ma
Reverse characteristics	$I_{sat}<25$ μamp $V_{max}>15$ volts (Voltage at which $I>100$ μamp) $r>750$ KΩ ($3\frac{1}{2}$ v) $C<15$ $\mu\mu$f ($3\frac{1}{2}$ v)
Reverse recovery time <0.15 μsec	Reverse recovery time is the time for the back resistance to recover to 100 K ($I<85$ μamp) when the test diode is switched from 2 ma forward current to 6 volts reverse bias (initial reverse current 6 ma).

Table II gives the physical design specifications for the Model II diode. The punch-through voltage is determined by the specified maximum reverse voltage. The resistivity was chosen so that for the anticipated forward current density the sum of the charge of the holes stored in forward bias and the space charge in reverse bias is a minimum (See Section IV-C). The base thickness is defined once both the punch-through voltage and resistivity are determined (5). The diameter of the alloy button is determined from the desired current-voltage characteristic. The maximum allowable saturation current determines the maximum diameter and the minimum allowable current at 0.11 volt forward determines the minimum diameter. Diodes made on a laboratory scale to the physical specifications in Table II have easily met the electrical specifications of Table I.

TABLE II*

PHYSICAL DESIGN SPECIFICATIONS FOR THE MODEL II VERY NARROW BASE DIODE

Resistivity of germanium	3.5 ohm-cm —4.5 ohm-cm
Diameter of alloy button	0.027–0.030 inch
Punch-through voltage	18–22 volts
Final base thickness	8–10 microns

* These physical specifications are based on an ohmic contact which has a generation velocity, s, of 50,000 cm/second.

B. Applications at UIIF

A reverse biased alloy junction is a capacitance which can be varied through variation of the bias voltage. Giacoletto and O'Connell[6] have described the application of a narrow base alloy diode as a variable capacitor at uhf. As indicated following (10) above, it should in principle be easy to design a very narrow base diode with a Q above 800 at 500 mcps. This value of Q, however, has not been achieved in diodes fabricated to date. These diodes have had a series resistance to majority carriers at uhf an order of magnitude larger than that expected from the calculation of the ohmic bulk resistance. We believe this increase in resistance is due to the ohmic contact and a program is under way to both further understand and improve this contact.

At frequencies at which the diode susceptance is less than its conductance the very narrow base diode should prove useful as a mixer.[14] The fabrication of successful mixer diodes also awaits further improvement of the ohmic contact.

[14] A. Uhlir, Jr., "Two terminal p-n junction devices for frequency conversion and computation," PROC. IRE, vol. 44, pp. 1183–1191; September, 1956.

ACKNOWLEDGMENT

The authors wish to thank C. R. Grant, L. Krohn, W. H. Laswell, and Mrs. M. L. Barney for their help in fabricating the diodes. We are indebted to J. Lowen for his help in solving the chemical problems associated with the bath etching process.

LIST OF SYMBOLS

A = junction area.
b = ratio of majority to minority carrier mobilities in base region.
C_T = junction transition-region capacitance.
D = diffusion constant for minority carriers in the base region.
f = frequency.
G = junction conductance.
I = diode current.
I_f = forward current.
I_r = maximum reverse current.
i = small-signal current amplitude.
J = diode current density.
$j = \sqrt{-1}$.
k = Boltzmann's constant.
L = diffusion length for minority carriers in base region.
N_D = net donor density in base region.
p = minority carrier density in base region.
p_n = equilibrium minority carrier density in base region.
Q = ratio of series reactance to series resistance.
Q_{sc} = charge in the space-charge layer when diode reverse biased.
Q_h = charge of the holes stored when diode forward biased.
q = electronic charge.
R = series bulk resistance.
s = generation velocity of the ohmic contact.
T = degrees Kelvin.
V_a = voltage applied in fabrication technique.
V_J = junction voltage.
V_j = junction voltage considered positive in reverse bias.
V_0 = a constant of (8).
V_p = punch-through voltage.
w = effective base width.
x = distance from the ohmic contact.
v_j = small signal amplitude of junction voltage.
ϵ = dielectric constant in rationalized units.
μ_n = mobility of majority carriers in base region.
μ_p = mobility of minority carriers in base region.
ρ_0 = resistivity of base region at low injection level.
τ = lifetime of minority carriers in the base region.
ω = angular frequency.

Application of the Smith Chart to General Impedance Transformations*

HARVEL N. DAWIRS†, SENIOR MEMBER, IRE

Summary—**The Smith Chart is not generally used for making impedance calculations when the characteristic impedance of the two terminal-pair network involved is anything but a real number because normalization of some terminating impedances to the complex characteristic impedance may result in a normalized impedance whose real part is negative, and a "propagation constant" whose magnitude is greater than one, even though no active elements are involved in the network.**

This paper shows how impedances may be calculated using the Smith Chart and associated techniques in much the same manner, and almost as conveniently, as for lossless transmission lines, even though the network may be unsymmetrical, and have complex image impedances and propagation constant.

The calculations are mathematically rigorous and simple using the Smith Chart only for converting back and forth between the complex numbers Γ in polar form and Z in rectangular form where Γ and Z are related by the mathematical expression

$$\Gamma = \frac{Z-1}{Z+1}.$$

No physical interpretation of these numbers is made during the computation as no such interpretation is necessary or useful as far as the method is concerned and may even confuse the main issue, that of a simple solution to a heretofore complex problem.

THE USE of the Smith Chart[1,2] in calculating the transformation of impedances through lossless transmission lines is well-known, and is so common, in fact, that many engineers have misgivings as to the use of the Smith Chart for any other purpose.

Even so, it is commonly accepted that a lossy transmission line has a complex characteristic impedance and that the input impedance of such a line may be plotted as a converging spiral on the Smith Chart. If the impedance plot is normalized to the characteristic impedance of the lossy line the spiral will converge to the center of the chart which now represents a complex number, the complex characteristic impedance of the line.

However, even though this idea may be accepted quite generally, very few engineers will agree with the consequent fact that the absolute value of the expression

$$\Gamma = \frac{z_0 - z_c}{z_0 + z_c},$$

usually known as the reflection coefficient, where z_c is the characteristic impedance of the transmission line and z_0 is the terminating impedance, may be greater than one. That is, if z_c is complex it is easy to find realizable values of z_0 which will make $|\Gamma| > 1$ even though the network is passive. This would seem to rule out the possibility of using the Smith Chart for calculating the impedance transformation through a network having a complex characteristic impedance. It is the purpose of this paper to show that generalized Smith Chart methods can in fact be applied to calculate the transformation of any impedance by any given linear, passive, bilateral two terminal-pair network. This applies equally well to microwave and lumped element circuits.

As an introduction consider the usual case of calculating the input impedance z_i of a transmission line of characteristic impedance z_c, and length l, when it is terminated in an arbitrary impedance z_0 as shown in Fig. 1. The characteristic impedance z_c is real and the

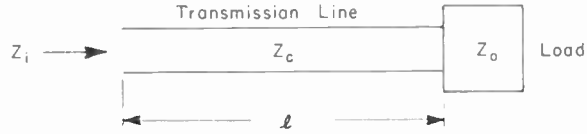

Fig. 1—Input impedance of an ordinary transmission line terminated in Z_0.

input impedance is given by the expression:

$$z_i = z_c \frac{z_0 + jz_c \tan \beta l}{z_c + jz_0 \tan \beta l} \tag{1}$$

or may be calculated as follows:

1) The terminating impedance is normalized to the characteristic impedance of the line. That is

$$Z_0 = \frac{z_0}{z_c}. \tag{2}$$

2) The output reflection coefficient Γ_0 is determined to be:

$$\Gamma_0 = \frac{Z_0 - 1}{Z_0 + 1} = \frac{z_0 - z_c}{z_0 + z_c}. \tag{3}$$

3) The input reflection coefficient is determined to be:

$$\Gamma_i = \Gamma_0 \epsilon^{-2j\beta l} \tag{4}$$

where

$$\Gamma_i = \frac{z_i - z_c}{z_i + z_c} = \frac{Z_i - 1}{Z_i + 1} \tag{5}$$

and

$$Z_i = \frac{z_i}{z_c}. \tag{6}$$

* Original manuscript received by the IRE, January 7, 1957. The research reported in this paper was sponsored in part by the Air Res. and Dev. Command, Wright Air Dev. Ctr.

† Dept. Elec. Eng., Ohio State University, Columbus, Ohio.

[1] P. H. Smith, "Transmission line calculator," *Electronics*, vol. 12, pp. 29–31; January, 1939.

[2] P. H. Smith, "An improved transmission line calculator," *Electronics*, vol. 17, pp. 130–133, 318–325; January, 1944.

4) The normalized input impedance can then be calculated to be:

$$Z_i = \frac{1 + \Gamma_i}{1 - \Gamma_i}. \tag{7}$$

5) It follows from (6) then that $z_i = z_c Z_i$.

It is well known that steps 2)–4) are greatly simplified by the use of the Smith Chart which conveniently converts impedances in rectangular form to reflection coefficients in polar form.

Now consider a general, passive, linear, bilateral, two-terminal network, with input and output image impedances of I_i and I_0 respectively and a propagation constant of $\gamma = \alpha + j\beta$, as shown in Fig. 2. It is well established[3] that when such a network is terminated in an impedance of z_0, the input impedance is:

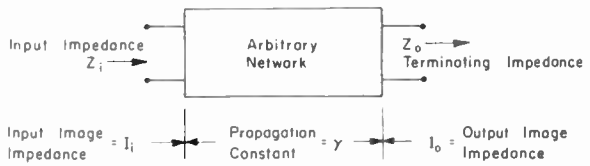

Fig. 2—Relation of impedances and parameters associated with the passive, linear, bilateral two-terminal network.

$$z_i = \frac{z_0 \sqrt{\frac{I_i}{I_0}} \cosh \gamma + \sqrt{I_i I_0} \sinh \gamma}{\sqrt{\frac{I_0}{I_i}} \cosh \gamma + \frac{z_0}{\sqrt{I_i I_0}} \sinh \gamma}. \tag{8}$$

[Note that (1) is just a special case of (8) in which $z_c = I_i = I_0$ and $\gamma = j\beta$.]

This can be put into much less complicated form as follows:

$$z_i = I_i \frac{z_0 \cosh \gamma + I_0 \sinh \gamma}{I_0 \cosh \gamma + z_0 \sinh \gamma} \tag{9a}$$

$$= I_i \frac{z_0 \frac{\epsilon^\gamma + \epsilon^{-\gamma}}{2} + I_0 \frac{\epsilon^\gamma - \epsilon^{-\gamma}}{2}}{I_0 \frac{\epsilon^\gamma + \epsilon^{-\gamma}}{2} + z_0 \frac{\epsilon^\gamma - \epsilon^{-\gamma}}{2}} \tag{9b}$$

$$= I_i \frac{\epsilon^\gamma (z_0 + I_0) + \epsilon^{-\gamma}(z_0 - I_0)}{\epsilon^\gamma (z_0 + I_0) - \epsilon^{-\gamma}(z_0 - I_0)} \tag{9c}$$

$$= I_i \frac{\epsilon^\gamma + \epsilon^{-\gamma} \frac{z_0 - I_0}{z_0 + I_0}}{\epsilon^\gamma - \epsilon^{-\gamma} \frac{z_0 - I_0}{z_0 + I_0}} \tag{9d}$$

$$= I_i \frac{\epsilon^\gamma + \Gamma_0 \epsilon^{-\gamma}}{\epsilon^\gamma - \Gamma_0 \epsilon^{-\gamma}} \tag{9e}$$

where

$$\Gamma_0 = \frac{z_0 - I_0}{z_0 + I_0} = \frac{Z_0 - 1}{Z_0 + 1} \tag{10}$$

and

$$Z_0 = \frac{z_0}{I_0}. \tag{11}$$

Note that (10) and (11) are very similar, respectively, to (3) and (2) but that in this case both z_0 and I_0 are complex numbers in which case the real part of Z_0 may be negative and $|\Gamma_0|$ may be greater than one, even though the real parts of I_0 and z_0 are positive indicating that the circuit is passive. Since this situation seems to violate the usual concept of reflection coefficient, Γ_0 will simply be regarded as a complex number defined by (10).

Now (9e) can be solved to obtain the expression:

$$\Gamma_0 = \frac{(z_i - I_i)\epsilon^\gamma}{(z_i + I_i)\epsilon^{-\gamma}} \tag{12a}$$

$$= \Gamma_i \epsilon^{2\gamma} \tag{12b}$$

where

$$\Gamma_i = \frac{z_i - I_i}{z_i + I_i} = \frac{Z_i - 1}{Z_i + 1} \tag{13}$$

and

$$Z_i = \frac{z_i}{I_i} \tag{14}$$

are analogous to (10) and (11) respectively.

Note that (12) is a general, complex form of (4) which can now be used to calculate the input impedance of a general network terminated in an arbitrary impedance z_0 in much the same manner as the transmission line calculation considered previously.

Such a calculation would proceed as follows:

1) Normalize the terminating impedance to the output image impedance

$$Z_0 = \frac{z_0}{I_0}. \tag{11}$$

2) Calculate

$$\Gamma_0 = \frac{Z_0 - 1}{Z_0 + 1}. \tag{10}$$

3) Calculate

$$\Gamma_i = \Gamma_0 \epsilon^{-2\gamma}, \text{ which follows from (12).} \tag{15}$$

4) Calculate

$$Z_i = \frac{1 + \Gamma_i}{1 - \Gamma_i} \tag{16}$$

which follows from (13).

[3] J. J. Karakash, "Transmission Lines and Filter Networks," The Macmillan Co., Inc., New York, N. Y., p. 178; 1950.

5) Calculate the input impedance

$$z_i = Z_i I_i$$

which follows from (14), where steps 2) and 4) can be carried out on a Smith Chart if $|\Gamma_0| < 1$ and $|\Gamma_i| < 1$.

Consider an expression of the form

$$\Gamma = \frac{Z - 1}{Z + 1}. \tag{17}$$

The conversion from Γ to Z and vice versa can be accomplished on a Smith Chart only if $|\Gamma| < 1$ (which implies that Re $Z > 0$ and conversely).

Define

$$\Gamma' = \frac{1}{\Gamma} \tag{18}$$

and

$$Z' = -Z. \tag{19}$$

Then when $|\Gamma| > 1$ and Re $Z < 0$, $|\Gamma'|$ will be less than one, Re Z' will be positive and

$$\Gamma' = \frac{1}{\Gamma} = \frac{Z + 1}{Z - 1} = \frac{Z' - 1}{Z' + 1} \tag{20}$$

by simple substitution of (18) and (19) into (17); or, in another form,

$$\frac{1}{\Gamma} = \frac{(-Z) - 1}{(-Z) + 1}. \tag{20a}$$

Thus if $|\Gamma_i| > 1$ or $|\Gamma_0| > 1$ steps 2) and 4) can be carried out on the Smith Chart with no difficulty by simply making use of (20). Step 3) then would become

$$\Gamma_i = \frac{1}{\Gamma_i} = \frac{1}{\Gamma_0 \epsilon^{-2\gamma}} = \Gamma_0' \epsilon^{2\gamma}. \tag{21}$$

Thus the transformation of an arbitrary impedance through a general network is not much more difficult than an impedance transformation through an ordinary transmission line.

Such transformations are useful whenever complex characteristic impedances arise such as in lossy transmission lines and filters.

This principle has been applied in the development of The Ohio State University's Filter Analysis Chart,[4-6] for symmetrical lossless filters where, of course, the characteristic impedance becomes purely imaginary in the rejection bands.

Note that in the above development the network may be nonsymmetrical in which case the image impedances are not equal. This property may be useful in analyzing terminating half sections, Tchebycheff distributions, etc.

When a number of symmetrical and identical networks are cascaded, as in the case of a filter, the relation

$$\Gamma_i = \Gamma_0 \epsilon^{-2n\gamma} \tag{22}$$

may be used, where γ is the propagation constant of each section and n is the number of sections. The characteristic impedance of the network is of course the same as that of the individual sections.

[4] H. N. Dawirs, "Graphical filter analysis," IRE TRANS., vol. MTT-3, pp. 15–21; January, 1955.
[5] H. N. Dawirs and E. K. Damon, "Application of The Ohio State University filter analysis chart," *Proc. Natl. Electronics Conf.*, vol. 10, pp. 303–309; February, 1955.
[6] H. N. Dawirs, "A chart for analyzing transmission-line filters from input impedance characteristics," PROC. IRE, vol. 43, pp. 436–443; April, 1955.

CORRECTION

Seymour B. Cohn, author of "Direct-Coupled-Resonator Filters," which appeared on pages 187–197 of the February, 1957 issue of PROCEEDINGS has requested the editors to make the following corrections to his paper.

The two equations at the bottom of Fig. 2, should read as follows:

$$A = 10 \log_{10}[1 + (10^{A_m/10} - 1) \cos^2 (n \cos^{-1}\omega')] \text{ db}, \omega' \leqq 1$$

$$A = 10 \log_{10}[1 + (10^{A_m/10} - 1) \cosh^2 (n \cosh^{-1}\omega')] \text{ db}, \quad \omega' \geqq 1.$$

In Fig. 3(a), insert ω_0 in denominator in formula for C_{jk}.

In both Fig. 3(a) and Fig. 3(b), change "For $f_2/f_1 < 0.05$:" to "For $f_2/f_1 < 1.05$:".

In Fig. 5, the formulas for ϕ_i and L should read as follows:

$$\phi_i = 180° - \tfrac{1}{2}[\tan^{-1}(2X_{i-1,\,i}) + \tan^{-1}(2X_{i,\,i+1})]$$

$$L = \frac{\pi}{\omega'_1}\left[\frac{\lambda_{g1} - \lambda_{g2}}{\lambda_{g1} + \lambda_{g2}}\right], \quad L \approx \frac{\pi}{2\omega'_1}\left(\frac{\lambda_{g0}}{\lambda_0}\right)^2\left(\frac{f_2 - f_1}{f_c}\right)$$

$$\text{for } \frac{f_2 - f_1}{f_0} < 0.01.$$

Behavior of Noise Figure in Junction Transistors*

EDWARD G. NIELSEN†, ASSOCIATE, IRE

Summary—It is well-known that generator resistance and dc-emitter current are two major factors in determining the noise figure of junction transistors. Other important factors are base resistance, low-frequency alpha, and alpha cutoff frequency. A method of calculating the noise figure in terms of these parameters, the frequency variation of the noise figure, and the conditions for minimizing the noise figure are presented. The results provide means for specifying transistor and circuit parameters to meet noise requirements.

In the absence of "excess" or $1/f$ noise, the noise figure as a function of frequency for the common base, common collector, and common emitter configurations is constant up to $\sqrt{1-\alpha_0}\, f_\alpha$. Here α_0 is the low-frequency alpha and f_α the alpha cutoff frequency. Above this frequency the noise figure increases toward an asymptote of 6 decibels per octave. Calculations show that for minimum noise figure the base resistance and emitter current should be small, α_0 should be close to one, f_α should be large, and the driving source resistance has an optimum value.

This work is based on a simplified version of a transistor noise equivalent circuit developed by van der Ziel.[1]

Introduction

As a result of considerable experimental work, much has been learned about the qualitative behavior of the noise figure in junction transistors.[2,3] As shown in Fig. 1 the noise figure is found to be

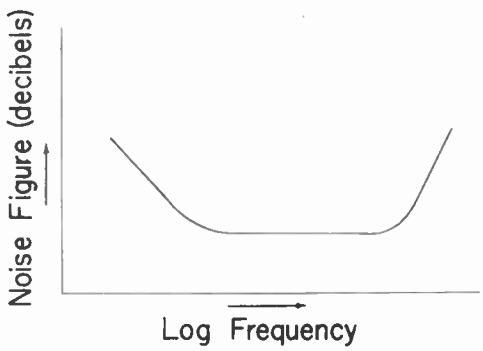

Fig. 1—Noise figure as a function of frequency.

high at low frequencies. This is caused by "excess" or $1/f$ noise. Fortunately, in many transistors "excess" noise is negligible above a frequency of 1 kilocycle.

In the center frequency region, the noise figure decreases to a minumum of about 2 to 6 db. It is essentially constant in this region (unless the excess noise is so large that the curve becomes V shaped). Finally at higher frequencies the noise figure increases. It has also been found experimentally that for minimum noise figure the emitter current should be small and the driving source resistance has an optimum value.

Except for the excess noise this behavior is predicted from the basic physical parameters in a transistor noise equivalent circuit. From this circuit the equations for the noise figure of the common base, common emitter, and common collector configurations will be calculated. The equations will be analyzed to determine the conditions for minimum noise figure and the effect of transistor and circuit parameters on the noise figure.

Noise Equivalent Circuit

The noise in a transistor is assumed to arise from three sources, diffusion fluctuations, recombination fluctuations in the base region, and ordinary thermal, or Johnson, noise in the base resistance. These fluctuations produce noise at the terminals of the transistor. For the purpose of circuit analysis, van der Ziel has represented the noise by equivalent noise generators attached to the transistor T equivalent circuit.[4] Two correlated generators, one at the emitter and one at the collector, represent the fluctuations due to diffusion and recombination in the base region. An independent generator in the base lead represents the thermal noise in the base resistance.

For frequencies below the alpha cutoff frequency, a simplified noise equivalent circuit, Fig. 2 gives good results. The principal simplifications over van der Ziel's circuit are:

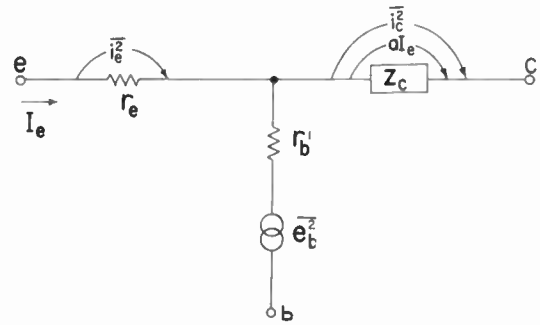

Fig. 2—Simplified noise equivalent circuit.

1) The frequency dependence of the emitter noise generator has been neglected;
2) The emitter and collector noise generators have been assumed independent;
3) The T equivalent circuit has been simplified by neglecting the effect of space charge layer widening, and neglecting the frequency characteristic of the emitter diode impedance.

* Original manuscript received by the IRE, January 28, 1957.
† Bell Telephone Labs., Inc., Murray Hill, N. J.
[1] A. van der Ziel, "Shot noise in junction diodes and transistors," PROC. IRE, vol. 43, pp. 1639–1646; November, 1955.
[2] H. C. Montgomery, "Transistor noise in circuit applications," PROC. IRE, vol. 40, pp. 1461–1471; November, 1952.
[3] P. M. Bargellini and M. B. Herscher, "Investigations of noise in audio frequency amplifiers using junction transistors," PROC. IRE, vol. 43, pp. 217–226; February, 1955.
[4] van der Ziel, *op. cit.*, pp. 1643–1645.

In practice, the noise figure calculated from this equivalent circuit is in good agreement with experiment to frequencies beyond the alpha cutoff frequency.

The noise at the emitter is represented by a mean square Norton generator, $\overline{i_e^2}$, connected across the junction

$$\overline{i_e^2} = 2qI_e df \tag{1}$$

where q is the electronic charge, I_e the dc emitter current, and df the frequency interval. This noise is frequently called "shot noise" because the "shot noise" in a temperature limited, vacuum diode is given by the same formula.

The noise at the collector is represented by the Norton generator

$$\overline{i_c^2} = 2qI_c\left[1 - \frac{|a|^2}{a_0}\right]df \tag{2}$$

where I_c is the dc collector current and a is the transistor's alpha.[5] This formula is the key to the transistor's high-frequency noise performance. As the frequency is increased the accompanying decrease in a causes $\overline{i_c^2}$ to increase. At high frequencies a approaches zero and the collector noise equation approaches the expression for full shot noise.

$$\overline{i_c^2}\big|_{a=0} = 2qI_c df.$$

At low frequencies $a = a_0$, and (2) becomes

$$\overline{i_c^2}\big|_{a=a_0} = 2qIc(1 - a_0)df$$

so that the collector noise is reduced by $(1 - a_0)$.

If a is replaced by the first order approximation

$$\frac{a_0}{1 + j\dfrac{f}{f_a}},$$

(2) becomes

$$\overline{i_c^2} = 2qI_c(1 - a_0)\frac{\left[1 + \left(\dfrac{f}{\sqrt{1 - a_0}\, f_a}\right)^2\right]df}{\left[1 + \left(\dfrac{f}{f_a}\right)^2\right]}. \tag{3}$$

The equation has the form of a doublet. It is constant with increasing frequency up to a corner frequency, $\sqrt{1-a_0}\, f_a$, and then increases at the rate of 6 db per octave. At f_a a second corner occurs and it becomes flat again.

To complete the noise picture, a noise generator, $\overline{e_b^2}$, must be added in series with the base resistance, r_b'. Since r_b' is an ohmic resistance, $\overline{e_b^2}$ is a thermal noise generator,

$$\overline{e_b^2} = 4kTr_b' df \tag{4}$$

where k is Boltzmann's constant and T the absolute temperature in degrees Kelvin.

The noise figure can be calculated from Fig. 2; however, at this point it is convenient to replace the Norton generators by their Thevenin equivalents. The resulting circuit is shown in Fig. 3. A resistor, R_g, and thermal

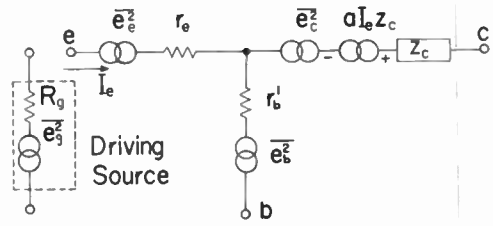

Fig. 3—Equivalent circuit with Thevenin generators.

noise generator, $\overline{e_g^2}$, have been added to represent the internal resistance and thermal noise of a driving source. The formulas for the noise voltage generators in the circuit are listed below.

$$\overline{e_b^2} = 4kTr_b' df \tag{4}$$

$$\overline{e_g^2} = 4kTR_g df \tag{5}$$

$$\overline{e_e^2} = 2kTr_e df \tag{6}$$

$$\overline{e_c^2} = \frac{2kTa_0(1 - a_0)\,|Z_c^2|\left[1 + \left(\dfrac{f}{\sqrt{1 - a_0}\, f_a}\right)^2\right]df}{r_e\left[1 + \left(\dfrac{f}{f_a}\right)^2\right]}. \tag{7}$$

Eqs. (6) and (7) were obtained, respectively, from (1) and (3). In (3) $a_0 I_e$ was substituted for I_c; and in (1) and (3) kT/r_e was substituted for qI_e.

Fig. 3 together with (4), (6), and (7) specify the noise characteristics of the transistor.

Calculation of Noise Figure

The noise figure, F, is most easily calculated using the definition:

$$F = \frac{\text{Total mean square noise voltage at output of transistor}}{\text{Mean square noise voltage at output resulting from thermal noise in } R_g}. \tag{8}$$

The noise figures for the common base and common emitter configurations, F_b and F_e, respectively, are found to be the same.[6]

[5] It is assumed in the development of this formula that a is not a function of emitter current. Furthermore, leakage currents and the collector reverse saturation current have been neglected.

[6] This is true under the assumptions that $R_g + r_b' \ll aZ_c$ and $R_g + r_e \ll aZ_c$. The common base noise figure is calculated in Appendix I.

$$F_b = F_e = 1 + \frac{r_b'}{R_g} + \frac{r_e}{2R_g} + \frac{(1-a_0)\left[1+\left(\frac{f}{\sqrt{1-a_0}\,f_a}\right)^2\right][R_g+r_b'+r_e]^2}{2a_0 r_e R_g}. \quad (9)$$

The "1" in (9) always occurs in noise figure equations. It is the ratio of the thermal noise from R_g appearing in the numerator of (8) to the same term in the denominator.

The second term in (9) is due to the noise in r_b', the third term to the noise in r_e, and the fourth term to the noise in the collector. The collector term is the only term that is a function of frequency. At low frequencies the contributions of all the terms are usually of the same order of magnitude, but above $\sqrt{1-a_0}\,f_a$ the collector term becomes dominant.

The behavior of the collector term is shown in Fig. 4.

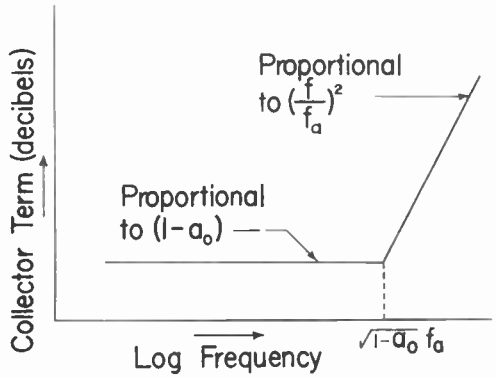

$$\text{Collector Term} = 10 \log_{10} \left\{ \frac{(1-a_0)\left[1+\left(\frac{f}{\sqrt{1-a_0}\,f_a}\right)^2\right](R_g+r_b'+r_e)^2}{2a_0 r_e R_g} \right\}$$

Fig. 4—Collector term.

For frequencies below $\sqrt{1-a_0}\,f_a$ it is proportional to $(1-a_0)$. Above $\sqrt{1-a_0}\,f_a$ it is proportional to $(f/f_a)^2$, and therefore increases at the rate of 6 db per octave of frequency. Clearly, reducing $(1-a_0)$ reduces the low-frequency noise and increasing f_a reduces the high-frequency noise.

Like the collector term, the noise figure will also have a 6 db per octave slope at high frequencies. Because of the first three terms in (9), its corner frequency will be greater than $\sqrt{1-a_0}\,f_a$. However, as a rule of thumb, it is often convenient to think of $\sqrt{1-a_0}\,f_a$ as an approximate corner for the noise figure. This frequency can be remembered as the geometric mean of the common emitter and common base cutoff frequencies.

The common collector noise figure, F_c, is the same as the common base and common emitter noise figures except for the last term.

$$F_c = 1 + \frac{r_b'}{R_g} + \frac{r_e}{2R_g} + \frac{a_0(1-a_0)\left[1+\left(\frac{f}{\sqrt{1-a_0}\,f_a}\right)^2\right][R_g+r_b']^2}{2r_e R_g\left[1+\left(\frac{f}{f_a}\right)^2\right]}. \quad (10)$$

Under most operating conditions

$$a_0 \approx 1$$
$$R_g + r_b' \approx R_g + r_b' + r_e$$
$$f < f_a$$

so that

$$F_c \approx F_b = F_e$$

and the noise figures for the three configurations are approximately equal. However, at frequencies above f_a the

$$\left[1+\left(\frac{f}{f_a}\right)^2\right]$$

term in (10) causes F_c to become constant with increasing frequency whereas F_b and F_e continue to increase.

The measured common emitter and common collector noise figures of a type 2N43 transistor are shown in Fig. 5 together with the calculated curves. F_e and F_c are constant with frequency to $\sqrt{1-a_0}\,f_a$ where they begin to increase. Above f_a the common collector noise figure becomes constant while the common emitter noise figure continues to increase. The calculated curves have the same shape and, except for the lowest frequencies, are within 2 decibels of the measured curves. These curves are typical of the experimental results which will be discussed in a later section.

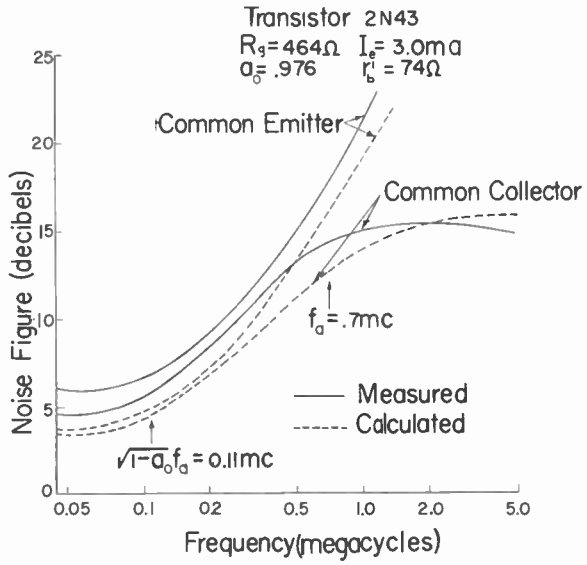

Fig. 5—Comparison of measured and calculated noise figure.

The Effect of the Driving Source Resistance on the Noise Figure

When plotted as a function of the driving source resistance, the noise figure has a minimum. Fig. 6 shows a typical set of measured and calculated values of noise figure vs source resistance for a type 2N94A transistor in the common emitter configuration. The measured curve has a minimum of 3.7 db at 700Ω, and the calculated curve has a minimum of 2.3 db at 800Ω.

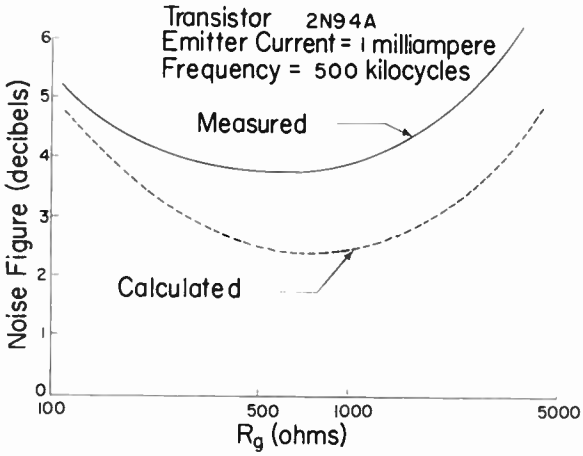

Fig. 6—Noise figure as a function of source resistance.

The source resistance for minimum noise figure, $R_{g(F\ \mathrm{opt})}$, is found by the usual process of setting $\partial F/\partial R_g$ equal to zero. For this step it is convenient to put (9) and (10) into a more compact form:

$$F = 1 + \frac{K_1}{R_g} + \frac{(K_2 + R_g)^2 K_3}{R_g} \tag{11}$$

where for the common base and common emitter configurations

$$K_1 = r_b' + \frac{r_e}{2}$$

$$K_2 = r_b' + r_e$$

$$K_3 = \frac{(1 - a_0)\left[1 + \left(\frac{f}{\sqrt{1 - a_0}\, f_a}\right)^2\right]}{2a_0 r_e}$$

and for the common collector configuration

$$K_1 = r_b' + \frac{r_e}{2}$$

$$K_2 = r_b'$$

$$K_3 = \frac{a_0(1 - a_0)\left[1 + \left(\frac{f}{\sqrt{1 - a_0}\, f_a}\right)^2\right]}{2r_e\left[1 + \left(\frac{f}{f_a}\right)^2\right]}.$$

The equation for $R_{g(F\ \mathrm{opt})}$ is:

$$R_{g(F\ \mathrm{opt})} = \left(K_2^2 + \frac{K_1}{K_3}\right)^{1/2}. \tag{12}$$

The only frequency dependent term is K_3 which causes $R_{g(F\ \mathrm{opt})}$ to decrease for frequencies between $\sqrt{1-a_0}\, f_a$ and f_a. At frequencies below f_a, $R_{g(F\ \mathrm{opt})}$ is approximately the same for the three configurations.

The magnitude of $R_{g(F\ \mathrm{opt})}$ as a function of emitter current is shown as the dotted curve in Fig. 7. The curve is plotted for a typical transistor ($a_0 = 0.98$, and $r_b' = 100\Omega$) at frequencies below $(1-a_0)f_a$. The values of source resistance for maximum available gain, $R_{g(\mathrm{Gain\ opt})}$ are plotted for the three configurations as solid lines.[7] The important relationship shown by Fig. 7 is that the source resistance for minimum noise figure is approximately equal to the source resistance for maximum, common emitter gain. In fact it can be shown that for reasonable transistor parameters and frequencies below $(1-a_0)f_a$, $R_{g(F\ \mathrm{opt})}$ is always within a factor of $\sqrt{2}$ of the common emitter, $R_{g(\mathrm{Gain\ opt})}$. From a standpoint of minimum low-frequency noise figure together with maximum low-frequency gain, common emitter configuration is clearly the better of the three.

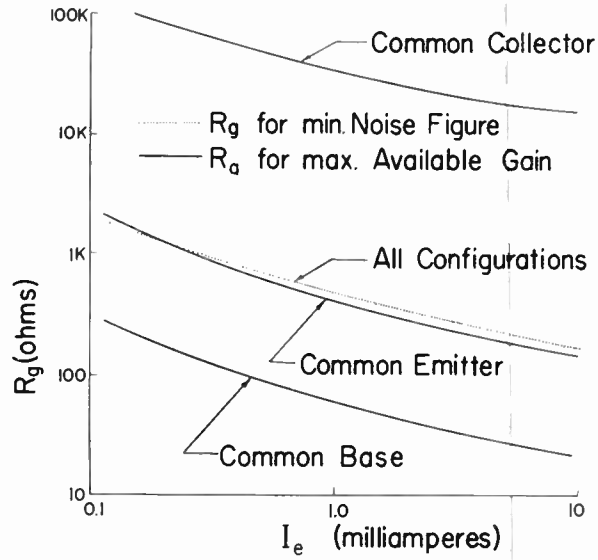

Fig. 7—Comparison of source resistance for minimum noise figure and for maximum available gain.

In designing circuits the question frequently arises, how much will the noise figure be degraded if the source resistance is not made equal to $R_{g(F\ \mathrm{opt})}$? The answer to this question is obtained by calculating $F/F_{\min}$ where $F_{\min}$ is the noise figure obtained when $R_g = R_{g(F\ \mathrm{opt})}$.[8]

$$\frac{F}{F_{\min}} = 1 + \frac{\frac{1}{2}\left(\frac{R_g}{R_{g(F\ \mathrm{opt})}} + \frac{R_{g(F\ \mathrm{opt})}}{R_g}\right) - 1}{1 + K} \tag{13}$$

[7] $R_{g(\mathrm{Gain\ opt})}$ is the source resistance for matched input and output conditions. Equations for $R_{g(\mathrm{Gain\ opt})}$ are given by F. R. Stansel, "Transistor equations," *Electronics*, vol. 26, pp. 156–158, March, 1953, where this resistance is called R_{GM}.

[8] This calculation is made in Appendix II.

where

$$K = \frac{K_2 + \dfrac{1}{2K_3}}{R_{g(F\ \mathrm{opt})}}.$$

The ratio is symmetrical in R_g about $R_{g(F\ \mathrm{opt})}$; for $R_g = R_{g(F\ \mathrm{opt})}$, the ratio is 1. K is a number that never gets smaller than 1; usually it is on the order of 2 or 3. The formula is plotted in Fig. 8 for values of K between 1 and 10. For $R_g \approx R_{g(F\ \mathrm{opt})}$ the curves are nearly flat. For R_g within a factor of 2 of $R_{g(F\ \mathrm{opt})}$ the noise figure will not increase more than 0.5 decibel; and for R_g within a factor of 5 of $R_{g(F\ \mathrm{opt})}$ the noise figure will not increase more than 2.5 db.

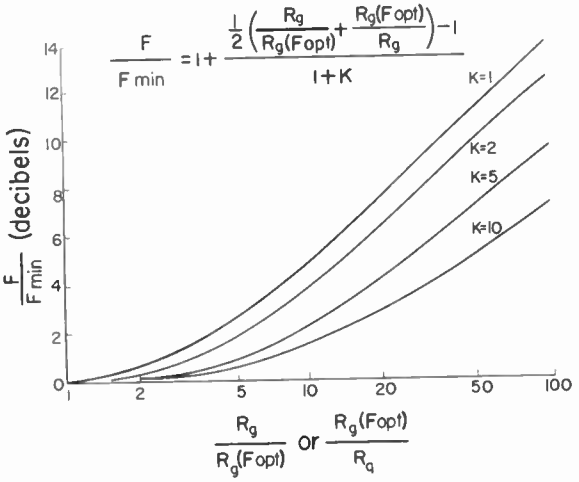

Fig. 8—Effect of nonoptimum source resistance on noise figure.

Conditions for Minimum Noise Figure

The noise figure can be minimized by suitably chosen transistor parameters. It was shown previously that decreasing $(1-a_0)$ and increasing f_a reduced the noise figure. It can also be seen that, since r_b' appears only in the numerators of (9) and (10), reducing the base resistance decreases the noise figure. It is interesting to note that the requirements on a_0, f_a, and r_b' for minimum noise figure are the same as the requirements on these parameters for high gain, wide-band amplification.

The effect of changing the emitter resistance is seen by expanding the equation for $F_{\min}$ so that the solution appears as the sum of a number of fractions. Among these fractions r_e appears only in the denominators. Therefore, r_e should be large and, hence, the emitter current should be small.

Fig. 9 is a plot of $F_{\min}$ vs emitter current. The curve was obtained by computing $R_{g(F\ \mathrm{opt})}$ for a number of values of I_e and using the computed values of $R_{g(F\ \mathrm{opt})}$ in a circuit in order to measure the noise figure. The curve is approximately constant at about 2.2 db for I_e below 0.5 ma. Above 0.5 ma, the noise figure increases slowly with increasing I_e. If the curves were extended to lower emitter currents, the noise figure would increase again. This would be caused by the decrease in alpha at low currents and the contribution of noise sources, such as the reverse saturation currents, neglected in the analysis.

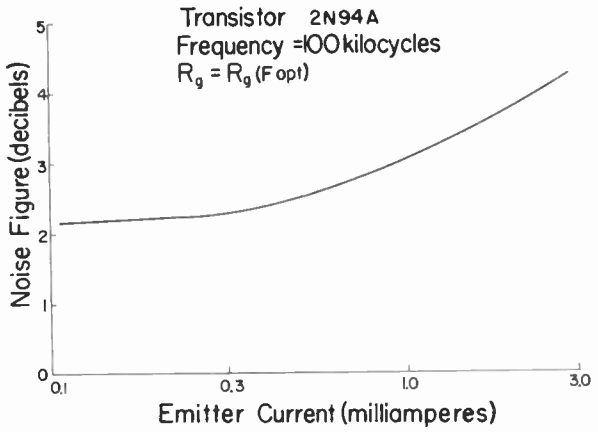

Fig. 9—Minimum noise figure as a function of emitter current.

Experimental Results

Most of the measurements have been made using the common emitter configuration, but a few common collector measurements have also been made. The transistors were alloy junction units with alpha cutoff frequencies in the range of 1 to 10 megacycles. Limited measurements on grown junction and surface barrier transistors have given similar results.

Fig. 5 and Fig. 6 are typical of the experimental data. Below $\sqrt{1-a_0}\, f_a$ the measured noise figure is usually 0 to $2\frac{1}{2}$ db greater than calculated. Above $\sqrt{1-a_0}\, f_a$ the measured noise figure increases with a slope of 4 to 6 db per octave as compared with the 6 db predicted by (9). In the common collector configuration the noise figure increases between $\sqrt{1-a_0}$ and f_a. The slope of the curve decreases above f_a although it does not always become flat as indicated by (10).

The fact that the measured noise figure is greater than calculated suggests that not all of the noise sources have been adequately accounted for or approximations in the development of the equations are resulting in error. An approximation, in addition to those mentioned,[5] that may cause such errors is

$$a = \frac{a_0}{1 + j\dfrac{f}{f_a}}.$$

The measurements indicate, however, that the gross behavior of the noise figure is well predicted by the van der Ziel circuit, and much useful design information can be obtained from it.

Conclusion

Except for excess noise, transistor noise is assumed to arise from diffusion and recombination fluctuations in the base region and thermal noise in the base resistance.

This noise is represented by noise generators connected in the legs of a T equivalent circuit. The emitter and base noise generators are independent of frequency, but the noise represented by the collector generator increases with frequency. This causes the transistor noise figure to increase at the rate of 6 db per octave for frequencies above $\sqrt{1-a_0}\,f_a$.

The noise figure for the three transistor configurations is approximately the same except above the alpha cutoff frequency. Here the common emitter and common base noise figures continue to increase with increasing frequency, but the common collector noise figure theoretically becomes constant.

For minimum noise figure, alpha should be close to 1, the alpha cutoff frequency should be large, and the base resistance should be small. These are the same requirements on the transistor as for high-gain, wide-band amplification. The emitter current should be small and the driving source resistance has an optimum value. For all configurations at low frequencies, the source resistance giving the minimum noise figure is approximately equal to the source resistance giving maximum, common emitter gain. This makes the common emitter configuration optimum for maximum gain and minimum noise at low frequencies.

For a source resistance close to the optimum, the noise figure varies slowly. It will not be degraded by more than 0.5 db by a source resistance that is a factor of 2 away from the optimum nor more than 2.5 db for a factor of 5 away.

The experimental results are in general agreement with theory and indicate that much useful design information can be obtained from the van der Ziel noise theory.

Appendix I

Calculation of Common Base Noise Figure

Using (8) the noise figure is calculated from the equivalent circuit shown in Fig. 10. For the purposes of the analysis the rms equivalent noise voltage generators, e_g, e_b, e_e, and e_c have been assigned arbitrary polarities.

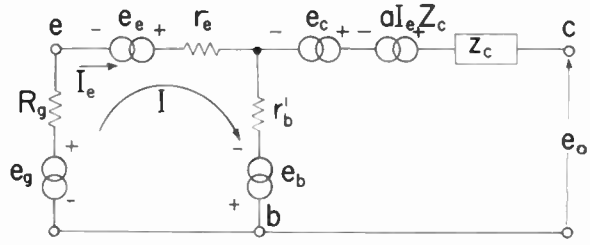

Fig. 10—Circuit for noise figure calculation.

By ordinary network analysis,

$$e_0 = -e_b + e_c + I(r_b' + aZ_c)$$

where

$$I = \frac{e_g + e_e + e_b}{R_g + r_b' + r_e}.$$

Combining and collecting terms

$$e_0 = \frac{e_g(r_b' + aZ_c)}{R_g + r_b' + r_e} + \frac{e_b(aZ_c - R_g - r_e)}{R_g + r_b' + r_e} + \frac{e_e(r_b' + aZ_c)}{R_g + r_b' + r_e} + e_c. \tag{14}$$

Assume

$$r_b' \ll aZ_c$$
$$R_g + r_e \ll aZ_c.$$

Taking the mean square value of both sides of (14), assuming no correlation between terms.

$$\overline{e_0^2} = \frac{\overline{e_g^2}\,|aZ_c|^2}{(R_g + r_b' + r_e)^2} + \frac{\overline{e_b^2}\,|aZ_c|^2}{(R_g + r_b' + r_e)^2} + \frac{\overline{e_e^2}\,|aZ_c|^2}{(R_g + r_b' + r_e)^2} + \overline{e_c^2}.$$

By (8) the noise figure is

$$F_b = \frac{\overline{e_0^2}(R_g + r_b' + r_e)^2}{\overline{e_g^2}\,|aZ_c|^2}$$

hence

$$F_b = 1 + \frac{\overline{e_b^2}}{\overline{e_g^2}} + \frac{\overline{e_e^2}}{\overline{e_g^2}} + \frac{\overline{e_c^2}(R_g + r_b' + r_e)^2}{\overline{e_g^2}\,|aZ_c|^2}. \tag{15}$$

Substituting (4) to (7) and

$$a_0 = \frac{a_0}{1 + j\dfrac{f}{f_a}}$$

into (15),

$$F = 1 + \frac{r_b'}{R_g} + \frac{r_e}{2R_g} + \frac{(1 - a_0)[R_g + r_b' + r_e]^2\left[1 + \left(\dfrac{f}{\sqrt{1 - a_0}\,f_a}\right)^2\right]}{2a_0 r_e R_g}.$$

Appendix II

Calculation of F/F_{min}

The last term of (11) is expanded and the equation put into the following form:

$$F = 1 + 2K_2K_3 + \frac{1}{R_g}(K_1 + K_2^2K_3) + R_gK_3.$$

Taking the ratio F/F_{min} we get

$$\frac{F}{F_{min}} = \frac{1 + 2K_2K_3 + \dfrac{1}{R_g}(K_1 + K_2^2K_3) + R_gK_3}{1 + 2K_2K_3 + \dfrac{1}{R_{g(F\ opt)}}(K_1 + K_2^2K_3) + R_{g(F\ opt)}K_3}.$$

By dividing the numerator and denominator by K_3, the term in the parentheses becomes $R_g^{2}{}_{(F\ \mathrm{opt})}$. Making this substitution

$$\frac{F}{F_{\min}} = \frac{\dfrac{1}{K_3} + 2K_2 + \dfrac{R_g^{2}{}_{(F\ \mathrm{opt})}}{R_g} + R_g}{\dfrac{1}{K_3} + 2K_2 + 2R_{g(F\ \mathrm{opt})}}.$$

Dividing the numerator and denominator by $2R_{g(F\ \mathrm{opt})}$,

$$\frac{F}{F_{\min}} = \frac{\dfrac{1}{R_{g(F\ \mathrm{opt})}}\left(\dfrac{1}{2K_3}+K_2\right)+\dfrac{1}{2}\left(\dfrac{R_{g(F\ \mathrm{opt})}}{R_g}+\dfrac{R_g}{R_{g(F\ \mathrm{opt})}}\right)}{\dfrac{1}{R_{g(F\ \mathrm{opt})}}\left(\dfrac{1}{2K_3}+K_2\right)+1}.$$

Letting

$$K = \frac{1}{R_{g(F\ \mathrm{opt})}}\left(\frac{1}{2K_3} + K_2\right),$$

and dividing the numerator by the denominator puts the equation into its final form:

$$\frac{F}{F_{\min}} = 1 + \frac{\dfrac{1}{2}\left(\dfrac{R_{g(F\ \mathrm{opt})}}{R_g} + \dfrac{R_g}{R_{g(F\ \mathrm{opt})}}\right) - 1}{K + 1}.$$

ACKNOWLEDGMENT

The author is indebted to A. van der Ziel and H. C. Montgomery for their information and discussions about the noise theory and to J. L. Robson for his painstaking measurements and analysis of data.

Improvement of Binary Transmission by Null-Zone Reception*

F. J. BLOOM†, ASSOCIATE, IRE, S. S. L. CHANG†, SENIOR MEMBER, IRE, B. HARRIS†, SENIOR MEMBER, IRE, A. HAUPTSCHEIN†, MEMBER, IRE, K. C. MORGAN†

Summary—**In the customary methods of transmitting binary data the receiver, as a result of the decision process made on each transmitted pulse, prints out one of two symbols. Schemes are considered here in which the receiver prints out one of three symbols (single-null zone reception) or one of four symbols (double-null zone reception). These extra symbols permit the receiver to indicate when the *a posteriori* probabilities of the two transmitted states are nearly equal. Single-null zone reception is shown to be capable, under optimum conditions, of achieving about one-half of the improvement in information rate theoretically attainable by increasing the number of receiver levels without limit. Double-null reception, which splits the null zone and thereby retains polarity information, offers only a slight additional increase in rate. It affords a significant advantage over single-null reception, though, because it is much less sensitive to variations in null level.**

INTRODUCTION

THE PROBLEM of improving the reliability of transmission in the presence of noise has commanded considerable attention in recent years. A large number of schemes have been proposed and studied toward this end. Prominent among these are the various pulse modulation schemes, including, as an important class, the pulse code modulation family. Analyses of pcm systems have indicated that, whereas a greater transmitted information rate is achieved by increasing the number of levels, the maximum reliability is obtained by reverting to binary transmission. This is particularly significant when the level of interference becomes appreciable.

The thorough analysis of binary transmission systems, therefore, becomes the *sine qua non* of any reliability study, and, indeed, a large number of papers have been published which pertain to this problem. This literature may be broadly grouped into two categories, depending on whether the analysis is concerned with the properties of an uncoded binary system or deals with various coding schemes. For this context the term coding is used in its defined sense in information theory, that is, if each element of an alphabet of 64 symbols is sent as a 6-digit binary pulse group, the system is considered uncoded. This paper will first consider a method of improving uncoded binary reception and then extend the results to various coding schemes.

THE TOTAL INFORMATION IN RECEIVED BINARY PULSES WITH GAUSSIAN INTERFERENCE

In conventional bilevel transmission an ideal band-limited video signal is sampled at the receiver at the Nyquist rate. These sampled values originate at the transmitter at one of two levels, x_1 or x_2, where, with no

* Original manuscript received by the IRE, August 17, 1956; revised manuscript received January 23, 1957. The research reported in this paper was performed at New York Univ. and sponsored by the Air Force Cambridge Res. Ctr., Air Res. and Dev. Command, under Contract AF 19(604)-1049.

† New York University, New York, N. Y

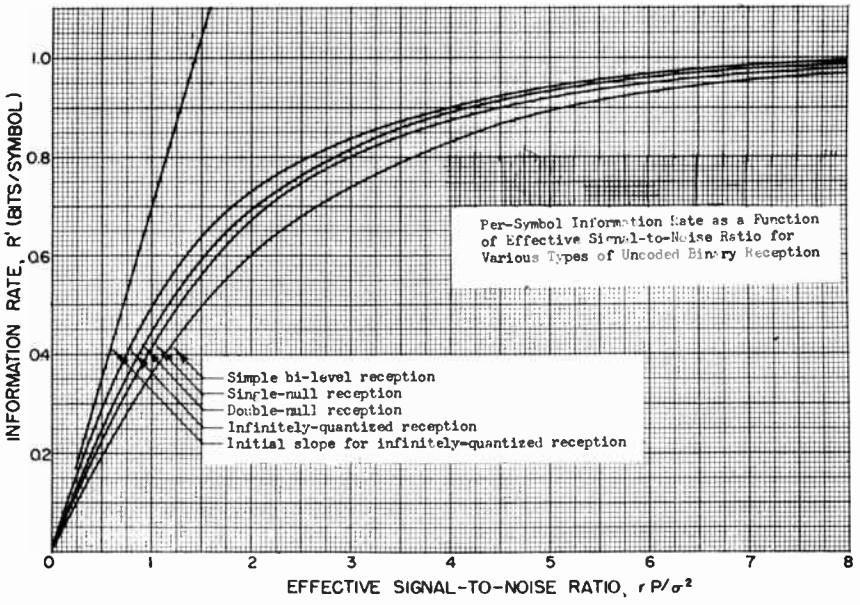

Fig. 1.

loss in generality, x_1 and x_2 may be considered to have equal amplitudes and opposite polarities. This paper will be further limited to binary symmetric transmission where the *a priori* probabilities of x_1 and x_2 will be considered equal.

At the receiver, a conventional decision device compares the incoming samples with a threshold set halfway between x_1 and x_2 and makes a corresponding bilevel decision. Such a decision, however, necessarily destroys some information, since it destroys all detailed knowledge of the noise structure, leaving no record of the sureness of the decision. It is, therefore, a matter of some interest to determine the theoretical upper limit on the amount of information which might be extracted, on the average, from a received binary symbol. This requires the assumption of an ideal decoder, which destroys no information in the process of making a decision. Such an ideal decoder, for example, would make an exact recording of the received signal; *i.e.*, employ an infinite number of receiving levels.

When the signal is transmitted at an average power P, and the noise is additive Gaussian of power σ^2 with a flat spectrum, a convenient parameter A_0 may be introduced, $A_0^2 = P/2\sigma^2$. The exact expression for the theoretical upper limit on the information rate in bits per symbol is then

$$R = \frac{-1}{\sqrt{\pi}\ln 2}\int_{-\infty}^{+\infty} du\, e^{-u^2} \ln \frac{1}{2}\left[1 + e^{-4A_0(u+A_0)}\right]. \quad (1)$$

A Taylor expansion of the nonexponential portion of the integrand yields the following result which is useful for $P/\sigma^2 \leq 0.6$.

$$R = \frac{1}{\ln 2}\left\{2A_0^2 - \ln\cosh 2A_0^2 - A_0^2\,\mathrm{sech}^2 2A_0^2 + A_0^4(3\,\mathrm{sech}^4 2A_0 - 2\,\mathrm{sech}^2 2A_0^2) + \cdots\right\}. \quad (2)$$

For larger values of P/σ^2 direct numerical integration was used, the result being shown in Fig. 1.

As a generalization, it can be shown that, if the transmitter sends each original pulse as a train of pulses r long, and if the receiver reconstructs the original pulse by integrating over the pulse train, then the information contained in a single recording of the integrated (summed) amplitudes is simply $R(rP/\sigma^2)$, that is, the same function given by (1) with P/σ^2 replaced by rP/σ^2. The quantity rP/σ^2 is plotted as the abscissa in Fig. 1 to permit the results to be interpreted either for single pulses or for an integrated series of pulses.

By way of comparison, Fig. 1 also shows the corresponding plot for the simple bilevel case. This comparison shows that an appreciable improvement in per-symbol rate is theoretically possible. More significant, perhaps, is the corresponding increase in reliability due to the decreased equivocation. Specifically, the decreased equivocation is equivalent to a saving of approximately 2 db in power.

Single-Null Reception

The preceding analysis indicates that an appreciable improvement in per-symbol information rate may be achieved by increasing the fineness of quantization at the receiver. Since decoder complexity will probably increase rapidly with an increase in the number of levels, it is logical to examine first the relatively simple three-level case. This permits the system to record "no information" whenever a guess is likely to result in wrong information. As will be seen, however, the adjustment of this null zone is important for proper operation of the system.

Consider a general binary symmetric channel where the two input levels x_1 and x_2 are transmitted with equal *a priori* probability. With a three-level decoder the received signal is assigned to one of three groups:

$$\begin{aligned} &\text{Group I} \quad y \geq k \\ &\text{Group II} \quad -k < y < k \\ &\text{Group III} \quad y \leq -k. \end{aligned} \tag{3}$$

Group I records as "x_1," Group III records as "x_2," and Group II records as "0."

Due to the symmetry of the system, and presuming the amplitude symmetry of the noise, the following relation then exists between the conditional probabilities:

$$\begin{aligned} p(\mathrm{I}/x_1) = p(\mathrm{III}/x_2), \qquad p(\mathrm{II}/x_1) = p(\mathrm{II}/x_2), \\ p(\mathrm{III}/x_1) = p(\mathrm{I}/x_2) \end{aligned} \tag{4}$$

and the expression for the rate in bits per symbol is[1]

$$\begin{aligned} R(k) = p(\mathrm{I}/x_1) \log_2 \frac{2p(\mathrm{I}/x_1)}{p(I/x_1) + p(\mathrm{III}/x_1)} \\ + p(\mathrm{III}/x_1) \log_2 \frac{2p(\mathrm{III}/x_1)}{p(\mathrm{I}/x_1) + p(\mathrm{III}/x_1)}. \end{aligned} \tag{5}$$

To justify the introduction of a single-null zone, it must be shown that this procedure can improve the information rate. Subject only to the reasonable limitation that the system be such that $p(\mathrm{I}/x_1) > p(\mathrm{III}/x_1)$, this can be demonstrated by showing, as in Appendix I, that $dR(0)/dk > 0$, for from this it necessarily follows that the rate attains a maximum at some $k > 0$.

The null adjustment at which the per-symbol rate is a maximum can be determined by setting dR/dk equal to zero. Since the derivative of the rate is

$$\begin{aligned} R'(k) = p'(\mathrm{I}/x_1) \log_2 \frac{2p(\mathrm{I}/x_1)}{p(\mathrm{I}/x_1) + p(\mathrm{III}/x_1)} \\ + p'(\mathrm{III}/x_1) \log_2 \frac{2p(\mathrm{III}/x_1)}{p(I/x_1) + p(\mathrm{III}/x_1)}, \end{aligned} \tag{6}$$

this optimum null adjustment occurs when (6) becomes zero.

Rate Improvement Due to Single-Null Reception

In order to ascertain numerically the degree of improvement that single-null reception achieves, various types of coded and uncoded systems will be considered. Since the nature of the improvement is dependent on the type of interference being combatted, two types of noise will be considered—additive Gaussian noise and peak limited noise possessing a uniform amplitude density. Both types of interference will be presumed uncorrelated at the sampling times.

Additive Gaussian Noise

Consider a binary symmetric channel where there are "r" transmitted samples per bit of information. When the interference is additive Gaussian and is uncorrelated at the sampling points, each received r-group with the same summed amplitude has the same *a posteriori* probability and thus can be combined into a single received level z.

When the null-zone boundaries are $\pm k$, a normalized signal amplitude A and a normalized boundary K can be conveniently defined as

$$A = \sqrt{\left(\frac{rP}{2\sigma^2}\right)} \quad \text{and} \quad K = \frac{k}{\sqrt{(2\sigma^2 r)}}. \tag{7}$$

The corresponding *a posteriori* probabilities are then simply (Appendix III)

$$\begin{aligned} p(\mathrm{I}/x_1) = \tfrac{1}{2}[1 + \Phi(A - K)] \\ p(\mathrm{III}/x_1) = \tfrac{1}{2}[1 - \Phi(A + K)] \end{aligned} \tag{8}$$

where $\Phi(x)$ is the error function

$$\Phi(x) = \frac{2}{\sqrt{\pi}} \int_0^x e^{-x^2} dx. \tag{9}$$

The analytic expression for the per-message-symbol rate for single-null reception can then be found from (5), while the corresponding optimum adjustment is obtained from (6).

The resulting per-symbol information rate for this optimum adjustment is shown in Fig. 1. This curve lies about midway between bilevel reception and infinite-level reception and thus indicates that in the presence of additive Gaussian noise the single-null scheme is capable of achieving about half the maximum possible improvement. Further quantization at the decoder is, of course, necessary to realize further improvement. This makes it desirable to analyze double-null reception to ascertain if a significant improvement in rate, over single-null, can be achieved.

Peak-Limited Noise with a Uniform Amplitude Distribution

It should be borne in mind, however, that the previous comparisons are based on the particular type of noise being combatted. In particular, by hypothesizing peak-limited noise with a flat distribution, it is possible to show that single-null reception is then a "natural" type of reception to employ. Indeed, in this instance, further quantization entails absolutely no further benefit.

The transmitted signal is again considered to have an average power P. It is further assumed that there are "r" transmitted pulses per bit of message information, but now the noise has a flat distribution between the peak limits of $\pm\hat{\sigma}$. The noise is presumed to be uncorrelated between sampled points.

When the peak noise power is less than the signal power, the system is capable of operation with an equivocation of zero because two clearly defined regions exist at the receiver, each of which uniquely indicates the corresponding transmitted signal. When the peak noise power exceeds the signal power, however, there are three regions at the receiver, namely

[1] C. E. Shannon, "A mathematical theory of communication," *Bell Sys. Tech. J.*, vol. 27, pp. 379–423, 623–656; 1948.

$$\begin{aligned}
&\text{Region I} && (\hat{\sigma} - \sqrt{P}) < y < (\hat{\sigma} + \sqrt{P}) \\
&\text{Region II} && -(\hat{\sigma} - \sqrt{P}) < y < (\hat{\sigma} - \sqrt{P}) \\
&\text{Region III} && -(\hat{\sigma} + \sqrt{P}) < y < -(\hat{\sigma} - \sqrt{P}). \qquad (10)
\end{aligned}$$

The significant characteristic of these regions is that the *a posteriori* probabilities are constant over the respective ranges, regions I and III uniquely indicating the transmitted signal, while region II is ambiguous. Thus there is a natural optimum boundary for the null zone, namely region II. (See Appendix II.) Furthermore, the single-null method of reception yields exactly the same rate as any larger number of levels, including the case of infinite quantization, the per-message-symbol rate being

$$R' = 1 - \left\{1 - \frac{P}{\hat{\sigma}^2}\right\}^r. \qquad (11)$$

To provide a comparison of the optimum null system with a bilevel system, the per-unit equivocation using a bilevel "integration" receiver was also determined. These results, shown in Fig. 2, indicate the advantages of single-null reception.

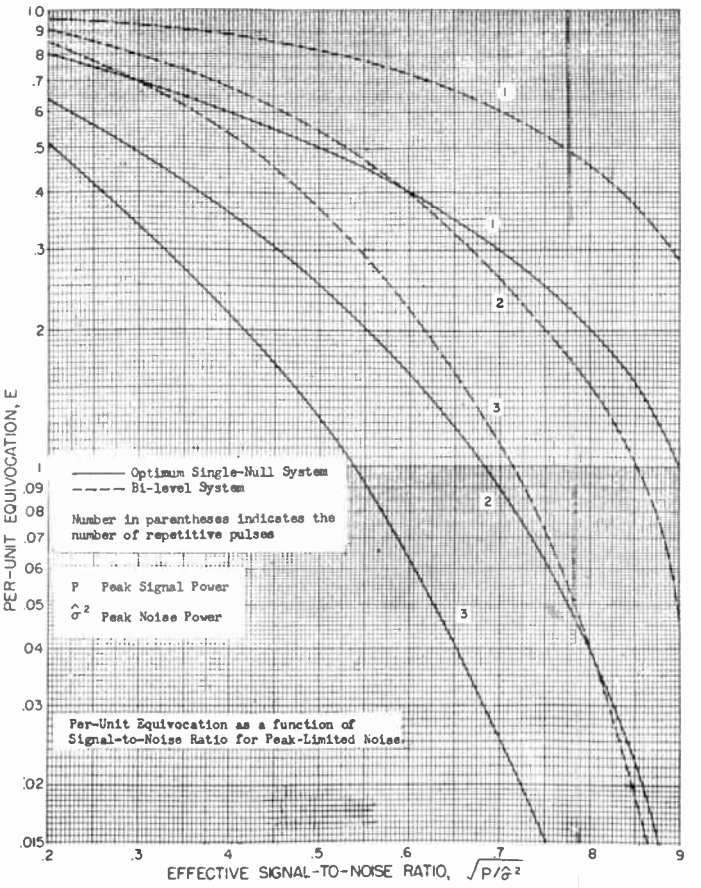

Fig. 2

Double-Null Reception

It has been demonstrated that an appreciable decrease in per-symbol equivocation can be achieved by introducing a single-null level at the receiver. The next problem is to ascertain whether the additional improvement to be expected from the introduction of still more receiver levels is sufficient to warrant the increased complexity of equipment.

Examination of Fig. 1 reveals that the single-null system yields an information rate about halfway between the simple binary and infinitely quantized cases. It is to be expected, therefore, and will be subsequently shown, that the use of further levels will, in general, produce only small additional amounts of improvement in equivocation.

However, the four-level, or double-null, case warrants investigation for at least two reasons. In the first place, for the assumed case of symmetrical transmission, it would appear to require only a moderate increase in equipment complexity, since the only basic change in the detector is the inclusion of a zero threshold to distinguish between "plus" and "minus" nulls. Increased complexity would result mostly from the greater demands on the decision device.

The second argument involves a consideration which has not been discussed yet, namely, the effect on the information rate of having the null boundaries set at other than the optimum levels. When the null zone is too large, the single-null system yields a large percentage of zeros which represents a considerable loss of information and a resulting over-all rate which is less than that of a simple binary system. The double-null system, however, would retain the essential polarity information, so that a suitable decision device could always extract at least as much message information as a simple binary decoder.

With such a four-level decoder the received signal is assigned to one of four groups:

$$\begin{aligned}
&\text{Group } A && y \geq k \\
&\text{Group } B && 0 \leq y < k \\
&\text{Group } C && -k \leq y < 0 \\
&\text{Group } D && y < -k.
\end{aligned}$$

Group A records as "x_1", Group B records as "0+," Group C records as "0−," and Group D records as "x_2." By setting 0+ and 0− equal to the zone 0, the double-null system includes the single-null system as a special case.

Due to the symmetry of the system, and presuming the symmetry of the interference, the following relations exist among the conditional probabilities.

$$\begin{aligned}
p(A/x_1) &= p(D/x_2) \qquad p(C/x_1) = p(B/x_2) \\
p(B/x_1) &= p(C/x_2) \qquad p(D/x_1) = p(A/x_2)
\end{aligned} \qquad (12)$$

whence the per-symbol information rate is

$$R(k) = p(A/x_1) \log_2 \frac{2p(A/x_1)}{p(A/x_1) + p(D/x_1)} + p(B/x_1) \log_2 \frac{2p(B/x_1)}{p(B/x_1) + p(C/x_1)}$$

$$+ p(C/x_1) \log_2 \frac{2p(C/x_1)}{p(B/x_1) + p(C/x_1)}$$
$$+ p(D/x_1) \log_2 \frac{2p(D/x_1)}{p(A/x_1) + p(D/x_1)} . \quad (13)$$

To justify the introduction of the double-null zones, it should be shown that this procedure at least improves the information rate over simple bilevel reception. As in the single-null case it can readily be established that $dR(0)/dk > 0$ and hence that the per-symbol rate achieves its maximum at $k > 0$ (Appendix I).

The setting of the null which actually achieves this maximum rate can be found from $dR/dk = 0$, where the derivative is

$$[R(k)]' = p'(A/x_1) \log_2 \frac{2p(A/x_1)}{p(A/x_1) + p(D/x_1)}$$
$$+ p'(B/x_1) \log_2 \frac{2p(B/x_1)}{p(B/x_1) + p(C/x_1)}$$
$$+ p'(C/x_1) \log_2 \frac{2p(C/x_1)}{p(C/x_1) + p(B/x_1)}$$
$$+ p'(D/x_1) \log_2 \frac{2p(D/x_1)}{p(D/x_1) + p(A/x_1)} . \quad (14)$$

Rate Improvement Due to Double-Null Reception

To determine numerically the degree of improvement that double-null reception achieves over single-null, it is necessary to assume the type of interference which is to be combatted. For convenience, the interference will again be assumed to be additive white Gaussian noise. The development of this case is then directly parallel to that for the single-null system. The corresponding transitional probabilities are

$$p(A/x_1) = \tfrac{1}{2}[1 + \Phi(A - K)]$$
$$p(B/x_1) = \tfrac{1}{2}[\Phi(A) - \Phi(A - K)]$$
$$p(C/x_1) = \tfrac{1}{2}[\Phi(A + K) - \Phi(A)]$$
$$p(D/x_1) = \tfrac{1}{2}[1 - \Phi(A + K)] \quad (15)$$

and the per-message-symbol rate for double-null reception follows from (13), while the optimum null condition follows from (14).

These relations can be solved by successive approximations to yield the curve shown in Fig. 1. This curve shows that double-null reception yields an improvement in rate over single-null reception which is equivalent to a few tenths of a db in power. The significant advantage of double-null reception, however, is not in this small improvement in rate, but rather in the fact that for any misadjustment of the null boundaries, the rate is always better than that of a simple bilevel system.

There remains the question of interpreting these extra levels at the receiver which were not present in the original transmission. For single-null reception the interpretation is clear, namely, that the conditional probabilities are too nearly alike to permit a decision. For double-null reception, however, the interpretation is not as simple. As will be later shown, this difficulty can be avoided by using double-null reception in conjunction with coded words to permit both the advantages of the better rate and the better adjustment characteristics, while maintaining an over-all single-null interpretation of the words.

Weak Signal Conditions

It is of interest to consider the behavior of these various systems at very low signal-to-noise ratios in order to permit ready comparison of the otherwise complicated relations for per-symbol rate. The procedure in each case is to expand the per-symbol rate equation by means of a Taylor's series about $A = 0$. In all cases the rate becomes proportional to the effective signal-to-noise ratio, the larger the coefficient of proportionality, the better the corresponding rate.

System	$R/(rP/\sigma^2)$	*Optimum K*
Bilevel	0.458	0
Single-null	0.585	0.43
Double-null	0.623	0.47
Infinite-level	0.721	—

It can be seen from these results that single-null reception is equivalent at low signal-to-noise ratios to a one db increase in power over a bilevel decoder, while double-null reception is only equivalent to a few tenths of a db improvement over single-null.

Effect of Variation of Null Level

The previous analysis has primarily considered the properties of the single- and double-null reception schemes when operating with the null boundaries at optimum levels. In actual practice, of course, the signal and noise levels might be expected to vary, and it would probably be impossible to maintain the null boundaries at the optimum levels. It is necessary, consequently, to examine the behavior of these systems as the null level varies. For this purpose it is convenient to introduce a new parameter Q, such that Q is the setting of the null normalized to the signal level.

$$Q = \frac{K}{A} = \frac{k}{r\sqrt{P}} . \quad (16)$$

Fig. 3 shows the variation of the null adjustment as a function of signal-to-noise ratio in the presence of additive Gaussian noise when the null is adjusted for optimum rate. To simplify the analysis, consider the system at high signal-to-noise ratios. The resulting asymptotic expression

$$\ln 2\, e^{4AK} \doteq (A + K)^2 + \ln (A + K) \quad (17)$$

indicates that in the limit as $A \to \infty$,

$$K \doteq \frac{\ln A}{A} \quad \text{or} \quad Q \doteq \frac{\ln A}{A^2} \quad (18)$$

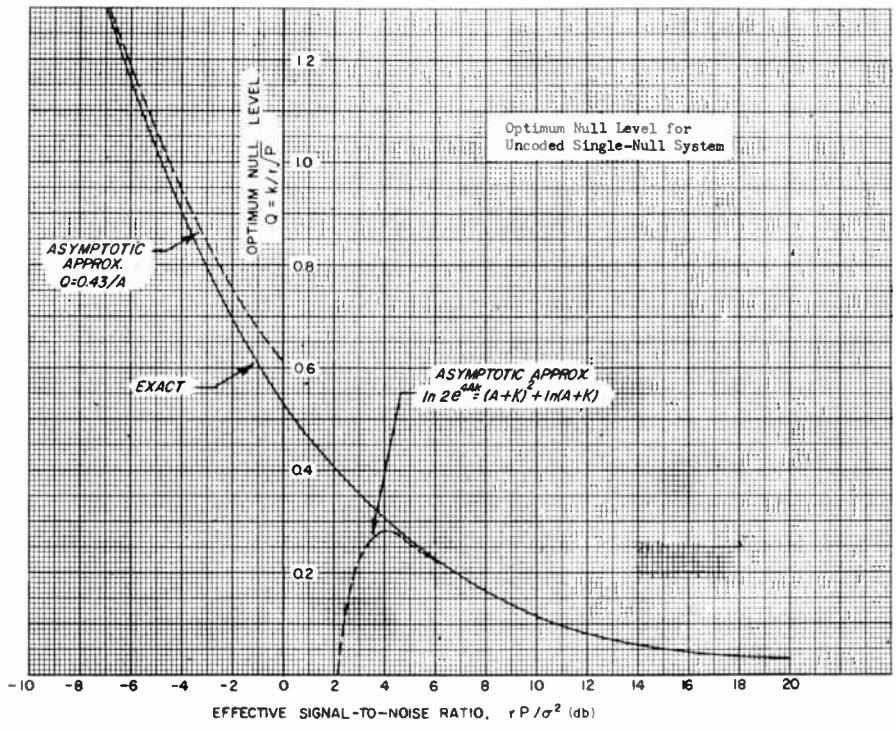

Fig. 3.

which clearly shows the monotonically decreasing character of K and Q.

On the other hand, when the signal-to-noise ratio is very small,

$$Q \doteq \frac{0.43}{A}. \tag{19}$$

Both these relations are shown in Fig. 3.

The suggestive feature of the optimum null-level curve is its monotonically decreasing characteristic with increasing signal-to-noise ratio. Consider Q fixed at a value which is optimum for some given signal-to-noise ratio. Then, for any smaller A, the null level will lie between zero and the optimum for that ratio, so that the per-unit equivocation will always be better than for an ordinary bilevel system in this range. However, for sufficiently high signal-to-noise ratios, the per-unit equivocation may become worse than for the no-null case.

That this is so is shown in Fig. 4 (opposite), where per-unit equivocation for a single-null system is plotted as a function of normalized null level for various signal-to-noise levels. From the almost parabolic character of the single-null curves near their minima, it is evident that when the null level is approximately twice its optimum value, the per-unit equivocation equals that of a system without the null. For larger K, the single-null system is actually the poorer one.

The behavior of the single-null curves at high signal-to-noise ratios can be found by using the asymptotic expression for the error function

$$\Phi(x) \doteq 1 - \frac{e^{-x^2}}{x\sqrt{\pi}}. \tag{20}$$

The asymptotic expression for the per-unit equivocation then becomes

$$E \doteq \frac{1}{2 \ln 2}\left\{\frac{\ln 2}{A(1-Q)\sqrt{\pi}}\, e^{-A^2(1-Q)^2} + \frac{A^2(1+Q)^2 + \ln A(1+Q)\sqrt{\pi}}{A(1+Q)\sqrt{\pi}}\, e^{-A^2(1+Q)^2}\right\}. \tag{21}$$

For a system without the null, $Q=0$, and the second term predominates.

$$E_0 \doteq \frac{A_0^2 + \ln A_0\sqrt{\pi}}{2A_0\sqrt{\pi}\ln 2}\, e^{-A^2}, \tag{22}$$

whereas for a single-null system $Q \neq 0$, and the first term predominates.

$$E \doteq \frac{e^{-A^2(1-Q)^2}}{2A(1-Q)\sqrt{\pi}}. \tag{23}$$

When the signal-to-noise ratio is very high, the exponents dominate, and E and E_0 have the same value when

$$A(1-Q) = A_0.$$

This means that, to achieve the same per-unit equivocation, the null system requires an increase in power by the factor $1/(1-Q)^2$ as compared with the no-null system, for very high signal-to-noise ratios. In effect, the introduction of a constant null level into an uncoded system increases the effective signal-to-noise ratio at low levels, but decreases it at large signal-to-noise ratios.

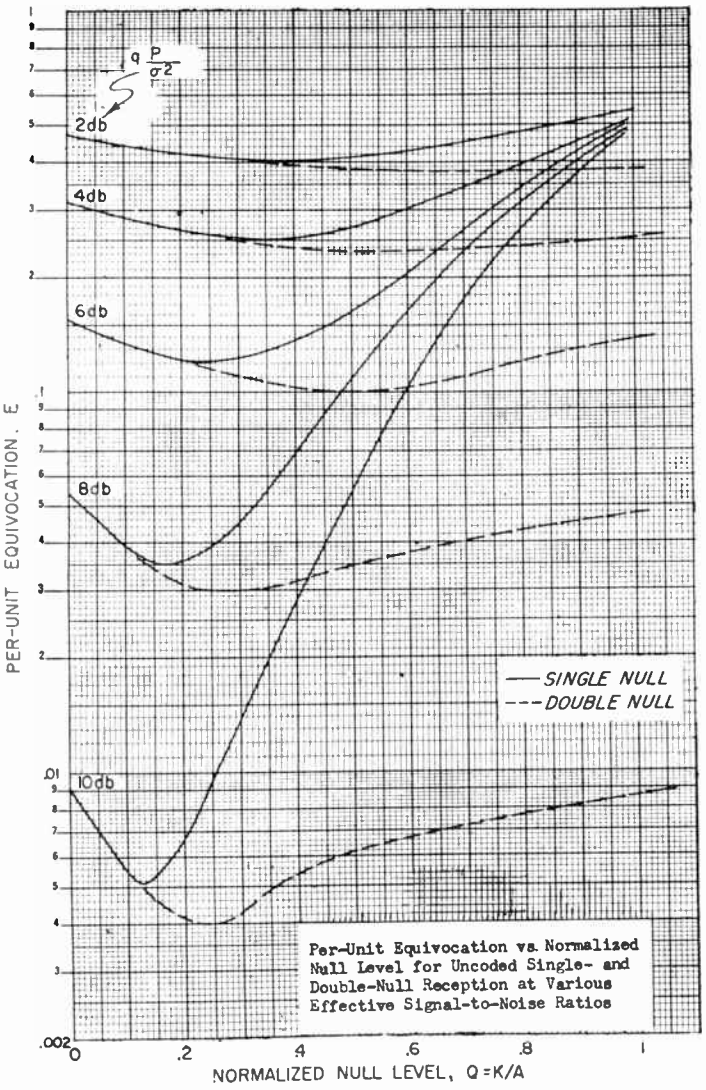

Fig. 4.

Single-null reception is thus seen to be capable of reducing per-unit equivocation, but it suffers from an unfortunate weakness—the sensitivity of the per-unit equivocation to the null level. The improvement is diminished appreciably, if the null boundary strays very far from the optimum, and can actually become a deterioration, if the null level becomes excessively high relative to the signal level for a given level of noise. There is no minimum fixed null level which can be used with a resultant improvement at all signal-to-noise ratios.

This is traceable to the fact that, in exchange for knowing where the most probable errors lie, the system destroys some of the information which would be available in simple binary reception. That is, a null gives no indication at all as to the probable sign of the original pulse, whereas in simple binary reception a weak pulse is recorded in accordance with the greater *a posteriori* probability, no matter how slight the difference. This characteristic of single-null reception is most troublesome in situations where a large number of nulls occur. Introduction of a double null, or split null, eliminates this difficulty.

Fig. 4 also shows the E vs Q characteristics of the double-null system. An immediate conclusion from these curves is that the per-unit equivocation of a double-null system is always better than or equal to that of a no-null system, for the same signal-to-noise ratio. This is because the null is split in two, and the polarity recorded, so that at least all of the information contained in a simple binary system is retained. This is in contrast to single-null reception, where misadjustment of the null level may destroy more information than is preserved by the presence of the null.

The per-symbol information rates of both single- and double-null systems are derived on the assumption that each received symbol is simply recorded as falling in one of the several established groups of levels. No further decision is implied. Because of the nulls, most of the errors that would be made with simple binary reception are avoided, and symbols received with a large degree of ambiguity are recorded as nulls. The information rate is improved, because no information at certain points is better than misinformation at these points.

It is clear that further benefit will accrue from such systems when two-way transmission is possible. Knowledge of the location of errors in the received message permits efficient systems for requesting selective retransmission to be developed. The double-null system offers a marked advantage over the single-null system here, in that the nulls are recorded with polarities, indicating at all times which *a posteriori* probability is greater. Hence decision can be made, when necessary, on the basis of the nulls.

Hamming Single-Error-Detecting Codes Modified by Null Reception

Binary transmissions are usually concerned, not with individual pulses, but rather with groups of pulses representing binary numbers or symbols of some alphabet. Hence the following analysis will deal with m-digit "words," where equivocation will be calculated on the basis of whether or not the word, as an entity, is properly interpreted and recorded.

Consider a Hamming code[2] of m message digits plus one additional digit for parity check. Normally, the presence of the extra digit permits the detection of single errors in the $(m+1)$-digit group. When the parity check fails, the m-digit word is not printed.

The registration of single nulls permits the single parity check to be used, not only for single error detecting, but, substantially, for single error correcting as well. Thus, if a single digit of the $(m+1)$ digits is registered as a null, the parity check is used to fill in the null, and the resultant word is printed. When two or more nulls are received, the word is not printed. When none of the

[2] R. W. Hamming, "Error detecting and error correcting codes," *Bell Sys. Tech. J.*, vol. 29, pp. 147–160; 1950.

digits are nulls, the word is printed if and only if parity checks.

The symbols q, p, and u are defined as the probabilities that the word is printed correctly, printed incorrectly, or not printed, respectively. These are related by

$$q + p + u = 1. \tag{24}$$

Similarly, q_0, p_0, and u_0 represent the corresponding single-digit probabilities of being correct, incorrect, or receiving a null. In the presence of additive Gaussian noise having a flat spectrum these become

$$\begin{aligned} q_0 &= \tfrac{1}{2}[1 + \Phi(A - K)] \\ p_0 &= \tfrac{1}{2}[1 - \Phi(A + K)] \\ u_0 &= \tfrac{1}{2}[\Phi(A + K) - \Phi(A - K)]. \end{aligned} \tag{25}$$

Assume that all permutations of the m-message digits are included in the group of words, or alphabet, which may be sent. Let Q_r represent the probability that a transmitted word will be received as another word r distance away. Since this requires the misinterpretation of an even number of digits, r is even. If no nulls are received, this misinterpretation can occur only when r errors are made. A misinterpretation may also occur, when one null is received, if r additional errors are made plus a correct interpretation of the null or if $(r-1)$ errors are made plus an incorrect interpretation of the null. Therefore,

$$\begin{aligned} Q = {} & q_0{}^{m+1-r}p_0{}^r + (m + 1 - r)q_0{}^{m-r}u_0p_0{}^r \\ & + rq_0{}^{m+1-r}u_0p_0{}^{r-1}. \end{aligned} \tag{26}$$

The corresponding number of words r distance away from the transmitted word is

$$\frac{(m + 1)!}{r!(m + 1 - r)!}.$$

When the input messages are equally probable and the noise is symmetrical, the output messages are also equally probable, and

$$\begin{aligned} p(x) &= 2^{-m} \\ p(y) &= (1 - u)2^{-m} = (p + q)2^{-m} \end{aligned}$$

where

$$(p + q) = \sum_{r=0,2,\cdots}^{m} \frac{(m + 1)!}{r!(m + 1 - r)!} Q_r. \tag{27}$$

The information rate in bits per word is then

$$\begin{aligned} R = {} & m(p + q) - (p + q)\log_2 (p + q) \\ & + \sum_{r=0,2,\cdots}^{m} \frac{(m + 1)!}{r!(m + 1 - r)!} Q_r \log_2 Q_r. \end{aligned} \tag{28}$$

Figs. 5 and 6 show the calculated per-unit equivocation characteristics of a two- and five-message-digit, single parity check code, in the presence of additive Gaussian noise, when single-null reception is employed. For comparison with bilevel reception it should be noted that a zero-null level corresponds to conventional binary reception.

The significant feature of these curves is that a minimum per-unit equivocation is obtained at some optimum setting of the null. Overadjusting the null zone boundaries to twice optimum yields a rate comparable with bilevel reception. Further overadjustment actually results in the destruction of information and a system which is poorer than a bilevel system.

In order to investigate analytically the characteristics of the optimum null adjustment, consider the system at high signal-to-noise ratios where the probability of multiple errors or multiple nulls is small. Then

$$Q_0 \gg Q_2 \gg Q_4 \cdots$$

and the information rate approaches

$$R \doteq mQ_0 \doteq mq. \tag{29}$$

The procedure of choosing a null level so as to maximize q or minimize $(u+p)$ is therefore equivalent, at high signal-to-noise ratios, to maximizing the information rate. This is particularly important from a computational point of view, because of the difficulty of handling the expressions required for maximizing the rate directly. Differentiating the expression for q results in

$$\frac{q_0'}{p_0'} \doteq \frac{q_0}{mu_0} \tag{30}$$

or, when additive Gaussian noise is present,

$$\exp(4AK) \doteq \frac{1 + \Phi(A - K)}{m[\Phi(A + K) - \Phi(A - K)]}. \tag{31}$$

From Figs. 5 and 6 (opposite) it can be seen that the procedure of maximizing q to maximize the rate yields a null level which is quite close to that corresponding to the minimum per-unit equivocation. At high signal-to-noise ratios, where the minimum is sharper, the expression is more accurate, while at low signal-to-noise ratios, where the discrepancy is greater, the curves are flatter in the region of the minima, and this reduces the significance of the discrepancy.

At high signal-to-noise ratios, the optimizing relation becomes

$$e^{4AK} \doteq \frac{2(A - K)\sqrt{\pi}}{m} e^{(A-K)^2} \tag{32}$$

which, since the exponents dominate when A is large, yields

$$4AK \doteq (A - K)^2 \tag{33}$$

or in numerical form,

$$Q = \frac{K}{A} \doteq (3 - 2\sqrt{2}) = 17.2 \text{ per cent.} \tag{34}$$

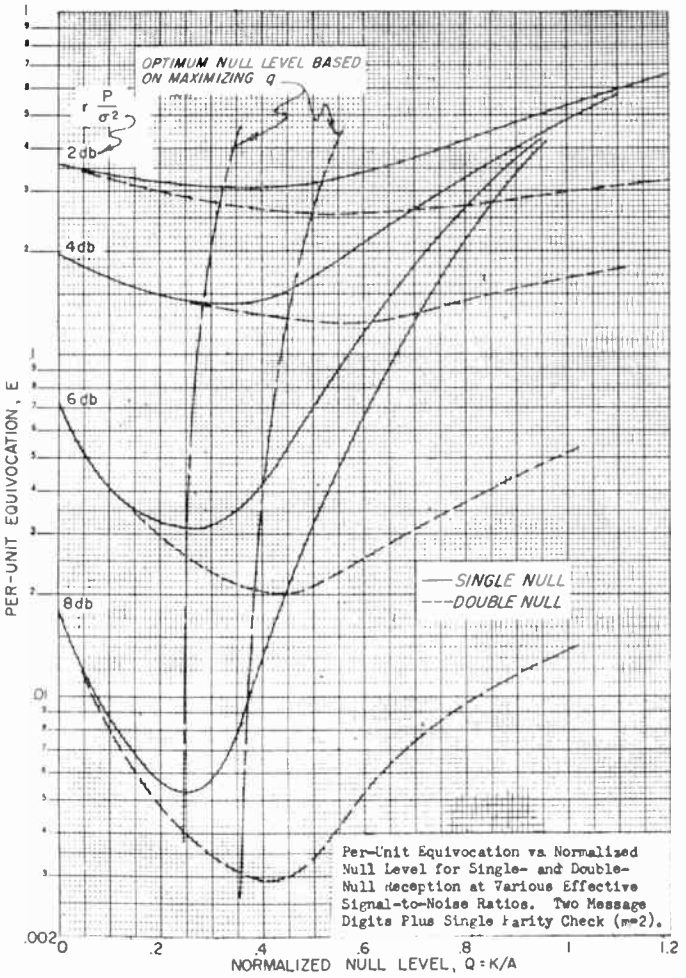

Fig. 5.

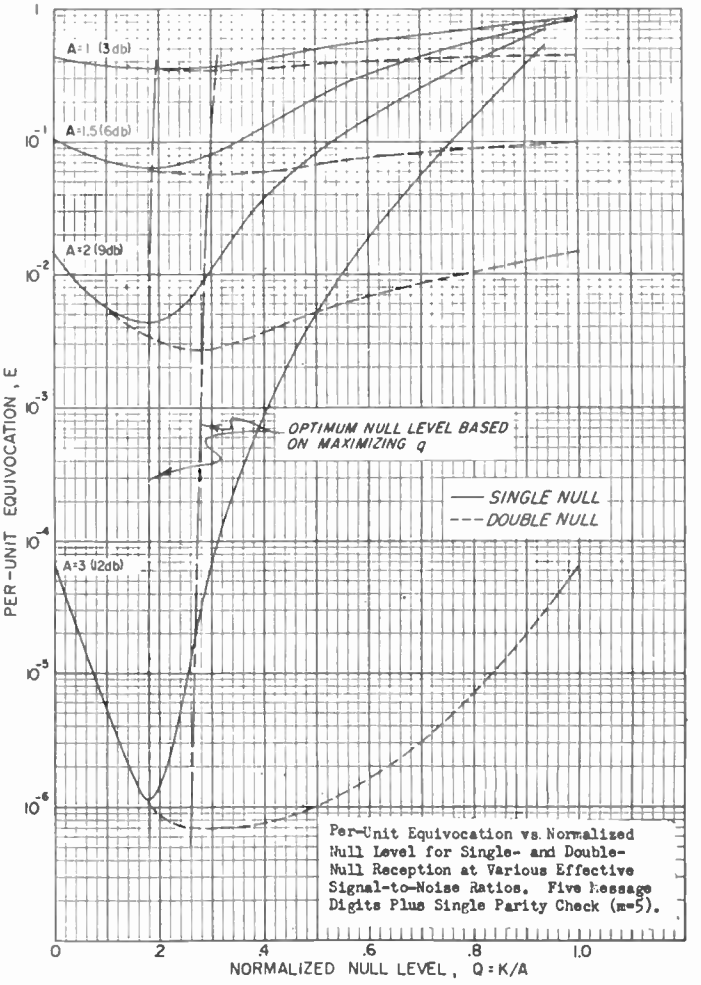

Fig. 6.

By comparing the expressions for u_0 and p_0 at high signal-to-noise ratios and at the optimum adjustment the interesting result is obtained that

$$\ln p_0 \doteq \ln \mu_0^2. \tag{35}$$

In effect, therefore, the optimum rate occurs, at high signal-to-noise ratios, when the null is adjusted so that the probability of a word having only one digit in error is equal to the probability of a word having two nulls.

The result of the optimum adjustment on the per-unit equivocation can be determined by expanding in a double Taylor expansion in u_0 and p_0

$$E \doteq (m+1)p_0 + \frac{m(m+1)}{2} u_0^2 + \cdots. \tag{36}$$

The optimum adjustment thus results in the per-unit equivocation being proportional to u_0^2 or,

$$-\ln E \doteq 2(A-K)^2$$

or

$$-\ln E \doteq 8(3-2\sqrt{2})A^2 \tag{37}$$

Without null reception, the per-unit equivocation is

$$E \doteq (m+1)p_0$$

or

$$-\ln E \doteq A^2. \tag{38}$$

The introduction of the single null zone thus represents an equivalent 1.4 db improvement in signal-to-noise ratio.

Equally significant as previously noted, is that, at high signal-to-noise ratios Q approaches $(3-\sqrt{8})$, or 17.2 per cent. This means that if the null level is fixed at 17.2 per cent of the effective peak voltage $r\sqrt{P}$, the per-unit equivocation will always be better than that for the system without a null. This is true for all signal-to-noise ratios and any number of message digits. This behavior is in sharp contrast to the system without a parity check, where no such lower bound exists. The single-null system nevertheless retains its characteristic disadvantage—namely, the misadjustment of the null level to too high a value can result in a situation where less information is received than in the corresponding simple binary case.

With double-null reception this is not true. As will be shown, the per-unit equivocation is always better than that of the system without nulls for any setting of the null level. Thus, if the sensitivity of the single-null system to the null-level setting proves to be a problem

in certain types of operational situations, double-null reception offers a straightforward solution.

With double-null reception the interpretation of the received signal is identical to that for single-null reception except when multiple nulls are received. Then, instead of always not printing the word, the word is printed if parity checks the digits indicated by the polarity of the nulls. As before, q_0 and p_0 represent the probabilities of receiving correct and incorrect digits, while q_1 and p_1 represent the probabilities of receiving the corresponding nulls. Then, in the presence of additive Gaussian noise,

$$\begin{aligned} q_0 &= \tfrac{1}{2}[1 + \Phi(A - K)] \\ q_1 &= \tfrac{1}{2}[\Phi(A) - \Phi(A - K)] \\ p_1 &= \tfrac{1}{2}[\Phi(A + K) - \Phi(A)] \\ p_0 &= \tfrac{1}{2}[1 - \Phi(A + K)]. \end{aligned} \tag{39}$$

Here interpretation of a transmitted word as another word r distance away is possible if parity checks the word indicated by any combination of nulls and digits with r errors. Misinterpretation is also possible, when only one null is received, if r incorrect digits are present and the null is altered from an incorrect null to a correct digit, or if $(r-1)$ incorrect digits are present and the null is altered from a correct null to an incorrect digit. Therefore, the probability of transmitting one word and receiving another r distance away is

$$\begin{aligned} Q_r = {} & (q_0 + q_1)^{m+1-r}(p_0 + p_1)^r + (m + 1 - r)q_0^{m-r}p_0p_1 \\ & + rq_0^{m+1-r}p_0^{r-1}q_1. \end{aligned} \tag{40}$$

The relation for the corresponding information rate in terms of Q_r is the same as that given for single-null reception. This relation is shown in Figs. 5 and 6 to permit ready comparison with single-null and bilevel reception. As previously stated, it is to be noted that the per-unit equivocation of a double-null system is always better than the single bilevel system or even the single-null system for all signal-to-noise ratios and all null settings.

Again, to examine analytically the behavior of the optimum null adjustment, consider the system at a high signal-to-noise ratio where the probability of multiple errors, or multiple nulls per word is small

$$Q_0 \gg Q_2 \gg Q_4 \cdots.$$

As for the single null analysis, the information rate then approaches

$$R \doteq mQ_0 \doteq mq. \tag{41}$$

Hence for double-null reception, as for single-null, the procedure of approximating the null level which maximizes the rate by choosing a null level which maximizes q is sound. Differentiating the expression for q yields

$$\frac{q_0'}{p_1'} = -\frac{q_0}{mp_1} \tag{42}$$

or, in the presence of additive Gaussian noise,

$$\exp(4AK) = \frac{1 + \Phi(A - K)}{m[\Phi(A + K) - \Phi(A)]}. \tag{43}$$

This relationship for the optimum null level, based on optimizing q, is not the same as for the single-null system, the optimum null level for the double-null system being higher than that for the single-null. In particular, at high signal-to-noise ratios this expression reduces to

$$e^{4AK} \doteq \frac{2A\sqrt{\pi}}{m}e^{A^2}. \tag{44}$$

Whence, for large A, since the exponents predominate,

$$Q = \frac{K}{A} \doteq 1/4. \tag{45}$$

To understand better the effect of this choice of null level, note that the digital probabilities, at high signal-to-noise ratio and at the optimum adjustment, correspond to setting

$$\ln p_0 \doteq \ln q_1p_1 \tag{46}$$

and hence the optimum adjustment closely corresponds to adjusting p_0 to approximately q_1p_1. Based on this adjustment the per-unit equivocation becomes

$$E \doteq (m + 1)(p_0 + mq_1p_1) \tag{47}$$

or

$$-\ln E \doteq \frac{25A^2}{16}.$$

The introduction of the double null zone, therefore, represents an equivalent 1.9 db improvement in power over bilevel reception or a 0.5 db improvement over single-null reception.

Fig. 7 shows the comparison of the per-unit equivocations of several five-message-digit binary systems. To compare the uncoded system with the ones employing a single parity check, the digit pulses are considered to be lengthened by $(m+1)/m$, to equalize the noise-free transmission rates. The interfering noise is assumed to be white. This corresponds, therefore, to an effective increase in the signal-to-noise power ratio of the uncoded system by the factor $(m+1)/m$.

The probability, Q_r, of receiving a word r distance away from the word transmitted is, for the uncoded cases,

$$Q_r = q_0^{m-r}p_0^r \tag{48}$$

and the per-word information rate then becomes, for equal input probabilities

$$R = m + \sum_{r=0}^{m} \frac{m!}{r!(m - r)!} Q_r \log_2 Q_r. \tag{49}$$

The important conclusions to be drawn from these curves are these. The introduction of single-null reception greatly improves the effectiveness of the single

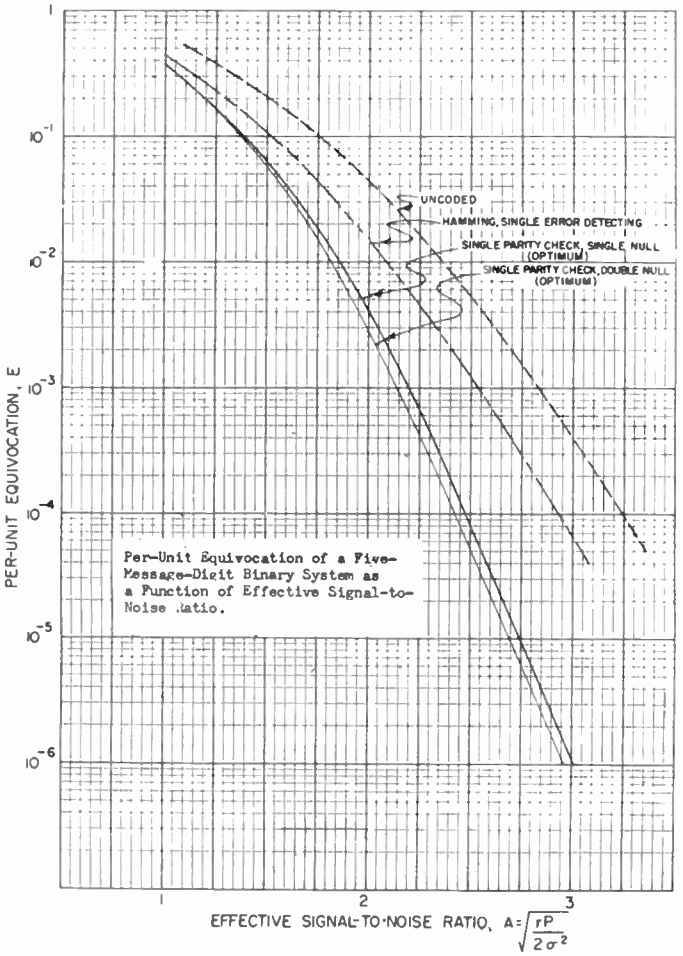

Fig. 7.

parity check. Double-null reception provides only a small additional improvement in per-unit equivocation. But if difficulties are encountered with single-null reception because of the sensitivity of the per-unit equivocation with respect to the setting of the null level, double-null reception offers a considerable advantage in this regard.

Appendix I

Proof that for a General Binary System with Single- or Double-Null Indication the Maximum Rate Occurs for $k>0$

The double-null relation will be considered first. If the received signal is considered a continuous variable and the noise is additive-symmetrical with a distribution p_n,

$$\begin{aligned} p(A/x_1) &= \int_k^\infty p_n(y-x_1)dy = \int_{k-x_1}^\infty p_n(z)dz \\ p(B/x_1) &= \int_0^k p_n(y-x_1)dy = \int_{-x_1}^{k-x_1} p_n(z)dz \\ p(C/x_1) &= \int_{-k}^0 p_n(y-x_1)dy = \int_{-k-x_1}^{-x_1} p_n(z)dz \\ p(D/x_1) &= \int_{-\infty}^{-k} p_n(y-x_1)dy = \int_{-\infty}^{-k-x_1} p_n(z)dz. \end{aligned} \quad (50)$$

Therefore, at $k=0$

$$\begin{aligned} p'(A/x_1) &= p'(D/x_1) = -p_n(-x_1) \\ p'(B/x_1) &= p'(C/x_1) = p_n(-x_1). \end{aligned} \quad (51)$$

Presuming that

$$\frac{p(B/x_1)}{p(C/x_1)} \to 1 \text{ as } k \to 0$$

it follows from (14) that

$$[R(0)]' = -p_n(-x_1)\log_2 \frac{4p(A/x_1)p(D/x_1)}{[p(A/x_1)+p(D/x_1)]^2}. \quad (52)$$

But from

$$[P(A/x_1) - P(D/x_1)]^2 > 0, \qquad p(A/x_1) \neq P(D/x_1)$$
$$[P(A/x_1) + P(D/x_1)^2]^2 > 4p(A/x_1)p(D/x_1)$$

so that

$$[R(0)]' > 0 \text{ if } p_n(-x_1) \neq 0. \quad (53)$$

For single-null reception the analogous relation

$$[R(0)]' = -p_n(-x)\log_2 \frac{4p(\mathrm{I}/x_1)\,p(\mathrm{III}/x_1)}{[p(\mathrm{I}/x_1)+p(\mathrm{III}/x_1)]^2} \quad (54)$$

is obtained. Whence it must follow that

$$[R(0)]' > 0 \text{ if } p_n(-x_1) \neq 0 \quad (55)$$

for both single- and double-null reception.

Appendix II

Analysis of Binary Single-Null-Level Reception in the Presence of Peak-Limited Noise with Flat Distribution

The transmitted samples are considered to have amplitudes of $+\sqrt{P}$ or $-\sqrt{P}$. It is assumed that there are r transmitted pulses per bit of message information and that the noise has a flat distribution between the peak limits $\pm\hat{\sigma}$.

If $\hat{\sigma}^2$ is smaller than P, the equivocation is zero and the solution is trivial. It is only necessary to consider the case where $\hat{\sigma}^2 > P$.

The *a posteriori* probability that $+\sqrt{P}$ was sent after receiving the y_i's is

$$p(\sqrt{P}/(y_1 \cdots y_r)\prod_{i=1}^{r} dy_i$$

$= 1$, if one or more y_i's are larger than $\hat{\sigma}-\sqrt{P}$

$= 1/2$, if all are in range $-(\hat{\sigma}-\sqrt{P}) < y_i < (\hat{\sigma}-\sqrt{P})$

$= 0$, if one or more $y_i < -(\hat{\sigma}-\sqrt{P})$. (56)

Thus, when arranged in accordance with their *a posteriori* probabilities, all possible received signals fall into three distinct ranges. Let these ranges be denoted by $+1$, 0, -1, respectively. If $+\sqrt{P}$ is transmitted, the conditional probability that all y_i's are in the range $|y_i| < (\hat{\sigma}-\sqrt{P})$ is

$$p(0/\sqrt{P}) = \left(1 - \sqrt{\frac{P}{\hat{\sigma}^2}}\right)^r. \tag{57}$$

Since it is not possible for any y_i to be more negative than $-(\hat{\sigma}-\sqrt{P})$,

$$p(-1/\sqrt{P}) = p(+1/-\sqrt{P}) = 0$$

$$p(+1/\sqrt{P}) = p(-1/-\sqrt{P}) = 1 - \left(1 - \sqrt{\frac{P}{\hat{\sigma}^2}}\right)^r. \tag{58}$$

Evidently, these three levels are natural optimum levels for indicating $+1$, 0, and -1. The net received information per message bit is

$$R = 1 - \left(1 - \sqrt{\frac{P}{\hat{\sigma}^2}}\right)^r. \tag{59}$$

To provide a comparison with the above optimum system, the per-unit equivocation of an "integration" system without a null level is calculated as follows. The integration system is defined such that, if $\sum_i y_i$ is positive, the receiver registers "$+1$" and, if $\sum_i y$ is negative, a "-1" is registered.

When the transmitted signal is $+\sqrt{P}$, the registration would be wrong if $\sum_i y<0$. Let a new set of variables z_i be defined such that $z_i=y_i-\sqrt{P}$. The possible values of z_i are in the range $|z_i| \leq \hat{\sigma}$. The condition for an erroneous registration when $a+\sqrt{P}$ is transmitted is

$$\sum_{i=1}^{r} z_i < -r\sqrt{P}. \tag{60}$$

For $r=1$, the probability for wrong registration is

$$p(-1/\sqrt{P}) = \frac{\hat{\sigma}-\sqrt{P}}{2\hat{\sigma}} = \frac{1}{2}\left(1 - \sqrt{\frac{P}{\hat{\sigma}^2}}\right). \tag{61}$$

For $r=2$, $p(0/+\sqrt{P})$ can be calculated by geometric means. The area of possible reception is shown as a square in Fig. 8. The boundary for registration is $z_1+z_2=-2\sqrt{P}$ and is a straight line. The area for wrong registration is heavily shaded in Fig. 8. Hence,

$$p(-1/\sqrt{P}) = \frac{\text{Heavily shaded area}}{\text{Total area}} = \frac{1}{2}\left(1 - \sqrt{\frac{P}{\hat{\sigma}^2}}\right)^2. \tag{62}$$

For $r>2$, $p(-1/+\sqrt{P})$ can be obtained from geometrical considerations in r-dimensional space. The space of possible registration is an r-dimensional cube of length $2\hat{\sigma}$ on each side. The space of wrong registration is a corner cut off from the r-dimensional cube by the $(r-1)$-dimensional hypersurface $\sum_{i=1}^{r} z_i=-r\sqrt{P}$. If P is in the range

$$\hat{\sigma}^2 > P > \left(\frac{r-2}{r}\right)^2 \hat{\sigma}^2,$$

the volume of the erroneous corner can be easily calculated. It is

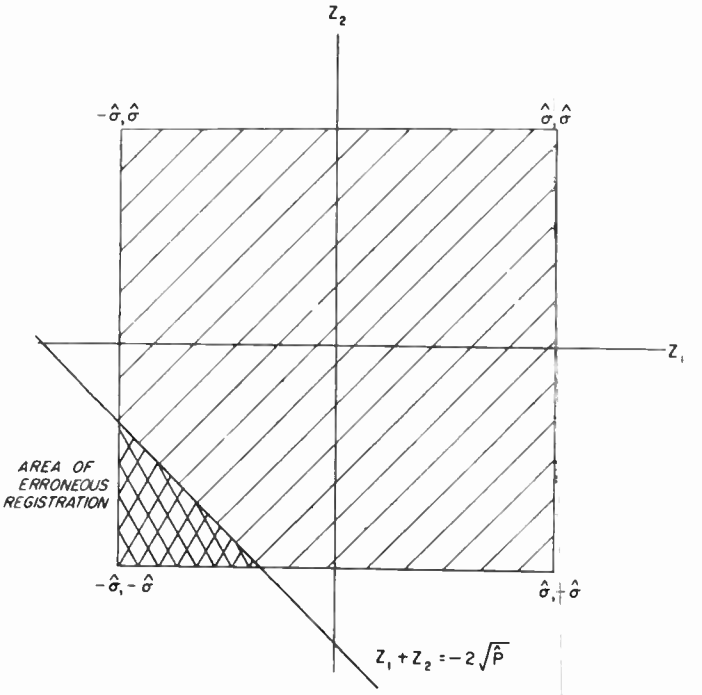

Geometrical Model of Received Signals for q = 2 (Peak Limited Noise)

Fig. 8.

$$\text{Vol}\,(-1/\sqrt{P}) = \frac{r^r}{r!}(\hat{\sigma}-\sqrt{P})^r \tag{63}$$

Therefore,

$$p(-1/\sqrt{P}) = \frac{\text{Vol}\,(-1/\sqrt{P})}{\text{Total volume}} \tag{64}$$

or,

$$p(-1/\sqrt{P}) = \left(\frac{r}{2}\right)^r \cdot \frac{1}{r!}\left\{1 - \sqrt{\frac{P}{\hat{\sigma}^2}}\right\}^r. \tag{65}$$

For smaller values of P, say for

$$r > 4 \text{ and } \left(\frac{r-2}{r}\right)^2 > \left(\frac{P}{\hat{\sigma}^2}\right) > \left(\frac{r-4}{r}\right)^2 \tag{66}$$

the results for $p(-1/\sqrt{P})$ are similar to that of relation (65) except the additional term

$$\left(\frac{r}{2}\right)^r \cdot \frac{1}{r!}\left[r\left(\frac{r-2}{r} - \sqrt{\frac{P}{\hat{\sigma}^2}}\right)^r\right] \tag{67}$$

must be subtracted. In a similar manner for

$$r > 6 \text{ and } \left(\frac{r-4}{r}\right)^2 > \left(\frac{P}{\hat{\sigma}^2}\right) > \left(\frac{r-6}{r}\right)^2 \tag{68}$$

the results of $p(-1/\sqrt{P})$ are similar to that for the condition (66) except a further additional term

$$\left(\frac{r}{2}\right)^r \frac{1}{r!}\left[\frac{r(r-1)}{2}\left(\frac{r-4}{r} - \sqrt{\frac{P}{\hat{\sigma}^2}}\right)^r\right] \tag{69}$$

must be added. These results may be compactly written in a form that holds for all r

$$p(-1/\sqrt{P}) = \left(\frac{r}{2}\right)^r \cdot \frac{1}{r!}\sum_{s=0}^{s_m}(-1)^s \frac{r!}{s!(r-s)!} \tag{70}$$

$$\cdot\left[\frac{r-2s}{r}-\sqrt{\frac{P}{\hat{\sigma}^2}}\right]^r$$

where

$$s_m \leq \frac{r}{2}\left(1-\sqrt{\frac{P}{\hat{\sigma}^2}}\right). \tag{71}$$

Knowing $p(-1/\sqrt{P})$ the per-unit equivocation can be calculated from

$$p(+1/\sqrt{P}) = 1 - p(-1/\sqrt{P}) \tag{72}$$

by the relation

$$E = -\,p(+1/\sqrt{P})\log_2 p(+1/\sqrt{P}) - p(-1/\sqrt{P})\log_2(-1/\sqrt{P}). \tag{73}$$

It has been called to the authors' attention that (70) also can be obtained by integrating the formula found on p. 260 of Laplace's "Theorie Analytique des Probabilities," Livre II, Paris; 1820.

Appendix III

Analysis of Binary Single-Null-Level Reception in the Presence of Additive Gaussian Noise with a Flat Spectrum

The transmitted samples are considered to have amplitudes of $+\sqrt{P}$ and $-\sqrt{P}$. It is assumed that there are r transmitted pulses per bit of message information and that the noise has a Gaussian amplitude distribution of power σ^2.

If the received value of the ith repeat is y_i, then the probability that the received signal is in the range from y_1 to y_1+dy_1, y_2 to y_2+dy_2, $\cdots$, y_r to y_r+dy_r is

$$p(y_1\cdots y_r/\sqrt{P})\prod_{i=1}^{r} dy_i = (2\pi\sigma^2)^{-r/2}\prod_{i=1}^{r} dy_i \exp\left[\frac{-1}{2\sigma^2}\sum_{i=1}^{r}(y_i-\sqrt{P})^2\right]. \tag{74}$$

A similar expression can be obtained for

$$p(y_1\cdots y_r/-\sqrt{P}).$$

If the received values are y_i the probability that $+\sqrt{P}$ was sent is

$$\prod_{i=1}^{r} dy_i p(+\sqrt{P}/y_1\cdots y_r) = \frac{p(y_1\cdots y_r/\sqrt{P})}{p(y_1\cdots y_r/\sqrt{P})+p(y_1\cdots y_r/-\sqrt{P})} = \frac{1}{1+\exp\left[\dfrac{-2\sqrt{P}}{\sigma^2}\displaystyle\sum_{i=1}^{r} y_i\right]}. \tag{75}$$

Thus groups with the same received $\sum_{i=1}^{r} y_i$ level have the same *a posteriori* probabilities and may be combined into the same z level,

$$z = \sum_{i=1}^{r} y_i. \tag{76}$$

The total probability that, if the transmitted signal is $+\sqrt{P}$, the received signal is in level z to $z+dz$ is

$$p(z/\sqrt{P}) = \int\int\int\cdots\int \prod_{i=1}^{r} dy_i p(y\cdots y_r/\sqrt{P}) \tag{77}$$

where $\sum_{i=1}^{r} y_i$ lies between z and $z+dz$.

This integration is taken over a hyper plane of thickness dz and can readily be integrated by a change of coordinates.

The summation

$$\sum_{i=1}^{r}(y_i-\sqrt{P})^2 \tag{78}$$

is the square of the distance from the point $(y_1, y_2, \cdots, y_r)$ to the point $(\sqrt{P}, \sqrt{P}, \cdots, \sqrt{P})$. If a new set of orthogonal coordinates, $u_1, u_2, \cdots, u_r$ are defined such that u_1 goes through the point $(\sqrt{P}, \sqrt{P}, \cdots, \sqrt{P})$, then the projection of the point $(y_1, y_2, \cdots, y_r)$ on the u_1 coordinate is

$$u_1 = \frac{1}{\sqrt{r}}\sum_{i=1}^{r} y_i. \tag{79}$$

The signal point is now located, on the new coordinate system, at $(\sqrt{rP}, 0, 0, \cdots, 0)$. As distance and volume are invariant for a change in coordinates

$$\sum_{i=1}^{r}(y_i-\sqrt{P})^2 = (u_1-\sqrt{rP})^2 + \sum_{i=1}^{r} u_i^2 \tag{80}$$

and

$$\prod_{i=1}^{r} dy_i = \prod_{i=1}^{r} du_i. \tag{81}$$

Substituting into (77)

$$p(z/\sqrt{P}) = \frac{1}{\sqrt{2\pi r\sigma^2}}\exp\left[\frac{-1}{2r\sigma^2}(z-r\sqrt{P})^2\right]. \tag{82}$$

Thus,

$$p(\mathrm{I}/\sqrt{P}) = \int_k^\infty p(z/\sqrt{P})dz = \tfrac{1}{2}[1+\Phi(Y_1)] \tag{83}$$

where

$$Y_1 = \frac{r\sqrt{P}-k}{\sqrt{2r\sigma^2}}$$

and $\Phi(Y)$ is the error function.

Similarly,

$$p(\mathrm{III}/\sqrt{P}) = \tfrac{1}{2}[1-\Phi(Y_2)]$$

where

$$Y_2 = \frac{r\sqrt{P}+k}{\sqrt{2r\sigma^2}}. \tag{84}$$

Using these relations both the rate and the optimum null adjustment can be obtained from (5) and (6).

Back Scattering from Water and Land at Centimeter and Millimeter Wavelengths*

C. R. GRANT†, MEMBER, IRE, AND B. S. YAPLEE†, MEMBER, IRE

Summary—**The back scattering from water and several land terrains has been measured at wavelengths of 3.2 cm, 1.25 cm, and 8.6 mm using vertical polarization only. σ°, the average radar cross section of water or land echo per unit area of the surface, has been plotted as a function of the angle of incidence for the three wavelengths. A family of curves at each of the three wavelengths shows the change in σ° with wind velocity for the water surface. σ° is also shown as a function of the angle of incidence for several land terrains. In general, σ° increases with frequency and also with wind velocity in the case of the water surface.**

Introduction

CONSIDERABLE WORK has been done in the past on measurements of back scattering from the sea at frequencies below 10 kmc.[1,2] Most of the data has been for grazing angles, and pulsed radars have been used. Recently, quantitative data have been obtained at frequencies as high as 48.7 kmc using cw Doppler radar.[2] In this work the back scattering was measured for large depression angles and for vertical incidence.

To obtain quantitative data on the back scattering from both land and sea an extensive study has been made of the scattering coefficient of a water surface and of several types of land terrain at wavelengths of 3.2 cm, 1.25 cm, and 8.6 mm.

The water surface data were taken on the Potomac River Bridge at Newburg, Md. where a catwalk 150 feet high provided an unobstructed view of the water at all angles from normal incidence to the horizon. The land terrain data were taken from bridges that had approaches at least 100 feet above relatively flat land. The bridges used were the Neches River Bridge at Port Arthur, Texas, the Huey P. Long Bridge at New Orleans, La., and the Eugene Talmadge Bridge at Savannah, Ga.

Equipment

The equipment used at each frequency was a two-antenna zero intermediate frequency superheterodyne continuous wave Doppler system. The antennas were spun aluminum parabolas, and vertical polarization was used. The antenna beamwidths between half-power points were 3.1° for the 3.2-cm (X-band), 3.4° for the 1.25-cm (K-band), and 2.4° for the 8.6-mm (Q-band) system. Fig. 1 is a block diagram that applies to all three systems. Low power klystron transmitting tubes were used, a 2K25 at X band, a 2K50 at K band, and a QK-291 at Q band. The transmitter was directly connected to the transmitting antenna, and local oscillator injection was provided by the directional coupler and variable attenuator which fed energy from the klystron to the balanced mixer. In all cases the output of the mixer was an audio signal which was amplified and displayed on a meter. In the water surface measurements, the difference in frequency between the transmitted and received signals was provided by the Doppler shift due to the motion of the water. The frequency response of the audio amplifier was linear down to 20 cycles per second. A radial velocity of about 0.6 knot on the X-band system and less than 0.2 knot on the Q-band system was necessary to give a 20-cycle Doppler frequency. Only in the case of extremely calm water were velocities lower than this encountered. For calm water and all the land terrain measurements the difference in frequency between transmitted and received signals was provided by frequency modulating the klystron transmitter.

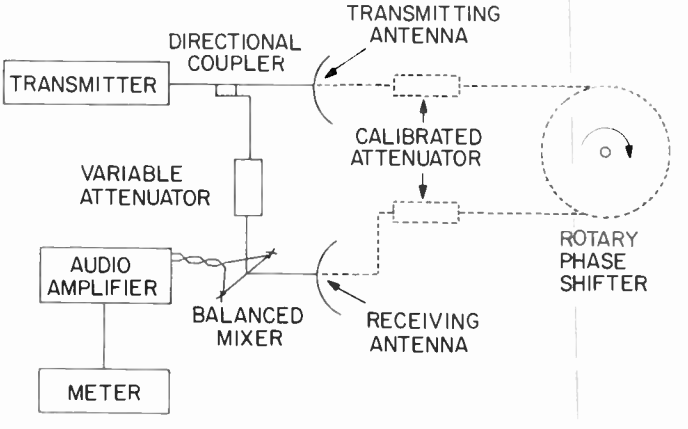

Fig. 1—System block diagram.

Calibration

The systems were calibrated by removing the antennas and placing a rotary phase shifter and calibrated attenuators between the transmitting and receiving arms as shown by the dotted lines in Fig. 1. The rotary phase shifter provided a simulated Doppler signal, and

* Original manuscript received by the IRE, October 5, 1956; revised manuscript received, March 20, 1957.

† Naval Research Laboratory, Washington, D. C.

[1] D. E. Kerr, "Propagation of Short Radio Waves," M.I.T. Rad. Lab. Ser. No. 13, McGraw-Hill Book Co., Inc., New York, N. Y.

[2] J. C. Wiltse, S. P. Schlesinger, and C. M. Johnson, "Back scattering characteristics of the sea in the region from 10 to 50 kcm," PROC. IRE, vol. 45, pp. 220–228; February, 1957.

by means of the attenuators the output meter was calibrated in terms of the ratio of power received to power transmitted. The calibration for fm operation was accomplished by frequency modulating the klystron transmitter and, using the same attenuators, the output meter was again calibrated in terms of the ratio of power received to power transmitted. The two calibrations were the same.

Measurement Procedure

The antennas were mounted on a horizontal rack which was secured to the bridge railing and extended beyond the railing far enough to give an unobstructed view of the terrain below at all angles from normal incidence to the horizon. (See Fig. 2.) Readings of the ratio of received power to transmitted power were made every 5° from 0–40° and every 10° from 40–80°. This procedure was repeated many times for each set of conditions. When reflectivity measurements of the water surface were made, wind velocity data were taken with a hand-held anemometer. A total of 421 runs were made, 191 over land and 230 over water.

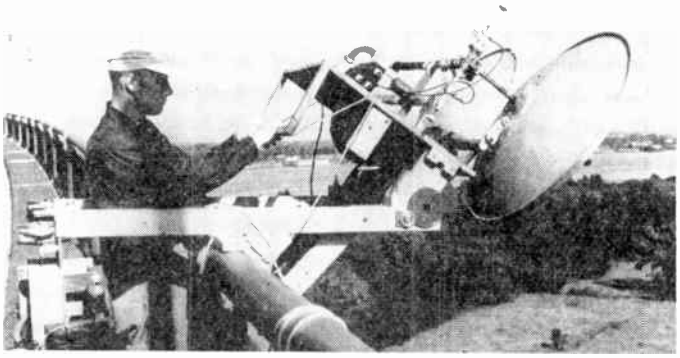

Fig. 2—3.2-cm system mounted on the Huey P. Long Bridge at New Orleans, La.

From the radar equation, if the true antenna beam of a given half-power width is approximated by a uniform antenna beam of the same width, the following expression for σ°, "the average radar cross section of sea echo per unit area of the sea surface" can be derived:

$$\sigma^0 = \frac{64R^4\lambda^2}{\pi^2 abd^4\eta^2}\,\frac{P_r}{P_t}.$$

In this equation

R = range
λ = wavelength
P_r = received power
P_t = transmitted power
d = diameter of the antenna
η = antenna efficiency (assumed to be 0.65)
a and b = semiaxes of the ellipse described on the surface by the half-power contour of the antenna beam pattern.

In the experimental work P_r/P_t was measured, and then σ° was calculated from the geometry and constants of the system. The values of σ° are an average over the beamwidth of the antenna. A graphical analysis indicated that the difference between this average value and the true value for a given angle is negligible at incident angles greater than 5°. The error introduced at smaller angles can be somewhat greater because of the rapid change in σ° with incident angle. Here, the value of σ° may be as much as 3 db too low at normal incidence.

Results—Sea Surface Reflectivity

Fig. 3 shows σ° as a function of the angle of incidence for each of the three frequencies tested. These curves were plotted from the average of all data and represent a wide range of sea states. Wind velocities from 2 to 25 knots were measured. The measurements were not made simultaneously at each frequency, but by making many runs at the same location and with a wide range of wind velocities it is believed that the average sea was approximately the same for each wavelength. In general σ° increases with frequency and was found to be 8 to 12 db greater for Q band than for X band. The high values of σ° near normal incidence (0°) indicate that there is considerable specular reflection present at these angles.

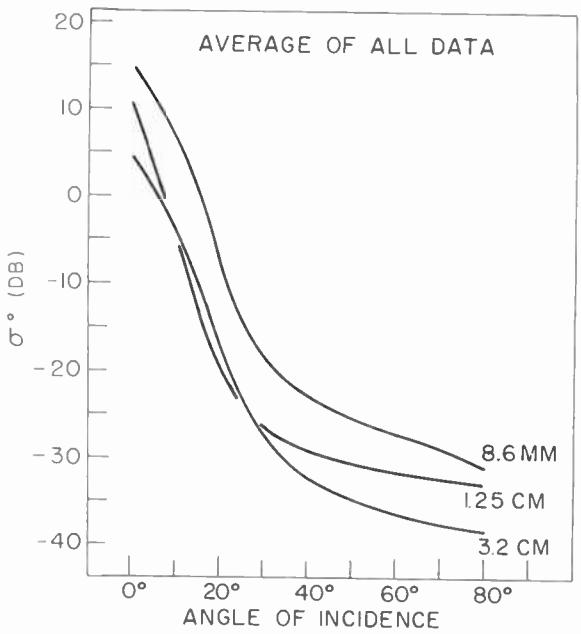

Fig. 3—σ° for the average sea.

In Fig. 4 the 8.6-mm data has been analyzed to show σ° as a function of the angle of incidence for several different wind velocities. As the wind velocity increases the specular reflection at normal incidence becomes slightly smaller while the scattering at large angles becomes much greater. For incidence angles over 20°, an increase in wind velocity of 20 knots caused an increase in σ° of over 20 db.

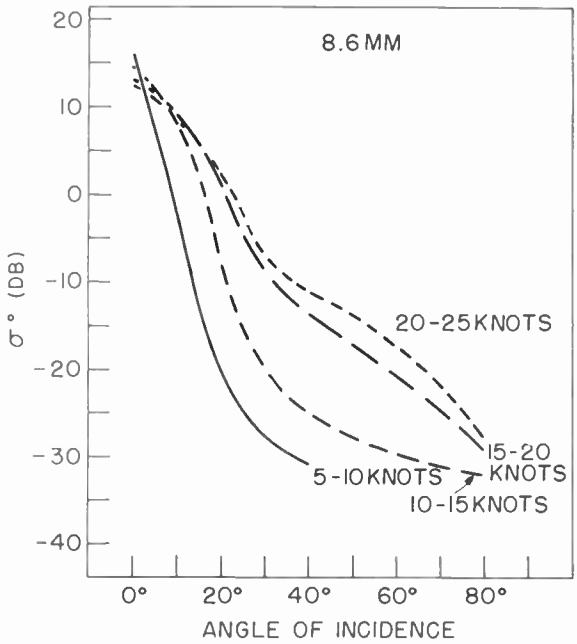

Fig. 4—σ° as a function of wind velocity, $\lambda = 8.6$ mm.

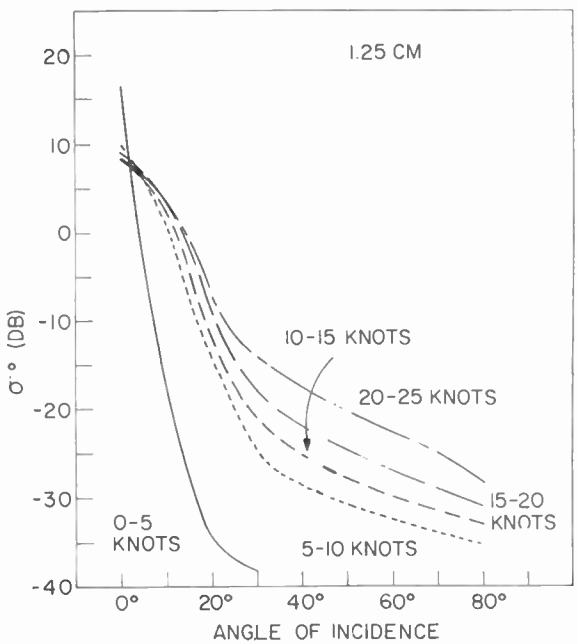

Fig. 5—σ° as a function of wind velocity, $\lambda = 1.25$ cm.

Fig. 5 is a similar family of curves for the 1.25-cm data. The curve for wind velocities under 5 knots is particularly interesting. The data for this curve were taken on a day when the river was very nearly calm and the water was glassy smooth. Under these conditions the specular reflection at normal incidence is extremely high and there is little evidence of any scattering at large angles. In 10°, σ° changed by nearly 35 db.

Fig. 6 is the family of curves for the 3.2-cm wavelength. This family is different from the other two in that σ° reaches a maximum value with wind velocities between 10 and 15 knots and then decreases as the wind

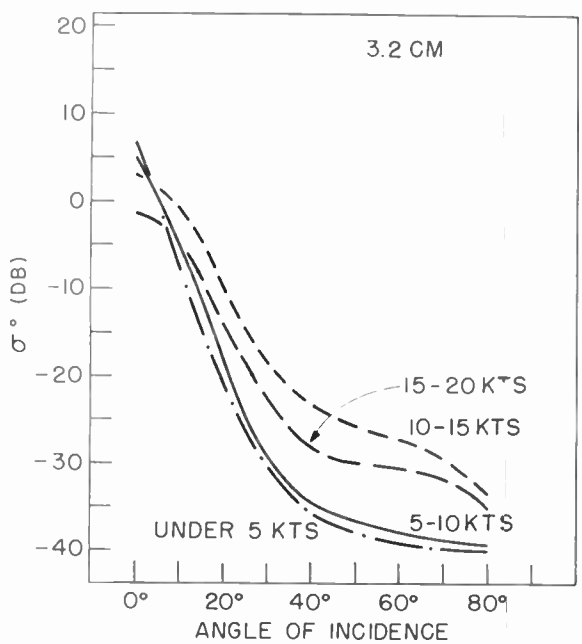

Fig. 6—σ° as a function of wind velocity, $\lambda = 3.2$ cm

velocity increases. No data were obtained for wind velocities over 20 knots.

The back-scattering cross section of water as a function of frequency is shown in Fig. 7 (opposite) for three different incident angles θ. Separate curves are shown for each wind velocity. At normal incidence σ° increases markedly with frequency at all wind velocities. At larger incident angles there are exceptions to this general trend.

Results—Land Surface Reflectivity

In contrast with the sea reflectivity curves where there is a large amount of specular reflection at normal incidence, are the land reflectivity curves shown in Fig. 8. This terrain, pictured in Figs. 9 and 10, was covered with trees in full foliage and was the nearest to an isotropic scatterer that was encountered. Here again σ° increases with frequency and at most angles is at least 10 db higher for Q band than for X band with K band falling in between. Fig. 11 (p. 980) shows σ° as a function of the angle of incidence for a terrain that was covered with tall dry weeds or flags. These curves are much the same as those of Fig. 8, and the dry weeds were also very close to an isotropic scatterer.

The data for Fig. 12 were taken at the same location as that for Fig. 11, but in the spring when the weeds were green and the ground wet. Figs. 13 and 14 are photographs of the terrain. Under these conditions there is considerable specular reflection evident at normal incidence particularly at Q and X bands. There appears to be an anomaly here in that σ° for 1.25 cm is lower than for 3.2 cm. This was found to be true whenever the reflectivity of green grass and weeds on wet ground was measured, and the anomaly may be associated with the water vapor absorption peak that occurs at this wave-

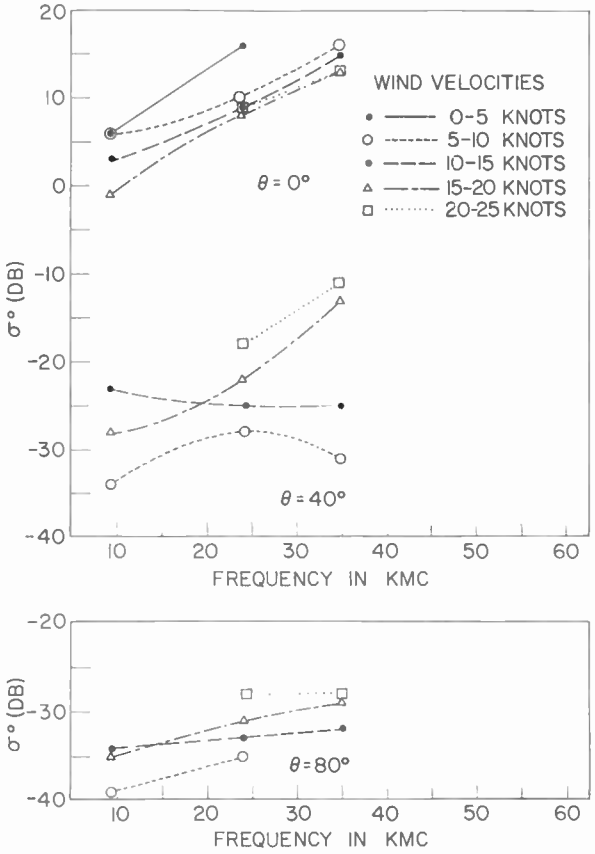

Fig. 7—σ° as a function of frequency.

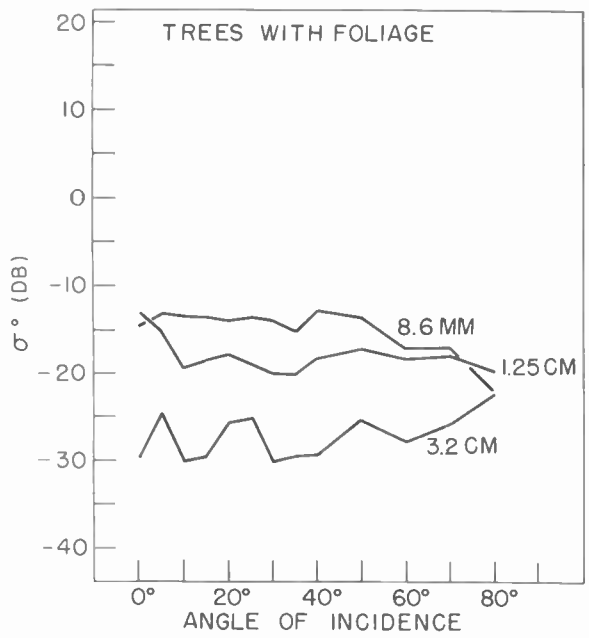

Fig. 8—σ° for a tree-covered terrain.

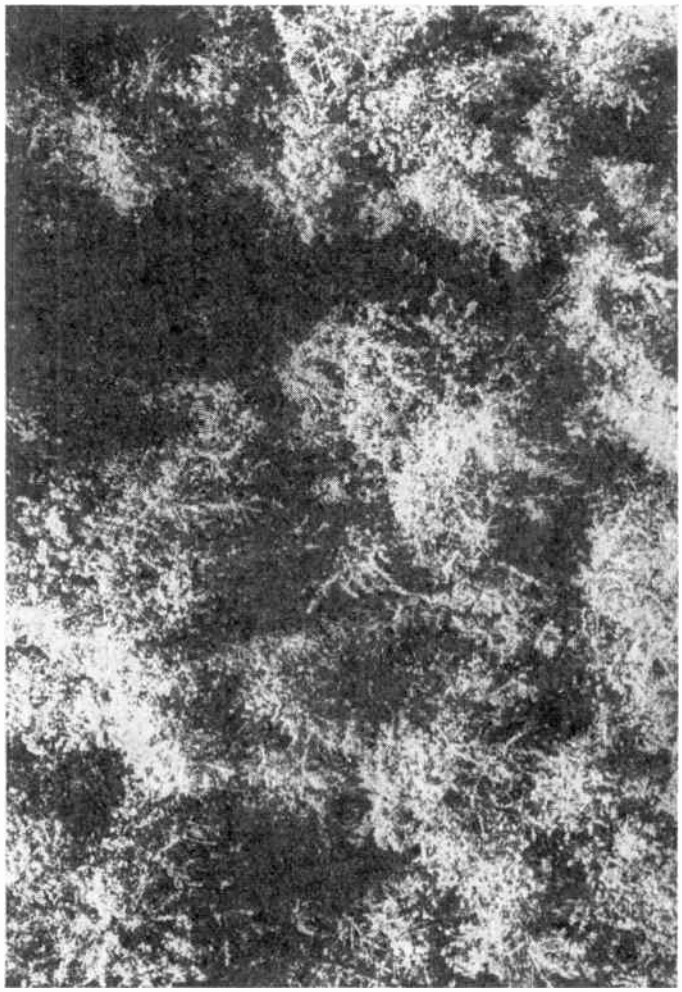

Fig. 9—Terrain at New Orleans covered with trees—view looking normal to the surface.

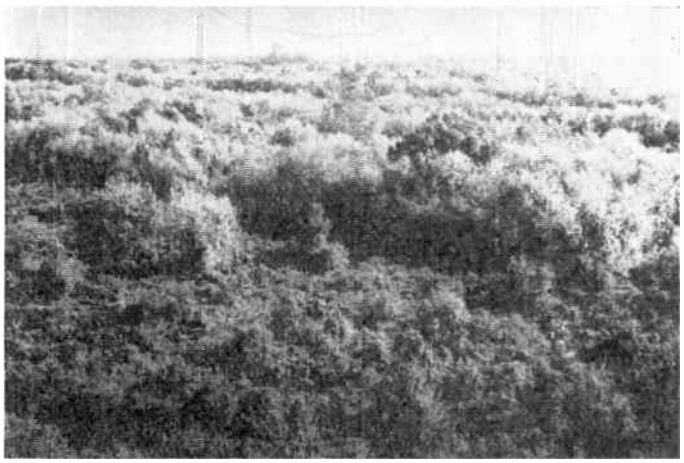

Fig. 10—Terrain at New Orleans covered with trees—view looking toward the horizon.

length. Another feature that is very noticeable in Fig. 12 is the increase in scattering at large angles at the 3.2-cm wavelength. This tendency for σ° to increase at large incidence angles was found in all the land measurements at this wavelength. This effect was not found at the higher frequencies.

The scattering by short dry grass and weeds as shown in Fig. 15 (p. 980) is much the same as for the tall dry grass. However, when bare ground is exposed a change is noticeable. Fig. 16 is a plot of σ° for the Mississippi River Levee at New Orleans. The levee was covered by short dry grass, but there was some bare sandy loam

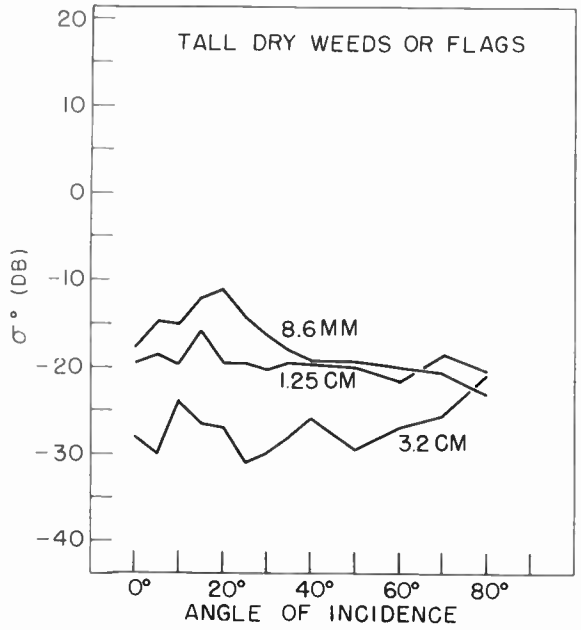

Fig. 11—σ° for a terrain covered with tall dry weeds

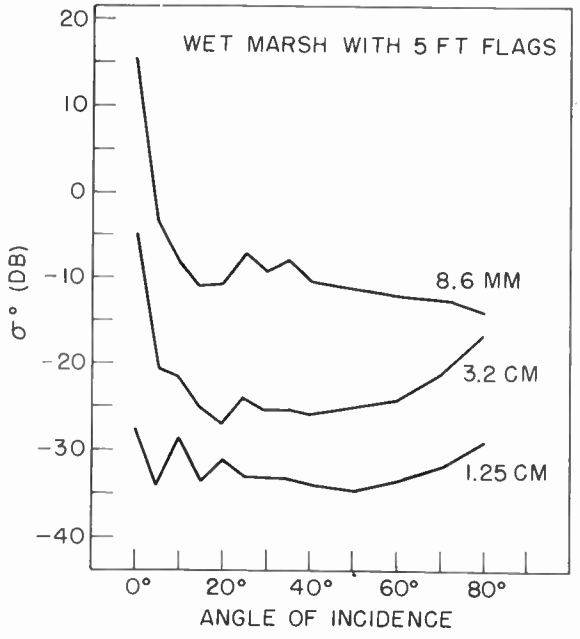

Fig. 12—σ° for a wet terrain covered with tall green weeds or flags.

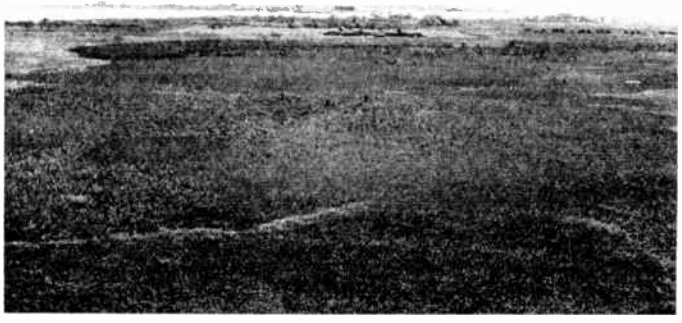

Fig. 13—Terrain at Port Arthur covered with tall weeds or flags—view from the bridge.

Fig. 14—Terrain at Port Arthur covered with tall weeds or flags—view from the ground.

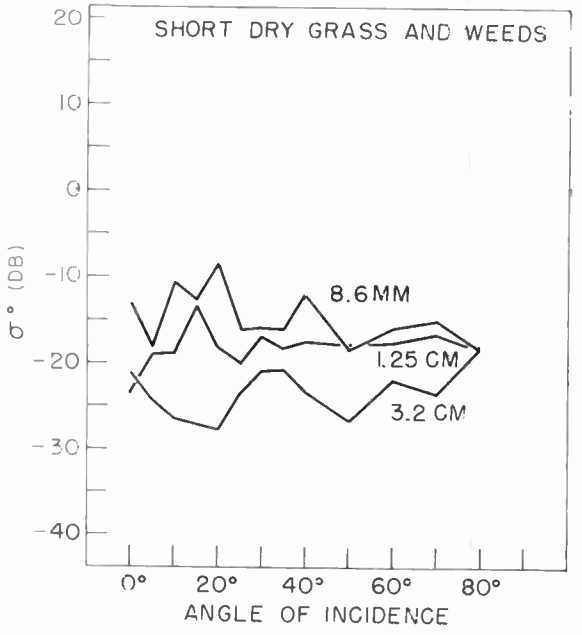

Fig. 15—σ° for a terrain covered with short dry grass and weeds

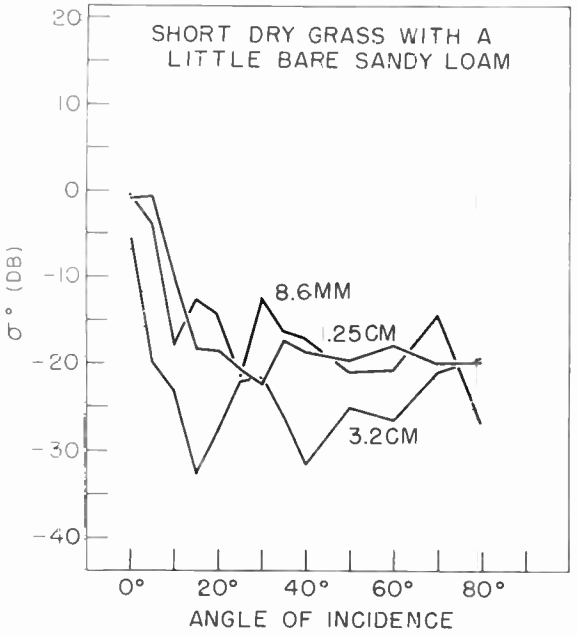

Fig. 16—σ° for a terrain partially covered with short dry grass.

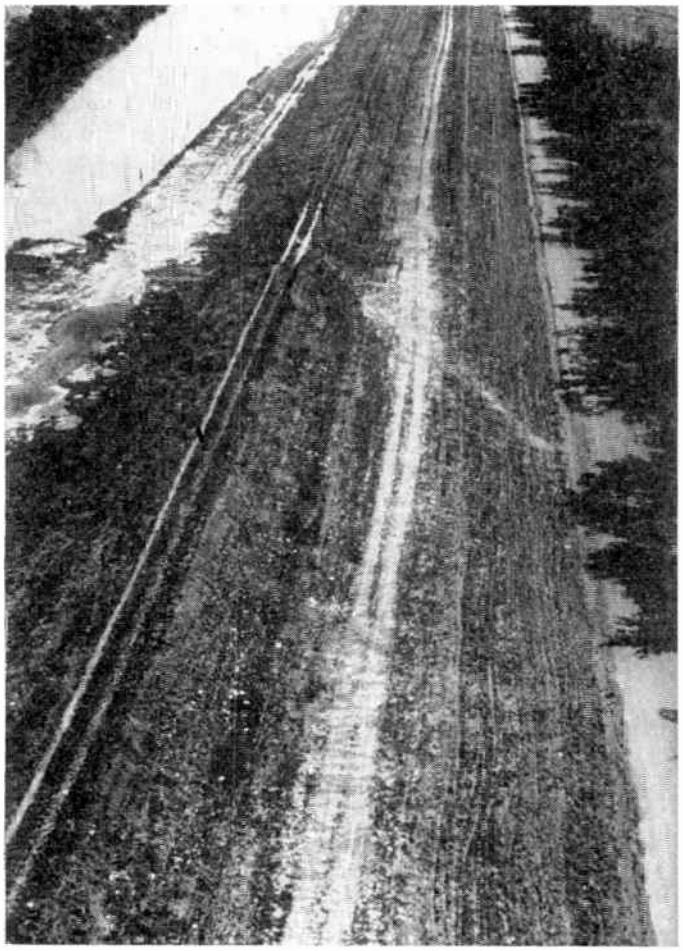

Fig. 17—Mississippi River Levee at New Orleans.

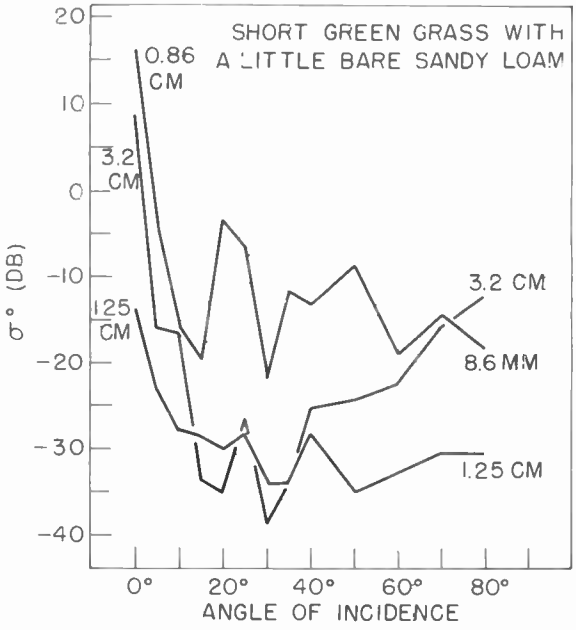

Fig. 18—σ° for a wet terrain partially covered with short green grass.

exposed. (See Fig. 17.) In this case there is some specular reflection at normal incidence due to the bare ground. Fig. 18 shows the scattering of the same spot in the spring when the grass was green and the ground wet. The specular reflection was much higher and here again σ° for 1.25 cm is lower than for 3.2 cm. The large discontinuities in these curves are due to a nonhomogeneous terrain.

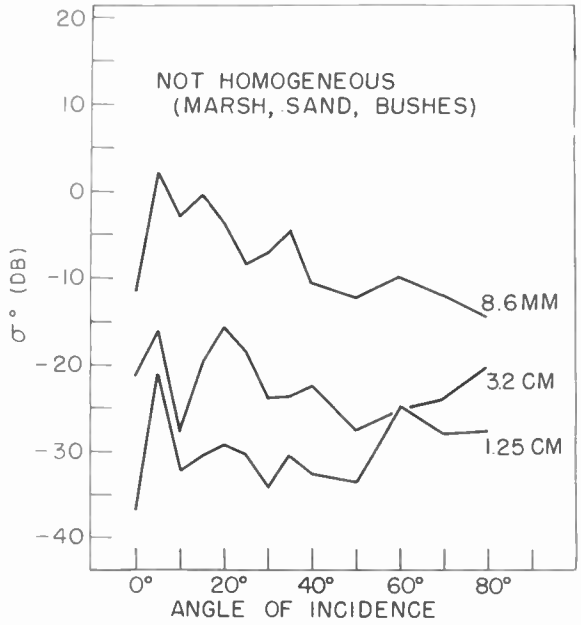

Fig. 19—σ° for a nonhomogeneous terrain.

Fig. 20—Nonhomogeneous terrain at Savannah, Ga.

The data for Fig. 19 were taken over a nonhomogeneous terrain of marsh, sand, and bushes. (See Fig. 20.) The minimum at normal incidence and the peak at 5° are due to debris under the bridge. Again the terrain was wet and σ° for 1.25 cm is low.

Fig. 21 (next page) shows the change in σ° from spring when the grass is green and the ground wet to fall when the grass and ground are dry. When the grass is green and the ground wet, the scattering at large angles is greater and there is specular reflection at normal incidence for both X and Q bands. At K band, however, the scattering by the green grass is much lower than for the dry grass, and there is very little evidence of any specular reflection.

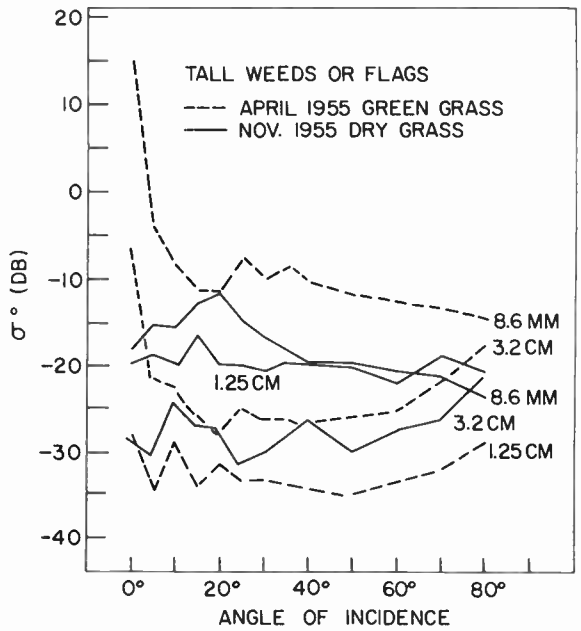

Fig. 21—Comparison of σ° for green grass and dry grass.

Conclusion

It can be concluded from these measurements that σ°, the average radar cross section of water echo per unit area of the water surface is a complicated function of wind velocity or water surface condition and of the frequency of the incident radiation, but in general σ° increases with frequency and with wind velocity. The back scattering of land is a function of the kind of terrain and of the frequency of the incident radiation, and under most conditions σ° increases with frequency. There is specular reflection present at normal incidence for all water surface conditions and for some land terrains. Terrain covered with vegetation that has matured and dried was found to be very nearly an isotropic scatterer.

Acknowledgment

The authors wish to acknowledge the help of Dr. Nancy Roman for many suggestions pertaining to the reduction of the data.

Correction

Dr. K. Pöschl, of Siemens & Halske Aktiengesellschaft, has brought the following correction to the attention of Ping King Tien, author of "Traveling-Wave Tube Helix Impedance," which appeared on pages 1617-1623 of the November, 1953 issue of PROCEEDINGS.

On page 1618, the curve in Fig. 2 is $\dfrac{1}{\eta^4 g_0}$ vs η. The curve for $\dfrac{1}{g_0}$ vs η should have appeared as indicated in the accompanying corrected Fig. 2.

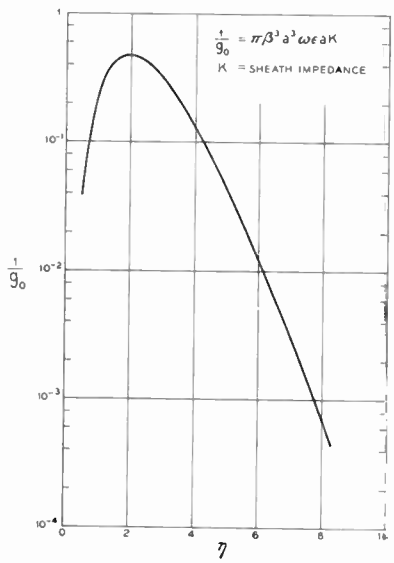

Corrected Fig. 2.

IRE Standards on Electron Tubes: Definitions of Terms, 1957*

(57 IRE 7. S2)

COMMITTEE PERSONNEL

1956-1957

Committee on Electron Tubes

P. A. REDHEAD, *Chairman*
G. A. ESPERSEN, *Vice-Chairman*

J. R. Adams
E. M. Boone
A. W. Coolidge
P. A. Fleming
K. Garoff
T. J. Henry
E. O. Johnson
W. J. Kleen
P. M. Lapostolle
R. M. Matheson
L. S. Nergaard
G. D. O'Neill
A. T. Potjer
H. J. Reich
A. C. Rockwood
H. Rothe
W. G. Shepherd
R. W. Slinkman
E. S. Stengel
R. G. Stoudenheimer
B. H. Vine
R. R. Warnecke
S. E. Webber

Subcommittee on Tubes in which Transit-Time is Not Essential

T. J. HENRY, *Chairman*

P. A. Eberhart
T. A. Elder
G. F. Hohn
W. T. Millis
C. J. Reynolds
E. E. Spitzer
R. W. Slinkman
A. K. Wing
A. H. Young

Subcommittee on Cathode-Ray and Television Tubes

J. R. ADAMS, *Chairman*

R. Dressler
H. J. Evans
J. T. Jans
L. T. Jansen
G. W. Pratt
R. Koppelon
J. C. Nonnekens
D. Van Ormer

Subcommittee on Storage Tubes

A. S. LUFTMAN, *Chairman*
J. A. BUCKBEE, *Secretary*

A. Bramley
A. E. Beckers
J. Burns
G. Chafaris
C. L. Corderman
M. Crost
D. Davis
Francis Darne
H. J. Evans
M. D. Harsh
H. Hook
B. Kazan
M. Knoll
J. A. McCarthy
W. E. Mutter
D. L. Schaefer
R. W. Sears
H. M. Smith
W. O. Unruh
P. Youtz

Subcommittee on Gas Tubes

A. W. COOLIDGE, *Chairman*

J. H. Burnett
E. J. Handley
R. A. Herring
D. E. Marshal
A. D. White
G. G. Riska
W. W. Watrous
H. H. Wittenberg

* Approved by the IRE Standards Committee, April, 1957. Reprints of this Standard, 57 IRE 7. S2, may be purchased while available from the Institute of Radio Engineers, 1 East 79th Street, New York, N. Y., at $1.00 per copy. A 20 per cent discount will be allowed for 100 or more copies mailed to one address.

Subcommittee on Methods of Test for TR and ATR Tubes

L. W. Roberts *Chairman*
A. Marchetti, *Secretary*

N. Cooper
H. Heins
F. Klawsnik
F. McCarthy
R. Walker
I. Reingold
R. Scudder
E. Vardon

Subcommittee on Phototubes

R. G. Stoudenheimer, *Chairman*

M. Adelman
H. H. Brauer
S. F. Essig
G. W. Iler
F. W. Schenkel
A. H. Sommer

Subcommittee on Camera Tubes

B. H. Vine, *Chairman*

B. R. Linden
M. Rome
D. L. Schaeffer
C. E. Thayer

Subcommittee on High-Vacuum Microwave Tubes

E. M. Boone, *Chairman*

J. H. Bryant
R. L. Cohoon
H. W. Cole
G. A. Espersen
M. S. Glass
P. M. Lally
R. A. LaPlante
H. L. McDowell
A. W. McEwan
R. R. Moats
M. Nowogrodzki
S. E. Webber

Subcommittee on Nonoperating Characteristics of Microwave Tubes

M. Nowogrodzki, *Chairman*
R. L. Cohoon, *Secretary*

M. S. Glass
R. C. Hergenrother
E. D. Reed
F. E. Vacarro

Subcommittee on Operating Measurements of Microwave Oscillator Tubes

R. R. Moats, *Chairman*
R. A. LaPlante, *Secretary*

T. P. Curtis
W. Ghen
G. I. Klein
J. T. Sadler
M. Siegman
W. W. Teich

Consultants

A. E. Harrison
J. F. Hull
T. Moreno
J. S. Needle
E. C. Okress
W. G. Shepherd

Subcommittee on Operating Measurements of Microwave Amplifier Tubes

P. M. Lally, *Chairman*
H. L. McDowell, *Secretary*

J. Berlin
H. W. Cole
H. J. Hersh
R. C. Knechtli
G. Weibel
A. W. McEwan
S. E. Webber

Subcommittee on Physical Electronics

R. M. Matheson, *Chairman*

R. W. Atkinson
J. G. Buck
L. Cronin
H. B. Frost
P. N. Hamblenton
J. M. Lafferty
J. E. White

Introduction

This Standard on Electron Tubes: Definitions of Terms supersedes the following:

Standards on Electron Tubes: Definitions of Terms, 1950 (50 IRE 7. S1).

Standards on Magnetrons: Definitions of Terms, 1952 (52 IRE 7. S1).

Standards on Gas-Filled Radiation Counter Tubes: Definitions of Terms, 1952 (52 IRE 7. S3).

Standards on Electron Devices: Methods of Measuring Noise (Appendix), (53 IRE 7. S1).

Standards on Electron Devices: Definitions of Terms Related to Phototubes, 1954 (54 IRE 7. S1).

Standards on Electron Devices: Definitions of Terms Related to Microwave Tubes (Klystrons, Magnetrons, and Traveling-Wave Tubes), 1956 (56 IRE 7. S1).

Standards on Electron Devices: Definitions of Terms Related to Storage Tubes, 1956 (56 IRE 7. S2).

Standards on Electron Tubes: TR and ATR Tube Definitions, 1956 (56 IRE 7. S3).

Standards on Electron Tubes: Physical Electronics Definitions, 1956 (57 IRE 7. S1).

This Standard combines the material published in the above Standards, with many revisions. Many new terms are also included.

Many definitions in this Standard are applicable to devices other than electron tubes—especially semiconductor devices. These definitions have been made as general as possible, but it should always be remembered in interpreting these definitions that they are primarily written for electron tubes.

Electron-Tube Admittance

As in the 1950 Standard, the familiar electron-tube coefficients have been generalized so that they apply to all types of linear electron-tube transducers at any frequency. The generalizations include the familiar low-frequency concepts. At sufficiently low frequencies, the effects of lead and socket reactance become negligible, and the admittances herein defined reduce to the familiar low-frequency coefficients. Further explanatory material may be found in Standards on Electron Tubes: Methods of Testing (50 IRE 7. S2).

When reference is made to alternating voltage or current components, the components are understood to be small enough so that linear relations hold between the various alternating voltages and currents.

In this Standard, an n-terminal electron tube is represented by a generalized network or transducer having n terminals, to each of which is flowing a complex alternating component of the current, and between each of which and a reference point (which may or may not be one of the n-network terminals) is applied a complex alternating voltage. The terms carrying an asterisk (*) refer to this network.

Terms defined elsewhere in this standard are indicated by italics.

Accelerating Electrode. An *Electrode* to which a potential is applied to increase the velocity of the electrons or ions in the beam.

Admittance.* See:

Driving-Point Admittance (between the jth Terminal and the Reference Terminal of an n-Terminal Network).

Electrode Admittance (of the jth Electrode of an n-Electrode Electron Tube).

Gap Admittance, Circuit.

Gap Admittance, Electronic.

Interelectrode Transadmittance (j-l Interelectrode Transadmittance of an n-Electrode Electron Tube).

Short-Circuit Driving-Point Admittance (of the jth Terminal of an n-Terminal Network).

Short-Circuit Feedback Admittance (of an Electron-Tube Transducer).

Short-Circuit Forward Admittance (of an Electron-Tube Transducer).

Short-Circuit Input Admittance (of an Electron-Tube Transducer).

Short-Circuit Output Admittance (of an Electron-Tube Transducer).

Short-Circuit Transfer Admittance (from the jth Terminal to the lth Terminal of an n-Terminal Network).

Transfer Admittance (from the jth Terminal to the lth Terminal of an n-Terminal Network).

Amplification Factor.* The *μ-Factor* for a specified *Electrode* and the *Control Grid* of an *Electron Tube* under the condition that the *Anode Current* is held constant.

Note 1: In a *Triode* this becomes the *μ-Factor* for the *Anode* and *Control-Grid* electrodes.

Note 2: In multielectrode tubes connected as *Triodes* the term *Anode* applies to the combination of *Electrodes* used as the *Anode.*

Amplifier. See:

Class-A Amplifier.

Class-AB Amplifier.

Class-B Amplifier.

Class-C Amplifier.

Amplitude Response (Camera Tubes). See:

Square-Wave Response.

Amplitude Response Characteristic (Camera Tubes). See:

Square-Wave Response Characteristic.

Angle. See:

Angle, Maximum-Deflection.

Bunching Angle (in an Electron Stream).

Effective Bunching Angle (Reflex Klystrons).

Optimum Bunching Angle.

Transit Angle.

Angle, Maximum-Deflection. The maximum plane angle subtended at the *Deflection Center* by the usable *Screen* area.

Note: In this term the hyphen is frequently omitted.

Anode (Electron Tubes). An *Electrode* through which a principal stream of electrons leaves the interelectrode space.

Anode Breakdown Voltage (Gas Tubes). See:

Breakdown Voltage (of an Electrode of a Gas Tube).

Anode Current. See: *Electrode Current.*

Anode Strap (Magnetrons). A metallic connector between selected anode segments of a *Multicavity Magnetron*, principally for the purpose of *Mode Separation.*

Anode Voltage. See: *Electrode Voltage.*

Anode Voltage Drop. See: *Tube Voltage Drop.*

Arc. A discharge of electricity through a gas, normally characterized by a voltage drop approximately equal to the ionization potential of the gas.

Arc-Back. The flow of a principal electron stream in the reverse direction owing to the formation of a *Cathode Spot* on an *Anode*, which results in a failure of the rectifying action.

Arc-Drop Loss (Gas Tubes). The product of the instantaneous values of *Tube Voltage Drop* and current averaged over a complete cycle of operation.

Arc-Drop Voltage (Gas Tubes). See:

Tube Voltage Drop.

Arc Loss (Switching Tubes). The decrease in radio-frequency power measured in a matched termination when a *Fired Tube*, mounted in a series or shunt junction with a waveguide, is inserted between a matched generator and the termination. In the case of a *Pre-TR Tube*, a matched output termination is also required for the tube.

Arc-Through (Multielectrode Gas Tubes). The loss of control resulting from the flow of a principal electron stream in the normal direction during a scheduled nonconducting period.

Astigmatism (Electron Optical). In an *Electron-Beam Tube*, a focus defect in which electrons in different axial planes come to focus at different points.

ATR (Anti-Transmit-Receive) Tube. A gas-filled radio-frequency switching tube used to isolate the transmitter during the interval for pulse reception.

Attenuator Tube. A gas-filled radio-frequency switching tube in which a gas discharge, initiated and regulated independently of radio-frequency power, is used to control this power by reflection or absorption.

Available Conversion Gain (of a Conversion Transducer). See:

Gain, Available Conversion (of a Conversion Transducer).

Available Power (at a Port). The maximum power which can be transferred from the *Port* to a load.

Note: At a specified frequency, maximum power transfer will take place when the impedance of the load is the conjugate of that of the source The source impedance must have a positive real part.

Available-Power Gain (of a Two-Port Linear Transducer). See:

Gain, Available-Power (of a Two-Port Linear Transducer).

Available-Power Gain, Maximum (of a Two-Port Linear Transducer). See:

Gain, Available-Power, Maximum (of a Two-Port Linear Transducer).

Avalanche. The cumulative process in which charged particles accelerated by an electric field produce additional charged particles through collision with neutral gas molecules or atoms.

Average Electrode Current. The value obtained by integrating the instantaneous *Electrode Current* over an averaging time and dividing by the averaging time.

Background Counts (Radiation Counters). *Counts* caused by *Radiation* coming from sources other than that to be measured.

Backplate (Camera Tubes). The *Electrode* to which the stored charge image is capacitively coupled.

Backward Wave (Traveling-Wave Tubes). A wave whose group velocity is opposite to the direction of electron-stream motion.

Band-Pass Tube (TR and Pre-TR Tubes). See:

Broad-Band Tube (TR and Pre-TR Tubes).

Beam Alignment (Camera Tubes). An adjustment of the electron beam, performed on tubes employing *Low-Velocity Scanning*, to cause the beam to be perpendicular to the *Target* at the *Target* surface.

Beam Bending (Camera Tubes). Deflection of the scanning beam by the electrostatic field of the charges stored on the *Target*.

Beam-Deflection Tube. An *Electron-Beam Tube* in which current to an output *Electrode* is controlled by the transverse movement of an electron beam.

Beam-Indexing Color Tube. A *Color Picture Tube* in which a signal, generated by an electron beam after deflection, is fed back to a control device or element in such a way as to provide an image in color.

Beam Modulation, Percentage (Image Orthicons). One hundred times the ratio of 1) the *Signal Output Current* for highlight illumination on the tube to 2) the *Dark Current*.

Beam Power Tube. An *Electron-Beam Tube* in which use is made of directed electron beams to contribute substantially to its power-handling capability, and in which the *Control Grid* and the *Screen Grid* are essentially aligned.

Blemish (Charge-Storage Tubes). An imperfection of the storage surface which produces a spurious output.

Breakdown (in a Gas Tube). A runaway increase in an *Electrode Current*.

Breakdown Transfer Characteristic (Gas Tubes). A relation between the *Breakdown Voltage* of an *Electrode* and the current to another *Electrode*.

Breakdown Voltage (of an Electrode of a Gas Tube). The voltage of an *Electrode* at which *Breakdown* occurs to that *Electrode*.

Note 1: The *Breakdown Voltage* is a function of the other *Electrode Voltages* or currents and of the environment.

Note 2: In special cases where the *Breakdown Voltage* of an *Electrode* is referred to an *Electrode* other than the *Cathode*, this reference *Electrode* shall be indicated.

Note 3: This term should be used in preference to "Pickup Voltage," "Firing Voltage," "Starting Voltage," etc., which are frequently used for specific types of *Gas Tubes* under specific conditions.

Note 4: See:

Critical Grid Voltage (Multielectrode Gas Tubes).

Broad-Band Tube (TR and Pre-TR Tubes). A gas-filled fixed-tuned tube incorporating a band-pass filter of geometry suitable for radio-frequency switching.

Bunching. The action in a velocity-modulated electron stream that produces an alternating convection-current component as a direct result of the differences of electron transit time produced by the *Velocity Modulation*. See:

Optimum Bunching.
Overbunching.
Reflex Bunching.
Space-Charge Debunching.
Underbunching.

Bunching Angle (in an Electron Stream). In a given *Drift Space*, the average *Transit Angle* between the processes of *Velocity Modulation* and energy extraction at the same or different gaps. See also:

Effective Bunching Angle (Reflex Klystrons).

Bunching, Optimum. See:

Optimum Bunching.

Bunching Parameter. One-half the product of 1) the *Bunching Angle* in the absence of *Velocity Modulation* and 2) the depth of *Velocity Modulation*.

Note: In a reflex klystron the *Effective Bunching Angle* must be used.

Camera Tube. An *Electron Tube* for the conversion of an optical image into an electrical signal by a scanning process.

Capacitance.* See:

Cathode Interface (Layer) Capacitance.
Electrode Capacitance (n-Terminal Electron Tubes).
Gap Capacitance, Effective.
Input Capacitance (n-Terminal Electron Tubes).
Interelectrode Capacitance (j-l Interelectrode Capacitance C_{jl} of an n-Terminal Electron Tube).
Output Capacitance (n-Terminal Electron Tubes).
Short-Circuit Input Capacitance (n-Terminal Electron Tubes).
Short-Circuit Output Capacitance (n-Terminal Electron Tubes).
Short-Circuit Transfer Capacitance (Electron Tubes).
Signal Electrode Capacitance.
Target Capacitance (Camera Tubes).

Cathode (Electron Tubes). An *Electrode* through which a primary stream of electrons enters the interelectrode space. See also:

Cold Cathode.
Filament.
Hot Cathode (*Thermionic Cathode*).
Indirectly Heated Cathode (*Equipotential Cathode, Unipotential Cathode*).
Ionic-Heated Cathode.
Photocathode.
Semitransparent Photocathode.

Cathode Coating Impedance. The impedance, excluding the *Cathode Interface* (*Layer*) *Impedance*, between the base metal and the emitting surface of a coated *Cathode*.

Cathode Current. See:
Electrode Current.

Cathode Glow. A luminous layer which covers all or part of the *Cathode* in a *Glow-Discharge Tube*.

Cathode Heating Time (Gas Tubes). The time required for a *Cathode* to attain operating temperature under stated operating conditions.

Cathode Heating Time (Vacuum Tubes). The time required for the time rate of change of the *Cathode Current* to reach maximum value.

Note 1: All *Electrode Voltages* are to remain constant during measurement. The tube *Elements* must all be at room temperature at the start of the test.

Note 2: See: *Operation Time.*

Cathode Interface (Layer) Capacitance. A capacitance which, in parallel with a suitable resistance, forms an impedance approximating the *Cathode Interface Impedance*.

Note: Because the *Cathode Interface Impedance* cannot be represented accurately by the two-element RC circuit, this value of capacitance is not unique.

Cathode Interface (Layer) Impedance. An impedance between the *Cathode* base and coating.

Note: This impedance may be the result of a layer of high resistivity or a poor mechanical bond between the *Cathode* base and coating.

Cathode Interface (Layer) Resistance. The low-frequency limit of *Cathode Interface Impedance*.

Cathode Preheating Time. The minimum period of time during which the heater voltage should be applied before the application of other *Electrode* voltages.

Cathode-Ray Tube. An *Electron-Beam Tube* in which the beam can be focused to a small cross section on a surface and varied in position and intensity.

Cathode Spot (of an Arc). An area, on the *Cathode* of an *Arc*, from which the electron emission density is extremely high.

Cell-Type Tube (TR, ATR, and Pre-TR Tubes). A gas-filled radio-frequency switching tube which operates in an external resonant circuit. A tuning mechanism may be incorporated in either the external resonant circuit or the tube.

Characteristic. See:
Breakdown Transfer Characteristic (*Gas Tubes*).
Constant-Current Characteristic.
Control Characteristic (*Gas Tubes*).
Counting-Rate-vs-Voltage Characteristic.
Decay Characteristic.
Diode Characteristic (*Multielectrode Tubes*).
Dynamic Characteristic (*Electron Tubes*).
Electrode Characteristic.
Emission Characteristic.
Grid Characteristic.
Grid-Drive Characteristic.
Knee of Transfer Characteristic (*Image Orthicons*).
Load (*Dynamic*) *Characteristic* (*Electron Tubes Connected in a Specified Operating Circuit at a Specified Frequency*).
Persistence Characteristic (*Camera Tubes*).
Persistence Characteristic (*Decay Characteristic*) (*of a Luminescent Screen*).
Spectral Characteristic (*of a Luminescent Screen*).
Spectral Sensitivity Characteristic (*Camera Tubes or Phototubes*).
Square-Wave Response Characteristic (*Camera Tubes*).
Static Characteristic (*Electron Tubes*).
Transfer Characteristic.
Transfer Characteristic (*Camera Tubes*).

Charge-Storage Tube. A *Storage Tube* in which information is retained on a surface in the form of electric charges.

Circuit Efficiency (of the Output Circuit of Electron Tubes). The ratio of 1) the power at the desired frequency delivered to a load at the output terminals of the output circuit of an oscillator or amplifier to 2) the power at the desired frequency delivered by the electron stream to the output circuit.

Circuit Gap Admittance. See:
Gap Admittance, Circuit.

Class-A Amplifier. An amplifier in which the *Grid Bias* and alternating *Grid Voltages* are such that *Anode Current* in a specific tube flows at all times.

Note: The suffix 1 is added to the letter or letters of the class identification to denote that *Grid Current* does not flow during any part of the input cycle. The suffix 2 is used to denote that current flows during some part of the cycle.

Class-AB Amplifier. An amplifier in which the *Grid Bias* and alternating *Grid Voltages* are such that *Anode Current* in a specific tube flows for appreciably more than half but less than the entire electrical cycle.

Note: The suffix 1 is added to the letter or letters of the class identification to denote that *Grid Current* does not flow during any part of the input cycle. The suffix 2 is used to denote that current flows during some part of the cycle.

Class-B Amplifier. An amplifier in which the *Grid Bias* is approximately equal to the cutoff value so that the *Anode Current* is approximately zero when no exciting *Grid Voltage* is applied, and so that *Anode Current* in a specific tube flows for approximately one half of each cycle when an alternating grid voltage is applied.

Note: The suffix 1 is added to the letter or letters of

the class identification to denote that *Grid Current* does not flow during any part of the input cycle. The suffix 2 is used to denote that current flows during some part of the cycle.

Class-C Amplifier. An amplifier in which the *Grid Bias* is appreciably greater than the cutoff value so that the *Anode Current* in each tube is zero when no alternating *Grid Voltage* is applied, and so that *Anode Current* in a specific tube flows for appreciably less than one half of each cycle when an alternating *Grid Voltage* is applied.

Note: The suffix 1 is added to the letter or letters of the class identification to denote that *Grid Current* does not flow during any part of the input cycle. The suffix 2 is used to denote that current flows during some part of the cycle.

Cloud Pulse (Charge-Storage Tubes). The output resulting from *Space-Charge* effects produced by the turning on or off of the electron beam.

Cold Cathode. A *Cathode* whose operation does not depend on its temperature being above the ambient temperature.

Cold-Cathode Tube. An *Electron Tube* containing a *Cold Cathode.*

Collector. An *Electrode* that collects electrons or ions which have completed their functions within the tube.

Color Cell. In a repeating pattern of phosphors on the *Screen* of a *Color Picture Tube*, the smallest area containing a complete set of all the primary colors contained in the pattern.

Note: If the cells are described by only one dimension as in the line type of *Screen*, the other dimension is determined by the resolution capabilities of the tube.

Color Center (Color Picture Tubes). A point or region (defined by a particular color-selecting electrode and *Screen* configuration) through which an electron beam must pass in order to strike the phosphor array of one primary color.

Note: This term is *not* to be used to define the *Color Triad* center of a *Color Picture Tube Screen.*

Color Field Corrector. A device located external to the tube producing an electric or magnetic field which affects the beam after deflection as an aid in the production of uniform color fields.

Color Picture Tube. An *Electron Tube* used to provide an image in color by the scanning of a *Raster* and by varying the intensity of excitation of phosphors to produce light of the chosen primary colors.

Color Plane (Multibeam Color Picture Tubes). A surface approximating a plane containing the *Color Centers.*

Color Purity Magnet. A magnet in the neck region of a *Color Picture Tube* to alter the electron beam path for the purpose of improving color purity.

Color-Selecting-Electrode System. A structure containing a plurality of openings mounted in the vicinity of the *Screen* of a *Color Picture Tube*, the function of this structure being to cause electron impingement on the proper *Screen* area by using either masking, focusing, deflection, reflection, or a combination of these effects.

Note: For examples, see:
Shadow Mask.
Focusing and Switching Grille.

Color-Selecting-Electrode System Transmission. The fraction of incident primary electron current which passes through the *Color-Selecting-Electrode System.*

Color Triad (of a Phosphor-Dot Screen). A *Color Cell* of a three-color phosphor-dot *Screen.*

Commutation Factor (Gas Tubes). The product of the rate of current decay and the rate of the inverse voltage rise immediately following such current decay.

Note: The rates are commonly stated in amperes per microsecond, and volts per microsecond.

Composite Controlling Voltage. The voltage of the *Anode* of an *Equivalent Diode* combining the effects of all individual *Electrode Voltages* in establishing the *Space-Charge-Limited Current.*

Compression Ratio (Gain or Amplification). The ratio of 1) the magnitude of the gain (or amplification) at a reference signal level to 2) its magnitude at a higher stated signal level.

Condensed-Mercury Temperature. The temperature measured on the outside of the tube envelope in the region where the mercury is condensing in a glass tube, or measured at a designated point on a metal tube.

Conductance. See:
Conductance for Rectification.
Conversion Transconductance (of a Heterodyne Conversion Transducer).
*Electrode Conductance.**
Equivalent Conductance (ATR Tubes).
Equivalent Noise Conductance.
*Interelectrode Transconductance (j-l Interelectrode Transconductance).**

Conductance for Rectification. The quotient of 1) the *Electrode* alternating current of low frequency by 2) the in-phase component of the *Electrode* alternating voltage of low frequency, a high-frequency sinusoidal voltage being applied to the same or another *Electrode* and all other *Electrode Voltages* being maintained constant.

Constant-Current Characteristic. The relation between the voltages of two *Electrodes* with the current to one of them as well as all other voltages maintained constant.

Contact Potential Difference. The difference between the *Work Functions* of two materials, divided by the electronic charge.

Control Characteristic (Gas Tubes). A relation between *Critical Grid Voltage* and *Anode Voltage.*

Control Electrode. An *Electrode* used to initiate or vary the current between two or more *Electrodes.*

Control-Electrode Discharge Recovery Time (Attenuator Tubes). The time required for the *Control-Electrode* discharge to deionize to a level such that a specified fraction of the *Critical High-Power Level* is required to ionize the tube.

Control Grid. A *Grid*, ordinarily placed between the *Cathode* and an *Anode*, for use as a *Control Electrode*.

Control Ratio (Gas Tubes). The ratio of the change in *Anode Voltage* to the corresponding change in *Critical Grid Voltage*, with all other operating conditions maintained constant.

Convection Current. In an electron stream, the time rate at which charge is transported through a given surface.

Convection-Current Modulation. The time variation in the magnitude of the *Convection Current* passing through a surface, or the process of directly producing such a variation.

Convergence (Multibeam Cathode-Ray Tubes). A condition in which the electron beams intersect at a specified point.

Convergence, Dynamic (Multibeam Cathode-Ray Tubes). The process whereby the locus of the point of convergence of electron beams is made to fall on a specified surface during scanning.

Convergence Electrode. An *Electrode* whose electric field converges two or more electron beams.

Convergence Magnet. A magnet assembly whose magnetic field converges two or more electron beams.

Convergence Plane (Multibeam Cathode-Ray Tubes). A plane containing the points at which the electron beams appear to experience a deflection applied for the purpose of obtaining *Convergence*.

Convergence Surface (Multibeam Cathode-Ray Tubes). The surface generated by the point of intersection of two or more electron beams during the scanning process.

Conversion Transconductance (of a Heterodyne Conversion Transducer). The quotient of 1) the magnitude of the desired output-frequency component of current by 2) the magnitude of the input-frequency (signal) component of voltage when the impedance of the output external termination is negligible for all of the frequencies which may affect the result.

Note: Unless otherwise stated, the term refers to the cases in which the input-frequency voltage is of infinitesimal magnitude. All direct *Electrode Voltages* and the magnitude of the local-oscillator voltage must remain constant.

Conversion Transducer. An electric transducer in which the input and the output frequencies are different.

Note: If the frequency-changing property of a *Conversion Transducer* depends upon a generator of frequency different from that of the input or output frequencies, the frequency and voltage or power of this generator are parameters of the *Conversion Transducer*.

Conversion Voltage Gain (of a Conversion Transducer). See:

Gain, Conversion Voltage (of a Conversion Transducer).

Converter Tube. An *Electron Tube* that combines the mixer and local-oscillator functions of a *Heterodyne Conversion Transducer*.

Count (Radiation Counters). A single response of the counting system.

Note: See also:

Tube Count.

Counter Tube, Externally Quenched. A radiation-counter tube that requires the use of an external quenching circuit to inhibit *Reignition*.

Counter Tube, Gas-Filled, Radiation. A *Gas Tube* used for detection of *Radiation* by means of gas ionization.

Counter Tube, Gas-Flow. A radiation-counter tube in which an appropriate atmosphere is maintained by a flow of gas through the tube.

Counter Tube, Geiger-Mueller. A radiation-counter tube operated in the *Geiger-Mueller Region*.

Counter-Tube, Proportional. A radiation-counter tube operated in the *Proportional Region*.

Counter Tube, Self-Quenched. A radiation-counter tube in which *Reignition* of the discharge is inhibited by internal processes.

Counting Efficiency (Radiation-Counter Tubes). The average fraction of the number of ionizing particles or quanta incident on the *Sensitive Volume* that produce *Tube Counts*. The operating conditions of the counter and the condition of irradiation must be specified.

Counting-Rate-vs-Voltage Characteristic. The relation between counting rate and voltage applied to a radiation-counter tube for constant *Radiation* intensity.

Coupling Coefficient, Small Signal (for an Electron Stream). The ratio of 1) the maximum change in energy of an electron traversing the *Interaction Space* to 2) the product of the *Peak Alternating Gap Voltage* by the electronic charge.

Critical Anode Voltage (Multielectrode Gas Tubes). Synonymous with *Anode Breakdown Voltage (Gas Tubes)*.

Critical Field (Magnetrons). The smallest theoretical value of steady magnetic flux density, at a steady *Anode Voltage*, that would prevent an electron emitted from the *Cathode* at zero velocity from reaching the *Anode*.

Critical Grid Current (Multielectrode Gas Tubes). The *Grid Current* corresponding to the *Critical Grid Voltage*, before anode *Breakdown*.

Note: The *Critical Grid Current* is a function of the other *Electrode Voltages* or currents and of the environment.

Critical Grid Voltage (Multielectrode Gas Tubes). The *Grid Voltage* at which anode *Breakdown* occurs.

Note 1: The *Critical Grid Voltage* is a function of the other *Electrode Voltages* or currents and of the environment.

Note 2: See:

Breakdown Voltage (of an Electrode of a Gas Tube).

Critical High-Power Level (Attenuator Tubes). The radio-frequency power level at which ionization is produced in the absence of a *Control-Electrode* discharge.

Critical Voltage (Magnetrons). The highest theoretical

value of steady *Anode Voltage*, at a given steady magnetic flux density, at which electrons emitted from the *Cathode* at zero velocity would fail to reach the *Anode*.

Current. See:
Average Electrode Current.
Convection Current.
Critical Grid Current (Multielectrode Gas Tubes).
Dark Current.
Electrode Current (Electron Tubes).
Electrode Dark Current (Camera Tubes or Phototubes).
Equivalent Noise Current.
Fault Electrode Current.
Field-Free Emission Current (of a Cathode).
Flection-Point Emission Current.
Gas (Ionization) Current (Vacuum Tubes).
Inflection-Point Emission Current.
Inverse Electrode Current.
Peak Cathode Current (Steady State).
Peak Electrode Current.
Preoscillation Current.
Signal Output Current (Camera Tubes or Phototubes).
Space-Charge-Limited Current (Vacuum Tubes).
Starting Current of an Oscillator.
Transfer Current (Gas Tubes).

Current Amplification (Multiplier Phototubes). The ratio of 1) the *Signal Output Current* to 2) the photoelectric signal current from the *Photocathode*.

Current Generator. A two-terminal circuit element with a terminal current independent of the voltage between its terminals.

Note: A *Current Generator* has zero internal admittance.

Cutoff Field (Magnetrons). See:
Critical Field (Magnetrons).

Cutoff Voltage (Electron Tubes). That *Electrode Voltage* which reduces the value of the dependent variable of an *Electron Tube* characteristic to a specified low value.

Note: A specific cutoff characteristic should be identified as follows: current-vs-grid-cutoff voltage, spot-brightness-vs-grid-cutoff voltage, etc.

Cutoff Voltage (Magnetrons). See:
Critical Voltage (Magnetrons).

Cyclotron Frequency. The frequency at which a charged particle traverses an orbit in a steady, uniform, magnetic field, and zero electric field.

Cyclotron-Frequency Magnetron Oscillations. Those oscillations whose frequency is substantially the *Cyclotron Frequency*.

Dark Current (Camera Tubes or Phototubes). See:
Electrode Dark Current.

Dead Time (Radiation Counters). The time interval, after the start of a *Count*, during which a *Radiation Counter* is insensitive to further *Ionizing Events*.

Note: See also:
Recovery Time.

DC Electron-Stream Resistance. The quotient of *Electron-Stream Potential* and the direct-current component of stream current.

Decay (Charge-Storage Tubes). The reduction in magnitude of stored charge by any cause other than *Erasing*.

Decay Characteristic. See:
Persistence Characteristic.

Decay Time (Charge-Storage Tubes). The time interval during which the magnitude of the stored charge decays to a stated fraction of its initial value.

Note: The fraction is commonly $1/e$, where e is the base of natural logarithms.

Decelerating Electrode (Electron-Beam Tubes). An *Electrode* the potential of which provides an electric field to decrease the velocity of the beam electrons.

Deflecting Electrode. An *Electrode* the potential of which provides an electric field to produce deflection of an electron beam.

Deflection Center. The intersection of the forward projection of the electron path prior to deflection and the backward projection of the electron path in the field-free space after deflection.

Deflection Factor (Cathode-Ray Tubes). The reciprocal of the *Deflection Sensitivity*.

Deflection Plane. A plane perpendicular to the tube axis containing the *Deflection Center*.

Deflection Sensitivity (Cathode-Ray Tubes). The quotient of the displacement of the electron beam at the *Target* or *Screen* by the change in the magnitude of the deflecting field.

Note: Deflection Sensitivity is usually expressed in millimeters (or inches) per volt applied between the *Deflecting Electrodes*, or in millimeters (or inches) per ampere in the deflecting coil.

Deflection Yoke. An assembly of one or more electromagnets to produce deflection of one or more electron beams.

Deflection-Yoke Pull-Back.
1) **Color.** The distance between the maximum possible forward position of the yoke and the position of the yoke to obtain optimum color purity.
2) **Monochrome.** The maximum distance the yoke can be moved along the tube axis without producing neck shadow.

Deionization Time (Gas Tubes). The time required for a tube to regain its preconduction characteristics after anode-current interruption.

Note: See also:
Recovery Time.

Depth of Velocity Modulation, Small-Signal. The ratio of the peak amplitude of the *Velocity Modulation* of an electron stream, expressed in equivalent volts, to the *Electron-Stream Potential*.

Diode (Electron Tube). A two-electrode *Electron Tube* containing an *Anode* and a *Cathode*.

Note: See also:
Equivalent Diode.

Diode Characteristic (Multielectrode Tubes). The composite *Electrode* characteristic taken with all *Electrodes* except the *Cathode* connected together.

Direct-Coupled Attenuation (TR, Pre-TR, and Attenuator Tubes). The *Insertion Loss* measured with the *Resonant Gaps*, or their functional equivalent, short-circuited.

Direct Grid Bias. The direct component of *Grid Voltage*.

Note: This is commonly called "grid bias."

Discharge. See:

Glow Discharge.

Ignitor Discharge (*Switching Tubes*).

Dissector Tube. See:

Image Dissector Tube.

Distortion, Barrel (Camera Tubes or Image Tubes). A distortion which results in a monotonic decrease in radial magnification in the reproduced image away from the axis of symmetry of the electron optical system.

Note: For a *Camera Tube*, the reproducer is assumed to have no geometric distortion.

Distortion, Keystone (Camera Tubes). A distortion such that the slope or the length of a horizontal line *Trace* or scan line is linearly related to its vertical displacement.

Note: A system having *Keystone Distortion* distorts a rectangular pattern into a trapezoidal pattern.

Distortion, Pincushion (Camera Tubes or Image Tubes). A distortion which results in a monotonic increase in radial magnification in the reproduced image away from the axis of symmetry of the electron optical system.

Note: For a *Camera Tube*, the reproducer is assumed to have no geometric distortion.

Distortion, S. See: *Distortion, Spiral.*

Distortion, Spiral (in Camera Tubes or Image Tubes using Magnetic Focusing). A distortion in which image rotation varies with distance from the axis of symmetry of the electron optical system.

Drift Rate (Voltage Regulators or Reference Tubes). The slope at a stated time of the smoothed curve of *Tube Voltage Drop* with time at constant operating conditions.

Drift Space. In an *Electron Tube*, a region substantially free of externally applied alternating fields, in which a relative repositioning of the electrons takes place.

Driving-Point Admittance (between the *j*th Terminal and the Reference Terminal of an *n*-Terminal Network).* The quotient of 1) the complex alternating component I_j of the current flowing to the *j*th terminal from its external termination by 2) the complex alternating component V_j of the voltage applied to the *j*th terminal with respect to the reference point when all other terminals have arbitrary external terminations.

Note: In specifying the *Driving-Point Admittance* of a given pair of terminals of a network or transducer having two or more pairs of terminals, no two pairs of which contain a common terminal, all other pairs of terminals are connected to arbitrary admittances.

Dynamic Characteristic (Electron Tubes). See:

Load Characteristic (*Electron Tubes*).

Dynode (Electron Tubes). An *Electrode* which performs a useful function by means of *Secondary Emission*.

Dynode Current. See: *Electrode Current.*

Dynode Spots (Image Orthicons). A spurious signal caused by variations in the *Secondary-Emission Ratio* across the surface of a *Dynode* which is scanned by the electron beam.

Effective Bunching Angle (Reflex Klystrons). In a given *Drift Space*, the *Transit Angle* that would be required in a hypothetical *Drift Space* in which the potentials vary linearly over the same range as in the given space and in which the bunching action is the same as in the given space.

Efficiency. See:

Circuit Efficiency (*of the Output Circuits of Electron Tubes*).

Efficiency (*Radiation-Counter Tubes*).

Electronic Efficiency.

Electron-Stream Transmission Efficiency.

Efficiency (Radiation-Counter Tubes). The probability that a *Tube Count* will take place with a specified particle or quantum incident in a specified manner.

Electrode (Electron Tubes). A conducting *Element* that performs one or more of the functions of emitting, collecting, or controlling, by an electromagnetic field, the movements of electrons or ions. See:

Accelerating Electrode.
Anode (*Electron Tubes*).
Backplate (*Camera Tubes*).
Cathode.
Collector.
Color-Selecting-Electrode System.
Control Electrode.
Control Grid.
Convergence Electrode.
Decelerating Electrode (*Electron-Beam Tubes*).
Deflecting Electrode.
Dynode (*Electron Tubes*).
Filament.
Focusing Electrode.
Grid.
Ignitor Electrode.
Intensifier Electrode.
Modulating Electrode.
Starter (*Gas Tubes*).
Target (*Camera Tubes*).

Electrode Admittance (of the *j*th Electrode of an *n*-Electrode Electron Tube).* The *Short-Circuit Driving-Point Admittance* between the *j*th *Electrode* and the reference point measured directly at the *j*th *Electrode*.

Note: To be able to determine the intrinsic electronic merit of an *Electron Tube*, the *Driving-Point* and *Transfer Admittances* must be defined as if measured directly at the *Electrodes* inside the

tube. The definitions of *Electrode Admittance* and *Electrode Impedance* are included for this reason.

Electrode Capacitance (*n*-Terminal Electron Tubes).* The capacitance determined from the *Short-Circuit Driving-Point Admittance* at that *Electrode*.

Electrode Characteristic. A relation between the *Electrode Voltage* and the current to an *Electrode*, all other *Electrode Voltages* being maintained constant.

Electrode Conductance.* The real part of the *Electrode Admittance*.

Electrode Current (Electron Tubes). The net current from an *Electrode* into the interelectrode space.

Note: The terms *Cathode Current*, *Grid Current*, *Anode Current*, *Plate Current*, and so forth, are used to designate *Electrode Currents* for these specific *Electrodes*. Unless otherwise stated, an *Electrode Current* is measured at the available terminal.

Electrode-Current Averaging Time. The time interval over which the current is averaged in defining the operating capabilities of the *Electrode*.

Electrode Dark Current (Camera Tubes or Phototubes). *Electrode Current* under specified conditions of *Radiation* shielding.

Electrode Dissipation. The power dissipated in the form of heat by an *Electrode* as a result of electron and/or ion bombardment.

Electrode Impedance.* The reciprocal of the *Electrode Admittance*.

Electrode Resistance.* The reciprocal of the *Electrode Conductance*.

Note: This is the effective parallel resistance and is not the real component of the *Electrode Impedance*.

Electrode Voltage. The voltage between an *Electrode* and the *Cathode* or a specified point of a filamentary *Cathode*.

Note: The terms *Grid Voltage*, *Anode Voltage*, *Plate Voltage*, etc., are used to designate the voltage between these specific *Electrodes* and the *Cathode*. Unless otherwise stated, *Electrode Voltages* are understood to be measured at the available terminals.

Electrometer Tube. A high-vacuum tube having a very low *Control-Electrode* conductance to facilitate the measurement of extremely small direct current or voltage.

Electron-Beam Tube. An *Electron Tube*, the performance of which depends upon the formation and control of one or more electron beams.

Electron Device. A device in which conduction is principally by electrons moving through a vacuum, gas, or semiconductor.

Electron Emission. The liberation of electrons from an *Electrode* into the surrounding space.

Electron Gun. An *Electrode* structure which produces and may control, focus, deflect, and converge one or more electron beams.

Electron-Gun Density Multiplication. The ratio of the average current density at any specified aperture through which the stream passes to the average current density at the *Cathode* surface.

Electronic. Of or pertaining to devices, circuits, or systems utilizing electron devices. *Examples:* electronic control, electronic equipment, electronic instrument, and electronic circuit.

Electronic Efficiency. The ratio of 1) the power at the desired frequency delivered by the electron stream to the circuit in an oscillator or amplifier, to 2) the average power supplied to the stream.

Electronic Gap Admittance. See:

Gap Admittance, Electronic.

Electronics. That field of science and engineering which deals with *Electron Devices* and their utilization.

Electronics. (Used as an adjective) of or pertaining to the field of electronics. *Examples:* electronics engineer, electronics course, electronics laboratory, and electronics committee.

Electron Multiplier. A structure, within an *Electron Tube*, which employs secondary electron emission from solids to produce current amplification.

Electron-Stream Potential. At any point in an electron stream, the time average of the potential difference between that point and the electron-emitting surface.

Electron-Stream Transmission Efficiency. At an *Electrode* through which the electron stream passes, the ratio of 1) the average stream current through the *Electrode* to 2) the average stream current approaching the *Electrode*.

Note: In connection with multitransit tubes, the term "electron stream" should be taken to include only electrons approaching the *Electrode* for the first time.

Electron Tube. An *Electron Device* in which conduction takes place by electrons moving through a vacuum or gaseous medium within a gas-tight envelope.

Electron-Wave Tube. An *Electron Tube* in which mutually interacting streams of electrons having different velocities cause a signal modulation to change progressively along their length.

Electrostatic Focusing. A method of *Focusing* an electron beam by the action of an electric field.

Element (Electron Tubes). A constituent part of the tube that contributes directly to its electrical operation. See:

Storage Element (Charge-Storage Tubes).

Emission. See:

Electron Emission.
Field Emission.
Field-Enhanced Photoelectric Emission.
Field-Enhanced Secondary Emission.
Field-Free Emission Current (of a Cathode).
Flection-Point Emission Current.
Grid Emission.
Inflection-Point Emission Current.
Reverse Emission (Back Emission) (Vacuum Tubes).

Schottky Emission.
Secondary Emission.
Secondary Grid Emission.
Thermionic Emission.
Thermionic Grid Emission (*Primary Grid Emission*).

Emission Characteristic. The relation between the emission and a factor controlling the emission such as temperature, voltage, or current of the *Filament* or heater.

End Shield (Magnetrons). A shield for the purpose of confining the *Space Charge* to the *Interaction Space.*

Equivalent Conductance (ATR Tubes). The normalized conductance of the tube in its *Mount* measured at its resonance frequency.

Note: Normalization is with respect to the characteristic impedance of the transmission line at its junction with the tube *Mount.*

Equivalent Dark-Current Input (Phototubes). The incident luminous flux required to give a *Signal Output Current* equal to the *Dark Current.*

Equivalent Diode. The imaginary *Diode* consisting of the *Cathode* of a *Triode* or multigrid tube and a virtual anode to which is applied a *Composite Controlling Voltage* such that the *Cathode Current* is the same as in the *Triode* or multigrid tube.

Equivalent Noise Conductance. A quantitative representation in conductance units of the spectral density of a *Noise-Current Generator* at a specified frequency.

Note 1: The relation between the *Equivalent Noise Conductance* G_n and the spectral density W_i of the *Noise-Current Generator* is

$$G_n = \pi W_i/(kT_0)$$

where k is Boltzmann's constant and T_0 is the *Standard Noise Temperature*, 290°K, and $kT_0 = 4.00 \times 10^{-21}$ watt-seconds.

Note 2: The *Equivalent Noise Conductance* in terms of the mean-square noise-generator current $\overline{i^2}$ within a frequency increment Δf is

$$G_n = \overline{i^2}/(4kT_0\Delta f).$$

Equivalent Noise Current. A quantitative representation in current units of the spectral density of a *Noise-Current Generator* at a specified frequency.

Note 1: The relation between the *Equivalent Noise Current* I_n and the spectral density W_i of the *Noise-Current Generator* is

$$I_n = (2\pi W_i)/e$$

where e is the magnitude of the electronic change.

Note 2: The *Equivalent Noise Current* in terms of the mean square noise-generator current $\overline{i^2}$ within a frequency increment Δf is

$$I_n = \overline{i^2}/(2e\Delta f).$$

Equivalent Noise Resistance. A quantitative representation in resistance units of the spectral density of a *Noise-Voltage Generator* at a specified frequency.

Note 1: The relation between the *Equivalent Noise Resistance* R_n and the spectral density W_e of the *Noise-Voltage Generator* is

$$R_n = (\pi W_e)/(kT_0)$$

where k is Boltzmann's constant and T_0 is the *Standard Noise Temperature*, 290° K, and $kT_0 = 4.00 \times 10^{-21}$ watt-seconds.

Note 2: The *Equivalent Noise Resistance* in terms of the mean square noise-generator voltage $\overline{e^2}$ within a frequency increment Δf is

$$R_n = \overline{e^2}/(4kT_0\Delta f).$$

Equipotential Cathode. See: *Indirectly Heated Cathode.*

Erase (Charge-Storage Tubes). To charge or discharge *Storage Elements* to eliminate previously stored information.

Erasing Speed (Charge-Storage Tubes). The rate of *Erasing* successive *Storage Elements.*

Externally Quenched Counter Tube. See:
Counter Tube, Externally Quenched.

External Termination (of the *j*th Terminal of an *n*-Terminal Network).* That passive or active two-terminal network which is attached externally between the *j*th terminal and the reference point.

Factor. See:
Amplification Factor.
Commutation Factor (*Gas Tubes*).
Deflection Factor (*Cathode-Ray Tubes*).
Gas Amplification Factor (*Gas Phototubes*).
μ-Factor (*of an n-Terminal Electron Tube*).
Noise Factor (*Noise Figure*) (*of a Two-Port Transducer*).
Noise Factor (*Noise Figure*), *Average* (*of a Two-Port Transducer*).
Noise Factor (*Noise Figure*), *Spot.*
Rectification Factor.
Trans-μ-Factor (*Multibeam Electron Tubes*).
Transrectification Factor.

Fault Electrode Current. The current to an *Electrode* under fault conditions, such as *Arc-Backs* and load short circuits.

Field Emission. The liberation of electrons from a solid or liquid by a strong electric field at the surface.

Field-Enhanced Photoelectric Emission. The increased *Photoelectric Emission* resulting from the action of a strong electric field on the emitter.

Field-Enhanced Secondary Emission. The increased *Secondary Emission* resulting from the action of a strong electric field on the emitter.

Field-Free Emission Current (of a Cathode). The electron current emitted by a *Cathode* when the electric field at the surface of the *Cathode* is zero.

Filament. A *Cathode* of a *Thermionic Tube*, usually in the form of a wire or ribbon, to which heat may be supplied by passing current through it. This is also known as a filamentary cathode.

Fired Tube (TR, ATR, and Pre-TR Tubes). The condition of the tube during which a radio-frequency *Glow*

Discharge exists at either the *Resonant Gap*, *Resonant Window*, or both.

Firing Time, High-Level (Switching Tubes). See:
High-Level Firing Time (*Switching Tubes*).

Flat Leakage Power (TR and Pre-TR Tubes). The peak radio-frequency power transmitted through the tube after the establishment of the steady-state radio-frequency discharge.

Flection-Point Emission Current. That value of current on the *Diode Characteristic* for which the second derivative of the current with respect to the voltage has its maximum negative value. This current corresponds to the upper flection point of the *Diode Characteristic*.

Focusing. The process of controlling the electron paths within one or more beams for the purpose of obtaining a desired image or current density distribution.

Focusing and Switching Grille (Color Picture Tubes). A *Color-Selecting-Electrode System* in the form of an array of wires including at least two mutually-insulated sets of conductors in which the switching function is performed by varying the potential difference between them, and *Focusing* is accomplished by maintaining the proper average potentials on the array and on the phosphor *Screen*.

Focusing Coil or Focusing Magnet. An assembly producing a magnetic field for *Focusing* an electron beam.

Focusing, Dynamic (Picture Tubes). The process of *Focusing* in accordance with a specified signal in synchronism with scanning.

Focusing Electrode. An *Electrode* to which a potential is applied to control the cross-sectional area of the electron beam.

Forward Transadmittance. See:
Transadmittance, Forward.

Forward Wave (Traveling-Wave Tubes). A wave whose group velocity is in the same direction as the electron stream motion.

Frequency Pulling. A change of the generated frequency of an oscillator caused by a change in load impedance.

Frequency Range (of a Device). The range of frequencies over which the device may be considered useful with various circuit and operating conditions.

Note: Frequency range should be distinguished from bandwidth, which is a measure of useful range with fixed circuits and operating conditions.

Gain, Available Conversion (of a Conversion Transducer). The ratio of 1) the available output-frequency power from the output terminals of the transducer to 2) the available input-frequency power from the driving generator.

Note: The maximum *Available Conversion Gain* of a *Conversion Transducer* is obtained when the input termination admittance, at input frequency, is the conjugate of the input-frequency *Driving Point Admittance* of the *Conversion Transducer*.

Gain, Available-Power (of a Two-Port Linear Transducer). At a specified frequency, the ratio of 1) the available signal power from the output *Port* of the transducer, to 2) the available signal power from the input source.

Note: The available signal power at the output *Port* is a function of the match between the source impedance and the impedance of the input *Port*.

Gain, Available-Power, Maximum (of a Two-Port Linear Transducer). The gain of the transducer at a specified frequency obtained when the transducer is conjugately matched to source and load.

Note: The *Maximum Available-Power Gain* is not defined unless both the input and output impedances of the two-port transducer have positive real parts for arbitrary passive input and output terminations.

Gain, Conversion Voltage (of a Conversion Transducer). The ratio of 1) the magnitude of the output-frequency voltage across the output termination, with the transducer inserted between the input-frequency generator and the output termination, to 2) the magnitude of the input-frequency voltage across the input termination of the transducer.

Gain, Insertion (of a Two-Port Linear Transducer). At a specified frequency, the ratio of 1) the actual signal power transferred from the output *Port* of the transducer to its load, to 2) the signal power which the same load would receive if driven directly by the source.

Gain, Insertion Voltage (of an Electric Transducer). The complex ratio of 1) the alternating component of voltage across the *External Termination* of the output with the transducer inserted between the generator and the output termination, to 2) the voltage across the *External Termination* of the output when the generator is connected directly to the output termination.

Gain, Power (of a Two-Port Linear Transducer). At a specified frequency, the ratio of 1) the signal power that the transducer delivers to a specified load, to 2) the signal power delivered to its input *Port*.

Note: The *Power Gain* is not defined unless the input impedance of the transducer has a positive real part.

Gain, Transducer (of a Two-Port Linear Transducer). At a specified frequency, the ratio of 1) the actual signal power transferred from the output *Port* of the transducer to its load, to 2) the available signal power from the source driving the transducer.

Gamma (Picture or Camera Tubes). The exponent of that power law which is used to approximate the curve of output magnitude vs input magnitude over the region of interest.

Note: For quantitative evaluation, it is customary to plot the log of the output magnitude (ordinate) vs the log of the input magnitude (abscissa), as measured from a point corresponding to some reference black level, and select a straight line which approximates this plot over the region of interest and takes its slope. If the

plot departs seriously from linearity it cannot be adequately described by a single value of *Gamma*. Even when the plot is reasonably linear, the procedure for determining the approximation should be described.

Gap. See:
Input Gap.
Interaction Gap.
Main Gap (Glow-Discharge Tubes).
Output Gap.
Resonant Gap (TR Tubes).
Starter Gap (Gas Tubes).

Gap Admittance, Circuit. The admittance of the circuit at a gap in the absence of an electron stream.

Gap Admittance, Electronic. The difference between 1) the gap admittance with the electron stream traversing the gap and 2) the gap admittance with the stream absent.

Gap Capacitance, Effective. One half the rate of change with angular frequency of the resonator susceptance, measured at the gap, for frequencies near resonance.

Gap Loading, Multipactor. The *Electronic Gap Admittance*, resulting from a sustained *Secondary-Emission* discharge existing within a gap as a result of the motion of the secondary electrons in synchronism with the electric field in the gap.

Gap Loading, Primary Transit-Angle. The *Electronic Gap Admittance* that results from the traversal of the gap by an initially unmodulated electron stream.

Note: This is exclusive of *Secondary Emission* in the gap.

Gap Loading, Secondary Electron. The *Electronic Gap Admittance* which results from the traversal of a gap by secondary electrons originating in the gap.

Gas Amplification (Radiation-Counter Tubes). The ratio of the charge collected to the charge liberated by the *Initial Ionizing Event.*

Note: See also: *Methods of Testing.*

Gas Amplification Factor (Gas Phototubes). The ratio of *Radiant* or *Luminous Sensitivities* with and without ionization of the gas.

Gas (Ionization) Current (Vacuum Tubes). A positive-ion current produced by collisions between electrons and residual gas molecules.

Gas-Filled Radiation-Counter Tube. See:
Counter Tube, Gas-Filled, Radiation.

Gas-Flow Counter Tube. See:
Counter Tube, Gas-Flow.

Gas Focusing. A method of concentrating an electron beam by gas ionization within the beam.

Gas Ratio. The ratio of the ion current in a tube to the electron current that produces it.

Gas Tube. An *Electron Tube* in which the contained gas or vapor performs the primary role in the operation of the tube.

Geiger-Mueller Counter Tube. See:
Counter Tube, Geiger-Mueller.

Geiger-Mueller Region (Radiation-Counter Tubes). See:
Region, Geiger-Mueller (Radiation-Counter Tubes).

Geiger-Mueller Threshold (Radiation-Counter Tubes). The lowest applied voltage at which the charge collected per isolated *Tube Count* is substantially independent of the nature of the *Initial Ionizing Event.*

Generator. See:
Current Generator.
Noise-Current Generator.
Noise-Voltage Generator.
Voltage Generator.

Glow Discharge. A discharge of electricity through a gas, characterized by 1) a space potential in the vicinity of the *Cathode* that is much higher than the ionization potential of the gas; 2) the presence of a *Cathode Glow.*

Glow-Discharge Tube. A *Gas Tube* that depends for its operation on the properties of a *Glow Discharge.*

Grid. An *Electrode* having one or more openings for the passage of electrons or ions. See:
Control Grid.
Screen Grid.
Shield Grid.
Space-Charge Grid.
Suppressor Grid.

Grid Bias. See:
Direct Grid Bias.

Grid Characteristic. See:
Electrode Characteristic.

Grid Current. See:
Electrode Current.

Grid-Drive Characteristic. A relation between electrical or light output and *Control-Electrode* voltage measured from cutoff.

Grid Driving Power. The average product of the instantaneous value of the *Grid Current* and the alternating component of the *Grid Voltage* over a complete cycle.

Note: This comprises the power supplied to the biasing device and to the *Grid.*

Grid Emission. Electron or ion emission from a *Grid* of an *Electron Tube.*

Grid Voltage. See:
Electrode Voltage.

Harmonic Conversion Transducer (Frequency Multiplier, Frequency Divider). A *Conversion Transducer* in which the output-signal frequency is a multiple or submultiple of the input frequency.

Note: In general, the output-signal amplitude is a nonlinear function of the input-signal amplitude.

Harmonic Leakage Power (TR and Pre-TR Tubes). The total radio-frequency power transmitted through the *Fired Tube* in its *Mount* at frequencies other than the fundamental frequencies generated by the transmitter.

Heater. An electric heating *Element* for supplying heat to an indirectly heated *Cathode.*

Heater Warm-Up Time. See:
Methods of test (to be published).

Heating Time (Vacuum Tubes). See:
Cathode Heating Time (Vacuum Tubes).

Heptode. A seven-electrode *Electron Tube* containing an *Anode*, a *Cathode*, a *Control Electrode*, and four additional *Electrodes* that are ordinarily *Grids*.

Heterodyne Conversion Transducer (Converter). A *Conversion Transducer* in which the output frequency is the sum or difference of 1) the input frequency and 2) an integral multiple of the local oscillator frequency.

Note: The frequency and voltage or power of the local oscillator are parameters of the *Conversion Transducer*. Ordinarily, the output-signal amplitude is a linear function of the input-signal amplitude over its useful operating range.

Hexode. A six-electrode *Electron Tube* containing an *Anode*, *a Cathode*, a *Control Electrode*, and three additional *Electrodes* that are ordinarily *Grids*.

High-Level Firing Time (Switching Tubes). The time required to establish a radio-frequency discharge in the tube after the application of radio-frequency power.

High-Level Radio-Frequency Signal (TR, ATR, and Pre-TR Tubes). A radio-frequency signal of sufficient power to cause the tube to become fired.

High-Level VSWR (Switching Tubes). The vswr due to a *Fired Tube* in its *Mount* located between a generator and matched termination in the waveguide.

High-Velocity Scanning. See:
Scanning, High-Velocity.

Hold (Charge-Storage Tubes). To maintain *Storage Elements* at equilibrium potentials by electron bombardment.

Hot Cathode (Thermionic Cathode). A *Cathode* that functions primarily by the process of *Thermionic Emission.*

Hot-Cathode Tube. An *Electron Tube* containing a *Hot Cathode.*

Hysteresis (of an Oscillator). A behavior that may appear in an oscillator wherein multiple values of the output power and/or frequency correspond to given values of an operating parameter.

Hysteresis (Radiation-Counter Tubes). The temporary change in the *Counting-Rate-vs-Voltage Characteristic* caused by previous operation.

Ideal Noise Diode. A *Diode* that has an infinite internal impedance and in which the current exhibits *Full Shot Noise* fluctuations.

Iconoscope. A *Camera Tube* in which a beam of high-velocity electrons scans a photoemissive mosaic which is capable of storing an electrical charge pattern.

Ignitor. See:
Ignitor Electrode (Switching Tubes).

Ignitor Current. See:
Electrode Current.

Ignitor-Current Temperature Drift (TR, Pre-TR, and Attenuator Tubes). The variation in *Ignitor Electrode* current caused by a change in ambient temperature of the tube.

Ignitor Discharge (Switching Tubes). A dc *Glow Discharge*, between the *Ignitor Electrode* and a suitably located *Electrode*, used to facilitate radio-frequency ionization.

Ignitor Electrode (Switching Tubes). An *Electrode* used to initiate and sustain the *Ignitor Discharge.*

Ignitor Firing Time (Switching Tubes). The time interval between the application of a direct voltage to the *Ignitor Electrode* and the establishment of the *Ignitor Discharge.*

Ignitor Interaction (TR, Pre-TR, and Attenuator Tubes). The difference between the *Insertion Loss* measured at a specified *Ignitor Current* and that measured at zero *Ignitor Current.*

Ignitor Leakage Resistance (Switching Tubes). The insulation resistance, measured in the absence of an *Ignitor Discharge*, between the *Ignitor Electrode* terminal and the adjacent radio-frequency *Electrode.*

Ignitor Oscillations (TR, Pre-TR, and Attenuator Tubes). Relaxation oscillations in the *Ignitor* circuit.

Note: If present, these oscillations may limit the tube's characteristics.

Ignitor Voltage Drop (Switching Tubes). The direct voltage between the *Cathode* and the *Anode* of the *Ignitor Discharge* at a specified *Ignitor Current.*

Image Converter Tube. See:
Image Tube.

Image Dissector Tube (Dissector Tube). A *Camera Tube* in which an electron image produced by a photoemitting surface is focused in the plane of a defining aperture and is scanned past that aperture.

Image Iconoscope. A *Camera Tube* in which an electron image is produced by a photoemitting surface and focused on one side of a separate storage *Target* which is scanned on the same side by an electron beam, usually of high-velocity electrons.

Image Orthicon. A *Camera Tube* in which an electron image is produced by a photoemitting surface and focused on one side of a separate storage *Target* which is scanned on its opposite side by an electron beam, usually of low-velocity electrons.

Image Tube (Image Converter Tube). An *Electron Tube* which reproduces on its fluorescent screen an image of an irradiation pattern incident on its photosensitive surface.

Impedance. See:
Cathode Coating Impedance.
Cathode Interface (Layer) Impedance.
Electrode Impedance.
Interaction Impedance (Traveling-Wave Tubes).

Indicator Tube. An *Electron-Beam Tube* in which useful information is conveyed by the variation in cross section of the beam at a luminescent target.

Indirectly Heated Cathode (Equipotential Cathode, Unipotential Cathode). A *Cathode* of a *Thermionic Tube* to which heat is supplied by an independent *Heater Element.*

Inflection-Point Emission Current. That value of current on the *Diode Characteristic* for which the second

derivative of the current with respect to the voltage is zero.

Note: This current corresponds to the inflection point of the *Diode Characteristic* and is, under suitable conditions, an approximate measure of the maximum space-charge-limited emission current.

Initial Ionizing Event (Radiation-Counter Tubes). An ionizing event that initiates a *Tube Count*.

Input Capacitance (*n*-Terminal Electron Tubes).* The *Short-Circuit Transfer Capacitance* between the input terminal and all other terminals, except the output terminal, connected together.

Note: This quantity is equivalent to the sum of the *Interelectrode Capacitances* between the input *Electrode* and all other *Electrodes* except the output *Electrode*.

Input Gap. An *Interaction Gap* used to initiate a variation in an electron stream.

Insertion Gain (of a Two-Port Linear Transducer). See:

Gain, Insertion (of a Two-Port Linear Transducer).

Insertion Loss (TR, Pre-TR, and Attenuator Tubes). The decrease in power measured in a matched termination when the *Unfired Tube*, at a specified *Ignitor Current*, is inserted in the waveguide between a matched generator and the termination.

Insertion Voltage Gain (of an Electric Transducer). See:

Gain, Insertion Voltage (of an Electric Transducer).

Intensifier Electrode. An *Electrode* causing *Post Acceleration*.

Interaction Circuit Phase Velocity (Traveling-Wave Tubes). The phase velocity of a wave traveling on the circuit in the absence of electron flow.

Interaction Gap. An *Interaction Space* between *Electrodes*.

Interaction Impedance (Traveling-Wave Tubes). A measure of the radio-frequency field strength at the electron stream for a given power in the interaction circuit. It may be expressed by the following equation:

$$K = \frac{E^2}{2\left(\frac{\omega}{v}\right)^2 P}$$

where E is the peak value of the electric field at the position of electron flow, ω is the angular frequency, v is the *Interaction-Circuit Phase Velocity* and P is the propagating power. If the field strength is not uniform over the beam, an effective *Interaction Impedance* may be defined.

Interaction Space. A region of an *Electron Tube* in which electrons interact with an alternating electromagnetic field.

Interdigital Magnetron. A *Magnetron* having axial anode segments around the *Cathode*, alternate segments being connected together at one end, remaining segments connected together at the opposite end.

Interelectrode Capacitance (*j-l* Interelectrode Capacitance C_{jl} of an *n*-Terminal Electron Tube).* The capacitance determined from the *Short-Circuit Transfer Admittance* between the jth and the lth terminals.

Note: This quantity is often referred to as direct interelectrode capacitance.

Interelectrode Transadmittance (*j-l* Interelectrode Transadmittance of an *n*-Electrode Electron Tube).* The *Short-Circuit Transfer Admittance* from the jth electrode to the lth electrode.

Interelectrode Transconductance (*j-l* Interelectrode Transconductance).* The real part of the *j-l Interelectrode Transadmittance*.

Internal Correction Voltage (Electron Tubes). The voltage that is added to the *Composite Controlling Voltage* and is the voltage equivalent of such effects as those produced by initial electron velocity and *Contact Potential*.

Inverse Electrode Current. The current flowing through an *Electrode* in the direction opposite to that for which the tube is designed.

Ionic-Heated Cathode. A *Hot Cathode* that is heated primarily by ionic bombardment of the emitting surface.

Ionic-Heated-Cathode Tube. An *Electron Tube* containing an *Ionic-Heated Cathode*.

Ionization Current. See:

Gas Current.

Ionization Time (Gas Tubes). The time interval between the initiation of conditions for and the establishment of conduction at some stated value of *Tube Voltage Drop*.

Ionizing Event. Any interaction by which one or more ions are produced.

Ion Spot (Camera Tubes or Image Tubes). The spurious signal resulting from the bombardment or alteration of the *Target* or *Photocathode* by ions.

Ion Spot (on a Cathode-Ray-Tube Screen). An area of localized deterioration of luminescence caused by bombardment with negative ions.

Johnson Noise. See:

Thermal Noise.

Keep-Alive. Deprecated, see:

Ignitor.

Knee of Transfer Characteristic (Image Orthicons). The region of maximum curvature in the *Transfer Characteristic*.

Lag (Camera Tubes). A persistence of the electrical-charge image for a small number of frames.

Landing, Poor (Camera Tubes). See:

Porthole.

Leakage Power (TR and Pre-TR Tubes). The radio-frequency power transmitted through a *Fired Tube*. See:

Flat Leakage Power (TR and Pre-TR Tubes).

Harmonic Leakage Power (TR and Pre-TR Tubes).

Level (Charge-Storage Tubes). A charge value which can be stored in a given *Storage Element* and distinguished in the output from other charge values.

Line or Trace (Cathode-Ray Tubes). The path of the moving spot on the *Screen* or *Target*.

Load (Dynamic) Characteristic (of an Electron Tube Connected in a Specified Operating Circuit, at a Specified Frequency). A relation between the instantaneous values of a pair of variables such as *Electrode Voltage* and current, when all direct *Electrode* supply voltages are maintained constant.

Loaded *Q* (Switching Tubes). The *Unloaded Q* of the tube modified by the coupled impedances.

Note: As here used, *Q* is equal to 2π times the energy stored at the resonance frequency divided by the energy dissipated per cycle in the tube, or for *Cell-Type Tubes*, in the tube and its external resonant circuit.

Load Impedance Diagram (Oscillators). A chart showing performance of the oscillator with respect to variations in the load impedance. Ordinarily, contours of constant power and of constant frequency are drawn on a chart whose coordinates are the components of either the complex load impedance or of the reflection coefficient.

Note: See:

Rieke Diagram.

Local Oscillator Tube. An *Electron Tube* in a *Heterodyne Conversion Transducer* to provide the local heterodyning frequency for a *Mixer Tube.*

Loss. See:

Arc-Drop Loss (Gas Tubes).

Arc Loss (Switching Tubes).

Insertion Loss (TR, Pre-TR, and Attenuator Tubes).

Low-Level Radio-Frequency Signal (TR, ATR, and Pre-TR Tubes). A radio-frequency signal with insufficient power to cause the tube to become fired.

Low-Velocity Scanning. See:

Scanning, Low-Velocity.

Magnetic Focusing. A method of *Focusing* an electron beam by the action of a magnetic field.

Magnetron. An *Electron Tube* characterized by the interaction of electrons with the electric field of a circuit element in crossed steady electric and magnetic fields to produce ac power output. See:

Interdigital Magnetron.

Multicavity Magnetron.

Multisegment Magnetron.

Packaged Magnetron.

Rising-Sun Magnetron.

Split-Anode Magnetron.

Main Gap (Glow-Discharge Tubes). The conduction path between a principal *Cathode* and a principal *Anode.*

Maximum Available Power Gain (of a Two-Port Linear Transducer). See:

Gain, Available Power, Maximum (of a Two-Port Linear Transducer).

Memory Tube. Deprecated, see:

Storage Tube.

Mercury-Vapor Tube. A *Gas Tube* in which the active gas is mercury vapor.

Microphonism (Microphonics) (Electron Tubes). The modulation of one or more of the *Electrode Currents* resulting from the mechanical vibration of a tube *Element.*

Minimum Firing Power (Switching Tubes). The minimum radio-frequency power required to initiate a radio-frequency discharge in the tube at a specified *Ignitor Current.*

Mixer Tube. An *Electron Tube* that performs only the frequency-conversion function of a *Heterodyne Conversion Transducer* when it is supplied with voltage or power from an external oscillator.

Mode. A state of a vibrating system to which corresponds one of the possible resonance frequencies (or propagation constants).

Note 1: Not all dissipative systems have *Modes.*

Note 2: See:

Modes, Degenerate.

Mode of an Oscillator.

1) **Resonator Mode.** A condition of operation corresponding to a particular field configuration for which the electron stream introduces a negative conductance into the coupled circuit.
2) **Transit-Time Mode.** A condition of operation of an oscillator corresponding to a limited range of *Drift-Space Transit Angle* for which the electron stream introduces a negative conductance into the coupled circuit.

Mode Purity (ATR Tubes). The extent to which the tube in its *Mount* is free from undesirable *Mode* conversion.

Modes, Degenerate. A set of *Modes* having the same resonance frequency (or propagation constant).

Note: The members of a set of *Degenerate Modes* are not unique.

Mode Separation (Oscillators). The frequency difference between *Resonator Modes* of oscillation.

Modulation. See:

Beam Modulation, Percentage (Image Orthicons).

Convection-Current Modulation.

Depth of Velocity Modulation, Small-Signal.

Velocity Modulation.

Moire (in Television). The spurious pattern in the reproduced picture resulting from interference beats between two sets of periodic structures in the image.

Note: *Moires* may be produced, for example, by interference between regular patterns in the original subject and the *Target Grid* in an *Image Orthicon*, between patterns in the subject and the line pattern and the pattern of phosphor dots of a *Color Picture Tube*, and between any of these patterns and the pattern produced by the chrominance signal.

Monoscope. A signal-generating *Electron-Beam Tube* in which a picture signal is produced by scanning an *Electrode* which has a predetermined pattern of *Secondary-Emission* response over its surface.

Mount (Switching Tubes). The flange or other means by which the tube, or tube and cavity, are connected to a waveguide.

μ-Factor (n-Terminal Electron Tubes). The ratio of the magnitude of an infinitesimal change in the voltage at the jth *Electrode* to the magnitude of an infinitesimal change in the voltage at the lth *Electrode* under the conditions that the current to the mth *Electrode* remains unchanged, and the voltages of all other *Electrodes* are maintained constant.

Multicavity Magnetron. A *Magnetron* in which the circuit includes a plurality of cavities.

Multielectrode Tube. An *Electron Tube* containing more than three *Electrodes* associated with a single electron stream.

Multiple Tube Counts (Radiation-Counter Tubes). Spurious *Counts* induced by previous *Tube Counts*.

Multiple-Unit Tube. An *Electron Tube* containing within one envelope two or more groups of *Electrodes* associated with independent electron streams.

Note: A *Multiple-Unit Tube* may be so indicated, for example: duodiode, duotriode, diode-pentode, duodiode-triode, duodiode-pentode, or triode-pentode.

Multiplier Phototube. A *Phototube* with one or more *Dynodes* between its *Photocathode* and the output *Electrode*.

Multisegment Magnetron. A *Magnetron* with an *Anode* divided into more than two segments, usually by slots parallel to its axis.

Noise. See:

Johnson Noise.
Shot Noise.
Shot Noise, Full.
Shot Noise, Reduced.
Thermal Noise.

Noise-Current Generator. A *Current Generator*, the output of which is described by a random function of time.

Note: At a specified frequency, a *Noise-Current Generator* can often be adequately characterized by its mean-square current within the frequency increment Δf, or by its spectral density. If the circuit contains more than one *Noise-Voltage Generator* or *Noise-Current Generator*, the correlation coefficients among the generators must also be specified.

Noise Diode, Ideal. See:

Ideal Noise Diode.

Noise Factor (Noise Figure) (of a Two-Port Transducer). At a specified input frequency the ratio of 1) the total noise power per unit bandwidth at a corresponding output frequency available at the output *Port* to 2) that portion of 1) engendered at the input frequency by the input termination at the *Standard Noise Temperature* (290°K).

Note 1: For heterodyne systems there will be, in principle, more than one output frequency corresponding to a single input frequency, and vice versa; for each pair of corresponding frequencies a *Noise Factor* is defined.

Note 2: The phrase "available at the output *Port*" may be replaced by "delivered by system into an output termination."

Note 3: To characterize a system by a *Noise Factor* is meaningful only when the input termination is specified.

Noise Factor (Noise Figure), Average (of a Two-Port Transducer). The ratio of 1) the total noise power delivered by the transducer into its output termination when the *Noise Temperature* of its input termination is standard (290°K) at all frequencies, to 2) that portion of 1) engendered by the input termination.

Note 1: For heterodyne systems, 2) includes only that noise from the input termination which appears in the output via the principal-frequency transformation of the system, and does not include spurious contributions such as those from an image-frequency transformation.

Note 2: A quantitative relation between the *Average Noise Factor* $\overline{F}$ and the *Spot Noise Factor* $F(f)$ is

$$\overline{F} = \frac{\int F(f)G(f)df}{\int G(f)df}$$

where f is the input frequency, and $G(f)$ is the ratio of 1) the signal power delivered by the transducer into its output termination, to 2) the corresponding signal power available from the input termination at the input frequency. For heterodyne systems, 1) comprises only power appearing in the output via the principal-frequency transformation of the system: for example, power via image-frequency transformation is excluded.

Note 3: To characterize a system by an *Average Noise Factor* is meaningful only when the input termination is specified.

Noise Factor (Noise Figure), Spot. See:

Noise Factor (Noise Figure) (of a Two-Port Transducer).

Note: This term is used where it is desired to emphasize that the *Noise Factor* is a point function of input frequency.

Noise Temperature (at a Port). The temperature of a passive system having an available noise power per unit bandwidth equal to that of the actual *Port*, at a specified frequency.

Note: See:

Thermal Noise.

Noise Temperature, Standard. The standard reference temperature T_0 for noise measurements is 290°K.

Note: $kT_0/e = 0.0250$ volt, where e is the magnitude of the electronic charge and k is Boltzmann's constant.

Noise-Voltage Generator. A *Voltage Generator* the output of which is described by a random function of time.

Note: At a specified frequency, a *Noise-Voltage Generator* can often be adequately characterized by its mean-square voltage within the frequency increment Δf or by its spectral density. If the circuit contains more than one *Noise-Voltage Generator* or *Noise-Current Generator*, the correlation coefficients among the generators must also be specified.

Normalized Plateau Slope. See:

Plateau Slope, Normalized.

Number of Loops (in a Magnetically Focused Electron Beam). The number of maxima in the beam diameter between the *Electron Gun* and the *Target*, or between a point on the *Photocathode* and the *Target*.

Octode. An eight-electrode *Electron Tube* containing an *Anode*, a *Cathode*, a *Control Electrode*, and five additional *Electrodes* that are ordinarily *Grids*.

Operating Characteristic. See:

Load Characteristic.

Operation Time. The time after simultaneous application of all *Electrode Voltages* for a current to reach a stated fraction of its final value. Conventionally the final value is taken as that reached after a specified length of time.

Note: All *Electrode Voltages* are to remain constant during measurement. The tube *Elements* must all be at room temperature at the start of the test.

Optimum Bunching. The *Bunching* condition that produces maximum power at the desired frequency in an *Output Gap*.

Orthicon. A *Camera Tube* in which a beam of low-velocity electrons scans a photoemissive mosaic capable of storing an electrical-charge pattern.

Oscilloscope Tube (Oscillograph Tube). A *Cathode-Ray Tube* used to produce a visible pattern which is the graphical representation of electrical signals.

Output Capacitance (*n*-Terminal Electron Tubes).* The *Short-Circuit Transfer Capacitance* between the output terminal and all other terminals, except the input terminal, connected together.

Output Gap. An *Interaction Gap* by means of which usable power can be abstracted from an electron stream.

Overbunching. The *Bunching* condition produced by the continuation of the *Bunching* process beyond the optimum condition.

Overvoltage (Radiation-Counter Tubes). The amount by which the applied voltage exceeds the *Geiger-Mueller Threshold*.

Packaged Magnetron. An integral structure comprising a *Magnetron*, its magnetic circuit, and an output matching device.

Peak Alternating Gap Voltage. The negative of the line integral of the peak alternating electric field taken along a specified path across the gap.

Note: The path of integration must be stated.

Peak Cathode Current (Steady-State). The maximum instantaneous value of a periodically recurring *Cathode Current*.

Peak Electrode Current. The maximum instantaneous current that flows through an *Electrode*.

Peak Forward Anode Voltage. The maximum instantaneous *Anode Voltage* in the direction in which the tube is designed to pass current.

Peak Inverse Anode Voltage. The maximum instantaneous *Anode Voltage* in the direction opposite to that in which the tube is designed to pass current.

Pentode. A five-electrode *Electron Tube* containing an *Anode*, a *Cathode*, a *Control Electrode*, and two additional *Electrodes* that are ordinarily *Grids*.

Performance Chart (Magnetron Oscillators). A plot on coordinates of applied *Anode Voltage* and *Current* showing contours of constant magnetic field, power output, and over-all efficiency.

Persistence Characteristic (Decay Characteristic) (of a Luminescent Screen). A relation between luminance (or emitted radiant power) and time after excitation.

Persistence Characteristic (Camera Tubes). The temporal step response of a *Camera Tube* to illumination. See:

Methods of Measurement.

Perveance. The quotient of the space-charge-limited *Cathode Current* by the three-halves power of the *Anode Voltage* in a *Diode*.

Note: *Perveance* is the constant G appearing in the Child-Langmuir-Schottky equation

$$i_k = G e_b^{3/2}.$$

When the term *Perveance* is applied to a *Triode* or multigrid tube, the *Anode Voltage* e_b is replaced by the *Composite Controlling Voltage* e' of the *Equivalent Diode*.

Phase Recovery Time (TR and Pre-TR Tubes). The time required for a *Fired Tube* to deionize to such a level that a specified phase shift is produced in the *Low-Level Radio-Frequency Signal* transmitted through the tube.

Phase-Tuned Tube (TR Tubes). A fixed-tuned *Broad-Band TR Tube*, wherein the phase angle through and the reflection introduced by the tube are controlled within limits.

Photocathode. An *Electrode* used for obtaining *Photoelectric Emission*.

Photoelectric Emission. The ejection of electrons from a solid or liquid by electromagnetic radiation. See:

Field-Enhanced Photoelectric Emission.

Photomultiplier. See:

Multiplier Phototube.

Phototube. An *Electron Tube* that contains a *Photocathode* and has an output depending on the total *Photoelectric Emission* from the irradiated area of the *Photocathode*.

Pickup Tube. Deprecated, see:

Camera Tube.

π-Mode (Magnetrons). The *Mode* of operation for which the phases of the fields of successive *Anode* openings facing the *Interaction Space* differ by π radians.

Plate. A common name for the principal *Anode* in an *Electron Tube.*

Plateau (Radiation-Counter Tubes). The portion of the *Counting-Rate-vs-Voltage Characteristic* in which the counting rate is substantially independent of the applied voltage.

Plateau Length (Radiation-Counter Tubes). The range of applied voltage over which the *Plateau* extends.

Plateau Slope, Normalized (Radiation-Counter Tubes). The ratio, at the midpoint of the *Plateau*, of 1) the increment of counting rate divided by the threshold counting rate, to 2) the increment of applied voltage divided by the threshold voltage.

Plateau Slope, Relative (Radiation-Counter Tubes). The quotient, at the midpoint of the *Plateau* of 1) the increment of counting rate by 2) the product of counting rate and applied voltage increment.

Plate Characteristic. See:
Electrode Characteristic.

Plate Current. See:
Electrode Current.

Plate Voltage. See:
Electrode Voltage.

Port. A place of access to a system where energy may be supplied or withdrawn, or where system variables may be observed or measured.

Note 1: In any particular case, the *Ports* are determined by the way in which the system is used, and not by the structure alone.

Note 2: A designated pair of terminals is an example of a *Port.*

Porthole (Poor Landing) (Camera Tubes). A defect, in a properly aligned *Camera Tube* employing *Low-Velocity Scanning*, resulting in an increase in *Target Cutoff Voltage*, and a decrease in sensitivity toward the corners of the picture.

Positional Crosstalk (Multibeam Cathode-Ray Tubes). The variation in the path followed by any one electron beam as the result of a change impressed on any other beam in the tube.

Position of the Effective Short (Switching Tubes). The distance between a specified reference plane and the apparent short circuit of the *Fired Tube* in its *Mount.*

Post Acceleration (Electron-Beam Tubes). Acceleration of the beam electrons after deflection.

Power. See:
Available Power (at a Port).
Flat Leakage Power (TR and Pre-TR Tubes).
Grid Driving Power.
Harmonic Leakage Power (TR and Pre-TR Tubes).
Leakage Power (TR and Pre-TR Tubes).
Minimum Firing Power (Switching Tubes).

Power Gain (of a Two-Port Linear Transducer). See:
Gain, Power (of a Two-Port Linear Transducer).

Predissociation. A process by which a molecule that has absorbed energy dissociates before it loses energy by *Radiation.*

Preoscillation Current. See:
Starting Current of an Oscillator.

Pre-TR Tube. A gas-filled radio-frequency switching tube used to protect the *TR Tube* from excessively high power and the receiver from frequencies other than the fundamental.

Primary-Color Unit. The area within a *Color Cell* occupied by one primary color.

Prime (Charge-Storage Tubes). To charge or discharge *Storage Elements* to a potential suitable for writing.

Priming Speed (Charge-Storage Tubes). The rate of priming successive *Storage Elements.*

Proportional Counter Tube. See:
Counter Tube, Proportional.

Proportional Region (Radiation-Counter Tubes). See:
Region, Proportional (Radiation-Counter Tubes).

Pulling Figure of an Oscillator. The difference between the maximum and minimum frequencies reached by an oscillator when the phase angle of the reflection coefficient at the load impedance varies through 360° and the absolute value of this coefficient is constant and at a specified value, usually 0.20. (Voltage standing-wave ratio 1.5.)

Pushing Figure of an Oscillator. The change of oscillator frequency with a specified change in current, excluding thermal effects.

Note: See:
Tuning Sensitivity, Electronic.

Q. See:
Loaded Q (Switching Tubes).
Unloaded (Intrinsic) Q (Switching Tubes).

Quantum Efficiency (Photocathodes). The average number of electrons photoelectrically emitted from the *Photocathode* per incident photon of a given wavelength.

Note: The *Quantum Efficiency* varies with the wavelength, angle of incidence, and polarization of the incident *Radiation.*

Quenching (Radiation-Counter Tubes). The process of terminating a discharge in a *Radiation-Counter Tube* by inhibiting *Reignition.*

Radiation (Nuclear). In nuclear work, the usual meaning of *Radiation* is extended to include moving nuclear particles, charged or uncharged.

Radiation Counter. An instrument used for detecting or measuring *Radiation* by a counting process.

Radiation-Counter Tube. See:
Counter Tube, Externally Quenched.
Counter Tube, Gas-Filled, Radiation.
Counter Tube, Gas-Flow.
Counter Tube, Geiger-Mueller.
Counter Tube, Proportional.
Counter Tube, Self-Quenched.

Radio-Frequency Signal, High-Level (TR, ATR, and Pre-TR Tubes). See:

High-Level Radio-Frequency Signal (TR, ATR, and Pre-TR Tubes).

Radio-Frequency Signal, Low-Level (TR, ATR, and Pre-TR Tubes). See:

Low-Level Radio-Frequency Signal (TR, ATR and Pre-TR Tubes).

Raster. A predetermined pattern of scanning lines which provides substantially uniform coverage of an area.

Raster Burn (Camera Tubes). A change in the characteristics of that area of the *Target* which has been scanned, resulting in a spurious signal corresponding to that area when a larger or tilted *Raster* is scanned.

Ratio. See:

Compression Ratio (Gain or Amplification).
Control Ratio (Gas Tubes).
Gas Ratio.
Read-Around Ratio (Charge-Storage Tubes).
Secondary-Emission Ratio (Electrons).
Signal-to-Noise Ratio (Camera Tubes).
Transadmittance Compression Ratio.

Read (Charge-Storage Tubes). To generate an output corresponding to the stored charge pattern.

Read-Around Number (Charge-Storage Tubes). The number of times *Priming*, *Writing*, *Reading*, or *Erasing* operations can be performed on *Storage Elements* adjacent to any given *Element* without loss of information from that *Element*.

Note: The sequence of operations should be specified.

Read-Around Ratio (Charge-Storage Tubes). Deprecated, see:

Read-Around Number.

Read Number (Charge-Storage Tubes). The number of times a *Storage Element* is *Read* without rewriting.

Reading Speed (Charge-Storage Tubes). The rate of *Reading* successive *Storage Elements*.

Recovery Time (ATR Tubes). The time required for a *Fired Tube* to deionize to such a level that the normalized conductance and susceptance of the tube in its *Mount* are within specified ranges.

Note: Normalization is with respect to the characteristic admittance of the transmission line at its junction with the tube *Mount*.

Recovery Time (Gas Tubes). The time required for the *Control Electrode* to regain control after *Anode Current* interruption.

Note: To be exact, the *Deionization* and *Recovery Time* of a *Gas Tube* should be presented as families of curves relating such factors as *Condensed-Mercury Temperature*, *Anode Current*, *Anode* and *Control Electrode* voltages, and control circuit impedance.

Recovery Time (Geiger-Mueller Counters). The minimum time from the start of a counted pulse to the instant a succeeding pulse can attain a specified percentage of the maximum amplitude of the counted pulse.

Recovery Time (TR and Pre-TR Tubes). The time required for a *Fired Tube* to deionize to such a level that the attenuation of a *Low-Level Radio-Frequency Signal* transmitted through the tube is decreased to a specified value.

Rectification Factor. The quotient of 1) the change in average current of an *Electrode* by 2) the change in amplitude of the alternating sinusoidal voltage applied to the same *Electrode*, the direct voltages of this and other *Electrodes* being maintained constant.

Redistribution (Charge-Storage Tubes or Camera Tubes). The alteration of charges on an area of a storage surface by secondary electrons from any other area of the surface.

Reflection Color-Tube. A *Color Picture Tube* which produces an image by means of electron reflection techniques in the *Screen* region.

Reflector. See:

Repeller.

Reflex Bunching. The *Bunching* that occurs in an electron stream that has been made to reverse its direction in the *Drift Space*.

Regeneration (Charge-Storage Tubes). The replacing of charge to overcome *Decay* effects, including loss of charge by *Reading*.

Region, Geiger-Mueller (Radiation-Counter Tubes). The range of applied voltage in which the charge collected per isolated *Count* is independent of the charge liberated by the *Initial Ionizing Event*.

Region of Limited Proportionality (Radiation-Counter Tubes). The range of applied voltage below the *Geiger-Mueller Threshold* in which the *Gas Amplification* depends upon the charge liberated by the *Initial Ionizing Event*.

Region, Proportional (Radiation-Counter Tubes). The range of applied voltage in which the charge collected per isolated *Count* is proportional to the charge liberated by the *Initial Ionizing Event*.

Note 1: In this region the *Gas Amplification* is greater than unity and is independent of the charge liberated by the *Initial Ionizing Event*.

Note 2: The *Proportional Region* depends on the type and energy of the incident *Radiation*.

Regulation (Gas Tubes). The difference between the maximum and minimum *Tube Voltage Drops* within a specified range of *Anode Current*.

Reignition (Radiation-Counter Tubes). A process by which multiple *Counts* are generated within a counter tube by atoms or molecules excited or ionized in the discharge accompanying a *Tube Count*.

Relative Plateau Slope (Radiation-Counter Tubes). See:

Plateau Slope, Relative (Radiation-Counter Tubes).

Repeatability (Voltage Regulator, or Voltage Reference Tubes). The ability of a tube to attain the same voltage drop at a stated time after the beginning of any conducting period.

Note: The lack of repeatability is measured by the change in this voltage from one conducting period to any other, the operating conditions remaining unchanged.

Repeller. An *Electrode* whose primary function is to reverse the direction of an electron stream.

Note: The *Repeller* is sometimes called the *Reflector.*

Resistance. See:

Cathode Interface (Layer) Resistance.

Electrode Resistance.

Equivalent Noise Resistance.

Resolution (in Television). A measure of the ability to delineate picture detail.

Note: *Resolution* is usually expressed in terms of a number of *Lines* discriminated on a test chart. For a number of *Lines* N (normally alternate black and white lines) the width of each *Line* is $1/N$ times the picture height.

Resolution, Structural (Color Picture Tubes). The *Resolution* as limited by the size and shape of the *Screen* elements.

Resolving Time (Radiation Counters). The minimum achievable pulse spacing between *Counts.*

Note: This quantity is a property of the combination of the tube and recording circuit.

Resonant Gap (TR Tubes). The small region in a resonant structure interior to the tube, where the electric field is concentrated.

Resonator Mode. See:

Mode of an Oscillator.

Response. See:

Amplitude Response (Camera Tubes).

Square-Wave Response (Camera Tubes).

Retained Image (Image Burn). A change produced in or on the *Target* which remains for a large number of frames after the removal of a previously stationary light image and which yields a spurious electrical signal corresponding to that light image.

Retention Time, Maximum (Charge-Storage Tubes). The maximum time between *Writing* into and *Reading* an acceptable output from a *Storage Element.*

Reverse Emission (Back Emission) (Vacuum Tubes). The inverse *Electrode Current* from an *Anode* during that part of a cycle in which the *Anode* is negative with respect to the *Cathode.*

Rieke Diagram (of Oscillator Performance). A chart showing contours of constant power output and constant frequency drawn on a polar diagram whose coordinates represent the components of the complex reflection coefficient at the oscillator load. See:

Load Impedance Diagram.

Rising-Sun Magnetron. A *Multicavity Magnetron* in which resonators of two different resonance frequencies are arranged alternately for the purpose of *Mode Separation.*

Scanning, High-Velocity. The scanning of a *Target* with electrons of such velocity that the *Secondary-Emission Ratio* is greater than unity.

Scanning, Low-Velocity. The scanning of a *Target* with electrons of velocity less than the minimum velocity to give a *Secondary-Emission Ratio* of unity.

Schottky Emission. The increased *Thermionic Emission* resulting from an electric field at the surface of the *Cathode.*

Screen (Cathode-Ray Tubes). The surface of the tube upon which the visible pattern is produced.

Screen Grid. A *Grid* placed between a *Control Grid* and an *Anode,* and usually maintained at a fixed positive potential, for the purpose of reducing the electrostatic influence of the *Anode* in the space between the *Screen Grid* and the *Cathode.*

Screen-Grid Characteristic. See:

Electrode Characteristic.

Screen-Grid Current. See:

Electrode Current.

Secondary Emission. The ejection of electrons from a solid or liquid as a result of charged-particle impact. See: *Field-Enhanced Secondary Emission.*

Secondary-Emission Ratio (Electrons). The average number of electrons emitted from a surface per incident primary electron.

Note: The result of a sufficiently large number of events should be averaged to ensure that statistical fluctuations are negligible.

Secondary Grid Emission. *Electron Emission* from a *Grid* resulting directly from bombardment of its surface by electrons or other charged particles.

Self-Quenched Counter Tube. See:

Counter Tube, Self-Quenched.

Semitransparent Photocathode (Camera Tubes or Phototubes). A *Photocathode* in which radiant flux incident on one side produces *Photoelectric Emission* from the opposite side.

Sensitive Volume (Radiation-Counter Tubes). That portion of the tube responding to specific *Radiation.*

Sensitivity, Cathode Luminous (Photocathodes). The quotient of *Photoelectric Emission* current from the *Photocathode* by the incident luminous flux, under specified conditions of illumination.

Note 1: Since *Cathode Luminous Sensitivity* is not an absolute characteristic but depends on the spectral distribution of the incident flux, the term is commonly used to designate the sensitivity to radiation from a tungsten-filament lamp operating at a color temperature of 2870°K.

Note 2: *Cathode Luminous Sensitivity* is usually measured with a collimated beam at normal incidence.

Sensitivity, Cathode Radiant (Photocathodes). The quotient of the *Photoelectric Emission* current from the *Photocathode* by the incident radiant flux at a given wavelength, under specified conditions of irradiation.

Note: *Cathode Radiant Sensitivity* is usually measured with a collimated beam at normal incidence.

Sensitivity, Illumination (Camera Tubes or Phototubes). The quotient of *Signal Output Current* by the

incident illumination, under specified conditions of illumination.

Note 1: Since *Illumination Sensitivity* is not an absolute characteristic but depends on the spectral distribution of the incident flux, the term is commonly used to designate the sensitivity to radiation from a tungsten-filament lamp operating at a color temperature of 2870°K.

Note 2: *Illumination Sensitivity* is usually measured with a collimated beam at normal incidence.

Note 3: See:
Transfer Characteristic (Camera Tubes).

Sensitivity, Luminous (Camera Tubes or Phototubes). The quotient of *Signal Output Current* by incident luminous flux, under specified conditions of illumination.

Note 1: Since *Luminous Sensitivity* is not an absolute characteristic but depends on the spectral distribution of the incident flux, the term is commonly used to designate the sensitivity to radiation from a tungsten-filament lamp operating at a color temperature of 2870°K.

Note 2: *Luminous Sensitivity* is usually measured with a collimated beam at normal incidence.

Sensitivity, Radiant (Camera Tubes or Phototubes). The quotient of *Signal Output Current* by incident radiant flux at a given wavelength, under specified conditions of irradiation.

Note: *Radiant Sensitivity* is usually measured with a collimated beam at normal incidence.

Shading (Camera Tubes). A brightness gradient in the reproduced picture, not present in the original scene, but caused by the tube.

Shadow Mask (Color Picture Tubes). A *Color-Selecting-Electrode System* in the form of an electrically conductive sheet containing a plurality of holes which uses masking to effect color selection.

Shield Grid (Gas Tubes). A *Grid* which shields the *Control Grid* from electrostatic fields, thermal radiation, and deposition of thermionic emissive material, and which may also be used as an additional *Control Electrode.*

Short-Circuit Driving-Point Admittance (of the *j*th Terminal of an *n*-Terminal Network).* The *Driving-Point Admittance* between that terminal and the reference terminal when all other terminals have zero alternating components of voltage with respect to the reference point.

Short-Circuit Feedback Admittance (of an Electron-Tube Transducer).* The *Short-Circuit Transfer Admittance* from the physically available output terminals to the physically available input terminals of a specified socket, associated filters, and tube.

Short-Circuit Forward Admittance (of an Electron-Tube Transducer).* The *Short-Circuit Transfer Admittance* from the physically available input terminals to the physically available output terminals of a specified socket, associated filters, and tube.

Short-Circuit Input Admittance (of an Electron-Tube Transducer).* The *Short-Circuit Driving-Point Admittance* at the physically available input terminals of a specified socket, associated filters, and tube.

Short-Circuit Input Capacitance (of an *n*-Terminal Electron Tube).* The effective capacitance determined from the *Short-Circuit Input Admittance.*

Short-Circuit Output Admittance (of an Electron-Tube Transducer).* The *Short-Circuit Driving-Point Admittance* at the physically available output terminals of a specified socket, associated filters, and tube.

Short-Circuit Output Capacitance (of an *n*-Terminal Electron Tube).* The effective capacitance determined from the *Short-Circuit Output Admittance.*

Short-Circuit Transfer Admittance (from the *j*th Terminal to the *l*th Terminal of an *n*-Terminal Network).* The *Transfer Admittance* from terminal j to terminal l when all terminals except j have zero complex alternating components of voltage with respect to the reference point.

Short-Circuit Transfer Capacitance (Electron Tubes).* The effective capacitance determined from the *Short-Circuit Transfer Admittance.*

Shot Noise, Full. The fluctuation in the current of charge carriers passing through a surface at statistically independent times.

Note 1: Shot noise has a uniform spectral density W_i given by

$$W_i = \frac{eI_0}{2\pi}$$

where e is the charge of the carrier, and I_0 is the average current.

Note 2: The mean-square noise current $\overline{i^2}$ of *Full Shot Noise* within a frequency increment Δf is

$$\overline{i^2} = 2eI_0\Delta f.$$

Note 3: The mean-square noise current $\overline{i^2}$ within a frequency increment Δf associated with an average current I_0 is often expressed in terms of *Full Shot Noise* through a *Shot Noise* reduction factor Γ^2, in general a function of frequency, by the formula:

$$\overline{i^2} = \Gamma^2 2eI_0\Delta f.$$

When $\Gamma^2 < 1$, $\overline{i^2}$ is called *Reduced Shot Noise.*

Shot Noise, Reduced. See:
Shot Noise, Full.

Shot Noise Reduction Factor (Γ^2). See:
Shot Noise, Full (Note 3).

Signal Electrode Capacitance. See:
Electrode Capacitance (Note 3).

Signal Output Current (Camera Tubes or Phototubes). The absolute value of the difference between output current and *Dark Current.*

Signal-to-Noise Ratio (Camera Tubes). The ratio of peak-to-peak *Signal Output Current* to rms noise in the output current.

Sink (of an Oscillator). The region of a *Rieke Diagram* where the rate of change of frequency with respect to phase of the reflection coefficient is maximum. Operation in this region may lead to unsatisfactory performance by reason of cessation or instability of oscillations.

Small-Signal Forward Transadmittance. The value of the *Forward Transadmittance* obtained when the input voltage is small compared to the beam voltage.

Space Charge. The net electric charge within a given volume.

Space-Charge Debunching. Any process in which the mutual interactions between electrons in the stream disperse the electrons of a bunch.

Space-Charge Density. The net electric charge per unit volume.

Space-Charge Grid. A *Grid*, usually positive, that controls the position, area, and magnitude of a potential minimum or of a *Virtual Cathode* in a region adjacent to the *Grid*.

Space-Charge-Limited Current (Vacuum Tubes). The current passing through an interelectrode space when a *Virtual Cathode* exists therein.

Spectral Characteristic (of a Luminescent Screen). The relation between wavelength and emitted radiant power per unit wavelength interval.

Note: The radiant power is commonly expressed in arbitrary units.

Spectral Sensitivity Characteristic (Camera Tubes or Phototubes). The relation between the *Radiant Sensitivity* and the wavelength of the incident *Radiation*, under specified conditions of irradiation.

Note: *Spectral Sensitivity Characteristic* is usually measured with a collimated beam at normal incidence.

Spike Leakage Energy (TR and Pre-TR Tubes). The radio-frequency energy per pulse transmitted through the tube before and during the establishment of the steady-state radio-frequency discharge.

Spill (Charge-Storage Tubes). The loss of information from a *Storage Element* by *Redistribution*.

Split-Anode Magnetron. A *Magnetron* with an *Anode* divided into two segments, usually by slots parallel to its axis.

Spot. See:

Cathode Spot (of an Arc).
Dynode Spot.
Ion Spot (on a Cathode-Ray Tube Screen).
Ion Spot (Camera Tubes or Image Tubes).

Spurious Tube Counts (Radiation-Counter Tubes). *Counts*, other than *Background Counts* and those caused directly by the *Radiation* to be measured.

Note: *Spurious Counts* are caused by failure of the *Quenching* process, electrical leakage, and the like. *Spurious Counts* may seriously affect measurement of *Background Counts*.

Square-Wave Response (Camera Tubes). The ratio of 1) the peak-to-peak signal amplitude given by a test pattern consisting of alternate black and white bars of equal widths to 2) the difference in signal between large-area blacks and large-area whites having the same illuminations as the black and white bars in the test pattern.

Note: Horizontal *Square-Wave Response* is measured if the bars run perpendicular to the direction of horizontal scan. Vertical *Square-Wave Response* is measured if the bars run parallel to the direction of horizontal scan.

Square-Wave Response Characteristic (Camera Tubes). The relation between *Square-Wave Response* and the ratio of 1) a *Raster* dimension to 2) the bar width in the *Square-Wave Response* test pattern.

Note: Unless otherwise specified, the *Raster* dimension is the vertical height.

Starter (Gas Tubes). A *Control Electrode*, the principal function of which is to establish sufficient ionization to reduce the *Anode Breakdown Voltage*.

Note: This has sometimes been referred to as a "trigger *Electrode*."

Starter Breakdown Voltage (Gas Tubes). See:

Breakdown Voltage (of an Electrode of a Gas Tube).

Starter Gap (Gas Tubes). The conduction path between a *Starter* and the other *Electrode* to which starting voltage is applied.

Starter Voltage Drop (Gas Tubes). The *Starter* voltage during conduction to the *Starter*.

Starting Current of an Oscillator. The value of electron-stream current through an oscillator at which selfsustaining oscillations will start under specified conditions of loading.

Static Characteristic (Electron Tubes). A relation between a pair of variables such as *Electrode Voltage* and *Electrode Current*, with all other voltages maintained constant.

Sticking Picture. See: *Retained Image.*

Storage Element (Charge-Storage Tubes). An area of a storage surface which retains information distinguishable from that of adjacent areas.

Note: The *Storage Element* may be a discrete area or an arbitrary portion of a continuous storage surface.

Storage Time. Deprecated, see:

Decay Time.
Retention Time, Maximum.

Storage Tube. An *Electron Tube* into which information can be introduced and then extracted at a later time.

Suppressor Grid. A *Grid* that is interposed between two positive *Electrodes* (usually the *Screen Grid* and the *Anode*), primarily to reduce the flow of secondary electrons from one *Electrode* to the other.

Synchronous Voltage (Traveling-Wave Tubes). The voltage required to accelerate electrons from rest to a velocity equal to the phase velocity of a wave in the absence of electron flow.

Target (Camera Tubes). A structure employing a stor-

age surface which is scanned by an electron beam to generate a *Signal Output Current* corresponding to a charge-density pattern stored thereon.

Note: The structure may include the storage surface which is scanned by an electron beam, the *Backplate* and the intervening dielectric.

Target Capacitance (Camera Tubes). The capacitance between the scanned area of the *Target* and the *Backplate.*

Target Cutoff Voltage (Camera Tubes). The lowest *Target Voltage* at which any detectable electrical signal corresponding to a light image on the sensitive surface of the tube can be obtained.

Target Voltage (in a Camera Tube with Low-Velocity Scanning). The potential difference between the *Thermionic Cathode* and the *Backplate.*

Temperature. See:

Condensed-Mercury Temperature.
Ignitor-Current Temperature Drift (TR, Pre-TR, and Attenuator Tubes).
Noise Temperature.
Noise Temperature, Standard.

Temperature Coefficient of Voltage Drop (Glow-Discharge Tubes). The quotient of the change of *Tube Voltage Drop* (excluding any *Voltage Jumps*) by the change of ambient (or envelope) temperature.

Note: It must be indicated whether the quotient is taken with respect to ambient or envelope temperature.

Tetrode. A four-electrode *Electron Tube* containing an *Anode*, a *Cathode*, a *Control Electrode*, and one additional *Electrode* that is ordinarily a *Grid.*

Thermal Noise. The noise caused by thermal agitation in a dissipative body.

Note: The available thermal noise power N, from a resistor at temperature T, is $N = kT\Delta f$, where k is Boltzmann's constant and Δf is the frequency increment.

Thermal Tuning Time (Cooling). The time required to tune through a specified *Frequency Range* when the tuner power is instantaneously changed from the specified maximum to zero.

Note: The initial condition must be one of equilibrium.

Thermal Tuning Time (Heating). The time required to tune through a specified *Frequency Range* when the tuner power is instantaneously changed from zero to the specified maximum.

Note: The initial condition must be one of equilibrium.

Thermionic Cathode. See: *Hot Cathode.*

Thermionic Emission. The liberation of electrons or ions from a solid or liquid as a result of its thermal energy.

Thermionic Grid Emission (Primary Grid Emission). Current produced by electrons thermionically emitted from a *Grid.*

Thermionic Tube. An *Electron Tube* in which the heating of one or more of the *Electrodes* is for the purpose of causing electron or ion emission.

Thyratron. A *Hot-Cathode Gas Tube* in which one or more *Control Electrodes* initiate, but do not limit, the *Anode Current* except under certain operating conditions.

Time. See:

Control-Electrode Discharge Recovery Time (Attenuator Tubes).
Dead Time.
Decay Time (Charge-Storage Tubes).
Deionization Time (Gas Tubes).
Electrode-Current Averaging Time.
Heater Warm-Up Time.
High-Level Firing Time (Switching Tubes).
Ignitor Firing Time (Switching Tubes).
Ionization Time (Gas Tubes).
Operation Time.
Phase Recovery Time (TR and Pre-TR Tubes).
Recovery Time (ATR Tubes).
Recovery Time (Gas Tubes).
Recovery Time (Geiger-Mueller Counters).
Recovery Time (TR and Pre-TR Tubes).
Resolving Time (Radiation Counters).
Retention Time, Maximum (Charge-Storage Tubes).
Storage Time (Charge-Storage Tubes).
Thermal Tuning Time (Cooling).
Thermal Tuning Time (Heating).
Tube Heating Time (Mercury-Vapor Tubes).

TR (Transmit-Receive) Tube. A gas-filled radio-frequency switching tube used to protect the receiver in pulsed radio-frequency systems.

Transadmittance Compression Ratio. The ratio of the magnitude of the *Small-Signal Forward Transadmittance* of the tube to the magnitude of the *Forward Transadmittance* at a given input signal level.

Transadmittance.* See:

Interelectrode Transadmittance.
Small-Signal Forward Transadmittance.
Transadmittance, Forward.

Transadmittance, Forward. The complex quotient of 1) the fundamental component of the short-circuit current induced in the second of any two gaps and 2) the fundamental component of the voltage across the first.

Transconductance.* As most commonly used, the *Interelectrode Transconductance* between the *Control Grid* and the *Anode.* At low frequencies, *Transconductance* is the slope of the *Control-Grid-to-Anode Transfer Characteristic.* See:

Conversion Transconductance (of a Heterodyne Conversion Transducer).
Interelectrode Transconductance (j-l Interelectrode Transconductance).

Transducer. See:

Conversion Transducer.
Harmonic Conversion Transducer (Frequency Multiplier, Frequency Divider).
Heterodyne Conversion Transducer (Converter).

Transducer Gain (of a Two-Port Linear Transducer). See:

Gain, Transducer (of a Two-Port Linear Transducer).

Transfer Admittance (from the *j*th Terminal to the *l*th Terminal of an *n*-Terminal Network).* The quotient of 1) the complex alternating component I_l of the current flowing to the *l*th terminal from the *l*th external termination by 2) the complex alternating component V_j of the voltage applied to the *j*th terminal with respect to the reference point when all other terminals have arbitrary external terminations.

Transfer Characteristic. A relation between the voltage of one *Electrode* and the current to another *Electrode*, all other *Electrode Voltages* being maintained constant.

Transfer Characteristic (Camera Tubes). A relation between the illumination on the tube and the corresponding *Signal Output Current*, under specified conditions of illumination.

Note 1: See:

Sensitivity, Illumination.

Note 2: The relation is usually shown by a graph of the logarithm of the *Signal Output Current* as a function of the logarithm of the illumination.

Transfer Current (Gas Tubes). The current to one *Electrode* required to initiate *Breakdown* to another *Electrode*.

Note: The *Transfer Current* is a function of the voltage of the second *Electrode*.

Transit Angle. The product of angular frequency and the time taken for an electron to traverse a given path.

Transit-Time Mode. See:

Mode of an Oscillator.

Trans-μ-Factor (Multibeam Electron Tubes). The ratio of 1) the magnitude of an infinitesimal change in the voltage at the *Control Grid* of any one beam to 2) the magnitude of an infinitesimal change in the voltage at the *Control Grid* of a second beam. The current in the second beam and the voltage of all other *Electrodes* are maintained constant.

Transrectification Factor. The quotient of the change in average current of an *Electrode* by the change in amplitude of the alternating sinusoidal voltage applied to another *Electrode*, the direct voltages of this and other *Electrodes* being maintained constant.

Note: Unless otherwise stated, the term refers to cases in which the alternating sinusoidal voltage is of infinitesimal magnitude.

Transverse-Beam Traveling-Wave Tube. A *Traveling-wave Tube* in which the direction of motion of the electron beam is transverse to the average direction in which the signal wave moves.

Transverse-Field Traveling-Wave Tube. A *Traveling-Wave Tube* in which the traveling electric fields which interact with the electrons are essentially transverse to the average motion of the electrons.

Traveling-Wave Magnetron. A *Traveling-Wave Tube* in which the electrons move in crossed static electric and magnetic fields which are substantially normal to the direction of wave propagation.

Traveling-Wave Magnetron Oscillations. Oscillations sustained by the interaction between the *Space-Charge* cloud of a *Magnetron* and a traveling electromagnetic field whose phase velocity is approximately the same as the mean velocity of the cloud.

Traveling-Wave Tube. An *Electron Tube* in which a stream of electrons interacts continuously or repeatedly with a guided electromagnetic wave moving substantially in synchronism with it, and in such a way that there is a net transfer of energy from the stream to the wave. See:

Transverse-Beam Traveling-Wave Tube.
Transverse-Field Traveling-Wave Tube.

Traveling-Wave-Tube Interaction Circuit. An extended *Electrode* arrangement in a *Traveling-Wave Tube* designed to propagate an electromagnetic wave in such a manner that the traveling electromagnetic fields are retarded and extended into the space occupied by the electron stream.

Note: *Traveling-Wave Tubes* are often designated by the type of interaction circuit used, as in "Helix Traveling-Wave Tube."

Triode. A three-electrode *Electron Tube* containing an *Anode*, a *Cathode*, and a *Control Electrode*.

Tube. See:

ATR (Anti-Transit-Receive) Tube.
Attenuator Tube.
Beam-Deflection Tube.
Beam-Indexing Color Tube.
Beam-Power Tube.
Broad-Band Tube (TR and Pre-TR Tubes).
Camera Tube.
Cathode-Ray Tube.
Cell-Type Tube (TR, ATR, and Pre-TR Tubes).
Charge-Storage Tube.
Cold-Cathode Tube.
Color Picture Tube.
Converter Tube.
Counter Tube.
Dissector Tube.
Electrometer Tube.
Electron-Beam Tube.
Electron Tube.
Electron-Wave Tube.
Externally-Quenched Counter Tube.
Fired Tube (TR, ATR, and Pre-TR Tubes).
Gas-Filled Radiation-Counter Tube.
Gas-Flow Counter Tube.
Gas Tube.
Geiger-Mueller Counter Tube.
Glow-Discharge Tube.
Heptode.
Hexode.
Hot-Cathode Tube.
Iconoscope.
Image Dissector Tube.

Image Iconoscope.
Image Orthicon.
Image Tube.
Indicator Tube.
Ionic-Heated-Cathode Tube.
Local Oscillator Tube.
Magnetron.
Memory Tube.
Mercury-Vapor Tube.
Mixer Tube.
Monoscope.
Multielectrode Tube.
Multiple-Unit Tube.
Multiplier Phototube.
Multisegment Magnetron.
Octode.
Orthicon.
Oscilloscope Tube (Oscillograph Tube).
Pentode.
Phase-Tuned Tube (TR Tubes).
Photomultiplier.
Phototube.
Pickup Tube.
Pre-TR Tube.
Proportional Counter Tube.
Reflection Color Tube.
Self-Quenched Counter Tube.
Storage Tube.
Tetrode.
Thermionic Tube.
Thyratron.
TR (Transmit-Receive) Tube.
Transverse-Beam Traveling-Wave Tube.
Transverse-Field Traveling-Wave Tube.
Traveling-Wave Magnetron.
Traveling-Wave Tube.
Triode.
Vacuum Tube.
Variable-μ Tube.
Vidicon.
Voltage Reference Tube.
Voltage Regulator Tube.

Tube Count (Radiation-Counter Tubes). A terminated discharge produced by an *Ionizing Event*.

Tube Heating Time (Mercury-Vapor Tubes). The time required for the *Condensed-Mercury Temperature* to reach a specified value.

Tube Voltage Drop. The *Anode Voltage* during the conduction period.

Note: This voltage is not necessarily constant.

Tuning, Electronic. The process of changing the operating frequency of a system by changing the characteristics of a coupled electron stream. Characteristics involved are, for example: velocity, density, or geometry.

Tuning Range, Electronic. The *Frequency Range* of continuous tuning between two operating points of specified minimum power output for an electronically-tuned oscillator.

Note: The reference points are frequently the half-power points, but should always be specified.

Tuning Range (Switching Tubes). The *Frequency Range* over which the resonance frequency of the tube may be adjusted by the mechanical means provided on the tube or associated cavity.

Tuning Rate, Thermal. The initial time rate of change in frequency which occurs when the input power to the tuner is instantaneously changed by a specified amount.

Note: This rate is a function of the power input to the tuner as well as the sign and magnitude of the power change.

Tuning Sensitivity, Electronic. At a given operating point, the rate of change of oscillator frequency with the change of the controlling electron stream. For example, this change may be expressed in terms of an *Electrode Voltage* or current.

Note: See:
Pushing Figure of an Oscillator.

Tuning Sensitivity, Thermal. The rate of change of resonator equilibrium frequency with respect to applied thermal tuner power.

Tuning Susceptance (ATR Tubes). The normalized susceptance of the tube in its *Mount* due to the deviation of its resonance frequency from the desired resonance frequency.

Note: Normalization is with respect to the characteristic admittance of the transmission line at its junction with the tube *Mount*.

Tuning, Thermal. The process of changing the operating frequency of a system by using a controlled thermal expansion to alter the geometry of the system.

Tuning Time Constant, Thermal. The time required for the frequency to change by a fraction $(1-1/e)$ of the change in equilibrium frequency after an incremental change of the applied thermal tuner power.

Note 1: If the behavior is not exponential, the initial conditions must be stated.

Note 2: Here e is the base of natural logarithms.

Underbunching. A condition representing less than optimum *Bunching*.

Unfired Tube (TR, ATR, and Pre-TR Tubes). The condition of the tube during which there is no radio-frequency *Glow Discharge* at either the *Resonant Gap* or *Resonant Window*.

Unipotential Cathode. See:
Indirectly Heated Cathode.

Unloaded (Intrinsic) Q (Switching Tubes). The Q of a tube unloaded by either the generator or the termination.

Note: As here used, Q is equal to 2π times the energy stored at the resonance frequency divided by the energy dissipated per cycle in the tube or, for *Cell-Type Tubes*, in the tube and its external resonant circuit.

Vacuum Tube. An *Electron Tube* evacuated to such a degree that its electrical characteristics are essentially unaffected by the presence of residual gas or vapor.

Variable-μ Tube. An *Electron Tube* in which the *Amplification Factor* varies in a predetermined way with *Control-Grid* voltage.

Velocity Modulation. The process whereby a time variation in velocity is impressed on the electrons of a stream; also the condition existing in the stream subsequent to such a process.

Velocity Sorting. Any process of selecting electrons according to their velocities.

Vidicon. A *Camera Tube* in which a charge-density pattern is formed by photoconduction and stored on that surface of the photoconductor which is scanned by an electron beam, usually of low-velocity electrons.

Virtual Cathode. The locus of such a space-charge-potential minimum that only a portion of the electrons approaching it is transmitted, the remainder being reflected.

Voltage. See:
Anode Breakdown Voltage (*Gas Tubes*).
Anode Voltage Drop.
Breakdown Voltage (*of an Electrode of a Gas Tube*).
Composite Controlling Voltage.
Critical Anode Voltage (*Multielectrode Gas Tubes*).
Critical Grid Voltage (*Multielectrode Gas Tubes*).
Critical Voltage (*Magnetrons*).
Cutoff Voltage (*Electron Tubes*).
Electrode Voltage.
Ignitor Voltage Drop (*Switching Tubes*).
Internal Correction Voltage (*Electron Tubes*).
Overvoltage (*Radiation-Counter Tubes*).
Peak Alternating Gap Voltage.
Peak Forward Anode Voltage.
Peak Inverse Anode Voltage.
Starter Breakdown Voltage (*Gas Tubes*).
Starter Voltage Drop (*Gas Tubes*).
Synchronous Voltage (*Traveling-Wave Tubes*).
Target Cut-off Voltage (*Camera Tubes*).
Target Voltage (*in a Camera Tube with Low-Velocity Scanning*).
Tube Voltage Drop.

Voltage Generator. A two-terminal circuit element with a terminal voltage independent of the current through the element.

Note: A *Voltage Generator* has zero internal impedance.

Voltage Jump (Glow-Discharge Tubes). An abrupt change or discontinuity in *Tube Voltage Drop* during operation.

Note: This may occur either during life under constant operating conditions or as the current or temperature is varied over the operating range.

Voltage Reference Tube. A *Gas Tube* in which the *Tube Voltage Drop* is approximately constant over the operating range of current and relatively stable with time at fixed values of current and temperature.

Voltage Regulator Tube. A *Gas Tube* in which the *Tube Voltage Drop* is approximately constant over the operating range of current.

VSWR, High-Level (Switching Tubes). See:
High-Level VSWR (*Switching Tubes*).

Wave. See:
Backward Wave (*Traveling-Wave Tubes*).
Forward Wave (*Traveling-Wave Tubes*).

Work Function. The minimum energy required to remove an electron from the Fermi level of a material into field-free space.

Note: *Work Function* is commonly expressed in electron volts.

Write (Charge-Storage Tubes). To establish a charge pattern corresponding to the input.

Writing Speed (Charge-Storage Tubes). The rate of *Writing* on successive *Storage Elements.*

CORRECTION

The following corrections have been brought to the attention of the editors on "IRE Standards on Piezoelectric Crystals—The Piezoelectric Vibrator: Definitions and Methods of Measurement, 1957," which appeared on pages 353–358 of the March, 1957 issue of PROCEEDINGS.

Page 355, Table I, left-hand column, line 15:
Macimum Admittance should read Maximum Admittance.

Page 355, Table I, right-hand column, line 2:
$f_m\pi$ should read f_{mT}.

Page 355, Table I, right-hand column, line 5:
Combination Vibrator should read Combination of Vibrator.

Page 355, Table I, right-hand column, line 7:
Combination DF Vibrator should read Combination of Vibrator.

*Page 356, Table II, column 1, line 1: Insert in blank space *f*.

*Page 356, Table II, column 1, line 4:
Insert in the blank space f_a.

*Page 356, Table II, column 1, line 6 (last line):
p should read f_p.

Page 356, left-hand column, first paragraph, last line:
$-5\cdot10^{-7}$ should read $5\cdot10^{-7}$.

* In some copies of March issue, Table II appears correctly.

Correspondence

Theory of Shot Noise in Junction Diodes and Junction Transistors*

In the above paper,[1] the shot noise in junction transistors was calculated for a one-dimensional model, both for low and for high frequencies. The low-frequency calculation was exact, the high-frequency calculation was carried out under the assumption that the equilibrium hole concentration p_n in the base region and the excess hole concentration p_{c0}' at the collector junction were negligible.

The noise has now been calculated without these assumptions. It was found that the following equations, derived in my article,[1] are of general validity:

$$\langle i_{p1}^2\rangle_{av} = 4kTG_e df - 2eI_e df \quad (1)$$

$$\langle i_{p2}^2\rangle_{av} = 2eI_c df \quad (2)$$

$$\langle i_{p1}^* i_{p2}\rangle_{av} = -2kT\alpha Y_e df. \quad (3)$$

Here α is the current amplification factor, Y_e the emitter admittance, G_e the emitter conductance, i_{p1} the emitter current generator and i_{p2} the collector current generator. If $V_c<0$, and $|eV_c/kT|\gg 1$, the emitter and collector current may be written

$$I_e = I_{ee}(e^{eV/kT}-1) + \alpha_0 I_{cc} \quad (4)$$

$$I_c = \alpha_0 I_{ee}(e^{eV/kT}-1) + I_{cc}, \quad (5)$$

where α_0 is the low-frequency current amplification factor and the current $I_{ee}=I_{cc}$ has been defined.[1] Substituting (4) into (5) yields

$$I_c = \alpha_0 I_e + (I_c)_{sat}. \quad (6)$$

The quantity

$$(I_c)_{sat} = I_{cc}(1-\alpha_0^2) \quad (6a)$$

is known as the *collector saturated current*, that is the collector current for zero emitter current.

The noise current generator

$$i_p = i_{p2} + \alpha i_{p1}, \quad (7)$$

corresponding to the output noise current generator for open input, has also been introduced.[1] Substituting (1), (2), (3) and (6a), we obtain

$$\langle i_p^2\rangle_{av} = 2eI_c df - |\alpha|^2 2eI_e df$$
$$= 2e(\alpha_0 - |\alpha|^2)I_e df + 2e(I_c)_{sat} df. \quad (8)$$

For low frequencies this reduces to

$$\langle i_p^2\rangle_{av} = 2e\alpha_0(1-\alpha_0)I_e df + 2e(I_c)_{sat} df. \quad (8a)$$

The reader will recognize the first term as the partition noise term introduced by van der Ziel and the second term as the shot noise term due to the collector saturated current introduced by Montgomery and Clark.[2]

The collector saturated current thus gives full shot noise at all frequencies. This is in contrast with the statement,[1] according to which the collector saturated current should *not* give full shot noise. This discrepancy is caused by a wrong definition of $(I_c)_{sat}$; instead of (6a) the definition $(I_c)_{sat}=I_{cc}$ was used. The first term in (8) gives the high-frequency equivalent of the low-frequency partition noise term.

Eqs. (1), (2), and (3) do not give any reference to the one-dimensional model for which they were derived. It thus seems likely that they hold for all geometries.

The author is indebted to Dr. K. M. van Vliet, University of Minnesota, for stimulating discussions on the subject, and to Dr. R. L. Pritchard, General Electric Company, for pointing out the correct expression for $(I_c)_{sat}$.

ALDERT VAN DER ZIEL
Elec. Eng. Dept.
University of Minnesota
Minneapolis, Minn.

* Received by the IRE, November 6, 1956. Work supported by the U. S. Signal Corps.

[1] A. van der Ziel, PROC. IRE, vol. 43, pp. 1639–1646; November, 1955.

[2] H. C. Montgomery and M. A. Clark, "Shot noise in junction transistors," *J. Appl. Phys.*, vol. 24, pp. 1397–1398; November, 1953.
A. van der Ziel, "Note on shot and partition noise in junction transistors," *J. Appl. Phys.*, vol. 25, pp. 815–816; June, 1954.

Molecular Amplification and Generation of Microwaves*

My above paper[1] was not intended to give a comprehensive survey of the literature on molecular amplification, but was meant to give a brief description of the present state of the field and an idea of its scope and promise.

However, I should like to mention here, as I did not do in my article, that the possibility of obtaining microwave amplification by means of stimulated emission was pointed out by Weber at the Tenth Annual Conference on Electron Tubes at Ottawa, Can., in June, 1952, and in the IRE TRANSACTIONS ON ELECTRON DEVICES.[2]

JAMES P. WITTKE
RCA Laboratories
Princeton, N. J.

* Received by the IRE, March 22, 1957.

[1] Proc. IRE, vol. 45, pp. 291–316; March, 1957.

[2] J. Weber, "Amplification of microwave radiation by substances not in thermal equilibrium," IRE TRANS., PGED-3, pp. 1–4; June, 1953.

Alternatives to Cathode Bias for Vacuum Tubes*

Although the use of a cathode resistor, by-passed if desired, is by far the commonest way of providing bias for tubes when some self-regulation of the operating point is desired, there are alternatives which may be attractive under certain circumstances. If a fairly well regulated negative voltage is available, as often happens in such applications as instrumentation, the scheme shown in Fig. 1 may be used. The voltage divider formed by resistors R_1, R_2, and R_3, working between the plate voltage V_p and the negative supply voltage $-V_c$, holds the grid at the proper operating point, the cathode being grounded directly. The capacitor C_1 by-passes all signal frequencies preventing degeneration of the signals.

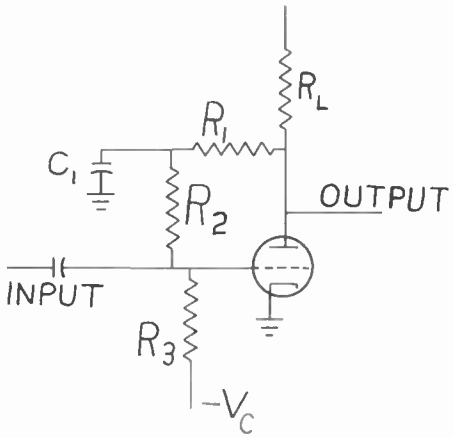

Fig. 1—The voltage divider bias system for a vacuum tube. By means of the divider chain, the plate voltage is compared with the fixed voltage $-V_c$, and the feedback from this comparison stabilizes the operating point.

It can be seen, from ordinary feedback theory, that any tendency of the operating point to change, due to a change in the properties of the tube, is attenuated approximately by a factor $\{1+(g_m R_L R_3)/(R_1+R_2+R_3)\}^{-1}$, g_m being the transconductance of the tube. If $R_1 \sim R_2 \sim R_3$, and $g_m R_L \gg 1$, this factor becomes approximately $3/(g_m R_L)$. When the bias is provided by a cathode resistor R_k, on the other hand, the factor is approximately $(1+g_m R_k)^{-1}$. Typically $g_m R_k \sim 1$, so the factor is around one half.

There are certain other possible advantages of the system shown in Fig. 1. Since R_1 will be as much as one thousand times as great as R_k would be for a similar situation, C_1 need be only about one thousandth the size of the capacitor required to by-pass R_k. This could mean savings in size, weight, and cost. Having the cathode grounded directly may help in reducing hum, and, in addition, it might be desirable if, for some reason, tubes with filamentary cathodes were to be used.

The same system may be used with a pentode. Fig. 2 shows another alternative which may be attractive here, especially when the screen has to be by-passed anyway. Here the screen provides the regulation, just as the plate did in the former circuit. Since the grid to screen and grid to plate

* Received by the IRE, April 1, 1957.

transconductances are in about the same ratio as the screen current and plate current, and the plate and screen run at about the same voltage, the attenuating factor for changes in the properties of the tube will be about the same when the regulation is taken from the screen as when it is taken from the plate. The screen method saves one resistor and one capacitor (if the screen has to be by-passed anyway), and is also useful if the plate load is something like a transformer, with a very low dc impedance.

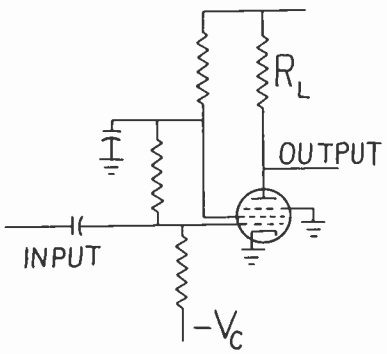

Fig. 2—The voltage divider bias system applied to a pentode by comparing the screen voltage with the fixed voltage. This method requires no additional capacitors, in case the screen has to be by-passed anyway.

HAROLD L. ARMSTRONG
Pacific Semiconductors, Inc.
Culver City, Calif.,
Formerly with Nat. Res. Council
Ottawa, Ont., Can.

A Linear Cathode-Ray Tube*

There have been numerous attempts to correct, for the nonlinear light output vs grid drive characteristic of cathode-ray tubes, (crt). In the rooter circuit developed by Oliver,[1] for instance, the crt is preceded by a circuit with a nonlinearity which is the inverse of that of the crt so that the over-all circuit is linear. It is not too difficult to match these nonlinearities with the precision required for most television applications. A further improvement in the precision of linearity, however, becomes increasingly difficult. In addition, a perfect match, if once obtained, would be difficult to maintain, since the two tubes involved would not age at precisely the proper relative rates.

The above objections are largely eliminated in a tube of the construction shown in Fig. 1. The first three electrodes are similar to the cathode, grid, and plate of a conventional lighthouse tube such as the 2C40, *i.e.*, a large area cathode, a parallel wire mesh control grid, and a parallel plate (screen grid in our tube), the plate, however, having a small hole through its center. Because of the parallel geometry, the electrons approach the plate perpendicularly, and a small, definite fraction of them penetrates the hole to form the beam which goes on to excite the phosphorescent screen. A large current (milliamperes) flows to the plate. However, this is at low (300) voltage. The power dissipated is less than that required in Oliver's rooter circuit. It is easily possible to force this plate current to vary linearly with the input voltage by using a conventional video feedback circuit. The beam current is a small, definite fraction of the plate current, and hence, its variation is accurately linear too. Note that aging of the tube no longer is a problem; it is corrected for by the feedback.

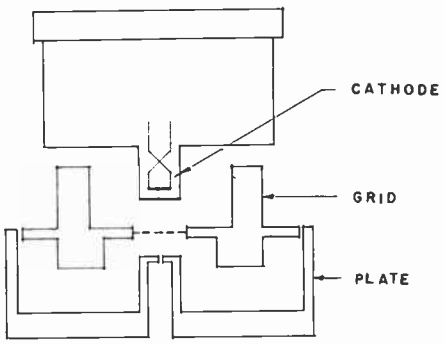

Fig. 1.

Conventional crt's can be corrected in this manner. However, the cathode current which must be sampled by the feedback circuit is so small that it becomes impossible to obtain the wide-band pass required in radar and television applications. The "g_m" on conventional tubes is of the order of 10 micromhos.

There remains the question of the linearity of the phosphor itself. As long as saturation is avoided, the phosphor in itself appears to be linear. However, its response falls off with temperature, and localized heating by the electron beam is sufficient to reduce the light out: beam current characteristic from a one to an approximate 0.8 power law within a 10 to 200 microampere current range. (Our tests have shown that P11, P15, and P16 phosphors behave this way.) It is possible, however, by properly under-correcting the gun nonlinearity, to make the over-all response sufficiently linear. The simplest feedback circuit which will do this is merely a selected cathode resistor.

The success of this device hinges upon obtaining accurate proportionality between the plate and beam currents. This is possible if several precautions are observed.

1) The grid-plate spacing should be large enough so that thermal motions of the electrons will be sufficient to fill in the "shadows" cast by the individual grid wires before the electrons reach the plate. If the hole in the plate is partially shadowed, the beam current may be too small at low currents.
2) The grid supporting structure should partially enclose the plate, as shown, to confine the field from the plate. Otherwise, as the grid bias decreases, some electrons hit the side of the plate and its supporting structure so that the fraction of the current going through the hole again is too small.
3) The space within the gun must be carefully shielded from the accelerating field to prevent electrons being drawn around rather than through the plate.

It is a pleasure to acknowledge the assistance of the staff of the University of Illinois, Electron Tube Laboratory, and especially that of Murray Babcock.

D. BITZER
AND R. D. RAWCLIFFE
Control Systems Lab.
University of Illinois
Urbana, Ill.

Quantum Derivation of Energy Relations Analogous to Those for Nonlinear Reactances*

In a paper by Manley and Rowe,[1] equations are given relating the average powers at the different frequencies in nonlinear reactances. These general energy relations are very interesting and give useful information regarding the gain and stability of nonlinear reactor modulators and demodulators. However, the derivation of the above equations involves a rather complicated Fourier analysis.

It is interesting to note that in a quantum mechanical system, the Manley-Rowe relations are almost selfevident. For example, (26) and (27) or (30) and (31) of Manley and Rowe,[1] applicable to a single-sideband modulator or demodulator, can be readily obtained by using the equivalent three-level quantum mechanical system shown in Fig. 1. The principle that one must utilize is that in the steady state, the total number of quanta per second leaving any level must equal the number arriving at that level. Therefore, one can write

$$\begin{aligned} N_{12} + N_{13} &= 0 \\ N_{12} &= N_{23} \end{aligned} \qquad (1)$$

where

N_{12} = no. of quanta per second going from level 1 to level 2
N_{13} = no. of quanta per second going from level 1 to level 3
N_{23} = no. of quanta per second going from level 2 to level 3
$N_{21} = -N_{12}$ = no. of quanta per second going from level 2 to level 1.

The energy in each quantum is hf where h is Planck's constant and f is the frequency of the transition. Therefore, $N_{12}hf_1$ is equal to W_1, the power in frequency f_1, with similar relations for N_{13} and N_{23}. One can therefore write (1) as follows:

* Received by the IRE, March 23, 1957.
[1] B. M. Oliver, "Tone rendition in television," PROC. IRE, vol. 38, pp. 1288–1300; November, 1950.

* Received by the IRE, April 2, 1957.
[1] J. M. Manley and H. E. Rowe, "Some general properties of nonlinear elements," PROC. IRE, vol. 44, pp. 904–913; July, 1956.

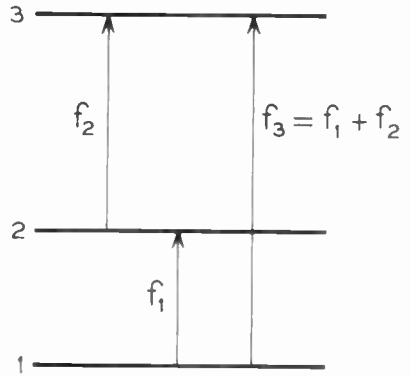

Fig. 1 —Quantum level scheme equivalent of single-sideband modulator or demodulator.

$$\frac{W_1}{f_1} + \frac{W_3}{f_3} = 0$$
$$\frac{W_1}{f_1} = \frac{W_2}{f_2}. \tag{2}$$

These equations are identical to (26) and (27) or (30) and (31) of Manley and Rowe,[1] by noting the difference in symbolism.

One can derive similar relations for the case of a nonlinear system in which both side bands carry power. Fig. 2 shows the

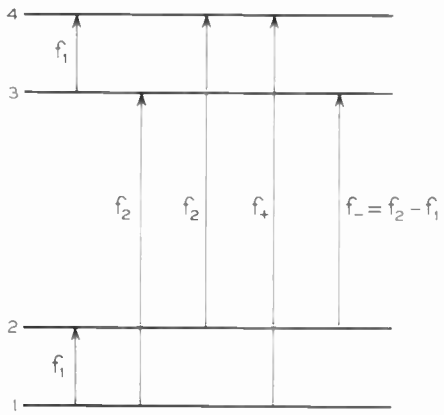

Fig. 2—Quantum level scheme equivalent of uppe and lower sideband modulator or demodulator.

equivalent quantum mechanical system which we shall analyze using the principle of conservation of quanta in the steady state.

$$N_{12} + N_{13} + N_{14} = 0$$
$$N_{23} + N_{24} - N_{12} = 0 \tag{3}$$
$$N_{34} - N_{13} - N_{23} = 0.$$

Combining the first two of (3) we get

$$N_{13} + N_{24} + N_{14} + N_{23} = 0.$$

Similarly, combining the first and last of (3) we get

$$N_{12} + N_{34} + N_{14} - N_{23} = 0.$$

Noting that $W_2 = (N_{13} + N_{24})hf_2$ and $W_1 = (N_{12} + N_{34})hf_1$ and substituting in the above equations, we obtain

$$\frac{W_2}{f_2} + \frac{W_+}{f_+} + \frac{W_-}{f_-} = 0$$
$$\frac{W_1}{f_1} + \frac{W_+}{f_+} - \frac{W_-}{f_-} = 0 \tag{4}$$

where W_+ and W_- are the upper and lower sideband powers respectively. These equations are again identical to those obtained from (24) and (25) of Manley and Rowe.[1]

One can alternatively derive the above relations by considering a photon interaction scheme rather than a multilevel quantum system. Thus, let us derive (4) by considering the following scheme. A material is irradiated with photons of frequency $f_+ = f_1 + f_2$ and of energy hf_+. We assume that this material is in a cavity which can absorb energy at frequencies f_1, f_2, and $f_- = f_2 - f_1$. Two different "decay" processes, shown in Fig. 3, are possible, In process A, a photon of energy hf_+ results in one photon of energy hf_1 and one photon of energy hf_2, so that energy is conserved. In process B a photon of energy hf_+ results in one photon of energy hf_- and two photons of energy hf_1, again conserving energy for this process.

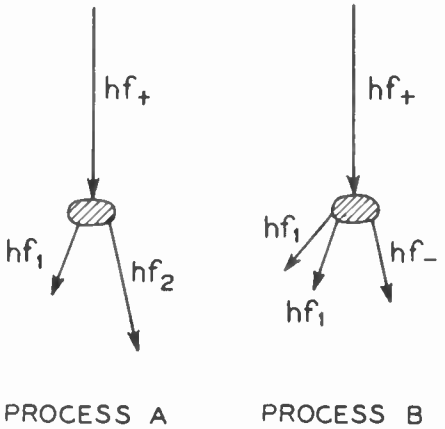

Fig. 3—Quantum interaction scheme equivalent of Fig. 2.

Let

$-N_{+A}$ = no. of hf_+ photons absorbed by process A in one second
$-N_{+B}$ = no. of hf_+ photons absorbed by process B in one second
N_{1A} = no. of hf_1 photons emitted by process A
N_{1B} = no. of hf_1 photons emitted by process B
N_2 = no. of photons of energy hf_2 emitted per second
N_- = no. of photons of energy hf_- emitted per second
$-N_+ = -(N_{+A} + N_{+B})$ = total no. of photons of energy hf_+ absorbed per second
$+N_1 = +(N_{1A} + N_{1B})$ = total no. of photons of energy hf_1 emitted per second.

From Fig. 3 one can readily see that the following equations hold:

$$\left.\begin{aligned} N_{1A} &= -N_{+A} \\ N_2 &= -N_{+A} \end{aligned}\right\} \text{process A} \tag{5}$$

$$\left.\begin{aligned} N_{1B} &= -2N_{+B} \\ N_- &= -N_{+B} \end{aligned}\right\} \text{process B.} \tag{6}$$

Combining the second of (5) with the second of (6) we obtain

$$N_2 + N_- = -(N_{+A} + N_{+B}) = -N_+$$

or

$$\frac{W_2}{f_2} + \frac{W_-}{f_-} + \frac{W_+}{f_+} = 0$$

which is identical to the second of (4).

Similarly, by combining the first of (5) and (6) we obtain

$$N_1 = N_{1A} + N_{1B} = -(N_{+A} + 2N_{+B})$$
$$= -N_+ - N_{+B} = -N_+ + N_-$$

or

$$N_1 + N_+ - N_- = 0$$

or

$$\frac{W_1}{f_1} + \frac{W_+}{f_+} - \frac{W_-}{f_-} = 0$$

which is the first of (4).

If one knows the relative probability of occurrence of process A to process B, one can, of course, obtain additional information regarding the powers at the different frequencies. Thus, if process A and process B were equally probable one can readily see that

$$\frac{W_1}{f_1} = -\frac{3}{2}\frac{W_+}{f_+}.$$

These simple energy relations are particularly significant in the analysis of the potentialities of the various multilevel solid-state maser[2] schemes.

MAX T. WEISS
Bell Telephone Labs., Inc.
Holmdel, N. J.

J. B. Wittke, "Molecular amplification and generation of microwaves," PROC. IRE, vol. 45, pp. 291–316; March, 1957.

Microwave Mixing and Frequency Dividing*

Data obtained from frequency mixing experiments and from related experiments in frequency division demonstrate the feasibility of achieving effective mixing and dividing in microwave tubes. In all of the experiments, the nonlinearity of an overmodulated electron beam was used to produce the desirable effects. As will be described in some detail below, mixing conversion gains as high as 30 db and strong divided-frequency signals have been obtained from traveling-wave-type tubes.

Interest in the traveling-wave mixer has been stimulated by certain characteristics which these tubes can possess. For example, such tubes may be designed to have wide IF bandwidths, to give IF outputs at microwave frequencies, to be free from burnout due to high-power inputs, to provide local-

* Received by the IRE, March 23, 1957. This paper prepared under Air Force Contract AF 19(604) 1847.

oscillator isolation from the signal input and to give high-level output power. The possibility of including the local oscillator within the tube envelope by using backward-wave structures has been investigated elsewhere by Gray.[1]

Much experimental data were obtained from an *S*-band traveling-wave tube having two identical helices as in Fig. 1. The tube was operated as a mixer with the local oscillator signal and the input signal applied to the input of the first helix. The IF signal was then obtained at the output of the second helix. In the experiment illustrated by Fig. 1, the measured gain through the first helix for both a high-level signal at f_1 and a low-level signal at f_2 was about 8 db. The second helix was operated at a higher voltage in the dispersive region in order to peak the gain at the difference frequency f_3. The measured gain through this helix for signals at f_3 was very nearly 0 db. The high-level signal served to drive the electron beam into a partially-saturated condition in order to produce a difference-frequency modulation on the beam. The difference-frequency modulation then was coupled to the second helix and hence to the mixer output. The conversion gain, defined as the ratio of the IF output power to the low-level signal input power, was +27 db.

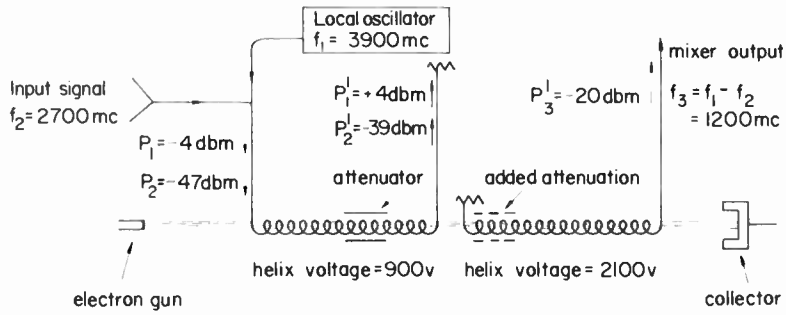

Fig. 1—Double-helix traveling-wave-tube mixer. The first helix was operated for broad-band amplification of *S*-band signals (including the frequencies f_1 and f_2) with a gain of +8 db. The second helix was operated in the dispersive region and was tuned for the IF frequency f_3, the gain for which was 0 db. In the experiment illustrated, the conversion gain, taken as the ratio of P_3' to P_2, was +27 db.

The above experiment was repeated after adding an external attenuator (marked "added attenuation") to the second helix. The purpose of the attenuator was to reduce the effects of possible feedback through the second helix. Such effects may have been partially responsible for the high conversion gain because the added attenuation resulted in lowering the conversion gain to +16 db.

The operation throughout the above experimentation was very stable. For example, even with the attenuator absent, a substantial increase in the beam current would still not produce oscillations. By increasing the beam current 50 per cent the conversion gain could be increased to +30 db. It is also interesting to note that by raising the input power levels, the tube's full saturation power output of +15 dbm was obtainable at the intermediate frequency. Consequently, high-level mixing can be accomplished in this type of tube.

[1] G. A. Gray, "Investigation of Mixing in Traveling-Wave Tube Amplifiers," Ser. No. 60, Issue No. 151, Elec. Res. Lab., University of Calif., Berkeley, Calif.; November 11, 1955.

Another mixer experiment was performed by using a conventional, helix-type *X*-band traveling-wave tube. An *S*-band resonant cavity was fitted over the tube envelope and positioned with the cavity gap concentric with the beam and located in the region between the helix output and the beam collector. A high-level signal at 10,100 mc and a low-level signal at 7600 mc were applied to the helix input. The cavity was tuned to 2500 mc and was excited by the difference frequency current present in the electron beam passing to the collector. A conversion gain of +11 db could be obtained. At the same time the tube gain as an amplifier was +32 db. Obviously this method of obtaining a mixer output was much less effective than the previous one.

An interesting application for the double-helix mixer tube of Fig. 1 is its use as a frequency divider. This mode of operation can be understood by assuming that the frequency of the high-level signal, f_1, is exactly twice that of the low-level signal, f_2. As a consequence, f_3 equals f_2. By adding a feedback path as in Fig. 2 the tube can be made to oscillate precisely at $f_2 = f_1/2$. This, of course, constitutes dividing by two.

Because of the gain mechanism inherent in the mixing process, the oscillations at f_2 will continue so long as the signal at f_1 is present. Since the straight-through gain for f_2 is too low to sustain oscillations, the oscillations cease when f_1 is removed.

The double-helix tube was tested as a frequency divider with good results. The frequency f_1 was chosen to be 4000 mc. For the best operation it was necessary to adjust the helix voltages to obtain proper phase relationships. Under these conditions, the system could easily be excited into oscillation at 2000 mc by supplying a high-level signal at 4000 mc to saturate the beam. Thus, the tube's full saturation power output was obtainable at the divided frequency.

Successful dividing was also obtained from a conventional (*i.e.*, a single-helix) *S*-band traveling-wave tube. Preliminary tests had shown that under the proper operating conditions the gain for the difference-frequency signal in this tube was substantially higher than the gain for either of the signals being mixed. This was precisely the characteristic which had permitted successful operation of the double-helix tube as a divider. Thus the conventional tube was connected with its output fed back through an attenuator to the input as in Fig. 2; except, of course, only one helix was present. The tube was operated as a frequency divider and gave successful performance over a bandwidth of about 10 mc. The operation was less stable and more critically dependent upon proper adjustment than in the case of the double-helix tube.

A number of experiments were made to investigate certain characteristics of the mixing. The results of a theoretical analysis by Putz[2] had indicated that for tubes of fixed dimensions the conversion gain should be proportional to the square of the intermediate frequency. These results were verified for low intermediate frequencies by taking the IF output signal directly from a traveling-wave-tube collector through a load resistor. As shown in Fig. 3, the variation

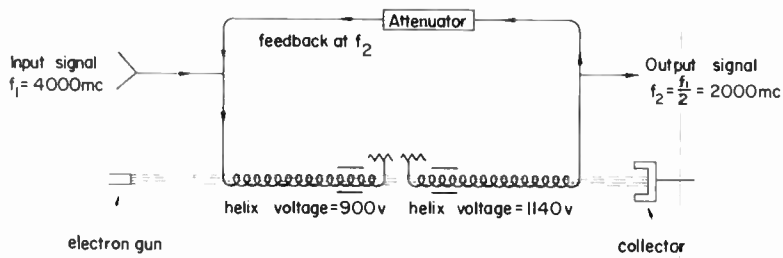

Fig. 2—Frequency divider employing a double-helix traveling-wave-tube mixer. The first helix was operated for broad-band amplification covering the 2000 to 4000-mc range. The second helix was tuned to peak the gain at 2000 mc.

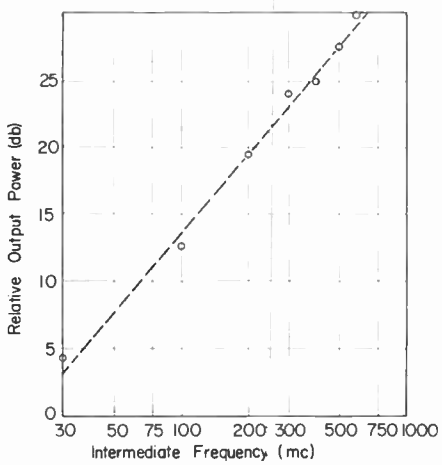

Fig. 3—Relative IF output power as a function of the intermediate frequency. For these data, the input power level of the signals which were mixed was held constant. The IF output was taken from a traveling-wave-tube collector operating into a 50-ohm load.

[2] J. L. Putz, "Nonlinear Phenomena in Traveling-Wave Amplifiers," Tech. Rep. No. 37 (N6onr 251), Elec. Res. Lab., Stanford University, Stanford, Calif.; October 15, 1951.

of the output power for constant input power (and thus the variation of the conversion gain) was as the square of the intermediate frequency. These data were taken with a 50-ohm collector load resistor. Since the collector capacity is fixed as in a pentode amplifier stage, the obtainable mixer conversion gain must be a function of bandwidth. This fact was verified by inserting a 30-mc tuned circuit as a collector load having a resonant impedance of about 16,000 ohms and a bandwidth of 0.6 mc. The conversion gain was thereby increased by 25 db. (This tube then had an over-all conversion gain of +7 db at 30 mc with a tube gain of 35 db.)

Additional experimental data were obtained from the above tube to determine the mixer saturation characteristics. These data are presented in Fig. 4. The relative conversion gain is shown as a function of the local oscillator input power. Also shown is the curve for the local oscillator ouput power from the traveling-wave-tube helix. As is apparent, the conversion gain reaches its peak well before large signal saturation, for the tube as an amplifier, sets in. Consequently, it is felt that a first-order mixing analysis can be used successfully to predict conversion gain and mixing effects in the useful region of operation of this type of tube. Such an analysis is being made at the present time.

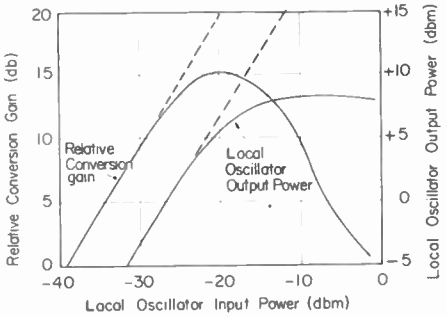

Fig. 4—Relative conversion gain and local oscillator output power as a function of local oscillator input power. The IF output was taken from the collector while the local oscillator output was taken from the helix of a traveling-wave tube.

R. W. DeGrasse
and G. Wade
Stanford Electronics Labs.
Stanford University
Stanford, Calif.

A Name and Unit for Handling Admittances Due to Coils*

The problem of a suitable name and unit for what has been called "inverse inductance" and "inverse mutual inductance" has been discussed several times in the correspondence columns of Proceedings. The inadequacy of names such as "inverse inductance" (or "inverse" anything), and of symbols that imply inversion, is more or less obvious. The need for a better name became a practical necessity, however, when it was required to develop a simplified approach to filter theory and design, which could be readily understood and applied at all levels of engineering.

It was clear from the start that the simplest approach was via nodal analysis rather than loop analysis, for the reason that node equations translate into equivalent circuits far more readily than do the corresponding mesh equations. But, an immediate difficulty was encountered in trying to present this approach for general consumption when it was found that a very large number of engineers tend to think of admittance as the inverse of impedance. Such a notion makes nodal analysis an impossibly complicated mental contortion. It proved most essential to replace this "inverted viewpoint" with a clear understanding of admittance as a measure of the ability to admit current—measured by the current that flows per volt applied.

In terms of nodal analysis, it was found that a considerable simplification of filter theory can be made by considering all filters as band-pass configurations made up of sections coupled by "mutuals" rather than by ponderable elements. High-pass, low-pass, stop filters, and so on, then drop out as special cases of this very simple and easily manipulated basic configuration. The approach is the opposite of the usual approach which makes the low-pass filter the basic configuration. Its success depends on the simplicity with which mutually-coupled circuits can be described in terms of admittances, provided coils are described in terms of parameters related to their admittances.

The admittance of coils has therefore been expressed in terms of their "*acceptance*," A, which is defined as a measure of the rate at which a coil accepts current. Thus, if a voltage, E, is applied to a pure acceptance, A, the current, i, that flows will be given by:

$$i = AEt.$$

The unit of acceptance is, therefore, one ampere per volt-second; hence acceptance is measured in amperes per volt-second. We can write this: i/et, where i stands for amperes, e for volts, and t for seconds; and the source of the somewhat whimsical, but completely descriptive name, "ippets" (spelled i/et), as the name for units of acceptance, is clear.

Acceptance, A, has been defined to include coefficients of magnetic coupling, therefore inductance, L, of a coil, is not simply the reciprocal of the coil's acceptance (except when the coil is not magnetically coupled to any other coils). In general, inductance, L, is related to acceptance, A, by:

$$L = \frac{1}{A(1 - \phi^2)}$$

where ϕ is the total effective coefficient of magnetic coupling. If a coil is magnetically coupled to other coils with individual coefficients of coupling, φ_{n1}, φ_{n2}, φ_{n3}, etc., then:

$$\phi^2 = \varphi_{n1}^2 + \varphi_{n2}^2 + \varphi_{n3}^2 \text{ etc.}$$

Magnetic coupling between any two coils can be replaced by a mutual acceptance, A_m. Corresponding mutual inductance, L_m, is related to mutual acceptance by:

$$L_m = \frac{\varphi^2}{A_m(1 - \varphi^2)}.$$

It will be noted that when magnetic coupling is replaced by a coil, as in Fig. 1,

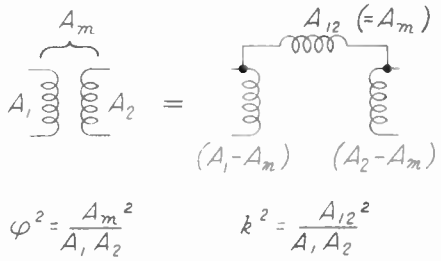

Fig. 1—Equivalent circuits and coefficients of coupling.

the coefficient of *magnetic* coupling, ϕ, becomes zero. It is replaced by the coefficient of coupling, k, which is given by:

$$k = \frac{A_{12}}{\sqrt{A_1 A_2}}$$

and the inductance of each of the coils in the equivalent π of Fig. 1 is then simply the reciprocal of the coil's acceptance. In terms of "ippets," a coil whose acceptance is 10^6 i/et (one "megippet") corresponds to a coil whose inductance is 10^{-6} henries (one microhenry) (when there are no magnetic couplings). "Megippet" is of course spelled Mi/et and "kilippet" (which corresponds to an inductance of 1 millihenry) is spelled ki/et.

The simplicity with which circuits containing mutual acceptance (or mutual inductance, which amounts to the same thing) can be handled in terms of acceptances and mutual acceptances, has indicated that it is advantageous to express a whole class of networks in terms of the mutually-coupled equivalents. Thus, the equivalent circuits of Fig. 1 are not restricted to coils. We may consider the coils to be any admittances whatsoever, coupled by a "mutual field" admittance y_m. There is then a coefficient of "field" coupling, φ, and this enters into the definition of the coupled admittances. When the circuit is eventually transformed back to a simple π, however, φ goes to zero and therefore the fact that it was ever anything other than zero can be ignored. In the same way, the presence of ϕ in the definition of inductance in terms of acceptance, can also be ignored, unless magnetically coupled circuits are to be actually constructed that way.

The filter study based on this approach is the subject of a report being prepared for the Air Force. The terms, acceptance, A, mutual acceptance, A_m, and ϕ for total effective coefficient of magnetic coupling, with φ for coefficient of magnetic coupling between any two coils, are introduced therein. The unit of acceptance, i/et, is also described, and the generalization of "field" coupling under the symbols, φ and ϕ, is used. Apart from this study, however, it was felt that the names and units for handling admittances due to coils, which have been described, would be of general interest.

* Received by the IRE, April 8, 1957.

F. Sutherland Macklem
Instruments for Industry, Inc.
Mineola, N. Y.

Two Theorems for Dissipationless Symmetrical Networks*

It is the purpose of this letter to derive two little known, but convenient theorems that enable one to quickly determine the insertion loss and insertion phase delay of a dissipationless, symmetric network from a knowledge of the input admittance of a half section of that network.

It is shown that the insertion loss $1/T^2$ of a dissipationless network of the type illustrated in Fig. 1 can be determined from

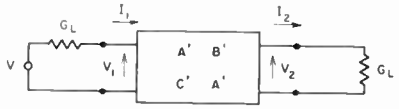

Fig. 1—Dissipationless symmetrical network.

the midplane admittance or impedance obtained when the network is terminated at each end in its load conductance $G_L=1/R_L$, by means of the relation[1]

$$\frac{1}{T^2}=1+\left[\frac{B_m}{G_m}\right]^2=1+\left[\frac{X_m}{R_m}\right]^2. \quad (1)$$

Here B_m/G_m is the ratio of midplane susceptance to conductance, while X_m/R_m is the ratio of midplane reactance to resistance. Similarly, the insertion phase of the network terminated at each end with conductance G_L can be determined from the susceptances

$$B_{oc}=-\frac{1}{X_{oc}} \quad \text{and} \quad B_{sc}=-\frac{1}{X_{sc}}$$

at the input terminals of the network, obtained when an open circuit and a short circuit are placed respectively at the midplane of the network. The relation is

$$\phi=\pi/2+\tan^{-1}\frac{B_{sc}}{G_L}+\tan^{-1}\frac{B_{oc}}{G_L}$$
$$=\frac{\pi}{2}+\tan^{-1}\frac{X_{sc}}{R_L}+\tan^{-1}\frac{X_{oc}}{R_L}. \quad (2)$$

These relations may be demonstrated in the following manner.

The insertion voltage ratio $1/T$ of the network shown in Fig. 1 is defined as the voltage at the load when no network is present divided by the voltage at the load when the network is present. The input and output voltages and currents of this network are related in terms of the A', B', C', D' constants by

$$\begin{aligned} V_1&=A'V_2+B'I_2 \\ I_1&=C'V_2+D'I_2. \end{aligned} \quad (3)$$

By applying the appropriate boundary conditions to (3) and remembering that $D'=A'$ in this symmetric network, it is easy to see that

$$\frac{1}{T}=A'+\frac{B'G_L}{2}+\frac{C'}{2G_L}. \quad (4)$$

It follows from elementary matrix theory that if the network in Fig. 1 is bisected as shown in Fig. 2 and that if the $ABCD$ matrix of the left-hand section is

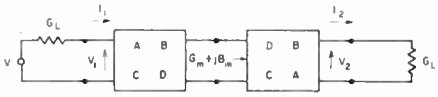

Fig. 2—Bisected dissipationless symmetrical network.

$$\begin{Vmatrix} A & B \\ C & D \end{Vmatrix}$$

then the $ABCD$ matrix of the right-hand section is

$$\begin{Vmatrix} D & B \\ C & A \end{Vmatrix}.$$

Therefore, the matrix of the whole symmetric network of Fig. 1 may be written as

$$\begin{Vmatrix} \frac{AD+BC}{2CD} & \frac{2AB}{AD+BC} \end{Vmatrix} \quad (5)$$

and the insertion voltage ratio for the whole network becomes

$$\frac{1}{T}=AD+BC+ABG_L+\frac{CD}{G_L}. \quad (6)$$

For a dissipationless network, it is well known that A and D are real while B and C are imaginary. Hence the insertion power ratio (*i.e.*, insertion loss) $1/T^2$ is

$$\frac{1}{T^2}=(AD+BC)^2-\left(ABG_L+\frac{CD}{G_L}\right)^2. \quad (7)$$

The insertion phase delay ϕ on the other hand is given by the relation

$$\tan\phi=-j\left[\frac{1}{G_L\left(\frac{A}{C}+\frac{B}{D}\right)}+\frac{G_L}{\left(\frac{C}{A}+\frac{D}{B}\right)}\right]. \quad (8)$$

By applying the reciprocity relation $AD-BC=1$, (7) becomes

$$\frac{1}{T^2}=1-\left[ABG_L-\frac{CD}{G_L}\right]^2. \quad (9)$$

The admittance Y_m of the right-hand half of the network of Fig. 2 as measured at the midplane is

$$Y_m=G_m+jB_m=\frac{G_L+CD-ABG_L^2}{D^2-B^2G_L^2}. \quad (10)$$

Substituting (10) in (9), one obtains (1), thus proving the first theorem.

Eq. (8) can be written in terms of B_{oc} and B_{sc} as

$$\tan\phi=\frac{1}{G_L\left[\frac{1}{B_{oc}}+\frac{1}{B_{sc}}\right]}-\frac{G_L}{B_{oc}+B_{sc}}$$
$$=\frac{B_{sc}B_{oc}-G_L^2}{G_L(B_{sc}+B_{oc})}. \quad (11)$$

Using the trigonometric relation for the cotangent of the sum of two angles, one finds

$$\tan\phi=-\cot\left[\tan^{-1}\frac{B_{sc}}{G_L}+\tan^{-1}\frac{B_{oc}}{G_L}\right]$$
$$=\tan\left(\frac{\pi}{2}+\tan^{-1}\frac{B_{oc}}{G_L}+\tan^{-1}\frac{B_{sc}}{G_L}\right) \quad (12)$$

thus proving (2).

E. M. T. Jones
and S. B. Cohn
Stanford Res. Inst.
Menlo Park, Calif.

* Received by the IRE, March 5, 1957; revised manuscript received, April 15, 1957.

[1] This relation has been stated without proof by J. Reed, "Low-Q microwave filters," PROC. IRE, vol. 38, pp. 793–796; July, 1950.

Smooth Random Functions Need Not Have Smooth Correlation Functions*

This note is concerned with certain questions relating to the behavior of autocorrelation functions, defined by

$$\rho(\tau)\equiv\lim_{T\to\infty}\frac{1}{2T}\int_{-T}^{T}f(t+\tau)f(t)dt \quad (1)$$

for functions $f(t)$ such that the limit (1) exists for every (real) value of τ. Sometimes this definition is modified by subtracting out the square of the mean, $\langle f\rangle^2$, where

$$\langle f\rangle\equiv\lim_{T\to\infty}\frac{1}{2T}\int_{-T}^{T}f(t)dt, \quad (2)$$

and dividing by the variance $\sigma^2\equiv\langle f^2\rangle-\langle f\rangle^2$, assumed positive. The two definitions coincide if $\langle f\rangle=0$ and $\sigma^2=1$, as we shall assume for the time being.

It is quite widely believed that the autocorrelation function obtained from an $f(t)$ with no "jump" discontinuities is differentiable at the origin. That is, it is thought that the graph of $\rho(\tau)$ necessarily has a horizontal tangent at $\tau=0$, provided only that $f(t)$ has no "jumps" such as those in an ideal square wave. This proposition seems to be some sort of "folk theorem;" *e.g.*, one finds:

> "Of course, the theoretical function . . . given in the figure cannot fit the data in the vicinity of the origin; this function has a finite slope [at the origin] which signifies infinitely sharp or steplike boundaries, a physical impossibility."[1]

This has even been cited as the basis, at least in part, for modifying or rejecting a proposed physical theory:

> "Finally, it should be noted that the first derivative of the correlation function (2) [exists] at the origin, as it must . . . to describe a physical process, and this eliminates one of the objections to the model proposed by Booker and Gordon which involved an exponential correlation function with a cusp at the origin."[2]

Such examples are quite common, and may be found in several branches of physics and engineering. However, there is one feature in common to every example—namely, that every time the "folk theorem" is invoked, it is always without reference to a proof. As a matter of fact, however, there is no hope of proving it; the object of this note is to point out that it is false, and to state mathematical conditions under which it is actually true that an autocorrelation function is differentiable at the origin. We shall also discuss certain practical considerations.

The fact that it is false has actually been known, though not widely so, since 1933, when Wiener[3] gave an example of a function

* Received by the IRE, March 15, 1957. This research was supported jointly by the U. S. Army, Navy, and Air Force under contract with the Mass. Inst. of Tech., Cambridge, Mass.

[1] L. Liebermann, "The effect of temperature inhomogeneities in the ocean on the propagation of sound," *J. Acoust. Soc. Amer.*, vol. 23, pp. 563–570; September, 1951.

[2] K. A. Norton, "Point-to-point radio relaying via the scatter mode of tropospheric propagation," IRE TRANS., vol. CS-4, p. 42; March, 1956.

[3] N. Wiener, "The Fourier Integral and Certain of its Applications," Cambridge University Press (reprinted, Dover Press, New York, N. Y.), p. 151; 1953.

that was everywhere *analytic* (not merely continuous!) and uniformly bounded, but which had the autocorrelation function

$$\rho(\tau) = \begin{cases} 1, & \tau = 0; \\ 0, & \tau \neq 0, \end{cases} \qquad (3)$$

which is not even continuous at the origin, let alone differentiable there. Once it is appreciated that the "folk theorem" is indeed false, it is not very difficult to give other counter-examples; *e.g.*, one can construct a uniformly-bounded function with continuous, everywhere-finite derivatives of *all* orders, and which has the correlation function $\rho(\tau) = \exp -|\tau|$.

It is of interest to state conditions under which it is unequivocally true that an autocorrelation function is differentiable at the origin. In order to do this, we shall first review some definitions. A function $f(t)$ is said to satisfy a uniform Lipschitz condition of order p if there is a number M such that for $|\tau| \leq 1$,

$$|f(t+\tau) - f(t)| \leq |\tau|^p M \qquad (4)$$

for all t. A function $f(t)$ is said to be "uniformly differentiable" if it is differentiable and if, given any $\epsilon > 0$, there is a $\delta > 0$ such that for every τ in $0 < |\tau| < \delta$,

$$\left| \frac{f(t+\tau) - f(t)}{\tau} - f'(t) \right| < \epsilon \qquad (5)$$

for all t. It is then true that $\rho(\tau)$ will have a horizontal tangent at the origin whenever any one of the following three conditions is satisfied:

1) $f(t)$ satisfies a uniform Lipschitz condition of order $p > \frac{1}{2}$.
2) $f(t)$ is uniformly differentiable and has a finite mean square derivative $\langle (f')^2 \rangle$.
3) $f(t)$ is uniformly differentiable and the limit $\langle ff' \rangle$ exists and is equal to zero.

Condition 1) follows readily from the easily established relation

$$\left| \frac{1-\rho(\tau)}{\tau} \right| = \frac{|\tau|^{2p-1}}{2\sigma^2} \operatorname*{Lim}_{T\to\infty} \frac{1}{2T} \int_{-T}^{T} \left[\frac{f(t+\tau) - f(t)}{\tau^p} \right]^2 dt \qquad (\tau \neq 0) \qquad (6)$$

where we now use the normalized definition of $\rho(\tau)$ mentioned after (1). Condition 2) follows from (6) (with $p = 1$) and the Schwarz inequality. Condition 3) follows from the trivial fact that, for $\tau \neq 0$,

$$\frac{1-\rho(\tau)}{\tau} = \frac{1}{\sigma^2} \operatorname*{Lim}_{T\to\infty} \frac{1}{2T} \int_{-T}^{T} f(t) \frac{f(t) - f(t+\tau)}{\tau} dt. \qquad (7)$$

In some sense, condition 1) is the most general of the three, and cannot be sharpened very much; in particular, it may happen that 2) or 3) implies 1).

It has been conjectured by Eckart[4] that a function with a finite mean square derivative essentially satisfies a Lipschitz condition, in the sense that if $\langle (f')^2 \rangle$ is finite, then there is a function $g(t)$ satisfying a uniform Lipschitz condition and such that $\langle (f-g)^2 \rangle = 0$. If so, this would shed light on 2). This conjecture is quite attractive, though it does not appear to be a simple matter to establish the true state of affairs concerning it.

We might remark that 1) will hold (with $p = 1$) if in particular $f(t)$ has a uniformly bounded first derivative. Condition 3) will hold if in particular

$$\operatorname*{Lim}_{|t|\to\infty} [f^2(t)/t] = 0$$

(*e.g.*, if f is uniformly bounded) and if f has a uniformly continuous first derivative. If $f(t)$ has a uniformly-bounded second derivative, then $f'(t)$ is uniformly continuous, which implies that $f(t)$ is uniformly differentiable.

It is clear from the conditions that it would certainly be safe to assume that one or more of them held in a great many practical cases. On the other hand, there are a great many practical cases where it would be equally safe to ignore the conditions, and use a model correlation function that did not have a horizontal tangent at the origin. For example, consider Fig. 1, which is an

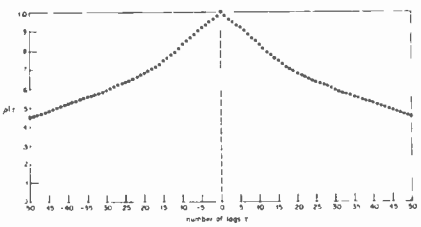

Fig. 1—Correlogram of the envelope of a fading radio wave.

empirical autocorrelogram of the envelope of a fading radio wave. One would be quite prepared to assume that one or more of the conditions held for the original envelope function. However, in spite of the fact that the correlogram has been computed with resolution a full order of magnitude better than is usually obtained [$1-\rho(1) = 0.01$ in Fig. 1], the obvious model correlation function to fit to the points of Fig. 1 would be one which did not have a derivative at the origin. (As a matter of fact, one of the form $\exp -|a\tau|$ does quite well.) The only circumstances in which this would be undesirable would be where some desired relation actually diverged or otherwise failed to exist in consequence of the nonexistent derivative,[5] in which case one would naturally use something else.

This situation is completely analogous to the many situations in physics and engineering where one uses (as a matter of convenience) the Rayleigh, normal, or some other probability distribution of a definitely unbounded sort to represent the distribution of a variable that would actually be bounded. For example, no one would actually expect to find gas molecules running about a room at speeds in excess of the velocity of light, even though the Maxwell-Boltzmann distribution would assign positive probability to this event. As always, such distributions are approximately valid only over certain finite ranges, which do not include either arbitrarily small or arbitrarily large values.

In the case of autocorrelation functions, meaningful questions will always involve values of τ bounded away from zero by some significant margin—*not* arbitrarily small values. The question of whether or not a given model correlation function actually has a derivative at the origin is thus ultimately vacuous, so far as physics is concerned, though the writer would be the last to deny the utility of classical analysis for physics and engineering. It might be added that analogous statements are true of the behavior of power spectra at high frequencies.

We might point out that (6) is useful in investigating the "reasonableness" of proposed model correlation functions at finite values of τ, and for interpreting the meaning of empirical correlograms. Setting $p = 1$, (6) yields the interpretation: The magnitude of the slope from the origin to the point $[\tau, \rho(\tau)]$ is equal to $(\tau/2)$ times the mean square slope of f (measured in units of the standard deviation σ) over intervals of fixed length τ. This is useful for, among other things, estimating limits of validity for proposed correlation functions.

The writer is indebted to several people, including Martin Balser, T. J. Carroll, Carl Eckart, C. L. Mack, and Robert Price for critical comments and stimulating discussions on various aspects of this subject.

Donald G. Brennan
Lincoln Laboratory
Mass. Inst. Tech.
Lexington, Mass.

[4] C. Eckart, Scripps Institution of Oceanography, La Jolla, Calif.; private communication.

[5] For example (3.3-11), of S. O. Rice, *Bell Sys. Tech. J.*, vol. 24, p. 54; January, 1945, could not be used with model correlation functions of this type.

Transient Response in FM*

In the above paper,[1] Gumowski derived expressions for the frequency-step and phase-step responses of networks in terms of the impulse responses of their zero-center-frequency analogs. This note is intended to present derivations which are considerably simpler and which sidestep the mathematical complications of Gumowski.[1]

Let the input be

$$e(t) = z(t) \exp(j\omega_0 t),$$

where $z(t)$ is, in general, a complex function. The output of the network may be written as

$$E(t) = Z(t) \exp(j\omega_0 t); \quad Z(t) = X(t) + jY(t);$$

and its instantaneous frequency is

$$\omega(t) = \omega_0 + d/dt[\tan^{-1}(Y/X)].$$

The zero-center-frequency analog $A(j\omega)$ of the network's transfer function $A'(j\omega)$ is defined by

$$A'(j\omega) \equiv A[j(\omega - \omega_0)].$$

* Received by the IRE, April 5, 1957.

[1] I. Gumowski, Proc. IRE, vol. 42, pp. 819–822; May, 1954.

Using a well-known transform property, $Z(t)$ may be found[2] as the response of the analog network $A(j\omega)$ to the excitation $z(t)$. In particular, $Z(t)$ may be expressed in terms of the impulse response $u(t)$ of the analog network $A(j\omega)$.[3]

As an example, consider deviations from center frequency and zero phase, starting at $t=0$; *i.e.*, let

$$z(t) = 1, \quad (t < 0)$$
$$= \exp [jF(t)], \quad (t>0).$$

The output $Z(t)$ consists of the superposition of three responses: The steady-state response to a unit dc input; the response to a negative unit step occurring at $t=0$; and the response to the input $\exp [jF(t)]$, applied at $t=0$. The first of these responses is simply $A(0)$. The other two may be written in terms of $u(t)$. One obtains immediately

$$Z(t)=A(0)-\int_0^t u(x)dx+\int_0^t e^{jF(t-x)}u(x)dx,$$

which is essentially (10) of Gumowski.[1] An input frequency jump from center frequency ω_0 to (ω_0+a) is described by $F(t)=\exp(jat)$. The corresponding output is[4]

$$Z(t)=A(0)-\int_0^t u(x)dx+e^{jat}\int_0^t e^{-jax}u(x)dx.$$

Similarly, $F(t)=\exp(j\Phi)$ represents a carrier phase jump from zero to Φ radians, and the output function is[5]

$$Z(t) = A(0) - (1 - e^{j\Phi})\int_0^t u(x)dx.$$

An extension of Gumowski's results will provide a final example: consider a frequency jump from (ω_0-b) to (ω_0+a). Here

$$z(t) = \exp(-jbt), \quad (t < (0)$$
$$= \exp(jat), \quad (t > 0).$$

Again considering the output as the sum of three responses, one may write

$$Z(t) = A(-jb)e^{-jbt} - \int_0^t e^{-j(b-x)}u(x)dx + \int_0^t e^{ja(t-x)}u(x)dx.$$

Inputs other than frequency and phase steps may be handled in the same manner. Further, the output $Z(t)$ can be expressed in terms of the unit step response of $A(j\omega)$ rather than its impulse response.

If the zero-frequency analog is realizable, *i.e.*, if the band-pass network is narrow and symmetrical, the above derivations may be rephrased in terms of in-phase and quadrature components. For example, an input frequency jump from ω_0 to (ω_0+a) corresponds to an input function

$$e(t) = \cos \omega_0 t, \quad (t < 0)$$
$$= \cos(\omega_0 + a)t, \quad (t > 0).$$

Alternatively,

$$e(t) = x(t)\cos\omega_0 t - y(t)\sin\omega_0 t,$$

where

$$x(t) = 1, \quad (t < 0)$$
$$= \cos at, \quad (t > 0)$$

and

$$y(t) = 0, \quad (t < 0)$$
$$= \sin at, \quad (t > 0).$$

The corresponding output is

$$E(t) = X(t)\cos\omega_0 t - Y(t)\sin\omega_0 t,$$

where $X(t)$ and $Y(t)$ are the responses of the low-pass analog to $x(t)$ and $y(t)$, respectively. The original network is thus represented by two identical low-pass analogs, one in the in-phase and one in the quadrature channel.[6] The instantaneous output frequency is again given by the time derivative of arc tan (Y/X).

DONALD A. LINDEN
Philco Corp.
Philadelphia, Pa.

[2] For example, E. A. Guillemin, "Communication Networks," John Wiley and Sons, New York, N. Y., vol. II, p. 470; 1935.

[3] The functions $z(t)$ and $Z(t)$ are "vector envelopes" in the sense defined by H. A. Wheeler, "The solution of unsymmetrical-sideband problems with the aid of zero-frequency carrier," PROC. IRE, vol. 29, pp. 446–458; August, 1941.

[4] Gumowski, *op. cit.*, (5a).

[5] *Ibid.*, (7a) represents the output in response to a carrier phase jump from Φ to zero radians, and is therefore not identical with this result.

[6] This concept has been used extensively by M. J. E. Golay in the analysis of fm phenomena.

Phase Error of a Two-Phase Resolver*

In the application of two-phase resolvers, it is sometimes useful to know the error resulting from an inequality between the two-phase voltages. This error may be expressed as the difference between the space angle of the rotor, θ_m, and the electrical angle of the rotor voltage, θ_e.

If the amplitude of the reference phase voltage is set equal to unity, and the amplitude of the quadrature voltage is A, then the phasor diagram (Fig. 1) can be drawn

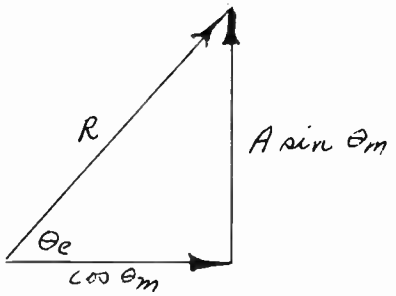

Fig. 1.

for the induced voltages in the rotor. This leads to the relationship:

$$\theta_e = \tan^{-1}(A\tan\theta_m).$$

Subtracting the angle θ_m from each side:

$$\theta_e - \theta_m = \tan^{-1}(A\tan\theta_m) - \theta_m.$$

This expression gives the angular error for any rotor position. The maximum angular error may be obtained by differentiating the above expression and setting the result equal to zero.

$$\frac{d(\theta_e-\theta_m)}{d\theta_m} = \frac{A\sec^2\theta_m}{1+A^2\tan^2\theta_m} - 1 = 0$$
$$A\sec^2\theta_m = 1 + A^2\tan^2\theta_m$$
$$A(1+\tan^2\theta_m) = 1 + A^2\tan^2\theta_m$$
$$\tan\theta_m = \sqrt{\frac{1}{A}}.$$

Substituting this result in the expression for the angular error and taking the tangent of both sides:

$$\tan(\theta_e-\theta_m) = \frac{\sqrt{A}-\frac{1}{\sqrt{A}}}{2}.$$

It can be seen from this result that an unbalance of only one per cent in the phase voltages will result in a maximum angular error of more than 17 minutes which is considerably in excess of the inherent error of many of these devices.

JACOB SCHACHTER
Pitometer Log Corp.
New York, N. Y.

* Received by the IRE, March 29, 1957.

A Simplified Procedure for Finding Fourier Coefficients*

Application of Gibbons' methods in the above article[1] to a different representation of the Fourier series may be of interest.

Consider the function $f(x)$ with period X and Fourier series:

$$\frac{a_0}{2} + \sum_{n=1}^{\infty}(a_n\cos\omega nx + b_n\sin\omega nx). \quad (1)$$

An alternate representation of $f(x)$ is

$$f(x) = \sum_{n=-\infty}^{\infty}\alpha_n e^{jn\omega x} \quad (2)$$

where

$$\omega = \frac{2\pi}{X}; \quad \alpha_n = \frac{1}{X}\int_0^X f(x)e^{-jn\omega x}dx \quad (3)$$

$$\alpha_n = \begin{cases}\frac{1}{2}(a_n + jb_n) & \text{if } n \geq 0\\ \alpha_{-n}^* & \text{if } n < 0\end{cases} \quad (4)$$

$$\int f(x)dx = \int\sum_{n=-\infty}^{\infty}\alpha_n e^{jn\omega x}dx$$
$$= \sum_{n=-\infty}^{\infty}{}'\frac{\alpha_n}{jn\omega}e^{jn\omega x} + \alpha_0 x + K. \quad (5)$$

Σ' indicates omission of the $n=0$ term.

The α_n's for a train of delta functions

$$\sum_{i=0}^{s}\sum_{j=0}^{\infty}\delta(x - x_i - jX);$$
$$0 \leq x_0 < x_1 < \cdots < x_s < X \quad (6)$$

* Received by the IRE, April 5, 1957.

[1] J. F. Gibbons, PROC. IRE, vol. 45, p. 243; February, 1957.

are

$$\sum_{i=0}^{s} \frac{1}{X} e^{-jn\omega x_i}. \tag{7}$$

Consider a function $g(x)$ which has $h(x)$ as its derivative. Since $g(x)$ is periodic, $h(x)$ is also periodic, and has zero average value.

$$g(x) = \sum_{n=-\infty}^{\infty}{}' \frac{\alpha_n}{jn\omega} + K. \tag{8}$$

Now, assume that by differentiating some function $g(x)$ m times, we arrive at a function $k(x)$ which is a sum of delta functions as given by (6). The α_n's are given by (7). That is,

$$\alpha_n = \frac{1}{X} \sum_{i=0}^{s} e^{-jn\omega x_i}.$$

Integrating m times gives

$$g(x) = \sum_{n=-\infty}^{\infty}{}' \frac{\alpha_n}{(jn\omega)^m} e^{jn\omega x} + K \tag{9}$$

$$= \sum_{n=-\infty}^{\infty} \alpha_{n0} e^{jn\omega x}. \tag{10}$$

In conclusion, to find the α_n's of a function $g(x)$, differentiate it until the mth derivative appears as a sum of delta functions. Find the α_n's of

$$\frac{d^m[g(x)]}{dx^m}.$$

Divide by $(jn\omega)^m$ to get the α_n's of $g(x)$. Add the average value of $g(x)$.

MARVIN I. GANG
1681 49th St.
Brooklyn 4, N. Y.

High Performance Silicon Tetrode Transistors*

Since the grown-diffused technique was announced one year ago,[1] this technique has been further exploited. The result is a developmental silicon tetrode transistor which seriously rivals germanium transistors in high-frequency performance.

Fig. 1 illustrates the frequency response possible for the common emitter and common base short-circuit current gains. The alpha cutoff frequency is approximately 350 megacycles.

One prevalent misconception concerning tetrode transistors is that tetrode operation necessarily precludes a high alpha. Referring to Fig. 1, it is seen that this unit has a low-frequency common emitter current gain of 37 db. Since the common emitter cutoff frequency is about 5 megacycles, this unit has a very large gain bandwidth product.

* Received by the IRE, April 1, 1957. This work was supported by the Signal Corps under Industrial Preparedness Study Contract No. DA-36-039-SC-72703.

[1] R. F. Stewart, B. Cornelison, and W. A. Adcock, "High-frequency tetrodes," 1956 IRE NATIONAL CONVENTION RECORD, Pt. 3, pp. 166–171.

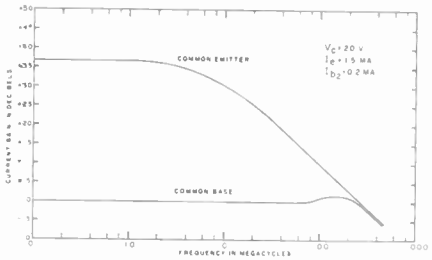

Fig. 1—Short-circuit current gain as a function of frequency in the common emitter and common base connections for a developmental grown-diffused silicon tetrode transistor.

The collector capacity for this type of unit is very low, approximately 0.6 mmf. The emitter and collector series bulk resistances are often thought to prohibit very high-frequency performance in a grown structure. However, with improved fabrication techniques these extrinsic elements may be reduced to quite low values. For this particular unit, the emitter series bulk resistance was about 0.5 ohm and the collector bulk resistance was 60 ohms. The high-frequency base resistance is 150 ohms at 150 megacycles.

Fig. 2 shows the power gain capabilities of this device. The curve was calculated assuming a common emitter conjugately matched input and ouptut stage with admittance neutralization. With moderate care, it is possible to realize within 2 or 3 db of this calculated power gain.

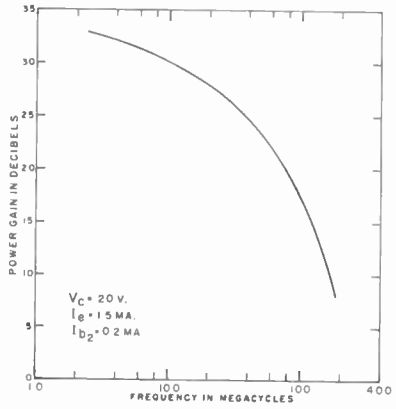

Fig. 2—Calculated common emitter power gain, assuming conjugate matched input and output and admittance neutralization.

The maximum collector to emitter voltage is 30 volts. The frequency response is relatively constant for collector voltages from 1.5 volts to 30 volts. The I_{co} has been a small fraction of a microampere as is usual in silicon transistors.

The tetrode bias current is not critical. A value of 0.2 ma was used in this example. It should be pointed out that in many applications, such as common emitter circuits, adequate tetrode bias may be obtained by merely connecting the second base to the emitter.

Fig. 3 illustrates not only the high tetrode alpha obtained but also the constancy of alpha with emitter current. Alpha remains essentially constant from 0.2 ma to greater than 15-ma emitter current.

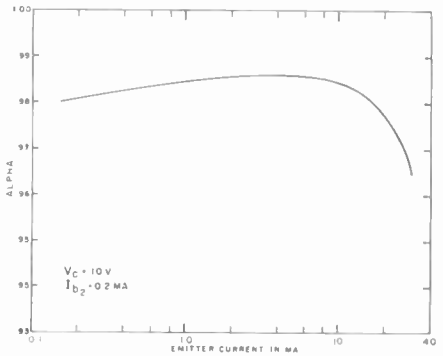

Fig. 3—Variation of tetrode alpha with emitter current.

In this effort, many individuals have made significant contributions. Members of the project group who contributed to the development and evaluation of these devices in addition to the author were W. C. Brower and Drs. R. E. Anderson, M. E. Jones, and W. R. Runyan.

RICHARD F. STEWART
Texas Instruments Inc.
Dallas, Texas

Relation Between Ratio of Diffusion Lengths of Minority Carriers and Ratio of Conductivities*

There is a simple relationship between the diffusion length L_p of the holes in the n region, L_n of the electrons in the p region, and the conductivities σ_n and σ_p of the n and p regions respectively. Namely,

$$\left(\frac{L_p}{L_n}\right)^2 = \frac{\sigma_p}{\sigma_n}. \tag{1}$$

Eq. (1) is derived on the basis of two commonly-made assumptions of junction transistor theory.

1) The conductivities in both regions can be closely approximated by that of the majority carriers alone.
2) The presence of injected minority carriers does not increase the number of majority carriers substantially enough to have detectable effect on the diffusion lengths.

Eq. (1) can be readily derived from the following well-established relations:

$$L_p^2 = D_p\tau_p = \frac{kT}{q}\mu_p\tau_p \tag{2}$$

$$L_n^2 = D_n\tau_n = \frac{kT}{q}\mu_n\tau_n \tag{3}$$

$$\tau_p = \frac{1}{rn_n} \tag{4}$$

$$\tau_n = \frac{1}{rp_p} \tag{5}$$

$$\sigma_p \approx q\mu_p p_p \tag{6}$$

$$\sigma_n \approx q\mu_n n_n. \tag{7}$$

* Received by the IRE, April 3, 1957.

In the above equations, τ_p and τ_n are lifetimes of holes and electrons as minority carriers; D_p, D_n and μ_p, μ_n are diffusion constants and mobilities of the holes and electrons, respectively. N_n and P_p are densities of majority carriers, q is the electronic charge and r is a constant of recombination. From (2) and (3),

$$\frac{L_p^2}{L_n^2} = \frac{\mu_p \tau_p}{\mu_n \tau_n} . \tag{8}$$

From (4) and (5),

$$\frac{\tau_p}{\tau_n} = \frac{p_p}{n_n} . \tag{9}$$

From (6) and (7),

$$\frac{\sigma_p}{\sigma_n} = \frac{\mu_p p_p}{\mu_n n_n} . \tag{10}$$

Eq. (1) follows from (8), (9), and (10).

As there are usually more than a single p region and a single n region, it is desirable to put (1) into an alternative form,

$$\sigma_j L_j^2 = \frac{kT}{r} \mu_p \mu_n \tag{11}$$

where σ_j is the conductivity of the majority carrier in the j-th region, and L_j is the diffusion length of the minority carrier in the j-th region. The right-hand side of (11) is a constant throughout the entire crystal, independent of the local densities of donors and acceptors. Eq. (11) can be easily derived for an n region from (2), (4), and (7), and for a p region from (3), (5), and (6).

SHELDON S. L. CHANG
Dept. of Elec. Eng.
New York University
New York, N. Y.

The Measurement and Specification of Nonlinear Amplitude Response Characteristics in Television*

It is gratifying to find Doba, in the above paper,[1] placing emphasis on linearity as such rather than on its effect—distortion. The widespread practice of specifying linearity in terms of the distortion which it produces has persisted too long.

I would, however, like to suggest an alternate procedure for plotting the linearity of an amplifier which is more direct and also simpler in application than the method of superposition of two signals. The term linearity refers specifically to an input-output characteristic and the definition of differential gain corresponds, in essence, to the slope of this curve at a particular point referred to some other point on the curve as a reference. If a ramp function is used for the input voltage waveform, the output waveform as plotted against a linear time base is the input-output characteristic. By means of a simple RC differentiating network, it is possible to differentiate the output waveform with respect to the input (since $e_{in} = kt$) and thus obtain a plot of the slope as a function of signal amplitude. The definition "differential gain" corresponds very closely to the "figure of demerit" which I proposed[2] and is defined in Fig. 1.

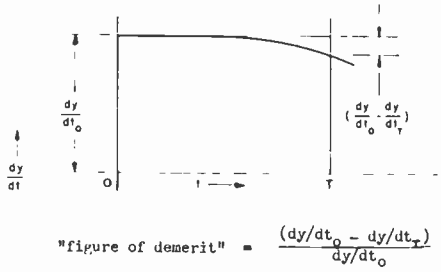

Fig. 1.

This procedure for plotting linearity requires fewer components, less bandwidth, and by use of a repetitive waveform of low-duty cycle permits measurements at power levels beyond the continuous duty ratings of the components involved.

STANLEY I. KRAMER
Guided Missiles Div.
Fairchild Engine and Airplane Corp.
Wyandanch, N. Y.

Author's Comment[3]

Although I am not in disagreement with Mr. Kramer's method of measuring and defining the "figure of demerit," I would like to point out that this is not quite the same as "differential gain."

The methods proposed by Mr. Kramer are correct for devices which have no time-storage effects. By this, I mean that they are valid when applied to a dc amplifier if the ramp function used as the input waveform changes at a "suitably" slow rate. As is obvious, in an ac amplifier there may be difficulty in making the ramp function too slow. With a finite bandwidth, there also may be difficulties in making it too fast. Hence, the determination of the meaning of the word "suitable" above may be quite a stumbling block, as was indicated by Mr. Kramer.

A more serious difficulty arises when we consider systems in general (such as feedback amplifiers), where the nonlinearity is a function of frequency. Here the distortion is affected not because of bandwidth limitations, but because a rapidly varying wave may be distorted differently from a slowly varying wave.

It is important then that the definitions and methods of measurement be stated clearly and without ambiguity. I believe our terms "differential gain" and "differential phase" are successful in meeting this objective. For the simple dc amplifier "differential gain" may be closely correlated with "figure of demerit." For more complex systems where it may be necessary to specify the "differential gain" as a function of frequency, this can be done without violence either to the definition or to the method of measurement.

STEPHEN DOBA, JR.
Bell Telephone Labs.
Murray Hill, N. J.

Automatic Dictionaries for Machine Translation*

Mechanical translation is one of the newer objectives of the communications engineer. Until now his concern has been chiefly with single-language messages. As communication has become more widespread it is more and more necessary to perform rapid multilingual transformations. An increasing number of communications engineers are concerned with the problems with which this note is concerned, and for which a partial solution is outlined.

In the field of machine translation, automatic dictionaries are generally recognized as the first requirement even by those who hope to go beyond word-for-word translation to sentence-for-sentence translation: "If translations better than word-for-word are wanted, work on an automatic dictionary should still be undertaken because any machine that translates will need a dictionary."[1]

At the present time, no translation machine, not even word-for-word, has been constructed which has a usefully large vocabulary.[2] The main problems for automatic translation machines are: 1) overcoming the many-one and one-many word relations which arise in translating words with several meanings; 2) reducing memory-search time; and 3) reducing input and output or print-out time. This note is addressed mainly to 2), although the word-for-word translation is evidently also a first approximation to a solution to 1).

As a specific kind of storage and retrieval device (a "pure memory" look-up system, rather than a computing system), an automatic dictionary is subject to the same logical considerations as storage and retrieval systems in general. Therefore an automatic dictionary involves two main processes: input of data, and search of stored data. Discussion of input is omitted here except for the observation that the information which can be gotten out of any storage and retrieval system can be no better than the information and organization put into it.

Now an automatic dictionary must search its word-memory either sequentially or by parallel (simultaneous) search. Obviously, parallel search is to be preferred for reduction of search time. Unfortunately, up to the present, the principal large-scale mem-

* Received by the IRE, March 29, 1957.
[1] S. Doba, Jr., PROC. IRE, vol. 45, pp. 161–165; February, 1957.

[2] S. I. Kramer, "A sensitive method for the measurement of amplitude linearity," PROC. IRE, vol. 44, pp. 1059–1060; August, 1956.
[3] Received by the IRE, April 11, 1957.

* Received by the IRE, April 11, 1957.
[1] V. H. Yngve, "The technical feasibility of translating languages by machine," *Elec. Eng.*, vol. 75, pp. 994–999 (p. 994); November, 1956.
[2] R. E. O'Dette, "Russian translation," *Science*, vol. 125, pp. 579–585 (p. 584); March 29 1957.

ories are tapes or their analogs, and cards, all of which require sequential search.

We have found that rapid, accurate parallel scanning of a large word-collection can be achieved by scanning, not the collection directly, but a class or classes of which the word sought is a member. We have constructed several systems for isolating class members, in the storage and retrieval of large collections of data.[3,4] They have the merit that access to an item can be had through a number of starting points, so that the devices are almost certain to deliver a word if it is in the system.

The operating principle is the construction of data storage classes from which it is possible to form logical products. Such products have continually decreasing membership as the number of products is increased: if a, b, c are the members of class X, and b, c, d are the members of class Y, then only b, c are the members of the class (X and Y). Further, if c, d, e are the members of class Z, then only c is a member of class [(X and Y) and Z]. If a device is set up which forms the logical product or "intersects" (in the form of an "and"-gate) classes X, Y, and Z, the intersection is simultaneous. The search is parallel search. In the case of a dictionary the final membership of the logical product is comprised of a word or words. The word-for-word dictionary restricts the output membership to a single word, but in the more general cases which may in time become feasible the dictionary could print out the entire set of translated words required to satisfy the one-many relationship.

Now there is a particularly easy way to locate words as members of classes, which is based upon the concept that the letters of words determine classes. If a letter of the alphabet is the name of a class, then a word is a member of the class formed by the logical intersection of its letter-classes. This is true for any language which has been alphabetized. In word-for-word translation, the input word is the intersection of the letter-classes which form it; and the output word is the intersection of other letter classes. However, it is not necessary to use this device for both input and output. Only the letters of the input word are needed, and of course only these are known initially. The output word can be considered as a single element. That is, in one-way translation the letters of the input terms are interpreted as the names of classes; the output terms as the members of these classes.

Suppose a French-to-English dictionary is to be used. The desired outputs will be English words, the input will be letters of the French words which are to be translated. Each letter of the French input will define a class which has as members a set of English words. The class distinguishes between the position of letters. Thus, the letter C in the French word, *chateau*, will be the class C_1, whereas the C's in *accomplir* will be C_2 and C_3; and the H in *chateau* will be H_2, etc. Consider now the normal procedure of looking up a word in a printed French-English dictionary, *e.g.*, the word *chateau*.

1) First look for the letter C (that is, for the French words beginning with C). This isolates from the total number of English words in the dictionary a partial set consisting of such members as: basket (cabas); coffee (café); hood (capuchon); ticket (carte); warm (chaud); cat (chat); hat (chapeau); castle (chateau); . . . swan (cygne); etc.
2) Next look for CH. This is equivalent to the class $(C_1 \cap H_2)$ and has as typical members: warm (chaud); hat (chapeau); and castle (chateau).
3) If the search is continued until it reaches the class $[(((((C_1 \cap H_2) \cap A_3) \cap T_4) \cap E_5) \cap A_6) \cap U_7]$, the output will be "castle," the single member of this class.

The above is a strictly accurate description only for a single word output (one-one) type dictionary such as would be used in an elementary word-for-word device. In general, in order to convert a printed dictionary to an automatic one, it is only necessary to construct a system of product circuits in which the selection of a set of switches (input letters) will select a single path through the system (the output word). In this case the system can be arranged as many-one or as one-one, depending on the ratio of input to output words. If the system is arranged as one-many, the reader of the translation has to do part of the work of final selection, since he has the different meanings of the input word presented to him. For example, the French noun *revers* might be printed out: (back, wrong side, back-stroke, counterpart, reverse, facing). As mentioned above, several devices using the class intersection principle have already been constructed for general storage and retrieval problems, and additional machines are under design.[3,4] These machines ordinarily have multiple outputs and multiple inputs as well. Thus modification to automatic dictionaries is a simple matter of substituting different meanings for the variables, namely, the input and output signals, by redefining what are regarded as classes and as members.

After basic design of the product-making automatic dictionary, certain interesting problems of efficiency remain. For instance, the sequential-scanning automatic dictionary may be operated on the assumption that the root of a word can be recognized by stripping away letters one by one, starting at the end of a word (that is, from right to left, in English). For example, the memory can be greatly reduced in size by storing only the root-stock *judg*, instead of *judge*, *judging*, *judgment*, etc.; and storing the endings separately. A product-making dictionary will proceed from the beginning of the word (*i.e.*, from left to right, in English). In many cases the last letters need not even be employed. Thus, the classes defined by C_1, H_2, A_3, T_4, E_5, A_6, U_7 and by C_1, H_2, A_3, T_4, E_5, A_6 have the same member. U_7 is redundant and can be disregarded. An efficient machine will not utilize products longer than are required to provide unique outputs. In our experience seven-letter intersections cover most cases, and need for more than ten is rare. And, of course, word-endings do not require separate storage.

The suggested solution for the search problem of automatic dictionaries has been directed mainly to word-for-word translation, on the assumption that this will come first. The principle should apply also in the case of dictionaries with many-one and one-many input-output relations. If such complexity can indeed be handled by a reasonably-sized memory, then the letter-class "and"-gate method appears to be the most efficient method of simultaneous search. The operating principle is that of the actual use of a dictionary: mere typing out of the input word forms the logical product. Not only will this save search time and some extra storage space, but the input typewriter itself can be a high-speed printer. The time for translation then will depend almost entirely on the output "readout" device.

M. Taube
and L. B. Heilprin
Documentation, Inc.
Washington, D. C

[3] E. Miller, "Final Report to the National Science Foundation on the MATREX Indexing Machine," Documentation, Inc., Washington, D. C.; January, 1957. See also, "The Prototype of the Mechanical Alpha-MATREX Indexing Machine," in "Studies in Coordinate Indexing," Documentation, Inc., vol. 4; June, 1957.

[4] M. Taube, *et al.*, "The Logic and Mechanics of Storage and Retrieval Systems," Tech. Rep. No. 14, prepared under Contract Nonr-1305(00) for the Office of Naval Res.; February, 1956. See also "Studies in Coordinate Indexing," Documentation, Inc., Washington, D. C., vol. 3, pp. 58–100; 1956.

On a Property of Wiener Filters*

The theory of optimum filters as originated by Wiener[1] and extended by many others[2] is invariably based upon a minimization of mean-squared error. A property of Wiener filters acting on stationary Gaussian inputs, which seems to have escaped general notice, is that they also minimize any function of the error of the form

$$f(|\epsilon|) = \sum_n \overline{|\epsilon(t)|^n},$$

where n is positive (but not necessarily an integer). This may be proved as follows.

If the input $\{x(t)\}$ to a linear time-invariant system $h(t)$ is Gaussian, the output $\{y(t)\}$ and hence the error

$$\{\epsilon(t)\} = \{y(t)\} - \{x(t+\alpha)\}$$

will also be Gaussian. Then

$$\overline{|\epsilon(t)|^n} = \frac{2}{\sqrt{2\pi\bar{\epsilon^2}}} \int_0^\infty \epsilon^n e^{-\epsilon^2/2\bar{\epsilon^2}} d\epsilon$$

$$= \frac{2^{n/2}}{\sqrt{\pi}} \Gamma\left(\frac{n+1}{2}\right) (\bar{\epsilon^2})^{n/2},$$

where

$$\bar{\epsilon^2} = \phi_{xx}(0) - 2\int_0^\infty h(\tau)\phi_{xx}(\tau+\alpha)d\tau + \int_0^\infty h(\tau_1)\int_0^\infty h(\tau_2)\phi_{xx}(\tau_1-\tau_2)d\tau_2 d\tau_1$$

* Received by the IRE, April 22, 1957.

[1] N. Wiener, "Extrapolation, Interpolation and Smoothing of Stationary Time Series," John Wiley and Sons, New York, N. Y.; 1949.

[2] J. Bendat, "A general theory of linear prediction and filtering," *J. Soc. Ind. Appl. Math.*, vol. 4, pp. 131–151; September, 1956.

and $\phi_{xx}(\tau)$ is the autocorrelation of the input $\{x(t)\}$. The minimization of $f(|\epsilon|)$ by the usual calculus of variations technique of varying $h(\tau)$ to $h(\tau)+ak(\tau)$, differentiating with respect to a, letting $a=0$, and subsequently setting this derivative equal to 0 gives

$$\left[\sum_n \frac{2^{n/2}n}{\sqrt{\pi}}\Gamma\left(\frac{n+1}{2}\right)(\bar{\epsilon^2})^{n/2-1}\right]\cdot\left[-\int_0^\infty k(\tau)\phi_{xx}(\tau+\alpha)d\tau + \int_0^\infty k(\tau_1)\int_0^\infty h(\tau_2)\phi_{xx}(\tau_1-\tau_2)d\tau_2 d\tau_1\right]=0$$

where $h(\tau)$ is the optimum filter impulse response. The quantity within the first brackets cannot vanish since $\epsilon^2>0$; hence a necessary condition for a minimum is that the second factor must vanish. This yields the requirement

$$\phi_{xx}(\tau+\alpha)=\int_0^\infty h(\sigma)\phi_{xx}(\tau-\sigma)d\sigma$$

which may be recognized as the Wiener-Hopf equation arising in the classical analysis based on the usual mean-square error criterion. The sufficiency of this condition may be proved in the usual manner.

T. R. Benedict
and M. M. Sondhi
Dept. of Elec. Eng.
University of Wisconsin
Madison, Wis

A Simplified Procedure for Finding Fourier Coefficients

*Letter from Mr. Brenner**

In the above article, Gibbons[1] pointed out that the Fourier series of periodic waveforms can be deduced with ease if successive differentiation of the waveform results in a simpler waveform, impulses being particularly desirable. The same technique can be applied to the problem of formulating the Fourier transform of pulse-type waveforms. If a pulse-type waveform is defined as a signal which lasts for a finite time and is Fourier transformable, *i.e.*,

$$f(t)\equiv 0, |t|\geq a, a \text{ positive}, \qquad (1)$$

then the (complex) Fourier transformation has the form:

$$f(t)=\frac{1}{2\pi}\int_{-\infty}^{+\infty}F(j\omega)\exp(j\omega t)d\omega \qquad (2a)$$

where

$$F(j\omega)=\mathfrak{F}f(t)=\int_{-a}^{+a}f(t)\exp(-j\omega t)dt. \qquad (2b)$$

From (2b) it follows that

$$i\omega F(j\omega)+f(a)\exp(-j\omega a)+f(-a)\exp(j\omega a)=\mathfrak{F}df/dt.$$

Since a has been chosen so that $f(a)=f(-a)=0$, one may write

$$\mathfrak{F}f(t)=1/(j\omega)\mathfrak{F}df/dt. \qquad (3)$$

In addition to (3), the relationship for the Fourier transform of the unit impulse

$$\mathfrak{F}\delta(t-b)=\exp(-j\omega b) \qquad (4)$$

is sufficient to find the Fourier transform of many waveforms. (The same scheme is applied to the Laplace transform if the waveform is shifted so that $f(t)=0$ for $t\leqq 0$.)

Examples

1) Find the Fourier transform of the rectangular pulse shown in Fig. 1(a). Solution: Since

$$f(t)=U(t)-U(t-T),$$
$$df/dt=\delta(t)-\delta(t-T)$$

as shown in Fig. 1(b). Hence

$$i\omega F(j\omega)=1-\exp(-j\omega T)$$

and

$$F(j\omega)=[1-\exp(-j\omega T)]/j\omega.$$

2) Find the Fourier transform of the pulse

$$f(t)=(V/T)tU(t)-(V/T)(t-T)U(t-T)-VU(t-T)$$

shown in Fig. 2(a). The derivative df/dt, shown in Fig. 2(b) has the form

$$df/dt=(V/T)U(t)-(V/T)U(t-T)-V\delta(t-T);$$

hence

$$\frac{d}{dt}[df/dt-V(t-T)]=(V/T)\delta(t)-\delta(t-T)$$

which corresponds to Fig. 1(b) (with a scale change). Hence

$$j\omega\mathfrak{F}[df/dt-V\delta(t-T)]=(V/T)[1-\exp(-j\omega T)]$$

and

$$\mathfrak{F}df/dt=(V/j\omega T)[1-\exp(-j\omega T)]-V\exp(-j\omega T)$$

so that

$$\mathfrak{F}f(t)=F(j\omega)=\frac{V}{T}\cdot\frac{1-\exp(-j\omega T)-j\omega T\exp(-j\omega T)}{(j\omega)^2}.$$

3) Find the Fourier transform of the sine pulse shown in Fig. 3(a):

$$f(t)=\sin(\omega_0 t)U(t)+\sin\omega_0(t-\pi/\omega_0)U(t-\pi/\omega_0).$$

For this pulse, the derivative [see Fig. 3(b)] is

$$df/dt=\omega_0\cos(\omega_0 t)U(t)+\omega_0\cos\omega_0(t-\pi/\omega_0)U(t-\pi/\omega_0)$$

and the second derivative [see Fig. 3(c)] is

$$d^2f/dt^2=-\omega_0^2\sin(\omega_0 t)U(t)-\omega_0^2\sin[\omega_0(t-\pi/\omega_0)U(t-\pi/\omega_0)]+\omega_0[\delta(t)+\delta(t-\pi/\omega_0)].$$

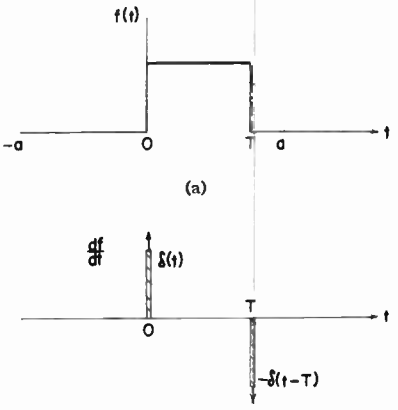

Fig. 1.

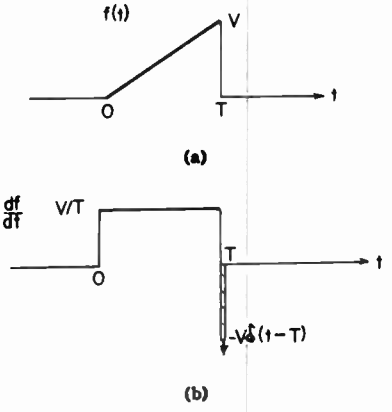

Fig. 2.

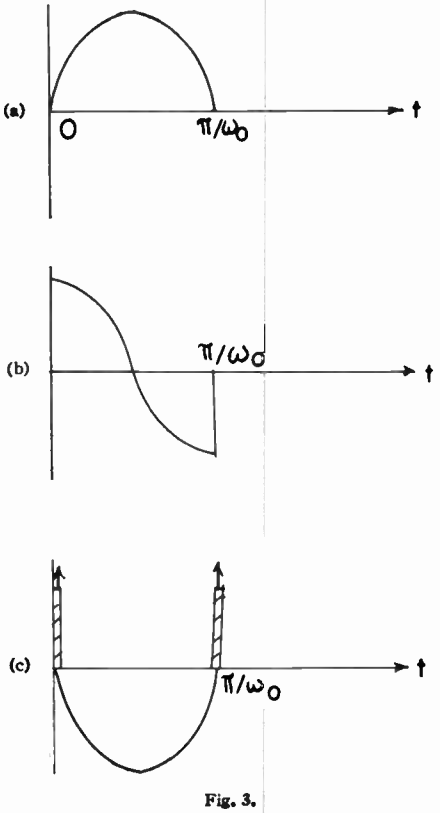

Fig. 3.

* Received by the IRE, March 22, 1957.
[1] J. F. Gibbons, Proc. IRE, vol. 45, p. 243; February, 1957.

Hence

$$\mathfrak{F}[\omega_0^2 f(t) + d^2f/dt^2] = \omega_0[1 + \exp(-j\omega\pi/\omega_0)],$$

so that

$$F(j\omega) = \frac{\omega_0[1 + \exp(-j\omega\pi/\omega_0)]}{\omega_0^2 + (j\omega)^2}.$$

EGON BRENNER
The City College of New York
New York 31, N. Y.

Letter from Dr. Fatehchand[2]

The simplified procedure for finding Fourier coefficients given by Gibbons[1] appears a most useful one. It may easily be extended to the transient case, when it is required to determine the frequency spectrum $g(\omega)$ of a time function $f(t)$. Here the Fourier integral relationships are necessary:

$$\left.\begin{aligned} g(\omega) &= \int_{-\infty}^{+\infty} f(t)e^{-i\omega t}dt \\ f(t) &= \frac{1}{2\pi}\int_{-\infty}^{+\infty} g(\omega)e^{i\omega t}d\omega \end{aligned}\right\}. \quad (1)$$

If $f^n(t)$ is the nth time derivative of $f(t)$ differentiating within the integral sign gives

$$\left.\begin{aligned} f^n(t) &= \frac{1}{2\pi}\int_{-\infty}^{+\infty} g(\omega)(i\omega)^n e^{i\omega t}d\omega \\ &= \frac{1}{2\pi}\int_{-\infty}^{+\infty} g_n(\omega)e^{i\omega t}d\omega \end{aligned}\right\}. \quad (2)$$

Therefore, if $g_n(\omega)$ is the frequency spectrum of $f^n(t)$, the frequency spectrum of $f(t)$ is given by

$$g_0(\omega) = g(\omega) = \frac{g_n(\omega)}{(i\omega)^n}. \quad (3)$$

We also have the result that if $\delta(t-T)$ is a δ function centered on $t=T$, and $h(t)$ is a function continuous in the neighborhood of $t=T$,

$$\int_{-\infty}^{+\infty} h(t)\delta(t-T)dt = h(T) \quad (4)$$

Hence the frequency spectrum of $\delta(t-T)$ is given by

$$\int_{-\infty}^{+\infty} e^{-i\omega t}\delta(t-T)dt = e^{-i\omega t}. \quad (5)$$

Thus, for example, if

$$f^n(t) = \delta(T-t), \quad g_n(\omega) = e^{-i\omega t}$$

and

$$g(\omega) = \frac{e^{-i\omega T}}{(i\omega)^n}.$$

As an illustration of the simplified method for deriving the frequency spectrum, consider a triangular pulse centered at $t=0$ (Fig. 1). The time function is differentiated until δ functions appear. In this case two differentiations are necessary (Figs. 2, 3). Then by (5):

$$g_2(\omega) = \frac{2}{T}e^{i\omega T/2} - \frac{4}{T} + \frac{2}{T}e^{-i\omega T/2}$$

[2] Received by the IRE, April 4, 1957.

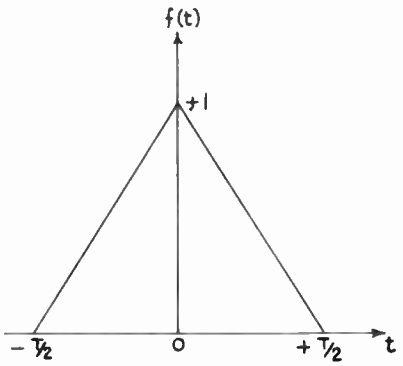

Fig. 1.

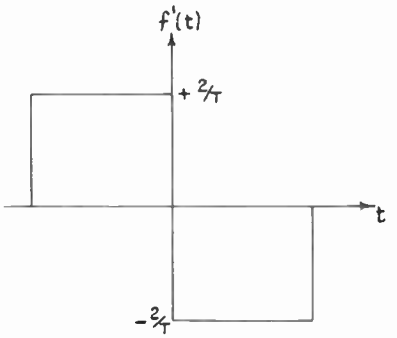

Fig. 2.

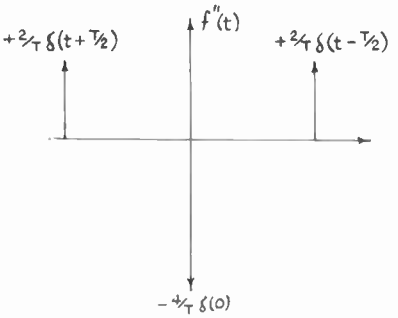

Fig. 3.

and

$$g(\omega) = \frac{4}{T}\cdot\frac{\cos\omega T/2 - 1}{(i\omega)^2}.$$

Here, the δ functions all appear at the same stage, but as Gibbons shows, this is not necessary for the solution. The method may obviously also be applied to the inverse problem, *i.e.*, to obtain the time function which corresponds to a given frequency spectrum.

RICHARD FATEHCHAND
British Broadcasting Corp.
London, England

Letter from Mr. Klotter[3]

Mr. Gibbons[1] has drawn attention to a very valuable tool for finding the Fourier coefficients of functions which exhibit discontinuities in the function itself or in any of its derivatives. Because his note does not quote any literature on the subject, it may be worth while to point out that the method has both a history and considerable ramifications, and to give some pertinent references.

After some early publications by Lalesco[4] and Abason[5] which failed to receive much attention, the first (and still best) presentation in English of the method for obtaining the Fourier coefficients from the discontinuities of a function's derivatives was given by Eagle.[6] In spite of its usefulness and the very adequate presentation by Eagle, the method seems to have gone generally unnoticed in the English-speaking countries. There seems to exist only a single reference to it and application of it by Jolley.[7]

On the European continent, however, the method caught on, was used extensively, and was developed further. Propagandists for and developers of the method were, in addition to the Roumanian school,[4,5,8] mainly Walther and his fellow workers in Germany. The first paper[9] of that group essentially reports on Eagle's work. Some items in that paper led to a discussion with Feinberg.[10,11] Later Zech[12] investigated some refinements and seemingly paradoxical results. A paper by Popesco[8] treats essentially the same items as Zech's paper.

The idea of finding the coefficients of expansions from the discontinuities of the function is not restricted to expansions into Fourier series but can be extended to other expansions; this was shown in a paper by Walther and Brinkmann.[13] Here the idea is extended to series progressing according to any orthogonal system with particular attention to expansions into spherical harmonics. The paper also gives an extensive list of references dealing with the development and applications of the method.

A fairly recent (English language) presentation of the essential features of the method has been given by Janssen.[14] In this paper, the method, furthermore, is extended and linked to the Fourier integrals, and it is shown how the frequency even of continuous functions may be found by suitably applying

[3] Received by the IRE, April 23, 1957.

[4] T. Lalesco, "Sur les fonctions polygonales périodiques," *Rev. Gén. Électr.*, vol. 5, pp. 43–45; January, 1919.
[5] E. Abason, "Asupra determinării pe cale grafică a armonicelor unei functiuni periodice (On finding the harmonics of a periodic function by graphical means)," *Gaz. mat.*, vol. 26, pp. 81–85, 105–108; 1920.
[6] A. Eagle, "Fourier's Theorem and Harmonic Analysis," Longman, Green and Co., London, England; 1925.
[7] L. B. W. Jolley, "Alternating Current Rectification and Allied Problems," Chapman and Hall, London, England, 3rd ed.; 1928.
[8] A. T. Popesco, "Sur l'application de la méthode des discontinuités a l'analyse harmonique des fonctions sinusoidales," *Bull. Math. Phys.*, (Ecole Polytech, Bucharest), vol. 9, p. 83; 1939.
[9] G. Koehler and A. Walther, "Fouriersche Analyse von Funktionen mit Sprüngen Ecken und ähnlichen Besonderheiten," *Arch. Elektrotech.*, vol. 25, pp. 747–758; October, 1931.
[10] R. Feinberg, "Bemerkung zu der Arbeit von G. Koehler und A. Walther über die Fouriersche Analyse von Funktionen mit Sprüngen, Ecken und ähnlichen Besonderheiten," *Arch. Elektrotech.*, vol. 27, pp. 15–19; January, 1933.
[11] A. Walther, "Stellungnahme zu der Bemerkung von Herrn Feinberg und geschichtliche Erganzung zur Fourierschen Analyse von Funktionen mit Sprüngen, Ecken und ähnlichen Besonderheiten," *Arch. Elektrotech.*, vol. 27, pp. 19–20; January, 1933.
[12] T. Zech, "Über das Sprungstellenverfahren zur harmonischen Analyse," *Arch. Elektrotech.*, vol. 36, pp. 322–328; May, 1942.
[13] A. Walther and K. Brinkmann, "Zum sprungstellen-verfahren, insbesondere für die entwicklung nach kugelfunktionen," *Ing.-Arch.*, vol. 13, pp. 1–8; January, 1942.
[14] J. M. L. Janssen, "The method of discontinuities in Fourier analysis," *Phillips Res. Rep.*, vol. 5, pp. 435–460; December, 1950.

the ideas of the "Method of Discontinuities."

The writer wishes to close with an appeal to the textbook authors in this country to take notice of this extremely useful method; especially because the ideas underlying the method are intimately related to intrinsic properties of the expansions which are treated in the textbooks anyway.

KARL KLOTTER
Stanford University
Stanford, Calif.

Unit-Distance Number-Representation Systems, a Generalization of the Gray Code*

A digit-distance function is any distance function, ρ, satisfying the metric space axioms, and defined on a finite set of digits. For binary digits, $\rho=0$ when the digits are the same and 1 when they are different. If d_1 and d_2 denote the numerical value of arbitrary digits, then for any base, β, one distance function is

$$\rho_1(d_1, d_2) = |d_1 - d_2|. \quad (1)$$

Another one is

$$\rho_2(d_1, d_2) = \min(|d_1 - d_2|, |d_1 - d_2 + \beta|, |d_2 - d_1 + \beta|). \quad (2)$$

If $\beta=2$, (1) and (2) reduce to the same function. This is false for $\beta>2$, since the maximum value of ρ in (1) is $\beta-1$, whereas in (2) it is the largest integer not greater than $\beta/2$. Digit-distance function (1) corresponds to placing the digits, in natural order, opposite the teeth of a rack, and measuring the distance between digits along the pitch line of the rack. Function (2) corresponds to placing the digits in natural order, opposite the teeth of a gear, and measuring the distance along the pitch circle of the gear.

Given a digit-distance function, we define an expression-distance function (syntactical distance) between two digit strings, e_1 and e_2, of length n, as the sum of the n digit-distance functions for corresponding digit pairs, d_{1i}, d_{2i}.

$$\rho_j^{(n)}(e_1, e_2) = \sum_{i=n}^{n} \rho_j(d_{1i}, d_{2i}) \quad (3)$$

where $j=1$ or $j=2$, or j may represent some other digit-distance function. This corresponds to metrizing the Cartesian product of the n individual metric spaces. It is known that a function of a finite number of factor metrics which vanishes if and only if all the factor metrics vanish, and which is subadditive and suitably isotone, is a product metric. The above is perhaps the simplest function having these properties.

We now assign some (or all) of these β^n-distinct n-digit strings as names of integers. At most, there will be β^n integers, and if all strings are used, there will be exactly that many. For example, let $n=2$, $\beta=3$, and the integers be 0 to 8 inclusive:

integer, i	string of n digits $e=\widehat{d_1 d_0}$
0	'00'
1	'01'
2	'02'
3	'12'
4	'10'
5	'11'
6	'21'
7	'22'
8	'20'.

The integers have a natural distance function:

$$p(i_1, i_2) = |i_1 - i_2|.$$

This integer distance function also induces a (semantical) expression-distance function

$$P(e_1, e_2) = p(i_1, i_2) = |i_1 - i_2|, \quad (4)$$

where i_j is the integer whose name (string of n digits) is e_j, $j=1, 2$.

A unit-distance code is one for which $P(e_1, e_2)=1 \Rightarrow \rho(e_1, e_2)=1$. The arrow is unilateral except in the degenerate case $\beta=2$.

Thus the names of two consecutive integers are at unit (syntactical) distance from each other, which for digit-distance functions (1) and (2) means that they differ only in a single digit and that those single digits are at unit digit distance from each other.

The Gray code ($\beta=2$) is the most familiar example of a unit-distance code. The writer, in a paper delivered orally at a meeting of the Association for Computing Machinery in 1951, gave examples of codes for $\beta>2$ based on digit-distance functions (1) and (2), calling the first type "reflecting" and the second type "progressive" and "retrogressive."

This terminology is based on the fact that in reflecting codes the digit cycle runs through the digits from smallest to largest, and then reflects and runs back down again, yielding a digit cycle of length twice the base. In the progressive code, the digit cycle is β times the base, and the digits increase to maximum, then dwell on the largest digit while another column changes, then they start with 0 again and progress (increase) until the next-to-the-largest digit, where another dwell occurs. The dwell precesses down to zero, at which point the digit cycle is complete. This system might be more natural (than the reflecting system) to mechanize on physical code wheels, since the wheels would always rotate in the same direction. A brief example is given above for $n=2$, $\beta=3$. One complete cycle of length 9 is shown for the least significant digit (d_0). The next digit (d_1) has a period of 27.

The retrogressive system is similar, except the digit cycle runs in the opposite direction and the dwell precesses through successively larger digits toward zero. It should be emphasized that all these codes reduce to the Gray code for $\beta=2$.

Since the generalized reflected code has been already discussed,[1] it does not seem necessary here to give any conversion rules for this code. The following conversion rules are for the progressive and retrogressive codes. Let d_i, Δ_i and δ_i be the ith digits of the name of a number, expressed in the progressive, retrogressive and ordinary number system, respectively, all to the base β. The 0th place or column contains the least significant, or units, digit.

Then

$$d_i = \delta_i \ominus_\beta \delta_{i+1},$$
$$\Delta_i = \delta_{i+1} \ominus_\beta \delta_i,$$

where $\ominus_\beta$ represents subtraction modulo β. In order to convert into normal code, we use the following equations:

$$\delta_i = \sum_{l=i}^{k}{}_{(\beta)}\, d_l,$$

$$\delta_i = \sum_{l=i}^{k}{}_{(\beta)}\, (-\Delta_l),$$

where k is any digit position such that all digits further to the left would be zero (if n were larger), and the addition is modulo β. The subscript (β) is thus a homomorphism operator mapping the sum onto the residue-class ring representatives 0 to $\beta-1$.

GEORGE W. PATTERSON
The Moore School of Elec. Eng.
University of Pennsylvania
Philadelphia, Pa.

On the Order of the Differential Equation Describing an Electrical Network*

The question of determining the order of the differential equation describing an electrical network without writing down and expanding the network determinant is quite basic and must have been answered correctly by many, even in the early years of network analysis. Yet, a search through literature failed to provide the writer with a full answer to the problem. Hence this note, in which the results of an investigation are presented, rather than the complete discussion.

The order of the differential equation describing an electrical network is equal to the number of energy-storing elements, *i.e.*, inductances and capacitances, less the number of certain independent algebraic equations which can be written for the network. One type of the equations relates currents through inductances, a second relates currents through capacitances, a third relates voltages across inductances, and a fourth relates voltages across capacitances. Such algebraic equations, when dealing with the currents, will be referred to as current-interdependence relations, and when dealing with the voltages, as voltage-interdependence relations.

Current-interdependence relations stem from Kirchhoff's first law, the law of currents, and arise when all the currents flowing between two parts of a network pass through

* Received by the IRE, April 11, 1957. This communication was prepared under the sponsorship of the Dept. of the Army, U. S. Army Signal Corps. Eng. Labs., Ft. Monmouth, N. J., Contract No. DA36-039 SC-72344.

[1] For example, I. Flores, "Reflected number systems," IRE TRANS., vol. EC-5, pp. 79–82; June, 1956.

* Received by the IRE, March 20, 1957.

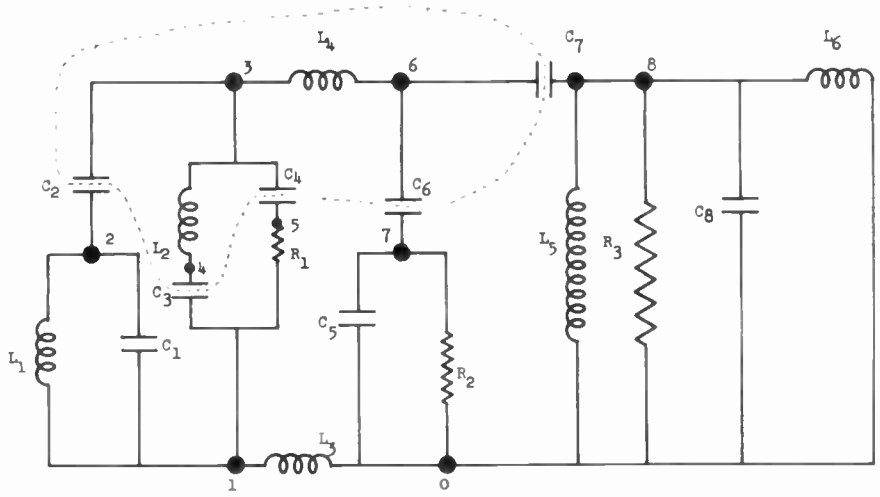

Fig. 1—The positive direction of currents and voltage-drops is chosen upwards and from left to right.

inductances (capacitances). In other words, a current-interdependence relation arises whenever a number of inductances (a number of capacitances) form a cut-set.[1] As a simple case of such an interdependence, consider two inductances (two capacitances) in series. For other examples, consider the network of Fig. 1. Examination of this network will show that the capacitances C_2, C_3, C_4, C_6, and C_7 form a cut-set, since they isolate nodes nos. 3, 4, and 6, from the rest of the network. This is indicated in Fig. 1 by a dotted line drawn through these capacitances. Thus, by Kirchhoff's law of currents, as applied to an isolated part of the network rather than to a single node, we have

$$I_{C_2} + I_{C_3} + I_{C_4} + I_{C_6} - I_{C_7} = 0. \quad (1)$$

Further examination of the network will show that the inductances L_3 and L_4 form a cut-set, and therefore by Kirchhoff's law of currents

$$I_{L_3} + I_{L_4} = 0. \quad (2)$$

We thus have two current-interdependence relations in the network.

Voltage-interdependence relations stem from Kirchhoff's second law, the law of voltages, and arise when a closed loop exists which consists of inductances only (capacitances only). As a simple case of such an interdependence relation, consider two inductances (two capacitances) in parallel. This is the case with the inductances L_5 and L_6 in Fig. 1. Thus, we have by Kirchhoff's law of voltages

$$V_{L_5} + V_{L_6} = 0. \quad (3)$$

A capacitance loop is created in this network by capacitances C_5, C_6, C_7, and C_8. By Kirchhoff's law of voltages, we have

$$V_{C_5} + V_{C_6} + V_{C_7} - V_{C_8} = 0. \quad (4)$$

Thus, there are two voltage-interdependence relations in the network.

The order of the differential equation describing the network of Fig. 1 will be 14 (the number of energy-storing elements), minus 4 (number of independent interdependence relations), or 10.

In most cases, as in the above example, the order of the differential equation can be obtained by rather simple inspection. For large and complicated networks, the question of counting all the independent interdependence relations is not a simple one. Care should be taken that dependent interdependence relations, *i.e.*, interdependence relations which are a linear combination of interdependence relations already counted, are not included. The procedure outlined herewith enables one to count quite easily the number of independent interdependence relations, even for large and complicated networks. The procedure applies to planar and nonplanar networks, including networks which cannot be mapped on a sphere.

Redraw the network, short-circuiting all the voltage sources and removing all the current sources. Disregard any mutual inductive coupling. Eliminate the ideal transformers by connecting the output from the secondary windings in parallel to the input of the primary. A network redrawn in this way will be referred to as the simplified network. Then follow these steps:

1) Count the number of the energy-storing elements.
2) Obtain the number of current-interdependence relations for capacitances by redrawing the simplified network, replacing any element other than a capacitance by a short-circuit. Count the total number of nodes.[2] If n_t is the total number of nodes, then $n=n_t-1$ will be the number of independent node-pairs,[3] which is equal to the number of current-interdependence relations for capacitances in the original network.
3) Obtain the number of independent current-interdependence relations for inductances by following step 2) and reading inductance, inductances, for capacitance, capacitances.
4) Obtain the number of independent voltage-interdependence relations for capacitances by removing from the simplified network all elements other than capacitances.[4] Let b be the number of elements, n the number of nodes, and s the number of separate parts in this final network. The number of independent loops of this final network is given by $l=b-n+s$, the number of independent voltage-interdependence relations for capacitances of the original network is equal to l.
5) Obtain the number of independent voltage-interdependence relations for inductances by following step 4) and reading inductances for capacitances.
6) Subtract the numbers obtained in steps 2)–5) from the number obtained in step 1).

The order of the differential equation determines the number of the independent voltage and current initial conditions that we are free to specify, and which determine all the currents and voltages in the network for $t>0$. Moreover, from a mathematical standpoint we can specify a number of "petrified" conditions which are superimposed on the solution and which remain constant unless forced to change by appropriate generators. These are dc currents circulating in loops of inductances, infinite frequency currents circulating in loops of capacitances, infinite frequency voltage-drops between parts of network separated by inductance cut-sets, and dc voltage-drops between parts of a network separated by capacitance cut-sets. Of these four cases, it seems that certain physical significance can be attached only to the last case.

Joseph Otterman
Eng. Res. Inst.
University of Michigan
Ann Arbor, Mich.

[1] For a definition of a cut-set, see E. A. Guillemin, "Introductory Circuit Theory," John Wiley and Sons, New York, N. Y., p. 21; 1953.

[2] We define a node as a junction of two or more elements, or a junction of two ends of the same element, or an isolated end of a single element.

[3] The discussion here is limited to the case when the simplified network consists of a single separate part. When this is not the case, determine the order of the differential equations separately for each separate part and add the results.

[4] The removal from the resulting network of all the capacitances that do not form part of any loop will simplify the count of elements and nodes but does not affect the answer.

Contributors

David J. Bates (S'55) was born in Portland, Ore., on October 22, 1928. He received the B.S. and M.S. degrees in physics from Oregon State College, Corvallis, Ore., in 1951 and 1953, respectively. He will receive the Ph.D. degree in applied physics from Stanford University, Stanford, Calif., in 1957.

D. J. Bates

From September, 1952 to May, 1957, Mr. Bates was a student at Stanford University and held appointments as research assistant and research associate at the Stanford Microwave Laboratory. In May, 1957, he joined the technical staff of the Electron Tube Laboratory at Hughes Aircraft Company, Los Angeles, Calif., where he is engaged in research in microwave electronics.

Mr. Bates is a member of Pi Mu Epsilon, Sigmi Pi Sigma, Sigma Xi, and the American Physical Society.

❖

Frank J. Bloom (A'49) was born on March 3, 1922 in New York. He received the B.E.E. and M.E.E. degrees from New York University in 1947 and 1948, respectively. He remained at New York University, first as a graduate assistant in the Electrical Engineering Department, and then as a research assistant. From 1948 to 1951, he was an instructor in electrical engineering, then he was appointed research associate. He was later designated as project director of the transmission measuring set project, director of the rf voltage measuring techniques project, and director of the digital communication project. In June, 1956, he was appointed technical coordinator for the electrical engineering research group.

F. J. Bloom

Mr. Bloom's technical experience has included fundamental research in memory devices, prosthetic devices, and, particularly, in advanced analysis concerned with accurate measurement problems in noise, cross-talk, voltage, and power measurements.

He has also conducted research in electronic pulse techniques, information theory, and digital communication systems. He is in charge of the Electrical Engineering Analog Computer Laboratory and is currently teaching graduate courses in analog and digital computers.

Mr. Bloom is a member of Sigma Xi and Eta Kappa Nu.

S. S. L. Chang (SM'53) was born in Peiping, China, in 1920. He received the M.S. in physics from Tsinghua University in China in 1944 and the Ph.D. in electrical engineering from Purdue University, Lafayette, Ind., in 1947. From 1947 to 1948, he taught at Purdue University.

S. S. L. Chang

He has been associated with Robbins and Myers, Inc., Springfield, Ohio since 1946. He joined the faculty of New York University in 1952 and is now associate professor of electrical engineering.

Dr. Chang is a member of the AIEE, ASEE, American Physical Society, Eta Kappa Nu, and Sigma Xi.

❖

H. N. Dawirs (S'39–A'52) was born in Colorado, on July 10, 1920. He received the B.S. in electrical engineering in 1942 from Colorado State College of Agriculture and Mechanic Arts, and the M.S. in mathematics from Ohio State University in 1952.

H. N. Dawirs

From 1942 to 1946 Mr. Dawirs worked in the engineering departments of a number of Westinghouse plants. From 1946 until 1948 he worked in the research department of the Curtiss Wright Corp., Columbus plant; and since 1948 he has been with the Antenna Laboratory of the Ohio State University Research Foundation, in Columbus, Ohio.

He is a member of Pi Mu Epsilon, Sigma Xi, and Eta Kappa Nu.

❖

Edward L. Ginzton (S'30–A'40–SM'46–F'51) was born in Russia on December 27, 1915, and came to the United States in 1929. He received the B.S. degree in electrical engineering from the University of California in 1936, and the M.S. degree in 1937. He received the E.E. degree in 1938, and the Ph.D. degree in 1940 from Stanford University, Stanford, Calif.

E. L. Ginzton

Dr. Ginzton is now a professor of applied physics and electrical engineering at Stanford University, and Director of the Microwave Laboratory there.

He has been a member of the Board of Directors of Varian Associates, Inc., Palo Alto, Calif., since that company's organization in 1948, and was appointed an assistant to the Chairman of the Board of Directors in 1957.

Dr. Ginzton is a member of Sigma Xi, Tau Beta Pi, and Eta Kappa Nu.

❖

Charles R. Grant (A'49–M'55) was born in Barrington, R. I., on November 24, 1908. He attended Northeastern University from 1940 to 1942 and received the B.E.E. degree from George Washington University in 1947.

C. R. Grant

Mr. Grant joined the Naval Research Laboratory in 1942 where he has been engaged in research in radar displays and airborne navigation systems. At the present time he is a member of the Radio Astronomy Branch of the Naval Research Laboratory.

❖

Bernard Harris (S'48–A'52) was born in New York City on October 13, 1927. He received the B.E.E. degree from Cooper Union in 1949 and the M.S. degree from Columbia University in 1951. He is a candidate for the D.Eng. Sc. degree at Columbia University.

B. Harris

From 1946 to 1947, Mr. Harris served in the United States Army as a radio instructor. He was a graduate assistant in the Electrical Engineering Department at Columbia University from 1949 to 1951. In 1951, he joined the staff of the New York Industry Service Laboratory, RCA Laboratory Division, as a television development engineer concerned with the design of uhf tuners and the application of transistors to broadcast band and television receivers. In 1954, Mr. Harris joined the research staff of the Electrical Engineering Department of New York University and contributed to a project concerned with the precision measurement of rf voltages. His present work is primarily concerned with the applications of information theory.

Mr. Harris is a member of Tau Beta Pi, Eta Kappa Nu, Sigma Xi, and is a registered Professional Engineer in New York State.

Arthur Hauptschein (S'47–A'50–M'55) was born on October 31, 1925 in New York, N. Y. He received the B.S. degree in electrical engineering from Pennsylvania State University, University Park, Pa., in June, 1947. In June, 1948, he received the M.S. degree in electrical engineering and and in February, 1957 the degree of Professional Electrical Engineer, both from Columbia University.

A. Hauptschein

From 1948 to 1952, he was employed by Airborne Instruments Laboratory, Mineola, N. Y. as a project engineer in the Antenna and Special Devices Section, and worked on the design of communication, navigation, and homing antennas for high-speed aircraft and helicopters.

Since 1952, Mr. Hauptschein has been associated with the Research Division of New York University, Department of Electrical Engineering, in the capacity of engineering scientist and instructor. At New York University he has been concerned with the design of a microwave impedance measuring bridge and is presently engaged in an evaluation study for communication systems. This latter work has resulted in the presentation and publication of several papers, in the fields of operations research and information theory, concerning the concept of merit criteria for the evaluation of communication systems.

Mr. Hauptschein is a member of Tau Beta Pi, Eta Kappa Nu, Pi Mu Epsilon, and Sigma Xi.

❖

Glenn L. Keister was born in Des Moines, Iowa, on June 2, 1924. He received the B.S., M.S., and Ph.D. degrees in physics from the University of Washington, Seattle, Wash., in 1949, 1951, and 1953. While a graduate student, he worked as a laboratory assistant at the University of Washington cyclotron and beta-ray spectrometer laboratories.

G. L. Keister

In October, 1953, Dr. Keister joined the Boeing Airplane Company and for the last two years has been investigating semiconductor device circuits and their susceptibility to various environments.

Dr. Keister is a member of the American Physical Society and Sigma Xi.

❖

Kenneth C. Morgan was born in New York, N. Y. in 1924. He received the M.E. degree from Stevens Institute of Technology in Hoboken, N. J., in 1944. After an interval on duty in the Navy Reserve, he returned to Stevens from 1947 to 1949 as an instructor in mathematics, physics, and mechanics. From 1949 to 1951, he studied graduate physics at Columbia University.

K. C. Morgan

He has been associated, since 1951, with the Research Division of New York University, Department of Electrical Engineering, in the capacity of associate research scientist and instructor. During that time, he designed major portions of an alternating voltage standard and an instantaneous signal analyzer, and for the past two years he has been concerned with the problem of optimizing and evaluating digital communications systems.

Mr. Morgan is a member of Sigma Xi.

❖

Edward G. Nielsen (S'49–A'52) was born in St. Paul, Minn., on January 11, 1927. In 1950, he received the B.S. degree in electrical engineering from the University of Minnesota, where he graduated with high distinction. Working under a Minneapolis-Honeywell Co. fellowship, he received the M.S. degree in electrical engineering from the same institution in 1952.

E. G. Nielsen

From 1951 to 1953 Mr. Nielsen was employed at the Electron Tube Research Laboratory of the University of Minnesota, electrical engineering department. Here he worked on the problem of flicker noise in vacuum tubes. Since 1953, he has been a member of the technical staff of Bell Telephone Laboratories where he has been working on transistor circuits.

Mr. Nielsen is a member of Eta Kappa Nu, Tau Beta Pi, and Gamma Alpha.

❖

Robert H. Rediker (A'53) was born in Brooklyn, N. Y. on June 7, 1924. He received the B.S. degree in electrical engineering in 1947 and the Ph.D. degree in physics in 1950, from the Massachusetts Institute of Technology, Cambridge, Mass. During 1950–1951, Dr. Rediker was a research associate in cosmic rays in the Physics Department of M.I.T. In April 1951, he became a staff member of the Lincoln Laboratory, M.I.T., Lexington, Mass.

R. H. Rediker

In October, 1952, he joined the Physics Department, Indiana University, Bloomington, Ind., returning in June, 1953, to the transistor device section of the Lincoln Laboratory.

Dr. Rediker is a member of the A.P.S. and Sigma Xi.

❖

David E. Sawyer (M'55) was born in Boston, Mass. on February 6, 1927. He served in the U. S. Navy from 1945 to 1946 and later from 1950 to 1952. He received the A.B. degree from Clark University, Worcester, Mass. in 1953 and the M.S. degree in physics from the University of Illinois, Urbana, Ill. in 1955. Since June, 1955, he has been a member of the device section of the solid state group of Lincoln Laboratory, Massachusetts Institute of Technology, Lexington, Mass.

D. E. Sawyer

❖

Harold V. Stewart, Jr. was born on June 12, 1923 at Easton, Pa. He received the Bachelor of Science degree in physics at Muhlenberg College, Allentown, Pa., in June, 1943. After serving three years in the Navy as Fire Control Officer aboard the USS Massachusetts, he returned to graduate school at Syracuse University, Syracuse, N. Y., and obtained the M.A. degree in physics in June, 1948.

H. V. Stewart

The following three years Mr. Stewart taught physics at Utica College, Utica, N. Y. In July of 1951, he joined the Boeing Airplane Company as a Research Engineer.

He is a member of Sigma Phi Sigma and Sigma Xi.

❖

Benjamin S. Yaplee (S'46—A'50-M'55) was born in Seattle, Washington on August 25, 1923. He received the B.S. degree in electrical engineering from the University of Washington in 1947.

B. S. Yaplee

Mr. Yaplee joined the Naval Research Laboratory in 1949 and was engaged in research on radio propagation with the Wave Propagation Branch from 1949 to July 1, 1954. He then joined the Radio Astronomy Branch where he has been engaged in research on navigation problems and more recently in centimeter wave radio astronomy.

IRE News and Radio Notes

Calendar of Coming Events and Deadline for Papers*

International Symposium on Physical Problems of Color Television, Paris, France, July 2–6

Automatic Control Conf., San Francisco, Calif., Aug. 19–20

WESCON, Fairmont Hotel and Cow Palace, San Francisco, Calif., Aug. 20–23

URSI General Assembly, Boulder, Colo., Aug. 22–Sept. 5

Special Technical Conference on Magnetic Amplifiers, Penn Sheraton Hotel, Pittsburgh, Pa., Sept. 4–6 (DL*: June 11, D. Feldman, Bell Tel. Labs., Whippany, N. J.)

Industrial Electronics Symp., Morrison Hotel, Chicago, Ill., Sept. 24–25

Nat'l Electronics Conference, Hotel Sherman, Chicago, Ill., Oct. 7–9 (DL*: June 1, V. H. Disney, Armour Res. Found., Chicago, Ill.)

IRE Canadian Convention, Exhibition Park, Toronto, Can., Oct. 16–18

East Coast Aero. & Nav. Conf., Lord Baltimore Hotel & 7th Reg. Armory, Balt., Md., Oct. 28–30

PGED Meeting, Shoreham Hotel, Wash., D. C., Oct. 31–Nov. 1 (DL*: Aug. 1, W. M. Webster, RCA, Somerville, N. J.)

PGNS Annual Meeting, Henry Hudson Hotel, New York City, Oct. 31–Nov. 1 (DL*: June 30, W. A. Higinbotham, Brookhaven Nat'l Labs., Upton, N. Y.)

Annual Symp. on Aero Commun., Hotel Utica, Utica, N. Y., Nov. 4–6

Radio Fall Meeting, King Edward Hotel, Toronto, Can., Nov. 11–13

PGI Conference, Atlanta-Biltmore Hotel, Atlanta, Ga., Nov. 11–13 (DL*: July 15, R. L. Whittle, Fed. Telecommun. Labs., 1389 Peachtree St., N.E., Atlanta 9, Ga.

Mid-America Electronics Convention, Kan. City Mun. Audit., Kan. City, Mo., Nov. 13–14.

New England Radio-Elec. Mtg., Mechanics' Bldg., Boston, Mass., Nov. 15–16

Conf. on Magnetism, Sheraton-Park Hotel, Wash., D. C., Nov. 18–20 (DL*: Aug. 15, L. R. Maxwell, U. S. Nav. Ordnance Lab., White Oak, Silver Spring, Md.)

Elec. Computer Exhibition, Olympia, London, England, Nov. 28–Dec. 4

PGVC Conf., Hotel Statler, Wash., D. C., Dec. 4–5 (DL*: July 1, G. E. Woodside Jr., 1145 19th St., N.W., Wash., D. C.

Eastern Joint Computer Conf., Park-Sheraton Hotel, Wash., D. C., Dec. 8–11

Nat'l Symp. on Reliability & Quality Control, Statler Hotel, Wash., D. C., Jan. 6–8, 1958

IRE Nat'l Convention, N. Y. Coliseum and Waldorf-Astoria Hotel, New York City, Mar. 24–27 (DL* Nov. 1, G. L. Haller, IRE Headquarters, New York City.)

* DL = Deadline for submitting abstracts

1958 Officers Are Nominated

At its May 15, 1957 meeting, the IRE Board of Directors received the recommendations of the Nominations Committee and the reports of the Regional Committees for officers and directors for 1958. They are:

President, 1958—D. G. Fink

Vice-President, 1958—C. E. Granqvist

Director-at-Large, 1958–1960 (two to be elected)—George H. Brown, Gordon S. Brown, W. H. Doherty, G. K. Teal

Regional Directors, 1958–1959 (one to be elected in each Region)

Region 1—R. L. McFarlan

Region 3—V. S. Carson, Joseph Weil

Region 5—R. E. Moe, E. H. Schulz

Region 7—G. A. Fowler, R. A. Kirkman

According to Article VI, Section 1 of the IRE Constitution, nominations by petition for any of the above offices may be made by letter to the Board of Directors, giving name of proposed candidate and office for which it is desired he be nominated. For acceptance a letter of petition must reach the executive office before noon on August 14, 1957, and shall be signed by at least one hundred voting members qualified to vote for the office of the candidate nominated.

Two-Way Radio Communication Attempt Made This Month

The first in a series of attempts to establish two-way radio communication by bouncing radio signals off man-made clouds of ionized gas will be made this month in a joint project of the U. S. Air Force and the country's amateur radio operators.

In March, 1956, an Aerobee rocket fired from the Holloman Air Force Base released a cloud of ionized gas detectable by radar. However, against the possibility that the radar reflection was a coincidence, "Operation Smoke-Puff" is going into effect.

Tests are planned for morning twilight, noon, evening twilight, and possibly night, in durations of ten to twenty minutes. Amateur frequency bands to be employed in these tests are those between 14 and 148 megacycles. Participants will receive radio warnings of intended rocket firings, but because of the earth's curvature the possibility of a signal bounce is limited to amateurs residing within a radius of seven hundred miles around Alamogordo, New Mexico.

For further information persons should contact the American Radio Relay League at West Hartford, Conn.

Seven PG Chapters Join IRE

The following Chapters were approved by the IRE Executive Committee at its meeting on May 14th: PG on Broadcast Transmission Systems, Omaha-Lincoln Section; PG on Circuit Theory, Tucson Section; PGs on Component Parts, Baltimore and Chicago Sections; PG on Electronic Components, Twin Cities Section; PG on Military Electronics, Central Florida Section; and PG on Reliability & Quality Control, Philadelphia Section.

November 1 is Deadline for 1958 IRE National Convention Papers

The 1958 IRE National Convention will be held at the Waldorf-Astoria Hotel and New York Coliseum, New York City, March 24–27, 1958. Prospective authors are requested to submit all of the following by November 1, 1957: 1) 100-word abstract *in triplicate*, title of paper, name and address; 2) 500-word summary *in triplicate*, title of paper, name and address; and an indication of the technical field in which the paper falls. The technical fields which may be covered are: Aeronautical & Navigational Electronics, Antennas & Propagation, Audio Automatic Control, Broadcast & Television Receivers, Broadcast Transmission Systems, Circuit Theory, Communications Systems, Component Parts, Education, Electron Devices, Electronic Computers, Engineering Management, Engineering Writing and Speech, Industrial Electronics, Information Theory, Instrumentation, Medical Electronics, Microwave Theory & Techniques, Military Electronics, Nuclear Science, Production Techniques, Reliability & Quality Control, Telemetry & Remote Control, Ultrasonics Engineering, and Vehicular Communications.

Original papers only will be considered, not published nor presented prior to the 1958 IRE National Convention; any necessary military or company clearance of paper granted prior to submittal.

Address all material to: G. L. Haller, Chairman, 1958 Technical Program Committee, The Institute of Radio Engineers, 1 East 79 St., New York 21, N. Y.

Los Angeles Section Met With Students and Military Men

The Los Angeles IRE Section recently held an important meeting, which was arranged by the Section and the Professional Group on Military Electronics and consisted of a military panel discussion on government technical manpower. Panelists were: Brig. Gen. O. J. Ritland, Capt. V. H. Soucek, Col. J. E. Johnston, S. R. Brentnall, C. B. Thornton, H. L. Hoffman, and W. F. Joyce.

The Section played host to 207 IRE Student Members from five universities at this meeting. Earlier in the afternoon seven Professional Groups contributed speakers and exhibits. Byron Coles, Section Student Relations Chairman, Jon Myer, Program Chairman, and J. K. Gossland of PGMIL were on the committee in charge of this meeting.

At the speakers' luncheon at the Annual Conference on Electronics in Industry, sponsored jointly by the PGIE and the Armour Research Foundation, were (left to right): E. A. Keller, Panellit Corp.; R. C. MacMillen, E. I. du Pont de Nemours & Co., Inc.; W. H. Howe, Foxboro Co.; R. C. Johnson, Barber-Coleman Co.; Eugene Mittelmann, Conference Chairman; E. H. Browning, Westinghouse Electric Corp.; and Harold Garbarino, Armour Research Foundation.

IRE Executive Committee Takes Action on Subsections

On April 10, the IRE Executive Committee approved the formation of the Northern Vermont Subsection of the Boston Section. On the following day, the status of the Shreveport Subsection of the Dallas Section was changed to that of a full Section.

Transistor-Circuits Volume to be Published by IRE-PGCT

The *Active-Networks* issue of the IRE Transactions in Circuit Theory to be published in September, 1957 will be the largest issue ever offered to its membership by the IRE Professional Group on Circuit Theory. This issue will contain over a dozen papers by authorities on various aspects of active networks. In addition, the issue will contain many of the papers given at the recent Conference on Transistor and Solid-State Circuits held in Philadelphia in February of this year. It will provide in carefully organized and edited form approximately 200 pages of the most up-to-date and comprehensive coverage of current developments in the important field of active networks.

Although comparable to a text book in size and content, it is being offered to IRE Members and to libraries at the low cost of $3.75 per copy, and to non-members at $7.50 per copy. Alternatively, IRE Members may receive this issue *plus* the other three quarterly issues of Transactions by joining the PGCT for only $3.

To insure that an adequate number of copies are printed, interested parties should place their orders immediately by sending their checks to IRE Headquarters, 1 East 79 Street, New York 21, N. Y.

Technical Societies Form New Control Systems Council

Representatives of the IRE, American Society of Mechanical Engineers, American Institute of Electrical Engineers, Instrument Society of America, and American Institute of Chemical Engineers met to form a joint council of American technical societies which conduct engineering and scientific activities in the broad field of control systems engineering. The delegates framed two initial objectives: cooperation in the organization and operation of a proposed international federation of control systems engineering, and coordination of the professional activities, conferences, symposia, and joint control meetings of American technical societies.

Rufus Oldenburger, Chairman of the Instruments & Regulators Division of the American Society of Mechanical Engineers, was elected chairman. He represented the newly-formed council at a meeting in Dusseldorf, Germany, where final plans were made for the first formal meeting of the proposed international federation of control. Dr. Oldenburger is a professor of mechanical engineering at Purdue University.

Other officers elected were: Vice-Chairman, H. E. Chestnut, Chairman of the AIEE's 1958 Feedback Control Systems Committee; and Secretary-Treasurer, W. E. Vannah, Technical Program Chairman of ASME's 1958 Instruments and Regulators Division Conference.

Additional members of the council are John Lozier, IRE, Bell Telephone Laboratories; E. M. Grabbe, IRE, Ramo-Wooldridge Corporation; Gerhart Heumann, AIEE, General Electric Company; Joel Hougen, AIChE, Monsanto Chemical Corporation; N. H. Ceaglske, AIChE, University of Minnesota; Robert Jeffries, ISA, Daystrom, Inc.; and John Johnston, JR., ISA, E. I. du Pont de Nemours & Co.

Automatic Control Conference Has Four Technical Sessions

The Automatic Control Conference will be held in San Francisco, Calif., August 19–20. The first day's program will consist of a nonlinear control symposium sponsored by the Professional Group on Automatic Control in which the AIEE and ASME will participate. The morning session will consist of a discussion of practical applications of nonlinear control. A panel discussion on the basic problems of nonlinear control will follow in the afternoon.

WESCON will sponsor the second day's program in which the Professional Group on Automatic Control will take part. The morning session will be on sampled data systems, while the afternoon session will be devoted to a general analysis of automatic control.

General chairman of this conference is E. M. Grabbe of Ramo-Wooldridge Corp. T. M. Stout, also of Ramo-Wooldridge, is technical program chairman, H. S. Robinson of Westinghouse is arrangements chairman, and J. M. Jones of Hughes Aircraft Co. is in charge of publicity.

Award winners of the Professional Group on Audio for 1956 were announced recently. H. E. Roys (*left*) won the IRE-PGA Achievement Award "for outstanding contributions to audio technology published in IRE publications over a long period of years." The IRE-PGA Senior Award went to J. R. Macdonald (*center*) for his paper entitled, "A Multi-Loop, Self-Balancing Power Amplifier," which appeared in the January–February, 1956 issue of the Transactions on Audio. H. H. Kajihara (*right*) also received an award for his paper entitled, "Miniaturized Audio Transformer Design for Transistor Application," which appeared in the January–February, 1956 issue of the Transactions on Audio.

J. T. Henderson, IRE President (*left*) visited the Cedar Rapids Section recently, and spoke at a meeting of the student branch, State University of Iowa, in Iowa City. During his Cedar Rapids visit, Dr. Henderson toured the facilities of the Collins Radio Company with section officers, W. B. Bruene (*center*), vice-chairman, and R. L. Olson (*right*), treasurer.

Magnetic Conference Recommends Subjects for Papers

A Conference on Magnetism and Magnetic Materials will take place at the Sheraton-Park Hotel, Washington, D. C., on November 18–20. The conference is being sponsored by the American Institute of Electrical Engineers in cooperation with the IRE, American Physical Society, American Institute of Mining and Metallurgical Engineers, and the Office of Naval Research.

Papers on the following subjects will be particularly welcome: garnets, hexagonal oxides, cobalt-doped ferrites, thin films, ferromagnetic resonance modes and nonlinear effects, anistropy, magnetostriction and magnetic annealing, switching phenomena, masers and nonreciprocal devices and their development. Preference will be given to papers dealing with basic exploration of magnetic phenomena having bearing upon potential engineering applications, and with the development of apparatus and techniques utilizing recent advances in magnetism.

The presentation of papers should take from 10 to 20 minutes each, and 200–500 word abstracts are due August 15. The completed papers should be handed in at the conference for publication in the conference proceedings.

Further details are obtainable from L. R. Maxwell, U. S. Naval Ordnance Lab., White Oak, Silver Spring, Md.

URSI Holds Twelfth Assembly

The Twelfth General Assembly of the URSI will be held in Boulder, Colorado, August 22 to September 5 this year. These meetings are held every three years; the last one was in The Hague, Holland, in 1954, and the only previous one in the United States was in 1927.

The meeting is for the promotion of world-wide cooperation in radio scientific projects. This is accomplished essentially by the holding of symposiums on the principal topics of interest, supplemented by administrative planning by representatives of the National Committees of the 26 member countries. The technical program is under the auspices of the seven scientific Commissions of URSI: I. Radio Measurements and Standards—Chairman, B. Decaux (France); USA Chairman, E. Weber; II. Radio and Troposphere—Chairman, R. L. Smith-Rose (England); USA Chairman, J. B. Smyth; III. Ionospheric Radio—Chairman, D. F. Martyn (Australia); USA Chairman, M. G. Morgan; IV. Radio Noise of Terrestrial Origin—Chairman, J. A. Ratcliffe (England); USA Chairman, A. W. Sullivan; V. Radio Astronomy—Chairman, M. Laffineur (France); USA Chairman, F. T. Haddock; VI. Radio Waves and Circuits—Chairman, S. Silver (United States); USA Chairman, J. B. Wiesner; and VII. Radio Electronics—Chairman, G. A. Woonton (Canada); USA Chairman, W. G. Shepherd.

The international officers of the URSI are: President, P. Lejay (France); Vice-Presidents, L. V. Berkner (United States), C. R. Burrows (United States), R. L. Smith-Rose (England), and B. D. H. Tellegen (Netherlands); Treasurer, C. H. Manneback (Belgium); and Secretary, E. Herbays (Belgium).

The officers of the U.S.A. National Committee of URSI are: Chairman, H. W. Wells; Vice-Chairman, W. E. Gordon; and Secretary-Treasurer, J. P. Hagen.

The General Assembly is managed by a General Arrangements Committee, as follows: Chairman, J. H. Dellinger; Finance, L. V. Berkner; Local Arrangements, K. A. Norton and A. H. Shapley; Foreign Arrangements, W. E. Gordon and H. W. Wells; Technical Program, A. H. Waynick and F. H. Dickson; Ladies Program, Mrs. K. A. Norton; Honorary, W. W. Atwood, Jr., F. W. Brown, and Quigg Newton.

The meeting is not open to the public. Participants are designated by the National Committees of the member countries.

Books

On Human Communication by Colin Cherry

Published (1957) by The Technology Press of Massachusetts Institute of Technology and John Wiley & Sons, Inc., 440 Fourth Ave., N. Y. 16, N. Y. 302 pages+9 index pages+5 appendix pages+16 pages of bibliography+xiv pages. Illus. 9¼×6¼. $6.75.

Colin Cherry writes from the midst of the field of communication theory, in which he is known particularly for his applications of Bayes' theorem. While he hails from the University of London, he has lectured in many countries and is welcome and appreciated everywhere. It is pleasant to meet him through a book based on some of his lectures.

Cherry writes of communication theory in broader terms than many Americans. The chapters discuss the evolution of communication science, signs and language, the analysis of signals, the statistical theory of communication, the logic of communication, and cognition and recognition. Those who have some acquaintance with communication theory are unlikely to be startled by the the contents of the book, but they will appreciate the wealth of illustration, and particularly the careful listing of sources and references for which one might otherwise search in exasperation and vain.

The book can be very valuable to technical men who know less about communication theory than they should. They will be safe in Mr. Cherry's hands, and he does a very good best to make a great many very important things simple and understandable.

I wish that the broader group of those who profess to be interested in science and in communication would read this book rather than what they do read. Alas, it says something which calls for thought, it is pleasing in a way which requires perception for appreciation, and it doesn't promise either to topple or to refound science, or to solve the readers' personal or political problems. In other words, it has nothing to make it popular except merit and my futile prayers.

J. R. Pierce
Bell Tel. Labs., Inc.
Murray Hill, N. J.

Television Receiving Equipment, 4th ed., by W. T. Cocking

Published (1957) by Philosophical Library, Inc., 15 E. 40 St., N. Y. 16, N. Y. 415 pages+4 index pages +30 pages of appendix+ix pages. Illus. 8¼×6. $15.00.

This is an elementary but comprehensive treatment of British TV standards and monochrome receiver practice. The use of British terminology and viewpoint makes this a special-purpose book which is not well correlated to American procedures. Some circuit considerations, such as intercarrier sound systems and weak signal fringe area performance which result from distinctions of American standards or usage, are not discussed. Other circuits such as automatic gain control, are discussed only from the British receiver viewpoint.

However, all monochrome receiver functions are discussed and the coverage of alternate circuit choices is good. The author indicates the circumstances or environmental conditions in which the particular circuits would be preferred. The text is easy to understand since it is essentially descriptive and does not press into theoretical detail. Emphasis is on the circuit functions and normal operation, with only nominal attention to design limits and specifications. The design engineer will find no new information. Since color signal transmission is not yet available in England there is no discussion of color receiver circuitry. The book would be of interest to students and junior engineers who are approaching TV circuit design responsibilities and to others interested in broadening their viewpoint by a knowledge of British television. Otherwise, the book does not rank high compared to standard texts.

W. P. Boothroyd
Philco Corp.
Philadelphia 34, Pa.

Les Semiconducteurs by G. Goudet and C. Meuleau

Published (1957) by Editions Eyrolles, 61, Boulevard Saint-Germain, Paris 6, France. 436 pages+5 index pages+17 pages of bibliography+1 appendix page. 108 figures. 9¾×6¾. 5.720 F.

Les Semiconducteurs is the most up-to-date and comprehensive treatment of the semiconductor field, covering the physics, the technology and the device applications excluding circuit aspects. It is the third major publication of this type in the free world literature and the first in French. However, the authors had to leave out many pertinent details in order to compress the immense material into 436 pages which, unfortunately, impairs the general usefulness of this volume. Essentially every topic of importance is, at least, mentioned and a good literature index for each chapter, arranged in chronological order, is most helpful for the reader interested in delving further into details. An author index would have added to its value as a reference book. The text is divided into three homogeneous parts.

The "General Theoretical Foundation" is well written and sufficiently complete as an introduction for nontheoretical readers, such as experimental physicists and electrical engineers. A minor blemish is the usage of mks units in the text mixed with cgs units in the figures.

The second part, entitled "Semiconductor Technology," encompasses much more than the verbal translation implies. Crystal structure, impurities and imperfections as well as preparation, purification and crystal growth methods and the underlying principles are included. Even the new compound semiconductors are mentioned briefly. The established methods for measuring physical properties are treated separately.

The third and most extensive part covers "The Major Semiconductor Applications." Starting with thermistors and varistors, it goes into the various types of rectifier structures and essentially all known transistors, mentioning the n-p-n-p structure, tetrodes and even the fieldistor. Photo-devices including radiation batteries and magnetic devices such as the Hall generator and magnetometer applications are touched upon besides some of the most recently invented special devices.

Les Semiconducteurs is a fine introduction to the semiconductor field. Although it is somewhat arbitrarily condensed, its usefulness as a reference book is greatly enhanced by the extensive bibliography.

D. A. Jenny
RCA Laboratories
Princeton, N. J

Professional Groups†

Aeronautical & Navigational Electronics—Joseph General, 6019 Highgate Dr., Baltimore 15, Md.

Antennas & Propagation—J. I. Bahnert, Code 5250, Naval Research Lab., Washington 25, D. C.

Audio—Dr. H. F. Olson, RCA Labs., Princeton, N. J.

Automatic Control—E. M. Grabbe, Ramo-Wooldridge Corp., Box 45067, Airport Station, Los Angeles 45, Calif.

Broadcast & Television Receivers—L. R. Fink, Research Lab., General Electric Company, Schenectady, N. Y.

Broadcast Transmission Systems—O. W. B. Reed, Jr., Jansky & Bailey, 1735 DeSales St., N.W., Washington, D. C.

Circuit Theory—H. J. Carlin, Microwave Res. Inst., Polytechnic Inst. of Brooklyn, 55 Johnson St., Brooklyn 1, N. Y.

Communications Systems—J. W. Worthington, Jr., USAF Rome Air Force Depot, Griffiss AFB, Rome, N. Y.

† Names listed are Group Chairmen.

Component Parts—R. M. Soria, American Phenolic Corp., 1830 S. 54 Ave., Chicago 50, Ill.

Electron Devices—T. M. Liimatainen, Diamond Ordnance Fuze Lab., Washington, D. C.

Electronic Computers—Werner Buchholz, IBM Engineering Lab., Poughkeepsie, N. Y.

Engineering Management—C. R. Burrows, Ford Instrument Co., 31-10 Thompson Ave., Long Island City 1, N. Y.

Engineering Writing and Speech—D. J. McNamara, Sperry Gyroscope Co., Great Neck, L. I., N. Y.

Industrial Electronics—W. R. Thurston, General Radio Co., 285 Massachusetts Ave., Cambridge 39, Mass.

Information Theory—W. B. Davenport, Jr., Lincoln Lab., M.I.T., Box 390, Cambridge 39, Mass.

Instrumentation—F. G. Marble, Boonton Radio Corporation, Intervale Road, Boonton, N. J.

Medical Electronics—L. B. Lusted, Clinical Center, National Institute of Health, Bethesda 14, Md.

Microwave Theory and Techniques—W. L. Pritchard, Raytheon Mfg. Co., 148 California St., Newton 58, Mass.

Military Electronics—Adm. W. E. Cleaves, 3807 Fanchurch Rd., Baltimore 18, Md.

Nuclear Science—W. E. Shoupp, Westinghouse Elec. Corp., Commercial Atomic Power Activities, P.O. Box 355, Pittsburgh 30, Pa.

Production Techniques—E. R. Gamson, Autonetics, 395-91, 12214 Lakewood Blvd., Downey, Calif.

Reliability and Quality Control—Victor Wouk, Beta Electric Corp., 333 E. 103rd St., New York 29, N. Y.

Telemetry and Remote Control—C. H. Doersam, Jr., 24 Winthrop Rd., Port Washington, L. I., N. Y.

Ultrasonics Engineering—C. M. Harris, 425 Riverside Dr., New York, N. Y.

Vehicular Communications—Newton Monk, Bell Labs., 463 West St., N. Y., N. Y.

Sections*

Akron (4)—H. F. Lanier, 2220—27th St., Cuyahoga Falls, Ohio; Charles Morrill, 2248—16th St., Cuyahoga Falls, Ohio.

Alamogordo-Holloman (6)—V. J. Lynch, 1105 Maple Dr., Alamogordo, N. Mex.; R. B. Kleinman, Box 1054, Holloman AFB, N. Mex.

Albuquerque-Los Alamos (7)—B. L. Basore, 2405 Parsifal, N.E., Albuquerque, N. Mex.; John McLay, 3369—48 Loop, Sandia Base, Albuquerque, N. Mex.

Atlanta (3)—W. B. Miller, 1369 Holly Lane, N.E., Atlanta 6, Ga.; W. H. White, 1454 S. Gordon St., S.W., Atlanta 10, Ga.

Baltimore (3)—M. I. Jacob, 1505 Tredegar Ave., Cotonsville 28, Md.; P. A. Hoffman, Hoover Electronics Co., 3640 Woodland Ave., Baltimore 15, Md.

Bay of Quinte (8)—W. D. Ryan, Cavalry House, Royal Military College, Kingston, Ont., Canada; R. Williamson, R.R. #3, Belleville, Ont., Canada.

Beaumont-Port Arthur (6)—J. G. Morgan, 508 Garland St., Beaumont, Tex.; B. J. Ballard, Box 2831, Rm. 608, Beaumont, Tex.

Binghamton (1)—Robert Nash, 12 Alice St., M.R. 97, Binghamton, N. Y.; Bruce Lockhart, R.D. 3, Binghamton, N. Y.

Boston (1)—R. A. Waters, Box 368, S. Sudbury, Mass.; T. F. Jones, Jr., 62 Bay St., Squantum, Mass.

Buenos Aires—A. H. Cassiet, Zavalia 2090 1 "B," Buenos Aires, Argentina; O. C. Fernandez, Transradio Internacional, 379 San Martin, Buenos Aires, Argentina.

Buffalo-Niagara (1)—W. S. Holmes, Cornell Aeronautical Labs., 4455 Genesee St., Buffalo 21, N. Y.; R. B. Odden, 573 Allenhurst Rd., Buffalo, N. Y.

Cedar Rapids (5)—J. L. Dalton, 2900 E. Ave., N.E., Cedar Rapids, Iowa; S. M. Morrison, 2034 Fourth Ave., S.E., Cedar Rapids, Iowa.

Central Florida (3)— G. F. Anderson, Dynatronics, Inc., 717 W. Amelia Ave., Orlando, Fla.; J. W. Downs, 1020 Highland Ave., Eau Gallie, Fla.

Central Pennsylvania (4)—W. J. Leiss, 1173 S. Atherton St., State College, Pa.; P. J. Freed, Hallor, Raymond & Brown, State College, Pa.

Chicago (5)—R. M. Soria, 1830 S. 54th Ave., Chicago 50, Ill.; G. H. Brittain, 3150 Summit Ave., Highland Park, Ill.

China Lake (7)—C. F. Freeman, 100-B Halsey St., China Lake, Calif.; P. K. S. Kim, 200-A Byrnes St., China Lake, Calif.

Cincinnati (4)—F. L. Weidig, Jr., 3819 Davenant Ave., Cincinnati 13, Ohio; H. E. Hancock, R.R. 4, Branch Hill Box 52, Loveland, Ohio.

Cleveland (4)—J. F. Keithley, 22775 Douglas Rd., Shaker Heights 22, Ohio; C. F. Schunemann, 2021 Sagamore Dr., Euclid 17, Ohio.

Columbus (4)—T. E. Tice, 2214 Jervis Rd., Columbus 21, Ohio; G. R. Jacoby, 78 N. James Rd., Columbus 13, Ohio.

Connecticut Valley (1)—H. A. Lucal, Univ. of Conn., Box U-37, Storrs, Conn.; A. R. Perrins, 951 Sperry Rd., Cheshire, Conn.

Dallas (6)—G. K. Teal, Texas Instruments Inc., 6000 Lemmon Ave., Dallas, Texas; John Albano, 4134 Park Lane, Dallas, Texas.

Dayton (4)—R. W. Ittelson, 724 Golfview Dr., Dayton 6, Ohio; Yale Jacobs, 310 Ryburn Ave., Dayton 5, Ohio.

Denver (6)—R. S. Kirby, 455 Hawthorne Ave., Boulder, Colo.; W. G. Worcester, 748 10th St., Boulder, Colo.

Detroit (4)—E. C. Johnson, 4417 Crooks Rd., Royal Oak, Mich.; G. E. Ryan, 5296 Devonshire Rd., Detroit 24, Mich.

Egypt—H. M. Mahmoud, Faculty of Engineering, Fouad I University, Giza, Cairo, Egypt; El Garhi I El Kashlan, Egyptian Broadcasting, 4, Shari Sherifein, Cairo, Egypt.

Elmira-Corning (1)—R. G. Larson, 220 Lynhurst Ave., Windsor Gardens, Horseheads, N. Y.; D. F. Aldrich, 1030 Hoffman St., Elmira, N. Y.

El Paso (6)—J. H. Maury, 328 Olivia Circle, El Paso, Tex.; W. A. Toland, 912 Brazil St., El Paso, Tex.

Emporium (4)—H. S. Hench, Jr., Sylvan Heights, Emporium, Pa.; H. J. Fromell, Sylvania Elec. Prod. Inc., Emporium, Pa.

Evansville-Owensboro (5)—D. D. Mickey, Jr., Engineering Department, General Electric Co., Owensboro, Ky.; C. L. Taylor, General Electric Co., 316 E. 9 St., Owensboro, Ky.

Florida West Coast (3)—(No chairman at present); Raymond Murphy, 12112 N. Edison Ave., Tampa 4, Fla.

Fort Huachuca (7)—J. H. Homsy, Box 123 San Jose Branch, Bisbee, Ariz.; R. E. Campbell, Box 553, Benson, Ariz.

Fort Wayne (5)—Gordon Collins, 3101 Lillie St., Fort Wayne, Ind.; H. D. Grosvenor, 1332 Maple Ave., Fort Wayne, Ind.

Fort Worth (6)—G. C. Sumner, 3900 Spurgeon, Fort Worth, Texas; C. W. Macune, 3132 Forest Park Blvd., Fort Worth, Texas.

Hamilton (8)—A. L. Fromanger, Box 507, Ancaster, Ont., Canada; C. J. Smith, Gilbert Ave., Dancaster Courts, Sub. Serv. 2, Ancaster, Ont., Canada.

Hawaii (7)—R. R. Hill, 219 Uilma St., Lanikai, T. H.; L. R. Dawson, 432 A Kalama St., Lanikai, T. H.

Houston (6)—M. A. Arthur, Humble Oil & Refining Co., P.O. Box 2180, Houston 1, Tex.; C. G. Turner, Communications Engineering Co., P.O. Box 12325, Houston 17, Tex.

Huntsville (3)—T. L. Greenwood, 1709 La Grande St., Huntsville, Ala.; W. J. Robinson, 715 Wharton Rd., Huntsville, Ala.

Indianapolis (5)—B. V. K. French, 4480 Marcy Lane, Apt. 62, Indianapolis 5, Ind.; N. G. Drilling, 3002 Ashland Ave., Indianapolis 26, Ind.

Israel—Franz Ollendorf, Box 910, Hebrew Inst. of Technology, Haifa, Israel; A. A. Wulkan, P.O.B. 1, Kiryat Motzkin, Haifa, Israel.

Ithaca (1)—H. S. McGaughan, Dept. of Elec. Eng., Cornell Univ., Ithaca, N. Y.; W. H. Murray, General Electric Co., Ithaca, N. Y.

Kansas City (6)—R. W. Butler, Box 1159 Kansas City 41, Mo.; Mrs. G. L. Curtis 6005 El Monte, Mission, Kan.

Little Rock (6)—J. D. Reid, 2210 Summit, Little Rock, Ark.; J. P. McRae, Route 1, Scott, Ark.

London (8)—J. C. Warder, 513 Princess Ave., London, Ont., Can.; J. D. B. Moore, 27 McClary Ave., London, Ont., Can.

Long Island (2)—E. G. Fubini, Airborne Instrument Labs., 160 Old Country Rd., Mineola, L. I., N. Y.; E. K. Stodola, 118 Stanton St., Northport, N. Y.

Los Angeles (7)—V. J. Braun, 2673 N. Raymond Ave., Altadena, Calif.; J. N. Whitaker, 323—15th St., Santa Monica, Calif.

Louisville (5)—O. W. Towner, WHAS Inc., 525 W. Broadway, Louisville 2, Ky.; F. M. Sweets, 114 S. First St., Louisville 2, Ky.

Lubbock (6)—E. W. Jenkins, Jr., Shell Oil Co., Admin. Dept., Box 1509, Midland, Tex.; J. J. Criswell, 511 50th St., Lubbock, Tex.

Miami (3)—W. H. Epperson, 5845 S.W. 108 St., Miami 43, Fla.; R. S. Rich, 7513 S.W. 54 Ct., S. Miami, Fla.

Milwaukee (5)—J. E. Jacobs, 6230 Hale Park Dr., Hales Corners, Wis.; L. C. Geiger, 2734 N. Farwell Ave., Milwaukee 11, Wis.

Montreal (8)—R. E. Penton, 6120 Cote St. Luc Rd., Apt. 6, Montreal, Quebec, Canada; R. Lumsden, 1680 Lepine St., St. Laurent, Montreal 9, Quebec, Canada.

Newfoundland (8)—J. B. Austin, Jr., Hq. 1805th AACS Wing, APO 862, c/o PM, New York, N. Y.; J. A. Willis, Canadian Marconi Co., Ltd., Pinetree-MEAC Depot, Pepperrill AFB, St. John's Newfoundland, Canada.

New Orleans (6)—M. F. Chapin, 8116 Hampson St., New Orleans, La.; G. A Hero, 1102 Lowerline St., New Orleans 18, La.

New York (2)—J. S. Smith, 3717 Clarendon Rd., Brooklyn, N. Y.; Joseph Reed, 52 Hillcrest Ave., New Rochelle, N. Y.

North Carolina-Virginia (3)—F. E. Brooks, Box 277, Colonial Ave., Colonial Beach, Va.; E. S. Busby, Jr., 1608 "B" St., Portsmouth, Va.

Northern Alberta (8)—J. E. Sacker, 10235—103rd St., Edmonton, Alberta, Canada; Frank Hollingworth, 9619—85th St., Edmonton, Alberta, Canada.

Northern New Jersey (2)—A. M. Skellett, 10 Midwood Terr., Madison, N. J.; G. D. Hulst, 37 College Ave., Upper Montclair, N. J.

Northwest Florida (3)—F. E. Howard, Jr., 573 E. Gardner Dr., Fort Walton, Fla.; W. W. Gamel, Canoga Corp., P.O. Box 188, Shalimar, Fla.

Oklahoma City (6)—Nicholas Battenburg, 2004 N.W. 30th St., Oklahoma City 6, Okla.; E. W. Foster, 5905 N.W. 42 St., Oklahoma City 12, Okla.

Omaha-Lincoln (5)—J. S. Petrik, c/o KETV, 27 & Douglas Sts., Omaha, Neb.; H. W. Becker, 1214 N. 34 St., Omaha 3, Neb.

* Numerals in parentheses following Section designate region number. First name designates Chairman, second name, Secretary.

Ottawa (8)—L. H. Doherty, 227 Barclay Rd., Ottawa 2, Ont., Canada; R. E. Thain, 54 Rossland Ave., Box 474, City View, Ont., Canada.

Philadelphia (3)—Nels Johnson, Philco Corp., 4700 Wissahickon Ave., Philadelphia 44, Pa.; R. E. Robertson, General Electric Co., 3198 Chestnut St., Philadelphia 4, Pa.

Phoenix (7)—Everett Eberhard, 30 E. Colter St., Phoenix, Ariz.; R. V. Baum, 1718 East Rancho Dr., Phoenix, Ariz.

Pittsburgh (4)—J. B. Woodford, Jr., Box 369, Carnegie Tech. P. O., Pittsburgh 13, Pa.; A. E. Anderson, 1124 Olympic Hts. Dr., Pittsburgh 35, Pa.

Portland (7)—R. R. Pooley, 3153 N.E. 83 Ave., Portland 20, Ore.; R. C. Raupach, 3920 N.E. Wistaria Dr., Portland 13, Ore.

Princeton (2)—J. L. Potter, Rutgers Univ., New Brunswick, N. J.; P. K. Weimer, RCA Laboratories, Princeton, N. J.

Regina (8)—William McKay, 2856 Retallack St., Regina, Saskatchewan, Canada; J. A. Funk, 138 Leopold Crescent, Regina, Saskatchewan, Canada.

Rio de Janeiro—M. P. deBritto Pereira, Caixa Postal 562, Rio de Janeiro, Brazil; Haroldo de Mattos, Rua Nascimento Silva 391, Rio de Janeiro, Brazil.

Rochester (1)—W. F. Bellor, 186 Dorsey Rd., Rochester 16, N. Y.; R. E. Vosteen, 473 Badkus Rd., Webster, N. Y.

Rome-Utica (1)—M. V. Ratynski, 205 W. Cedar St., Rome, N. Y.; Sidney Rosenberg, 907 Valentine Ave., Rome, N. Y.

Sacramento (7)—E. W. Berger, 3421—58 St., Sacramento 20, Calif.; P. K. Onnigian, 4003 Parkside Ct., Sacramento, Calif.

St. Louis (6)—C. E. Mosley, 8622 St. Charles Rock Rd., Overland 14, Mo.; R. D Rodenroth, 7701 Delmont, Affton 23, Mo.

Salt Lake City (7)—V. E. Clayton, 1525 Browning Ave., Salt Lake City, Utah; A. L. Gunderson, 3906 Parkview Dr., Salt Lake City 17, Utah.

San Antonio (6)—W. H. Hartwig, Dept. of Elec. Eng., University of Texas, Austin 12, Tex.; E. L. Hixson, Dept. of Elec. Eng., University of Texas, Austin 12, Tex.

San Diego (7)—E. J. Moore, 3601 Eighth St., San Diego 3, Calif.; R. J. Cary, Jr., 4561 Normandie Place, La Mesa, Calif.

San Francisco (7)—J. S. McCullough, 1781 Willow St., San Jose 25, Calif.; E. G. Goddard, Stanford Research Institute, Menlo Park, Calif.

Schenectady (1)—J. S. Hickey, Jr., General Electric Co., Box 1088, Schenectady, N. Y.; C. V. Jakowatz, 10 Cornelius Ave., Schenectady 9, N. Y.

Seattle (7)—R. H. Hoglund, 1825 E. Lynn St., Seattle 2, Wash.; L. C. Perkins, Box 307, Des Moines, Wash.

Shreveport (6)—H. H. Moreland, Hq. 2nd Air Force, Barksdale AFB, La.; M. C. Benson, P.O. Box 1316, Shreveport, La.

South Bend-Mishawaka (5)—J. L. Colten, 149 E. Tasher, South Bend, Ind.; P. G. Cox, R.R. 2, 10251 Harrison Rd., Osceola, Ind.

Southern Alberta (8)—W. K. Allan, 2025 29th Ave., S.W., Calgary, Alta., Canada; R. W. H. Lamb, Radio Station CFCN, 12th Ave. and Sixth St. E., Calgary, Alberta, Canada.

Syracuse (1)—P. W. Howells, General Electric Co., H.M.E.E. Dept., Bldg. 3, Industrial Park, Syracuse, N. Y.; G. M. Glasford, Elec. Eng. Dept., Syracuse University, Syracuse 10, N. Y.

Tokyo—Yasujiro Niwa, Tokyo Elec. Engineering College, 2-2 Kanda-Nishikicho, Chiyoda-Ku, Tokyo, Japan; Fumio Minozuma, 16 Ohara-Machi, Meguro-Ku, Tokyo, Japan.

Toledo (4)—M. E. Rosencrantz, 4744 Overland Parkway, Apt. 204, Toledo, Ohio; L. B. Chapman, 2459 Parkview Ave., Toledo 6, Ohio.

Toronto (8)—H. W. Jackson, 352 Laird Dr., Toronto 17, Ont., Canada; R. J. A. Turner, 66 Gage Ave., Scarborough, Ont., Canada

Tucson (7)—P. E. Russell, Elec. Eng. Dept., Univ. of Arizona, Tucson, Ariz.; C. L. Becker, 4411 E. Sixth St., Tucson, Arizona.

Tulsa (6)—R. L. Atchison, 415 E. 14 Pl., Tulsa 20, Okla.; B. H. Keller, 1412 S. Winston, Tulsa 12, Okla.

Twin Cities (5)—J. L. Hill, 25—17 Ave., N.E., North St. Paul 9, Minn.; F. C. Wagner, 16219 Tonkaway Rd., Wayzata, Minn.

Vancouver (8)—J. S. Gray, 4069 W. 13th Ave., Vancouver, B. C., Canada; L. R. Kersey, Department of Electrical Engineering, Univ. of British Columbia, Vancouver 8, B. C., Canada.

Washington (3)—R. I. Cole, 2208 Valley Circle, Alexandria, Va.; R. M. Page, 5400 Branch Ave., Washington 23, D. C.

Wichita (6)—W. K. Klatt, 2625 Garland, Wichita 4, Kan., A. T. Murphy, Univ. of Wichita, Dept. of Elec. Eng., Wichita 14, Kan.

Williamsport (4)—(No chairman at present); W. H. Bresee, 818 Park Ave., Williamsport, Pa.

Winnipeg (8)—C. J. Hopper, 332 Bronx Ave., Winnipeg 5, Man., Canada; T. J. White, 923 Waterford Ave., Fort Garry, Winnipeg 9, Manitoba, Canada.

Subsections

Berkshire (1)—A. H. Forman, Jr., O.P. 1-203, M.O.S.D., General Electric Co., 100 Plastics Ave., Pittsfield, Mass.; E. L. Pack, 62 Cole Ave., Pittsfield, Mass.

Buenaventure (7)—O. La Plant, 325 N. "J", St. Oxnard, Calif.; W. L. MacDonald 65 Glen Ellen Dr., Ventura, Calif.

Charleston (3)—A. Jonas, 105 Lancaster St., N. Charleston, S. C.; F. A. Smith, Route 4, Melrose Box 572, Charleston, S.C.

East Bay (7)—H. F. Gray, Jr., 2019 Mira Vista Dr., El Cerrito, Calif.; D. R. Cone, 6017 Chabolyn Terr., Oakland 18, Calif.

Erie (1)—J. D. Heibel, 310 W. Grandview, Erie, Pa.; D. H. Smith, 3025 State St., Erie, Pa.

Gainesville (3)—W. E. Lear, Dept. of Elec. Eng., Univ. of Fla., Gainesville, Fla. (Chairman)

Hampton Roads (3)—R. L. Lindell, WTAR Radio Corp., 720 Boush St., Norfolk 10, Va.; J. E. Eller, Waterview Apts., Apt. E-3, Portsmouth, Va.

Kitchener-Waterloo (8)—Jules Kadish, Raytheon Canada, Ltd., 61 Laurel St., Waterloo, Ont., Canada; G. C. Field, 48 Harber Ave., Kitchener, Ont., Canada.

Lancaster (3)—W. T. Dyall, 1415 Hillcrest Rd., Lancaster, Pa.; P. W. Kaseman, 405 S. School Lane, Lancaster, Pa.

Las Cruces-White Sands Proving Grounds (6)—(Chairman to be elected); M. Goldin, 1921 Calle de Suneos, Las Cruces, New Mex.

Lehigh Valley (3)—F. W. Smith, Dept. of Elec. Eng., Lafayette College, Alumni Hall of Eng., Easton, Pa.; L. G. McCracken, Dept. of Elec. Eng., Lehigh Univ., Bethlehem, Pa.

Memphis (3)—R. N. Clark, Box 227, Memphis State College, Memphis, Tenn. (Chairman)

Mid-Hudson (2)—Altman Lampe, Cramer Rd., R.D. 3, Poughkeepsie, N. Y.; M. R. Marshall, 208 Smith St., Poughkeepsie, N. Y.

Monmouth (2)—Edward Massell, Box 433, Locust, N. J.; Harrison Rowe, Box 107, Red Bank, N. J.

Nashville (3)—W. W. Stifler, Jr., Aladdin Electronics, Nashville 2, Tenn.; P. E. Dicker, Dept. of Elec. Eng., Vanderbilt Univ., Nashville 5, Tenn.

New Hampshire (1)—M. R. Richmond, 55 Raymond St., Nashua, N. H.; R. O. Goodwin, 86 Broad St., Nashua, N. H.

Northern Vermont (1)—Charles Horvath, 15 Iby St., S. Burlington, Vt.; (secretary to be elected)

Orange Belt (7)—J. Tampico, 2709 N. Garey Ave., Pomona, Calif.; R. E. Beekman, 113 N. Lillie, Fullerton, Calif.

Palo Alto (7)—W. B. Wholey, 25044 La Loma Dr., Los Altos, Calif.; A. M. Peterson, 14846 Manuella Ave., Los Altos, Calif.

Panama City (3)—C. B. Koesy, 1815 Moates Ave., St. Andrew Station, Panama City, Fla.; M. H. Naeseth, 1107 Buena Vista Blvd., Panama City, Fla.

Pasadena (7)—J. L. Stewart, Assoc. Prof. of Elec. Eng., Calif. Inst. of Tech., Pasadena, Calif.; J. E. Ranks, ElectroData, Pasadena, Calif.

Piedmont (3)—H. H. Arnold, 548 S. Westview Dr., Winston-Salem, N. C.; C. A. Norwood, 830 Gales Ave., Winston-Salem, N. C.

Quebec (8)—R. E. Collin, 590 Avenue Mon Repos, Ste. Foy, Quebec, Can.; R. M. Vaillancourt, 638 Avenue Mon Repos, Ste. Foy, Quebec, Canada.

Richland (7)—R. E. Connally, 515 Cottonwood Dr., Richland, Wash.; R. R. Cone-611 Thayer, Richland, Wash.

San Fernando (7)—J. C. Van Groos, 21051 Constanso St., Box 425, Woodland Hills, Calif.; F. E. La Fetra, 22700 Erwin St., Woodland Hills, Calif.

USAFIT (5)—(Officers to be elected.)

Westchester County (2)—D. S. Kellogg, 9 Bradley Farms, Chappaqua, N. Y.; M. J. Lichtenstein, 53 Beaumont Circle, Yonkers, N. Y.

Western North Carolina (3)—J. G. Carey, 1429 Lilac Rd., Charlotte, N. C.; R. W. Ramsey, Sr., 614 Clement Ave., Charlotte 4, N. C.

Abstracts of IRE Transactions

The following issues of "Transactions" have recently been published, and are now available from the Institute of Radio Engineers, Inc., 1 East 79th Street, New York 21, N. Y. at the following prices. The contents of each issue and, where available, abstracts of technical papers are given below.

Sponsoring Group	Publication	Group Members	IRE Members	Non-Members*
Aeronautical & Navigational Electronics	Vol. ANE-4, No. 1	$1.50	$2.25	$4.50
Circuit Theory	Vol. CT-4, No. 1	.65	.95	1.95
Component Parts	Vol. CP-4, No. 1	1.35	2.00	4.05
Microwave Theory & Techniques	Vol. MTT-5, No. 2	1.90	2.85	5.70
Production Techniques	PGPT-2	2.85	4.25	8.55
Vehicular Communications	PGVC-8	1.40	2.10	4.20

*** Public libraries and colleges may purchase copies at IRE Member rates.**

Aeronautical & Navigational Electronics

Vol. ANE-4, No. 1, March, 1957

Joseph General (p. 2)

Thoughts on an Improved ATC System—H. K. Morgan (p. 3)

In this paper, air traffic control is considered quite separately from navigation or general communications. An analysis of the fixed block, the timed block, and the timed intersection systems of air traffic control shows that the fixed block system presents certain advantages. After a discussion of methods of naming and numbering fixes, a scheme is proposed of numbered blocks between fixes, instead, as the control elements. A communication scheme for the signaling link is proposed as a time-shared, ground-controlled system to interrogate all aircraft sequentially for request and release of blocks several times a minute. General broadcasts of airport conditions periodically, followed by specific request when an aircraft is a half-hour from arrival, are proposed as a method of reserving airport landing time. Finally, the simplicity of an interlock system which can automatically reply with clearance to the pilot is proposed with certain remarks on comparative costs.

The Air Traffic Control Radar Beacon System—D. S. Crippen (p. 6)

This paper outlines the major advantages and limitations of the Air Traffic Control Radar Beacon System under evaluation at the Civil Aeronautics Administration Technical Development Center. It discusses the advantages and disadvantages of compatibility, the system traffic capacity problems, and the need for an operational doctrine to restrict the use of interrogators. System coverage, ground antenna, reply-code garbling, and reflection problems also are discussed. The paper points out specific applications of the beacon system, including its ability to improve the reliability of aircraft position information, to provide identity for specific aircraft targets in a traffic situation, and to furnish the information required for a filtered air traffic control display with a very rapid and flexible cross-reference between aircraft identification, plan position, and altitude.

Airborne Storm Avoidance Radar Training—M. E. Balzer (p. 16)

In training scheduled air carrier flight crews in the use of airborne storm avoidance radar, a twofold problem is encountered. The utility of the instrument must be sold to the doubting Thomas who has many thousands of hours flying in thunderstorm conditions, and its limitations must be defined for those who see it as a miracle maker. In overcoming these problems, United Air Lines, training program has emphasized basic scope interpretation with special reference to severe storms and their appearance on a plan-position indicator (ppi) display. Flight crew reaction to the training and to the radar installations in United's fleet has been favorable and is described.

Study of the Feasibility of Airborne HF Direction-Finding Antenna Systems—P. S. Carter, Jr. (p. 19)

High-frequency (2–24 mc) airborne direction-finding antennas are, in general, limited in accuracy, due to the undesired coupling between the antenna and the airframe which is electrically resonant in this frequency range.

This paper describes the results of laboratory and flight test studies of antennas designed to eliminate such coupling and to achieve the necessary direction-finding accuracy. The radiation patterns of one particular antenna design —the wing H-Adcock—are discussed.

It is concluded that hf airborne direction-finding is not feasible except in very restricted circumstances over narrow portions of the hf band.

Effect of Precipitation on the Design of Radio Altimeters—R. K. Moore (p. 24)

Radio altimeters operating in the microwave region must distinguish between desired signals returned from the ground and undesired signals returned from precipitation. Calculation of the relative ground and precipitation returns for a 0.1 microsecond pulse-duration altimeter requiring 10 to 1 desired-undesired signal ratio indicates a minimum wavelength of about 2 cm may be used for reliable operation in heavy precipitation.

Curves have been computed for minimum wavelength at a given altitude for fixed range to rain and for equal rain and ground ranges, for various beam widths. Minimum wavelengths as long as 20 cm are indicated for some conditions. Use of circular polarization may permit altimeter operations at wavelengths less than 2 cm, even with intense precipitation.

A One-Kilowatt Airborne-Radio-Frequency Power Amplifier—J. B. Humfeld (p. 30)

A miniaturized airborne rf power amplifier with continuous coverage of the 4–30-mc frequency range and with 1-kw average power output is described. Complete oil immersion for heat transfer and voltage insulation plus a novel six-phase self-rectifying power amplifier circuit give a high-power density unit capable of operating under extreme environmental conditions. The maximum usable power level is now limited by the aircraft antennas available.

Synthesis of Delay Line Networks—D. A. Linden and B. D. Steinberg (p. 34)

Radar video information may be processed on a continuous-trace (as opposed to range-gated) basis by using delay elements whose delay times are integral multiples of the repetition period τ. Networks consisting of such lines and of linear amplifiers and adders yield periodic pass bands. Their properties may be analyzed most conveniently by the transformation $z = e^{p\tau}$, where p is the complex frequency variable.

A systematic synthesis procedure is presented which realizes a prescribed delay-line transfer function as a cascade of elementary building blocks. Flow-graph techniques may be used to obtain different embodiments corresponding to the same transfer function.

It is shown that the required number of delay elements is equal to the number of poles of the z-transfer-function which are located away from the origin, or to the number of zeros, whichever is larger.

PGANE News (p. 40)

Contributors (p. 41)

Circuit Theory

Vol. CT-4, No. 1, March, 1957

Abstracts of Papers in This Issue

Q Factors of a Transmission Line Cavity—Leo Young (p. 3)

On investigating the properties of a transmission line cavity, new expressions for the Q factor and logarithmic decrement δ were derived, and were compared with the expressions for a single shunt or series LCR circuit. It was expected that the expressions for Q and π/δ would be very similar, if not the same, as is the case with LCR circuits. That this expectation was not realized was attributed to the finite velocity of wave propagation. The two expressions are the same only so long as the transfer of influence is assumed instantaneous or the losses are uniformly distributed.

It is possible to define a Q of steady-state oscillations ("wave-meter Q" and a Q of decaying oscillations ("echobox Q"). The expressions for these two Q factors are the same in the case of an LCR circuit, but for a transmission line cavity the two formulas contain different transcendental functions of the circuit parameters, and tend towards equality only for large Q, or no external loading.

Bandwidth Limitations in Equalizers and Transistor Output Circuits—J. L. Stewart (p. 5)

The attenuation-integral theorem shows that a limit exists to the power gain times bandwidth product when an ideal current generator drives a network having a finite capacitance in shunt with the input. This paper derives a comparable theorem which includes both capacitance and device behavior like the α-cutoff effect in transistors. The result of the theorem is the familiar $\pi/(2RC)$ when α cutoff can be ignored. The result depends upon both capacitance and α cutoff in general. The analysis is somewhat different from the classical method

and hence can be considered to provide an alternate derivation of the attenuation-integral theorem. The results can also be interpreted to indicate the limitations of general amplitude equalization by means of a single network driven from a current source.

Specific nonminimum-phase networks suitable for equalizing output networks when the (transistor) current source behaves as $\delta/(p+\delta)$ are the subject of the second half of this paper. Both networks and convenient design relations are given, as well as a specific example which increases δ-cutoff bandwidth by a factor of 10.

Degenerate Solutions and an Algebraic Approach to the Multiple-Input Linear Filter Design Problem—R. M. Stewart and R. J. Parks (p. 10)

This paper describes three common types of multiple-input filter design problems; in each case Wiener's general optimum multiple-input solution is reduced to a simpler equivalent single-input solution. The first type of situation discussed is the "distortionless dual-input system." Conditions under which this additional criterion of fidelity may be advisable are discussed, two general distortionless systems are shown, and it is demonstrated that Wiener's single-input solution may be used in designing such a system. The second semigeneral solution obtained (or semispecial, as the case may be) pertains to a situation in which interference is present in one channel which is statistically similar to, but still independent of, the actual signal of interest. The third case is probably the most interesting of all in that when several signal sources are available, such as in a diversity receiving system, each corrupted by additive independent noises, the optimum system is one in which all channels are added together directly (after possible simple gain adjustments) and then passed through a single filter. It is demonstrated that this result is true even though the signal-to-noise ratios are quite different for the various input channels.

Optimum Filters for Independent Measurements of Two Related Perturbed Messages—J. S. Bendat (p. 14)

A general technique is developed for designing an optimum filter to smooth a perturbed message (signal plus noise) by employing separate and independent information about a second perturbed message whose signal portion is related to the first. For example, the second signal might be the first derivative of the original signal, or its second derivative, or its delay value, etc. The two noises are required to be statistically distinguishable. The method involves four steps: 1) feeding both sources of information into the same device, 2) utilizing known relations between the signal portions so as to remove the signal portions and leave noise terms only, 3) designing a subsidiary system to pass one of the two noise terms in an optimal way, and 4) recombining with one of the original messages so as to furnish an optimum smoothed estimate of the desired signal.

A second question considered in the paper shows how one might smooth simultaneously both of the perturbed messages with a single compact system. The main ideas are illustrated in detail in a practical physical problem involving independent measurements of a signal and its derivative, such as occurs in guidance and control problems using radar equipment. Optimum physically realizable system designs are derived for handling this example.

On Matrices of Residues of the Impedance or Admittances Matrices of N-Ports—Israel Cederbaum (p. 20)

In the paper some properties of matrices of residues for the open-circuit impedance or the short-circuit admittance representation of n-ports are discussed. It is shown that at a simple pole, located wherever in the complex plane, the matrix of residues of the impedance or admittance matrix is, in general, highly degenerate. The rank of the matrix of residues of the impedance matrix cannot exceed the nullity of the numerator of the admittance matrix, and vice versa. The above proposition turns out to be a special case of a more general theorem for multiple poles. At a multiple pole, instead of the matrix of residues, the matrix of the first coefficients in the Laurent expansion about this singular point is to be considered. At poles on the imaginary axis where, according to Cauer, the matrix of residues is positive definite or semidefinite, the application of the above discussion shows that such a matrix is, in general, semidefinite (and of unit rank) and it may be positive definite only in very special cases.

Correction (p. 21)

Reviews of Current Literature—On the Design of Distributed Constant Networks—Nobuichi Ikeno. (Report of Electrical Communication Laboratories, NTT, Japan). . . . Reviewed by H. Ozaki and J. Ishii (p. 22)

Abstracts of Foreign Language Articles on Circuit Theory—Analytic Representation of Active Fourpoles—Johanna Piesch (in German) (p. 24)

Theory of a Triode Oscillator with Feedback—V. A. Zorye (English translation) (p. 24)

Some Transformations of Four-Terminal Networks—J. E. Colin (in French) (p. 24)

Graphic Construction of Image Attenuation of a Ladder Filter with One or Two Cut-Off Frequencies With or Without Losses—J. Bimont (in French) (p. 24)

Relationship of Physical Applications of Fourier Transforms in Various Fields of Wave Theory and Circuitry—E. F. Bolinder (in English) (p. 24)

Experimental Investigation of Subharmonic Oscillations in a Nonlinear System—K. Gorausson and L. Hansson (in English) (p. 24)

The Calculation of Filters by Synthesis—G. DeLotto and M. Trinchieri (in Italian) (p. 24)

Some Aspects of Intermediate Frequency Filtering in a Receiver—J. Carteron (in French) (p. 24)

Correspondence (p. 25)

PGCT News (p. 25)

Component Parts

Vol. CP-4, No. 1, March, 1957

Sendust Flake—A New Magnetic Material for Low-Frequency Application—W. M. Hubbard, E. Adams, and J. F. Haben (p. 2)

A high permeability, low-loss core was prepared by compacting Sendust flakes, which were produced by warm rolling Sendust powder. Sendust, a brittle magnetic alloy of iron, silicon, and aluminum, was discovered by the Japanese in 1936 and is used extensively by them in cast and powder form. The low permeability values (70–80) of Sendust powder cores precluded their acceptance in this country to any extent. The improved magnetic properties of the new flake cores, called Flakenol I, make them an attractive nonstrategic substitute for applications which now require powdered high nickel alloys. The permeability values as measured on compacts of this new flake core ranged from 150–280, with electrical losses as low as present powder cores. The very low eddy-current loss coefficient value measured on Sendust flake cores indicates their usefulness at higher frequencies than possible for present high permeability powder cores. The flake cores, which have a negative temperature coefficient of permeability, were stabilized by the addition of Alfenol flake material. The comparatively simple techniques for processing Sendust flake cores from the cast alloy are described, along with the factors which most influence their ultimate magnetic characteristics.

The Application of Pulse-Forming Networks—Alfred Graydon (p. 7)

This paper is intended to aid engineers—especially modulator and component engineers with their pulse-forming network application problems. The discussion includes an analysis of the circuitry in which pulse-forming networks are used, a discussion of case size limiting parameters, and a procedure indicating the calculations required to determine the approximate case size of new network requirement.

The Insulation Resistance of Capacitors After Long-Time Electrification—F. W. Grahame and D. F. Schmidt (p. 14)

In recent months design engineers have been interested in capacitors with extremely high values of insulation resistance not normally achieved in the common one- or two-minute electrification period. After long periods of electrification, insulation resistance values in the order of 100-million megohm microfarads and more can be achieved with some types of capacitors. Such high values can be accurately measured by the special measuring technique described in this paper, which also discusses the interpretation of test data taken at various temperatures and voltages on some typical Mylar capacitors. The concepts of instantaneous and equivalent parallel insulation resistance are developed and their significance discussed.

Environmental Effects on Precision Potentiometers—A. W. Green and K. S. Schulz (p. 18)

Current trends in design of military equipment have imposed on precision potentiometer manufacturers the necessity of meeting rigid environmental requirements. To fulfill these requirements, the authors' company inaugurated a test program to determine causes and effects of severe environmental conditions on precision potentiometer performance.

This paper is based on results obtained during three years of this program. The goals of this program were: 1) to determine the effects of increasingly severe environments on performance, 2) to determine what design changes were required to give the desired performance.

Special test techniques applicable to precision potentiometers were developed and potentiometer characteristics affected by each environment were determined.

Where design improvements in current models were found to be inadequate, the design of a new line of potentiometers using improved techniques and materials resulted in the desired improvement.

A Novel Construction Concept for Linear Delay Lines—Daniel Elders (p. 24)

Previous attempts to design lumped parameter delay lines having linear phase characteristics required the use of compensating capacitors or coils. This paper presents a novel concept in construction techniques which results in a linear phase delay line without the necessity of resorting to any compensating components. A step-by-step design procedure for a low-loss linear delay line is used to illustrate this new construction technique. This novel line has a nominal characteristic impedance of 500 ohms, delay of 10 microseconds, low attenuation, and a cutoff frequency of 4 megacycles.

This new work is based upon the theoretical treatment of the ideal low-pass filter by Golay. The ideal parameter relationships have been reduced to practical design considerations involving unique geometric placements of ferrite cored components.

Sealing Metal and Ceramic Parts by Forming Reactive Alloys—J. E. Beggs (p. 28)

Metal and ceramic parts are sealed by introducing a molten solder or by inserting a thin

sheet of metal that will form a reactive alloy. A wide choice of materials can be used, including many that seal at high temperatures with little metallic evaporation. Materials can be used that can be predegassed at temperatures considerably above those used for final sealing. The seals can be made in vacuum or in an inert gas. The parts can be stacked one on the other so that a multiplicity of seals can be made at the same time. By using a metal such as titanium, and ceramic parts having an expansion characteristic similar to that of titanium, seals can be made that are strong and can operate for many hours at temperatures as high as 800°C.

Microwave Theory & Techniques

VOL. MTT-5, NO, 2, APRIL, 1957

A method is presented for determining the capacitance of electrostatic fields which have hitherto proved intractable because their solutions required the evaluation of hyperelliptic integrals. The method is illustrated by applying it to the determination of the characteristic impedance of a strip transmission line. The results compare favorably with the results of existing solutions. The method is then used to determine the characteristic impedance of coupled strip transmission lines with inner conductors of rectangular shape. Curves are included which permit the determination of this impedance over a wide range of line proportions.

Analysis is given for the problem of reflection of a plane wave at oblique incidence on a wire grid which is parallel to a plane interface between two homogeneous dielectrics. It is assumed that the wire grid is a periodic structure and consists of thin cylindrical wires of homogeneous material. The equivalent circuit is derived where it is shown that the space on either side of the interface can be represented by a transmission line, and the grid itself is represented by a pure shunt element across one of the lines.

The two-dimensional Helmholtz equation is solved in a rectangle having two semicircular projections in the center of its broad faces. More particularly, the lowest two eigenvalues are determined for Neumann's boundary condition, and the lowest eigenvalue for Dirichlet's boundary condition. The results are of interest in various fields of physics, such as vibrations of a membrane, but are of particular importance in the study of waveguide propagation. The latter application is stressed in the article, in accordance with the practical importance of ridged waveguides.

This paper deals with the development of a new model for a class of microwave filters. With this model one can reproduce and systematize from a general viewpoint results now in the literature. Its most prominent feature, however, is that the use of the model permits the development of a synthesis procedure for the wide-band filter. From this single model a wide variety of structural realizations are readily obtained. Designs employing this model, and the appropriate synthesis, show significant improvement of desired characteristics over conventional designs. The general multiple quarter wave matching transformer problem is also discussed.

A single grounded dielectric slab can support either TM or TE modes, but cannot propagate both with the same velocity. This paper concerns a modification of the single slab which enables either polarization to propagate with the same velocity. Such a structure could transmit a circularly polarized wave, and would be be useful in transmission, feeder, and antenna applications.

The structure consists of a grounded dielectric slab with parallel metal plates imbedded in the dielectric, normal to and in contact with the ground plane. The plates do not reach the top of the slab. Propagation is *along* the plates, whereas corrugated surfaces propagate across the vanes. For small plate thickness, the TE field is undisturbed; hence, the entire slab thickness controls the velocity. The TM field, however, has an electric field component parallel to the plates, which is shorted out by the plates; thus, only the thickness of slab above the plates controls this mode, and the two modes can be independently controlled.

Since the plates are not a perfect short circuit, a boundary value analysis is given which finds the higher mode amplitudes, and the variation of effective short circuit with parameters. This analysis sets up a sum of modes in each region, and then solves the resulting sets of simultaneous transcendental equations by a contour integration-residue theory technique. The theory is illustrated by a specific example.

Reflections from randomly spaced transmission line discontinuities can cause serious attenuation and distortion of pulses in the lines, and the presence of reflections at the sending end may be undesirable. The effect of these discontinuities may be described in terms of the mathematics for combining outputs from oscillators with random frequencies. The location of the discontinuity corresponds to the frequency of an oscillator. The phase constant of the transmission line is analogous to time for the oscillators. Use of spectrum and filter analogies permits approximate determination of discontinuity locations from measurements. Use of known space and size distributions permits statistical prediction of attenuation and of size of reflected wave at the sending end.

The problem of predicting the probability distribution of vswr for many randomly spaced discontinuities is solved using the "central limit theorem." Assuming that reflection factors add in the complex plane and using the "central limit theorem" the result is shown to be a Rayleigh distribution in terms of the reflection factor.

The probability of the vswr over a band of frequencies is calculated using the concept that this band of frequencies can be considered as a number of statistically independent samples.

Because of growing applications of millimeter wave measurements, a fairly thorough investigation of what could be expected from sources and detectors in the 3 mm region was made. The sources consisted of fourth-harmonic generators from a 1.25 cm fundamental. A type of crystal holder for both harmonic generators and detectors in which a small crystal wafer is positioned in the broad wall of the millimeter waveguide, being contacted by a whisker passing across the waveguide (the open-guide type) was found to be superior in general to units using crystal cartridges or modifications thereof. Factors affecting the performance of these units have been investigated statistically. It was found that the short-circuit current sensitivity in microamperes per microwatt of a good crystal detector of the type described above is not greatly less than the value for crystals at lower microwave frequencies, so that the minimum detectable signal is about the same. As an additional result, evidence for an important effect in which the harmonic generation process degrades the signal-to-noise ratio of the source is presented and discussed.

A new group of circularly polarized microwave cavity filters is described. With a single circularly polarized cavity, a reflectionless filter is achieved that couples nearly 100 per cent of the energy from the main waveguide at the cavity resonant frequency. Two degenerate cavity modes may be excited, to produce a circularly polarized field, by coupling to the transverse and longitudinal waveguide magnetic fields or to the transverse electric and magnetic waveguide fields.

A theoretical analysis is presented as well as experimental results. The loss between the band-pass terminals of the reflectionless circularly polarized filter is identical with the loss in a conventional reflection-type band-pass filter with the same bandwidth and cavity-wall losses. The null at resonance between the band-elimination terminals of the reflectionless circularly polarized filter is limited only by the asymmetries of the cavity and not by the cavity-wall losses. Design equations and curves are given for eight of the lower order, circularly cylindrical, degenerate cavity modes that are coupled to a rectangular waveguide at the point of circularly polarized waveguide magnetic fields.

The design problems in a reference cavity include coupling, cavity Q, temperature compensation, stability, and hysteresis. Temperature compensation is shown to be a problem in second order compensation theory and is solved by material changes. Stability is achieved by novel mechanical design and by elimination of hysteresis producing members.

A procedure is presented for connecting some known physical applications of Fourier transform pairs in different branches of the theory of waves and circuitry. After an investigation of the cases of diffraction, reflection, and coupling of waves, deflection of particles (which includes the cathode-ray-tube case and so-called gap effect) and the closely related scanning problem are examined. Finally, extension to random functions is discussed briefly.

Projective constructions are described for deducing the iconocenter of a two-port junction from input reflection coefficient measurements taken with a short circuit placed in various positions in the output waveguide. The wavelength in the output line is deduced from a four-point measurement. If this wavelength is known in advance, a three-point measurement gives all the information needed to construct the iconocenter.

Production Techniques

PGPT-2, April, 1957

The purpose of this paper is to illustrate the responsibilities of product engineering and design in evolving printed wire products. The short cuts are the results of planning with maximum standardization. The products to be used for illustration are 23 servo-amplifier designs used in military airborne equipment. The quantity of amplifiers to be produced is not large and might be classified as a short-run type production. Printed wiring was decided upon on the basis of reduced unit cost and consistency of amplifier performance. It is important to point out that the products mentioned are part of a large system within a large company. Many of the principles illustrated herein are necessary because of the great coordination a large program requires.

The applied experimental psychologist, or human engineer, can be of great assistance in the design, production, and maintenance of simple or complex electronic equipment. By his knowledge of human sensory and motor characteristics, by systematic application of fundamental principles of psychology, physiology, and anthropometry, and by application of psychophysiological research techniques to machine problems, he can contribute to the development of compatible and more efficient man-machine systems. In many applications, reduction of human factor errors can be as important as the reduction of electromechanical errors.

This paper points out the relationship between human engineering, design approach, and engineering management. Application of electronic packaging with printed circuit design is discussed and several slides illustrating finished units are shown. A modern design approach is explained, both from management's standpoint and the design engineer's point of view. Design procedure is discussed and the various functions and responsibilities of a design group are outlined.

This paper discusses the basic concept of utilizing functional circuits and packaging them into modular end products. As the modular philosophy has advanced, the size of the modular assembly itself has decreased. Several different modes of encapsulation are discussed. Encapsulation by casting is presented. Trimming operations on the cast module are discussed. Encapsulation by pressure molding is compared to casting methods. It is shown that many of the disadvantages of the individual methods can be eliminated by the combination of these two encapsulation methods.

At the 1955 IRE National Convention, the author delivered a paper entitled "Guided Missile Reliability and Electronic Production Techniques." A general description was given of several contemporary concepts of automation-for-electronics. The present paper is a sequel to the previous report. An attempt is made to view objectively the various improved concepts and their advancing techniques, and to evaluate them in terms of present trends for their use. Three needed basic improvements for automatic electronic assembly machines are outlined, and a prediction is made that the early incorporation of these improvements will rapidly advance the acceptance and application of automation-for-electronics.

This paper describes the manufacture of the major sub-assemblies for the general purpose wire spring relay. Their mass production to close tolerances and at low cost has required the development of entirely new and different machines and techniques. Several machines of the type discussed are already in operation and more are under construction to satisfy the ever-increasing demand for these excellent relays.

The combination of such widely different kinds of processes into integrated machine units is a great step forward in the march toward the automatic factory so widely acclaimed in these modern times. Knowledge gained during this development has already been used by Western Electric in planning the manufacture of future communication apparatus and in lowering the cost of present Bell System products.

It will doubtless be recognized that automatic facilities of the type described require a major capital investment, the justification for which must depend upon a large and continuing demand as well as a stable product design.

The techniques of automation have been experiencing a rapid expansion in the past few years. It became apparent that standards should be arrived at to prevent chaos in this relatively new means of production.

In August of 1954, the Radio-Electronics-Television Manufacturers' Association organized a committee to propose standards in this field of automation. The great interest shown, by industry in general, indicated the urgent need for this type of action.

The progress, observations, and results of this standardization activity will be described and outlined in detail.

Progress in the mechanization of production testing of electronic products is reviewed. Several test equipments are described and evaluated. The necessity for considering the quality monitoring function of production as a continuous and integrated system is emphasized. This approach enables the test process planner to utilize the powerful tools of operations research in determining the nature of the test equipment and procedures required for optimum operation. A test system for the automatic factory is described. This system calls for the more efficient use of statistical sampling techniques as well as the more efficient feed-back of test data. Within the framework of this system, new requirements on test equipment have been developed. The activities of an industry-wide RETMA Task Group on Standards for Product Testing in Mechanized Production is described.

The trend today is the use of electronic variable speed drives in applications which normally would have been filled by rotating conversion units. Physically, electronic drives have a space and weight advantage over rotating equipment. Electrically, they lend themselves to precise control and rapid response to error signals.

Small drives using thyratrons to supply and control d-c motors are quite common. Large Ignitron and Excitron drives have been in successful use for many years. An electronic drive, the Xatron, using a grid controlled rectifier has been marketed in the 30 to 100 horsepower range. It is believed that this drive will capture the mass market for packaged drives within five to ten years. Chief use will be in the machine tool industry and for process control.

The optimum automatic process control system requires a continuous flow of information relating to the process variations. Radiation gauges utilizing absorption or scattering of radiation produced by a radioisotope source as a means of measuring thickness, weight per unit area, or density of a product offer a means for obtaining this information. Process control utilizing these gauges differs from the usual control system in that large delays exist between the measuring point and the control point. The existence of such delays requires the use of specialized control systems, usually utilizing interrupted control. A typical control system of this type is described and the safety precautions required to prevent malfunction or damage are discussed.

Rapidly rising steam temperatures and pressures in addition to new design techniques have vastly increased both the quantity and quality of x-ray and ultrasonic testing required. Consequently, the development pressure, particularly in ultrasonics, which in its modern form is of postwar birth, has been heavy. Some of the techniques, equipment and circuitry of present day inspection are described and the characteristics and operation of ultrasonic transducers noted.

Sodium iodide, the linear accelerator, and industrial television have brought the promise of mechanization to the examination of large castings, while the promulgation of acceptance standards and the use of ABC scan representation and recording gives equal promise of speeding up the inspection and quality control of forgings. Preliminary experiments and electronic design work towards these objectives are described.

An interesting development is the use of ultrasonics in nozzle-area determination, wall-thickness measurements on large castings, and liquid-level indication. Possibilities exist for automatic control of machining operations and liquid-level control. Distances and cross sections can be checked with accuracies of 0.1%. As a control device, the feedback nature of the system will tend to suppress dependence on machine or template accuracies.

Nearly every problem encountered in engineering at some time proceeds from the qualitative to the quantitative phase where the results of mathematical analysis must be applied in actual computation. Most often the computation is short enough that automatic means are not necessary. However, more and more problems are requiring powerful aids to calculation. This increase is due as much to expanded thinking encouraged by the mere availability of computers as to any actual backlog of work. Therefore it is to the engineer's advantage to know what computers can do for him, even though he may take his problem to someone else for final preparation and programming.

The following text presents some examples in which automatic calculation is being used. The logic used in choosing the computing meth-

ods is shown based on the characteristics of problem and computer. As background for the examples the most important of these characteristics are presented briefly in the next section.

Computers—The Key to Modern Manufacturing Scheduling—J. P. J. Gravel and T. F. Kavanagh (p. 90)

Manufacturing operations with poor scheduling plans are headed for trouble. Load capacity analysis is a technique for measuring the feasibility and desirability of proposed scheduling plans. Simply stated mathematically, load capacity analysis consists of a series of multiplications and additions. However, the numerous computations in a typical problem usually take more time than can be allowed. The paper describes a special purpose analog computer specifically designed to solve this problem in a matter of minutes.

A Tank Farm Data Reduction System—D. J. Gimpel (p. 94)

A tank farm data reduction system has been developed for the new Tidewater Oil Company installation in Delaware by the Armour Research Foundation and Panellit, Inc. The function of the unit is to secure the temperature corrected volume of fluid in each of the approximately 100 tanks in the field. The inputs to the system are the fluid height and average tank temperature. Fluid volume is tabulated digitally as a function of the height on magnetic tape. The system automatically searches the tape for the indicated volume and multiplies the number by the temperature correction factor. This paper describes the operation of the multiplier, the tape search elements, and the sensing instruments employed in the field. The factors governing the selection of the specific elements in the storage and computing system are also discussed.

(*Third Industrial Electronics Conference, Detroit, Mich., Sept. 28–29, 1955*)

Automation Re-Examined—J. J. Graham (p. 101)

The author re-examines the subject to reorient thinking along constructive lines which will utilize the concept as we use the many other valuable tools in our industrial storeroom. The mechanization involved in the production of printed boards is discussed. The requirements for numbers and training of people are increased rather than decreased, as outlined by the author.

The Industrial Electronics Concept—E. Mittleman (Abstract) (p. 103)

Analysis of a Motor Speed-Control System with an Analog Computer—W. J. Bradburn Abstract) (p. 103)

(*WESCON, Los Angeles, Calif., August 21–24, 1956*)

Problems of Semi-Mechanized Assembly of Electronic Test Equipment—C. S. Selby (p. 104)

This paper describes a method-system for assembly of precision electronic test equipment. It is pointed out, when considering all segments of the electronics industry, that assembly methods vary from one extreme to the other. On the one hand, simple bench methods are used for single and limited-unit production; while at the 1000-per-day end of the production spectrum, highly mechanized power-driven conveyor assembly is in order. It is emphasized, although the precision electronic test equipment manufacturer has the same general assembly problems, that his specific assembly requirements lie midway between the two assembly method extremes.

The production requirements of this typical test equipment manufacturer are summarized as varying from 10 per year to several hundred per month, with 30 per month as an average for their 280 different instruments. Two previous method-systems are discussed from which has evolved the present "Roller-Skate" conveyor system. The earlier "walk-around" system was used for large instruments and small-quantity production runs, while its companion "push-along" system was favored for smaller units especially if the production quantity was 50 or more. A 10% assembly-time saving is indicated when using the "push-along" method as compared to the "walk-around" method.

The present "Roller-Skate" conveyor system is described as built in 50-foot-bench units, at a total cost of $80.00 per 10-foot length. It is reported that assembly time was further reduced by 15 to 25%. Several other unanticipated benefits are listed such as taking advantage of the "flow" of sub-assemblies, inspection, testing calibrating, and shipping—to provide the required day-to-day output. A discussion of the 1-minute versus 8-minute time cycle is given. The conclusion is reached that assembly time was reduced, while using semi-skilled workers and with an improved quality of the product.

Eyelet Failure in Etched Wiring—W. J. Hodges (p. 109)

This paper points out that eyelets used on etched wiring boards, to receive component-part leads and to provide wiring connections, have been a source of unreliability. A study of the eyelet-failure problem is described, based upon microscopic examination of over 1500 eyeleted connections on defective assemblies. Inspection of failed eyelet connections shows solder separations between the crimped eyelet flanges and the etched conductors of as much as four thousandths of an inch. Laminate deformation and conductor lifting at the eyelet are also observed. The large thermal expansion of the board during soldering, and eyelet relaxation appear to place large stresses on the eyelets, resulting in failures. Solder joints made with tightly crimped eyelets are found to be mechanically weak, due to the lack of an adequate solder fillet.

This study helps to explain why circuit failures occur at eyelets and shows how they may be minimized through the use of improved design. An eyelet with a tapered flange is described which provides a much stronger solder joint, with a possible smaller diameter, and with a greater effective lead-entrance diameter.

Mechanical Design Consideration in the ERMA System—R. W. Melville (p. 115)

This paper examines some of the early 1954 design concepts of ERMA (Electronic Recording Machine, Accounting), developed for the Bank of America to record commercial checking-account activity. Standardized plug-in circuit and relay modules are described which include printed wiring, an adapter for in-rack testing, and controlled air flow. Emphasis is placed on reliability and easy access for maintenance and repair, by the use of integrated inter-rack raceway wiring, internal rack printed-wiring busses, and rear-access inter-connector wiring. The exclusive adoption of solderless connections for inter-package wiring, and the use of stock parts in preference to "specials" is stressed. It is discussed how standardization was accomplished in 22 different forms of 1500 electronic circuit packages, in the areas of connector pins, supply voltages, and distribution circuits.

An integrated method of cooling is outlined beginning with module-guiding metal rails fastened to a hollow shelf assembly; embracing shelf, rack, and cabinet ducts; and completed with under-floor plenums. The associated closed-loop cooling and filtering system is shown, which used a bypassed chilled-water arrangement and an electrostatic air filter.

Special equipment such as magnetic drums, cross-bar switch assemblies, and tape-transport mechanisms are treated. It is pointed out, when any complex device such as ERMA is being pioneered, that the design of the individual components must often be based on incomplete information—leading to a change in specifications as functional relationships become more apparent. A specific warning is sounded that the number of inter-rack leads are usually underestimated, with an attendant poor access to terminals. Sixteen photographs contribute to a detailed presentation of the completed design.

The Selection of Coatings for Printed Wiring—R. A. Martel and L. J. Martin (p. 125)

It is pointed out that printed wiring has given rise to a serious surface leakage problem, in contrast to standard wiring where volume leakage is predominant. Suitable insulating coatings are credited with protection against contamination and moisture entry, as well as with control of corona at high altitudes.

A coating material suitable for use on printed wiring boards is described as needing to possess high insulation resistance, superior humidity resistance, good adherence to both metals and plastics, chemical and physical stability under variable environments, and good mechanical properties. It is stated that practical consideration requires that the material be transparent so that component-part coding can be seen, that the cure temperature be tolerable to the boards and component parts, that application may easily and uniformly be made, and that factory and field repair be possible. Test procedures used in evaluating coatings for these properties are outlined and discussed. Examples of coated boards are shown.

A total of 48 coating materials, consisting of solvent proprietary blends and laboratory formulations, are evaluated. From the test results, a sprayable epoxy-polyamide formulation is found acceptable for use on printed wiring. The importance of the volume-resistance of a coating is indicated.

Calendar of Coming Events (p. 131)
News of the Chapters (p. 134)

Vehicular Communications

PGVC-8, May, 1957

(*Seventh Annual Meeting, Detroit, Mich., Nov. 29–30, 1956*)

Foreword—L. E. Kearney (p. 1)

Field Application of Transmission Quality Control in Mobile Radio Systems—R. D. Smith (p. 3)

An improved method is presented whereby a radio repairman can test the audio performance of a phase modulated transmitter in a mobile unit at an isolated location using a minimum of time and test equipment. Testing is done with signals at normal operating levels, as well as above limiting, to obtain a more uniform adjustment of modulation in different transmitters. When this is combined with other measurements that are more familiar, the repairman can obtain an index of audio performance at the mobile unit for both transmitting and receiving conditions. A reliable index is particularly useful in connection with narrow band operation as well as in wide band systems that are large enough to include mobile relay stations or multiple repeaters. Examples are given showing that previous methods of adjusting modulation in the field are inadequate for some present applications.

Railroad Radio Communication—L. E. Kearney (p. 11)

Mobile-Type radio equipment is employed in the railroad industry for communication on trains, between trains, between wayside stations and trains and between trains and railroad personnel on the ground and in other vehicles. It is also employed, particularly in ter-

minal areas, for communication between various groups of employees and their base of operations. Radio has been found to be capable of contributing to the safety, efficiency and economy of railroad operation.

A Selective Calling System to 106A Standards Employing Cold Cathode Thyratrons—W. Ornstein (p. 17)

A selective calling device is described which operates with the same coding signal as the 106A selector used by many common carrier companies. The unit is intended mainly for use in the land and maritime mobile services.

It differs from existing designs in the use of cold cathode thyratrons in sequential counter circuits in place of the presently used electromechanical devices.

The unit employs a printed circuit board, subminiature tubes and printed components to ensure compact construction and ease of maintenance. Cold cathode tubes are used to ensure reliability and to eliminate problems of heat generation.

The Important Role of Mobile Radio in the Growth of the Power Utilities—T. G. Humphreys, Jr. (p. 27)

The Design and Life of Planar Microwave Transmitting Tubes—H. D. Doolittle (p. 31)

The principal design features of planar triode transmitting tubes are reviewed: ruggedness, low inductance leads, cathode area, electrode spacings and cathode emission requirements. A progress report is given on life improvement from a few hundred to a few thousand hours for mobile equipment and to many thousands of hours for less critical applications. Some details are given on cathode evaluation studies with particular emphasis on tube life.

Obtaining Optimum Performance in a Mobile Communications System—E. A. Miller (p. 36)

Electronics Application in the County of Los Angeles—W. C. Collins (p. 45)

Mobile Radio Doesn't Cost, It Pays—R. L. Abel (p. 47)

Mobile radio has come of age within the trucking industry and let there be no doubt about it, it's here to stay. There are a number of reasons for this, but only two which I wish to discuss in detail. And the two reasons are probably the most important factors in the growth of mobile radio within the trucking industry.

Motor carriers have discovered that operating efficiency can be increased from the utilization of mobile radio. This is the primary reason for adopting mobile radio to trucking operations. The secondary reason is found in the economic advantages derived from this increased operating efficiency.

These advantages accrue ultimately to the shipping public and consumer.

Industry Prospers With Radio's Progress—E. L. White (p. 50)

A Low Power Industrial Communication Unit—A. F. Freeland (p. 54)

Two way radio communication units for industrial service have requirements which differ from those for transportation vehicles due to FCC regulations and the nature of industrial trucks. A unit designed especially for low power industrial service consists of a filamentary tube transmitter-receiver and a vibrator power supply capable of operation on a variety of voltage sources. The requirements and the unit itself are discussed.

Noise in Communications Antennas—Survey—M. W. Scheldorf (p. 60)

A study was made to determine the possibility of contributing to signal-to-noise ratio in communication systems by virtue of changes in design in the antenna used.

1. A thorough study of existing literature was made, in order to become acquainted with the sources of noise and the methods employed in the past to improve the antenna.

2. A customer survey was made to evaluate the various kinds of noise and to establish conditions which would permit improvement by antenna design.

Radio Speeds the Flow of Oil—J. E. Keller (p. 66)

Reasons For Establishing a "Service"—C. B. Plummer (p. 74)

Abstracts and References

Compiled by the Radio Research Organization of the Department of Scientific and Industrial Research, London, England, and Published by Arrangement with that Department and the *Electronic and Radio Engineer*, incorporating *Wireless Engineer*, London, England

NOTE: The Institute of Radio Engineers does not have available copies of the publications mentioned in these pages, nor does it have reprints of the articles abstracted. Correspondence regarding these articles and requests for their procurement should be addressed to the individual publications, not to the IRE.

The number in heavy type at the upper left of each Abstract is its Universal Decimal Classification number and is not to be confused with the Decimal Classification used by the United States National Bureau of Standards. The number in heavy type at the top right is the serial number of the Abstract. DC numbers marked with a dagger (†) must be regarded as provisional.

The Index to the Abstracts and References published in the PROC. IRE from February, 1956 through January, 1957 is published by the PROC. IRE, May, 1957, Part II. It is also published by *Electronic and Radio Engineer*, incorporating *Wireless Engineer*, and included in the March, 1957 issue of that journal. Included with the Index is a selected list of journals scanned for abstracting with publishers' addresses.

ACOUSTICS AND AUDIO FREQUENCIES

534.121 1623

The Composition Product of Difference Operators: Application to the Vibrations of Embedded Panels—J. Hersch. (*C.R. Acad. Sci., Paris*, vol. 244, pp. 299–302; January 14, 1957.)

534.213 1624

Propagation of Elastic Waves in Medium with Cylindrical Ducts—V. V. Tyutekin. (*Akust. Z.*, vol. 2, pp. 291–301; July–September, 1956.)

534.213.4 1625

Acoustic Constants for Tubes of Small Cross-Section—I. Barducci. (*Alta Frequenza*, vol. 25, pp. 355–377; October, 1956.) New formulas are derived for the calculation of primary and secondary acoustic constants, which allow for viscosity and thermal conduction but are not restricted by frequency and tube diameter limitations. The constants can be found with the aid of the graphs and tables given.

534.23:533.7 1626

Sound Radiation Pressure According to the Kinetic Theory of Gases—V. Gavreau. (*J. Phys. Radium*, vol. 17, pp. 899–904; October, 1956.)

534.231.3 1627

Influence of the Subsonic Stream Velocity on the Radiation Impedance of a Piston with an Infinite Flange—D. N. Chetaev. (*Akust. Z.*, vol. 2, pp. 302–309; July–September, 1956.) A theoretical paper.

534.232 1628

Calculation of Radiation Impedance of some Distributed Radiator Systems—M. I. Karnovski. (*Akust. Z.*, vol. 2, pp. 267–278; July–September, 1956.) The real component of radiation impedance of various distributed systems of coherent radiators is determined. Groups of spherical radiators are considered.

534.232:546.431.824-31 1629

Cylindrical Radiator of Barium Titanate Ceramic Radiating along its Axis—A. A. Anan'eva. (*Akust. Z.*, vol. 2, pp. 323–325; July–September, 1956.)

534.61–8 1630

Theory of the Ultrasonic Interferometer—V. A. Solov'ev. (*Akust. Z.*, vol. 2, pp. 285–290; July–September, 1956.) New formulas are given for calculating the absorption coefficient for ultrasonic waves from the results of interferometric measurements.

534.7 1631

Significance of Time Factors in the Perception of Complex Sounds—L. A. Chistovich. (*Akust. Z.*, vol. 2, pp. 310–316; July–September, 1956.) Results are reported of experiments on the perception of sound in the presence of noise or interference.

534.78:621.396.5 1632

Instantaneous Speech Compressor—C. R. Rutherford. (*Electronics*, vol. 30, pp. 168–169; February 1, 1957.) A miniature transistor compressor, for incorporation in the microphone lead of an aircraft transmitter, enables sideband power to be increased, giving greater range of communication.

534.84 1633

New Coefficients for the Assessment of Quality of Room Acoustics—E. E. Golikov. (*Akust. Z.*, vol. 2, pp. 255–266; July–September, 1956.)

534.851:681.85 1634

Locked Concentric-Grooved Disk for Use in Measurements of Disk-Reproducer Performance—J. Feinstein. (*J. Audio Eng. Soc.*, vol. 4, pp. 76–81; April, 1956.) The relative merits of signal grooves and closed concentric grooves for test records are discussed and some experimental results are given.

534.86:681.84 1635

The Radial Tone Arm—an Unconventional Phonograph Pickup Suspension—H. E. Roys and E. E. Masterson. (*J. Audio Eng. Soc.*, vol. 4, pp. 101–104; July, 1956.) The arrangement described uses a smooth rotating rod as lead screw and permits the pickup to follow a radial line, thus eliminating tracking error.

621.395.61.089.6 1636

Free-Field Technique for Secondary Standard Calibration of Microphones—A. L. Seligson. (*J. Audio Eng. Soc.*, vol. 4, pp. 110–115; July, 1956.) The method described includes automatic compensation for sound output-level changes with frequency of the source.

621.395.616:621.375.232.3 1637

A Cathode-Follower Pre-amplifier for Condenser Microphones—Riéty. (See 1709.)

621.395.623.52 1638

A Semicircular Exponential Horn—R. M. Cares. (*Audio*, vol. 40, pp. 26–29, 90; October, 1956.)An approximately semicircular horn made up of five square-pyramidal sections is described and illustrated; good response is obtained at frequencies down to 40 cps.

621.395.623.7 1639

Recent Investigations of "Son Rauque" in Loudspeakers—J. B. Fischer. (*Arch. elekt. Übertragung*, vol. 10, pp. 441–454; October, 1956.) The conditions giving rise to subharmonic vibrations of loudspeaker cones are studied. Low mass, high stiffness, and, above all, high damping of the cone material are desirable, in order to keep such vibrations to a minimum. A certain amount of subharmonic vibration is tolerable; distortion due to this cause does not provide a criterion for subjectively perceived distortion. The vibration waveforms of a number of cones were observed; they indicate that the load exerts a radial rather than an axial action. Improvement is achieved by providing damping rings on the outer third of the cone.

621.395.623.743 1640

The Isophase Loudspeaker—T. Lindenberg. (*J. Audio Eng. Soc.*, vol. 4, pp. 56–59; April, 1956.) Brief description of two models of a push-pull "inert-diaphragm;" *e.g.*, loudspeaker having a large diaphragm area. Their frequency response is flat from 400 cps and 1000 cps respectively up to 20 kc.

621.395.625.3+534.862 1641

New Products and New Applications in the Magnetic-Tape and Film Fields—E. W. Franck and E. Schmidt. (*J. Audio Eng. Soc.*, vol. 4, pp. 90–100; July, 1956.) An outline of progress achieved up to 1954 with illustrations of some American equipment.

621.395.625.3:621.397.5:535.623 1642

Color TV on Tape—Lamont. (See 1920.)

ANTENNAS AND TRANSMISSION LINES

621.315.2:621.317.341.3 1643

Variation of Cable Loss with Standing Wave Ratio—E. G. Hamer. (*J. Brit. IRE*, vol. 17, pp. 121–124; February, 1957.) Formulas and nomograms are derived.

621.372 1644

Influence of Inhomogeneities on the Propagation of Electromagnetic Waves in Periodic

Structures—V. I. Bespalov and A. V. Gaponov. (*Radiotekhnika i Elektronika*, vol. 1, pp. 772–784; June, 1956.) The effect on the propagation of em waves of random inhomogeneities in transmission lines with periodic-profile guide surfaces is considered theoretically using equivalent circuits. The treatment leads to a difference equation of the second order with random coefficients which is solved by pertubation methods. Formulas are obtained for the dispersion of the reflection coefficient at the entrance to the inhomogeneous section of the line. Examples considered include a comb. delay line and an interdigital system.

621.372.2 1645
Dilemmas in Transmission-Line Theory—E. G. Godfrey; I. F. Macdiarmid and H. J. Orchard; R. A. Chipman. (*Electronic Radio Eng.*, vol. 34, p. 150; April, 1957.) Comments on 984 of 1957 and author's reply.

621.372.2 1646
Capacitance of Shielded Balanced-Pair Transmission Line—A. W. Gent. (*Elect. Commun.*, vol. 33, pp. 234–240; September, 1956.) A concise formula for the capacitance is derived by the method of images, and its range of validity is shown to be wider than that of formulas previously obtained by various authors.

621.372.2:621.37.049.75 1647
Printed-Circuit Directional Coupler—(*Electronic Radio Eng.*, vol. 34, pp. 133–134; April, 1957.) Description of a printed-circuit equivalent of the coaxial-cable directional coupler described by Monteath (2522 of 1955).

621.372.2.029.6:621.318.134:621.318.57 1648
Microwave Ferrite Phase Shifter—S. Sensiper. (PROC. IRE, vol. 45, p. 359; March, 1957.) A helical transmission line with a ferrite tube mounted inside the helix is described, and the performance as a sideband modulator is described and analyzed.

621.372.51.012 1649
L-Network Design—Mathis. (See 1686.)

621.372.8 1650
Note on Coaxial-Line/Waveguide Junctions. The Case of Thin Structures—A. Leblond. (*Ann. Radioélect.*, vol. 11, pp. 331–338; October, 1956.) The general equations for the components of the input impedance are derived and the concept of "thin structure" is defined. A method of determining the transmission parameters for such structures is described.

621.372.8 1651
Graphical Method of Determining the Efficiency of Two-Port Networks—E. F. Bolinder. (PROC. IRE, vol. 45, p. 361; March, 1957.)

621.372.8:621.376.22.029.64 1652
Amplitude Modulation of Microwaves by Tunable Transmission Waveguide Filters—M. H. N. Potok and J. Barbour. (*J. Brit. IRE*, vol. 17, pp. 109–113; February, 1957.) Modulation is effected by shifting the pass band of the waveguide filter by the modulating signal. A linear response and a bandwidth 4 kc have been obtained using simple components and circuits.

621.396.67.012.12:523.16 1653
Investigation of Aerials using Cosmic Sources of Radio Emission with Finite Dimensions—O. A. Boguslavtsev, A. P. Molchanov, P. V. Olyanyuk, and L. M. Ponomarenko. (*Radiotekhnika i Elektronika*, vol. 1, pp. 873–877; June, 1956.) The use of radiation from the sun and moon in determining antenna directivity characteristics is considered theoretically. Uniform disk brightness is assumed.

621.396.67.029.6 1654
A Universal Scanning Curve for Wide-Angle Mirrors and Lenses—J. F. Ramsay. (*Marconi Rev.*, vol. 19, pp. 150–159; 4th Quarter, 1956.) A curve is derived showing loss of gain on scanning of a coma-corrected focusing element-lens or mirror. Although normalized to an aperture of 100λ and $F=1$, it is applicable to other diameters and focal lengths at any wavelength, subject to restrictions dependent on the assumptions. Agreement with measured performances is shown. The use of the curve in determining the scanning performance of offset fed mirrors of circular profile symmetry is described.

621.396.67.029.64 1655
Misfocusing and the Near-Field of Microwave Aerials—D. H. Shinn. (*Marconi Rev.*, vol. 19, pp. 141–149; 4th Quarter, 1956.) "Curves are presented showing: *a*) the theoretical radiation patterns of a misfocused lens or mirror with a circular boundary and *b*) the near-field of the same antenna correctly focused. Some practical applications of these are briefly discussed."

621.396.677.75:621.396.965 1656
Ferrod Radiator System—F. Reggia, E. G, Spencer, R. D. Hatcher, and J. E. Tompkins. (PROC. IRE, vol. 45, pp. 344–352; March, 1957.) Arrays of microwave (3-cm-λ) ferrite dielectric tapered-rod antennas are described. The high dielectric constant of the ferrite allows the rod diameters to be about $\frac{1}{4}$ inch and a short feed section forming the mechanical support simplifies adjustment and reduces tolerances necessary for the rods. Methods of changing the polar diagram by magnetic switching have also been developed.

AUTOMATIC COMPUTERS

681.142 1657
An Accumulator Unit for a Dekatron Calculator—R. Townsend and K. Camm. (*Electronic Eng. London*, vol. 29, pp. 58–64; February, 1957.) Decimal numbers may be added or subtracted, the sum being returned to the main store multiplied or divided by ten or unity. The calculator has a punched-card input.

681.142:51 1658
Introduction to a Theory of Ensembles based on the Prime Numbers Assimilable by Electronic Computers—S. Sabliet. (*C.R. Acad. Sci., Paris*, vol. 244, pp. 35–38; January 2, 1957.) Computers of "ordinator" type can be made to provide algebraic solutions of equations by coding the functions to be operated on as prime numbers.

681.142:621.314.2 1659
Application of a Digital Computer to the Design of Power Transformers to Specification—C. L. Moore, W. T. Duboc, and P. A. Zaphyr. (*Commun. & Electronics*, no. 24, pp. 134–137; May, 1956. Discussion, pp. 137–138.)

681.142:621.314.63 1660
Application of Semiconductor Diodes in Circuits of Nonlinear Units of Electrical Analogue Apparatus—G. M. Petrov. (*Avtomatika i Telemekhanika*, vol. 17, pp. 707–716; August, 1956.)

681.142:621.316.11 1661
Automatic Network Analysis with a Digital Computation System–S. Y. Wong and M. Kochen. (*Commun. & Electronics*, no. 24, pp. 172–175; May, 1956. Discussion, p. 176.) A general outline of the procedure and a method of solution are given.

681.142:621.318.134 1662
Ferrite Apertured Plate for Random Access Memory—J. A. Rajchman. (PROC. IRE, vol. 45, pp. 325–334; March, 1957.) An experimental prototype plate has 256 holes of 0.025 inch in a 0.830-inch square. A current of 330 ma reverses the magnetization around a hole in 1.5 μsec and produces 30 mv. The hysteresis loop has good rectangularity and the properties of the holes are uniform within ± 5 per cent. Several novel switching principles are proposed, and it is claimed that the construction of a ferrite memory plate system with printed windings requires much less time and labor than corresponding techniques with conventional cores.

681.142:621.375.3 1663
A Magnetic-Amplifier Switching Matrix—D. Katz. (*Commun. & Electronics*, no. 24, pp. 236–241; May, 1956.) The circuit described translates a four-digit binary code into an electronically displayed decimal output.

681.142:621.395.625.3 1664
High-Density [magnetic-] Tape Recording for Digital Computers—(*Elec. Mfg.*, vol. 56, pp. 153, 290; November, 1955.) Digital pulse densities of up to 700/inch can be recorded by the method described which was developed by the National Bureau of Standards for use with the SEAC computer. See also 31 of 1956.

681.142.002.2 1665
Factory for Eelectronic Digital Computers—(*Engineer, London*, vol. 202, p. 593; October 26, 1956.) Design features of the "Pegasus" and "Mercury" computers are discussed.

CIRCUITS AND CIRCUIT ELEMENTS

621.314.6.01 1666
Rectifier and Contact-Rectifier Circuits—O. B. Lupanov. (*C.R. Acad. Sci. U.R.S.S.*, vol. 111, pp. 1171–1174; December 21, 1956. In Russian.) The synthesis of circuits realizing given functions and comprising a minimum number of elements is considered mathematically.

621.318.57 1667
Frequency-Sensitive Switching Circuit—J. B. Earnshaw. (*Rev. Sci. Instr.*, vol. 27, pp. 1041–1043; December, 1956.) "A frequency-sensitive switching circuit is described which automatically selects between two ranges of an otherwise conventional frequency meter by switching the leak resistor of the integrating circuit."

621.318.57:621.387 1668
Dekatron Drive Circuit and Application—M. Graham, W. A. Higinbotham, and S. Rankowitz. (*Rev. Sci. Instr.*, vol. 27, pp. 1059–1061; December, 1956.) "A reliable, one-tube drive circuit for decade glow-transfer counter tubes is described. Application of the circuit is illustrated in a ten-channel glow-tube register with automatic electric-typewriter readout."

621.319.4 1669
Capacitors Subjected to Voltage Pulses: Prediction of Heating Effects—J. Peyssou. (*Ann. Radioélect.*, vol. 11, pp. 281–292; October, 1956.) Heat dissipation can be calculated for pulse conditions by assuming the simultaneous application to the capacitor of all components of the Fourier analysis.

621.319.43 1670
Calculation of the Capacitance of a Variable High-Precision Capacitor with Plane Plates—R. Lacoste and G. Giralt. (*C.R. Acad. Sci., Paris*, vol. 244, pp. 321–324; January 14, 1957.) A systematic investigation is made of possible sources of error, and an upper limit for errors is determined as a function of the mechanical characteristics.

621.319.47:621.385.833.032.2 1671
Potential in Doubly Curved Condensers—Albrecht. (See 1877.)

621.37.049.75:621.3.032.5 1672
New Design in Ruggedized P.C. [printed-

circuit] Connectors—H. E. Ruehlemann. (*Electronic Ind. Tele-Tech*, vol. 15, pp. 62–63, 162; October, 1956.)

621.37.049.75:621.319.4 1673
A Unique Printed-Circuit Capacitor—J. R. Woods. (*Electronic Ind. Tele-Tech*, vol. 15, pp. 59, 157; October, 1956.) Description of a commercially produced ceramic capacitor which is leadless and flat, suitable for insertion into slots in the printed-circuit board prior to dip-soldering.

621.372.01 1674
Some Considerations on the Realizability of Electrical Circuits—I. Gumowski. (*C.R. Acad. Sci., Paris*, vol. 244, pp. 317–319; January 14, 1957.)

621.372.029.64:538.569.4 1675
Molecular Amplification and Generation of Microwaves—Wittke. (See 1733.)

621.372.029.64:538.569.4 1676
Molecular-Beam Oscillator—Bason. (See 1734.)

621.372.2:621.314.2 1677
Properties of an Adjustable Line Transformer—H. K. Ruppersberg. (*Arch. elekt. Übertragung*, vol. 10, pp. 438–440; October, 1956.) Use of a six-terminal network with uniform input and output lines is discussed, and an analysis is made of the effect on the location of the input and output transformation reference points, and on the transformation factor, of moving a short-circuit along the second output line.

621.372.4 1678
The Decomposition into Energy Terms of the Operational Impedance of a Two-Terminal Network—L. Lunelli. (*Alta Frequenza*, vol. 25, pp. 391–410; October, 1956.) Derivation of further theorems with reference to earlier work (39 and 3295 of 1956).

621.372.412.029.45:549.514.51 1679
Flexural-Mode Quartz Crystals as A.F. Resonators—Bechmann and Hale. (See 1836).

621.372.413:[537.226+538.221 1680
Note on Cavity Perturbation Theory—E. G. Spencer, R. C. LeCraw, and L. A. Ault. (*J. Appl. Phys.*, vol. 28, pp. 130–132; January, 1957.) A criterion for the validity of the theory is presented.

621.372.5 1681
Synthesis of Linear Systems with the Aid of *RLC* Elements—R. Kulikowski. (*Bull. Acad. Polon. Sci., Classe 4e*, vol. 4, pp. 287–292; 1956. In English.)

621.372.5 1682
Synthesis of Transfer Functions with Poles Restricted to the Negative Real Axis into Two Parallel RC Ladders and an Ideal Transformer—M. G. Malti and Hun Hsuan Sun. (*Commun. & Electronics*, no. 24, pp. 165–171; May, 1956. Discussion, p. 171.)

621.372.5 1683
Network Synthesis for a Prescribed Impulse Response using a Real-Part Approximation—R. A. Pucel. (*J. Appl. Phys.*, vol. 28, pp. 124–129; January, 1957.) A semi-graphical scheme is presented with examples illustrating synthesis procedure.

621.372.5.011.1 1684
The Synthesis of Loss-Free Quadripoles from Lines with Nonuniform Characteristic Impedance—H. Meinke. (*Nachrichtentech. Z.*, vol. 9, pp. 457–461; October, 1956.) Approximation methods of solving impedance transformation problems by means of series expansions are outlined.

621.372.51 1685
Network Matching Problems—E. L. Topple. (*Electronic Radio Eng.*, vol. 34, p. 151; April, 1957.) Comment on 1019 of 1957 (Deignan).

621.372.51.012 1686
L-Network Design—H. F. Mathis. (*Electronics*, vol. 30, pp. 186, 188; February 1, 1957.) Description of a technique for using a Smith chart to determine transducing networks for transmission lines and waveguides.

621.372.54 1687
Some Quadripole Transformations—J. E. Colin. (*Câbles & Transm.*, vol. 10, pp. 314–334; October, 1956.) Norton's method of transformation is applied to several types of filter circuit and used to form three-branch networks. The negative capacitance arising from the transformation can be suppressed in the case of a band-pass filter derived from a low-pass filter. A summary of transformation formulas is appended.

621.372.54 1688
Graphical Construction of the Image Attenuation, with or without Losses, of a Ladder Filter with One or Two Cut-Off Frequencies—J. Bimont. (*Câbles & Transm.*, vol. 10, pp. 335–355; October, 1956.) The nomogram method described is illustrated by a numerical example.

621.372.54 1689
The Transmission Constants of Networks with a Given Transient Response—V. Fetzer. (*Nachrichtentech. Z.*, vol. 9, pp. 462–468; October, 1956.) The constants for low-pass and narrow band-pass filters are calculated by means of Laplace transformations. Formulas and curves are given for a number of input and response functions. See also 960 of 1955.

621.372.54 1690
The Characteristics of Parallel-T *RC* Networks—D. H. Smith. (*Electronic Eng., London*, vol. 29, pp. 71–77; February, 1957.) Balanced and unbalanced networks are analyzed and typical curves of magnitude and phase of the transmission ratio are given. The use of the unbalanced type in an oscillator is described.

621.372.54:621.396.621.54 1691
Some Aspects of Intermediate-Frequency Filtering in a Receiver—J. Carteron. (*Câbles & Transm.*, vol. 10, pp. 263–278; October, 1956.) The design of ladder-type half-sections, including those of variable selectivity, and of improved crystal-filter networks is discussed. Examples of filter design calculations are given with tabulated values of attenuation and phase shift.

621.372.54+621.372.553:621.397.24 1692
Filters and Delay Equalizers for Television Transmission on Cables—Keil. (See 1917.)

621.372.56.029.62 1693
V.H.F. Variable Attenuators—B. G. Martindill. (*Wireless World*, vol. 63, pp. 181–182; April, 1957.) Continuously variable ladder attenuators suitable for use up to 200 mc are formed by press stamping from a thin insulator base with a carbon coating.

621.372.57 1694
The Analytical Representation of Active Quadripoles—J. Piesch. (*Arch. elekt. Übertragung*, vol. 10, pp. 429–437; October, 1956.)

621.372.57 1695
The Theory of Noisy Quadripoles and its Application—(*Telefunken röhre*, no. 33, pp. 1–145 and A1–A89; October, 1956.) A group of papers covering modern theory and applications. Sixty-eight references are given some of which have been noted previously [*e.g.*, 2665 of 1956 (Rothe and Dahlke) and 636 of 1957 (Bauer and Rothe)].

621.373:621.317.361 1696
Theory of the Spectral Line Width of Radio-Frequency Generators and its Measurement by the Method of I. L. Bershtein—V. S. Troitski. (*Radiotekhnika i Elektronika*, vol. 1, pp. 818–830; June, 1956.) For Bershtein's paper (*Zh. Tekh. Fiz.*, vol. 11, pp. 305–316; 1941), see 1649 of 1942.

621.373.029.64:621.396.822 1697
Noise-Diode Generator for the 3-cm Band—S. I. Averkov, V. I. Anikin, D. M. Bravo-Zhivotovski, A. V. Gaponov, M. T. Grekhova, V. S. Ergakov, V. A. Lopyrev, M. A. Miller, and V. A. Flyagin. (*Radiotekhnika i Elektronika*, vol. 1, pp. 758–771; June, 1956.) The construction and operation of a microwave noise generator in the form of a coaxial diode slot-coupled to a waveguide T-junction is described.

621.373.42:621.316.86 1698
The Use of Thermistors for the Compensation of Thermal Drift in Self-Oscillating Circuits—P. Guené. (*Ann. Radioélect.*, vol. 11, pp. 317–330; October, 1956.) Formulas for calculating frequency drift are derived theoretically. Examples show that in the case of a particular 0.75–1.5-mc oscillator the frequency drift can be reduced to about 3 parts in 10^6 per °C.

621.373.42:621.373.1.029.4 1699
Very-Low-Frequency Generator—P. Dupin. (*C.R. Acad. Sci., Paris*, vol. 244, pp. 319–321; January 14, 1957.) The arrangement described comprises a pair of rotating capacitors of complementary configuration connected in series and associated with an inductance so as to form a resonant circuit. A hf voltage of constant amplitude is applied, and sinusoidal-envelope voltages in phase opposition are derived from the two capacitances and rectified. The output frequency is dependent on the rotation rate.

621.373.421 1700
Constant-Frequency Oscillators—D. A. Bell. (*Electronic Radio Eng.*, vol. 34, p. 150; April, 1957.) Comment on 697 of 1956 (Gladwin).

621.373.431:621.385.5 1701
Relaxation Oscillator using a Gated Beam Tube—C. E. Tschiegg. (*Rev. Sci. Instr.*, vol. 27, pp. 1085–1086; December, 1956.)

621.373.52:681.142 1702
Linear Sweep-Voltage Generators and Precision Amplitude Comparator using Transistors—L. C. Merrill and T. L. Slater. (*Elect. Commun.*, vol. 33, pp. 228–233; September, 1956.)

621.374:621.372.5 1703
Pulse Shaping to a Given Monotonic Discharge Function—K. G. Fancourt and J. K. Skwirzynski. (*Marconi Rev.*, vol. 19, pp. 176–182; 4th Quarter, 1956.) A method of approximating a required discharge function is described; it is realizable in the form of a *RC* network.

621.374.4 1704
Electronic Multiplier Circuit—L. Sideriades and J. Brunel. (*C.R. Acad. Sci., Paris*, vol. 244, pp. 176–178; January 7, 1957.) A multiplier derived from the four-position flip-flop circuit described by Sideriades (2339 of 1956) is discussed.

621.374.4:621.396.41 1705
Reference Generator for S.S.B. Systems—M. I. Jacob. (*Electronics*, vol. 30, pp. 152–155; February 1, 1957.) "Applicable to scatter propagation, equipment uses stable frequency

generator employing phase-locked oscillators to provide accurate reference frequencies for ssb generator. Beam-switching tube used in frequency-dividing circuits permits coverage of 2 to 30-mc range in 1-kc steps."

621.375.2.029.3 1706
Inexpensive High-Quality Amplifier—P. J. Baxandall. (*Wireless World*, vol. 63, pp. 108–113, March; pp. 168–172, April, 1957.) Design and construction details of an af amplifier with 5-w push-pull output stage are given with results of measurements and comparative listening tests.

621.375.2.029.3 1707
Design for a 50-Watt Amplifier—W. I. Heath and G. R. Woodville. (*Wireless World*, vol. 63, pp. 158–163; April, 1957.) Incorporates two pentodes Type KT88 in an "ultralinear" output stage.

621.375.232.029.4 1708
An Output-Transformerless Amplifier—H. Amemiya. (*J. Audio Eng. Soc.*, vol. 4, pp. 72–75; April, 1956.) The amplifier described has a flat frequency response up to 30 kc with 20 db negative feedback; its output is 3 w into 600 Ω for an input of 0.8 v.

621.375.232.3:621.395.616 1709
A Cathode-Follower Pre-amplifier for Condenser Microphones—P. Riéty. (*Ann. Télécommun.*, vol. 11, pp. 198–206; October, 1956.) Several practical circuits are analyzed with special attention to stability and low background noise.

621.375.3 1710
Magnetic Amplifiers—(*Electronic Radio Eng.*, vol. 34, pp. 118–123; April, 1957.) A general discussion of the principles of operation, advantages, and limitations is followed by a brief description of their various applications.

621.375.4 1711
Stability and Power Gain of Tuned Transistor Amplifiers—A. P. Stern. (PROC. IRE, vol. 45, pp. 335–343; March, 1957.) The theoretical maximum power gain realizable as a function of a required degree of stability is discussed for single- and multi-stage amplifiers.

GENERAL PHYSICS

530.1:51 1712
On the Perturbation Theory of Small Disturbances—A. Dalgarno and A. L. Stewart. (*Proc. Roy. Soc. A*, vol. 238, pp. 269–275; December 18, 1956.) Conventional perturbation theory is re-examined and a number of useful properties are emphasized.

530.16 1713
Causality and the Dispersion Relation: Logical Foundations—J. S. Toll. (*Phys. Rev.*, vol. 104, pp. 1760–1770; December 15, 1956.) A rigorous proof is given, for a linear system, of the logical equivalence of strict causality ("no output before the input") and the validity of a dispersion relation; *e.g.*, the relation expressing the real part of a generalized scattering amplitude as an integral involving the imaginary part.

535.14 1714
Light Waves and Photons—(*Electronic Radio Eng.*, vol. 34, pp. 130–133; April, 1957.) A discussion of the particle theory of light in which the author endeavors to describe in simple terms the nature of the photon.

535.22 1715
New Method of Measuring the Velocity of Light—K. S. Vul'fson. (*C.R. Acad. Sci. U.R.S.S.*, vol. 109, pp. 929–930; August 11, 1956. In Russian.) A modified version of Fizeau's method is proposed. The equipment comprises a triggered light-pulse source, distant mirror, photocell, and pulse amplifier, the output of which is used to trigger the source. The pulse repetition frequency is a function of the circuit delay constant, the light path length and the velocity of light. Using pulses of 10^{-7}–10^{-8} sec and a path a few meters long a result accurate to one part in 10^7–10^8 should be attainable.

535.33.07 1716
The Role of the Receiver in the Determination of the Elements of a Grating Spectrometer: Application to the Far Infrared ($20\mu < \lambda < 1000\mu$)—M. A. Hadni. (*Ann. Phys., Paris*, vol. 1, pp. 765–778; September/October, 1956.) The prospects of improving resolution by using more powerful signal sources and appropriately designed radiation detectors are discussed.

537.226:530.145:538.569.4 1717
Quantum Theory of Dielectric Relaxation—E. P. Gross and J. L. Lebowitz. (*Phys. Rev.*, vol. 104, pp. 1528–1531; December 15, 1956.) The statistical behavior of a system coupled to a reservoir at constant temperature is treated, assuming that the interactions are impulsive.

537.311 1718
The Electron-Phonon Interaction, according to the Adiabatic Approximation—J. C. Taylor. (*Proc. Camb. Phil. Soc.*, vol. 52, pp. 693–697; October, 1956.) Further application of Ziman's work (1355 of 1956) to calculate the self-energy of conduction electrons.

537.523:621.314.6 1719
Studies of Rectification in a Gas (Nitrogen) Discharge between Coaxial Cylindrical Electrodes: Part 3—Rectification in Full Ozonizers—V. L. Talekar. (*J. Electronics*, vol. 2, pp. 341–357; January, 1957.) Potential variation of rectification is studied at pressures from 6 to 350 mm Hg. Parts 1 and 2: 1391 of 1957.

537.525 1720
The Generation of Direct Current by a High-Frequency Discharge: Part 1—M. Chenot. (*J. Phys. Radium*, vol. 17, pp. 842–848; October, 1956.) Discussion of the results of further experiments on the effects previously investigated (2262 of 1955 and back references).

537.525:621.396.822:621.317.7.029.6 1721
Helix-Type Gaseous-Discharge Noise Sources at Low Plasma Densities—H. Schnitger. (*J. Electronics*, vol. 2, pp. 368–377; January, 1957.) The behavior of the positive column of a helium discharge is investigated theoretically and experimentally at 1.8 kmc. The measured attenuation shows good agreement with theory, but the noise figure is too low for the value predicted by the ambipolar diffusion theory.

537.525.5:538.561 1722
An 8-Volt Cold-Cathode Mercury Arc Emitting Microwaves—K. D. Froome. (*Nature, London*, vol. 179, pp. 267–268; February 2, 1957.) A vacuum arc struck between a liquid Hg cathode and a vertical thin tungsten-wire anode emits microwave noise when running at minimum arc length. With the arc coupled to a coaxial-line resonator, the measured output was about 50 μw in a band approximately 200 mc wide centered on 3 kmc; under these conditions the potential difference across the arc was less than 7.5 v dc.

537.533 1723
Electron Emission from Mechanically Worked Metal Surfaces on Oxidation—J. Lohff. (*Z. Phys.*, vol. 146, pp. 436–446; October 16, 1956.) Experimental results indicate that chemically active metals, after surface treatment with a steel brush, emit electron currents whose intensities are markedly sensitive to the presence of oxygen in the containing vessel, but not of nitrogen. The intensities are lower at higher temperatures. As a function of time after the treatment, the emission first increases and then decreases. Irradiation by uv or X rays gives rise to practically no delayed emission. These results are not consistent with the trap mechanism suggested; *e.g.*, by Seeger (2914 of 1955).

537.533:537.534.8 1724
Effect of Monolayer Adsorption on the Ejection of Electrons from Metals by Ions—H. D. Hagstrum. (*Phys. Rev.*, vol. 104, pp. 1516–1527; December 15, 1956.) Monolayer adsorption of a foreign gas (N_2, N_2, or CO) on an atomically clean tungsten surface decreases the electron yield, primarily at the expense of the faster electrons ejected from the metal.

537.56:533.7 1725
On the Dynamics of a Nonuniform Electrically Conducting Fluid—G. H. A. Cole. (*Nuovo Cim.*, vol. 4, pp. 779–785; October 1, 1956. In English.) First steps are taken towards building up a kinetic theory of ionized fluids under nonuniform conditions. The Boltzmann-Maxwell and Fokker-Planck equations are related to molecular data, and in this way the approximations involved in their use are made clear.

537.56:536.7 1726
Solution of Boltzmann's Equation for an Imperfect Lorenz Gas. Application to Weakly Ionized Gases—M. Bayet, J. L. Delcroix, and J. F. Denisse. (*C.R. Acad. Sci., Paris*, vol. 244, pp. 171–173; January 7, 1957.) Extension of theory presented previously.

538.13 1727
Microinhomogeneities in Magnetic Fields—H. H. Brown, Jr., and F. Bitter. (*Rev. Sci. Instr.*, vol. 27, pp. 1009–1012; December, 1956.) For a given magnet pole face, the field variations were found to be all about the same size; they decreased exponentially from the pole face.

538.56:536.33 1728
Thermal Radiation of Good Conductors—M. L. Levin. (*Zh. Eksp. teor. Fiz.*, vol. 31, pp. 302–316; August, 1956.) The radiation in the wave zone is calculated by methods of the electrodynamical theory of thermal fluctuations for the limiting cases of wavelengths small and large in comparison with the radiator dimensions. The radiation from bodies with surface anisotropies is studied. The fluctuation field near conducting surfaces (metallic plane, focus of parabolic mirror, and center of spherical mirror) is considered. Fluctuation surface charges are calculated.

538.56:537.5 1729
Observation of Gyromagnetic Resonance of Electrons in a Disintegrating Plasma—Yu. V. Gorokhov. (*Radiotekhnika i Elektronika*, vol. 1, pp. 794–797; June, 1956.) The experiments reported were performed on hydrogen and helium gas at pressures between 3×10^{-3} and 4 mm Hg in an antenna switch placed in a constant magnetic field.

538.566:535.42]+534.26 1730
On the Propagation of Pulses: Part 1—Diffraction of Pulses by Wedges—F. Oberhettinger. (*Z. Phys.*, vol. 146, pp. 423–435; October 16, 1956. In English.) Diffraction of an em or an acoustic pulse by a perfectly reflecting wedge is investigated, using a method based on representation of a function by a Laplace transform and on the solution of the corresponding time-harmonic problem.

538.566.2 1731
Propagation in a Gyrational Medium—L. G.

Chambers. (*Quart. J. Mech. Appl. Math.*, vol. 9, pp. 360–370; September, 1956.) "The electromagnetic properties of media such that $\mathbf{D}=\epsilon\mathbf{E}+\zeta\mathbf{H}$, $\mathbf{B}=\zeta\mathbf{E}+\mu\mathbf{H}$ are discussed. It is shown that each field component obeys the equation $\nabla^2\mathbf{F}+i\omega(\zeta-\xi)\nabla\times\mathbf{F}+\omega^2(\mu\epsilon-\zeta\xi)\mathbf{F}=0$ and that such media are accordingly doubly refracting. Integral forms for Maxwell's equations are also discussed."

538.569.4:621.372.029.64 1732

Geometrical Representation of the Schrödinger Equation for Solving Maser Problems—R. P. Feynman, F. L. Vernon, Jr., and R. W. Hellwarth. (*J. Appl. Phys.*, vol. 28, pp. 49–52; January, 1957.) A simple rigorous geometrical picture is developed to describe the resonance behavior of a quantum system when only a pair of energy levels is involved.

538.569.4:621.372.029.64 1733

Molecular Amplification and Generation of Microwaves—J. P. Wittke. (PROC. IRE, vol. 45, pp. 291–316; March, 1957.) A survey of theory and methods is given. At present, means of achieving low-noise low-level amplification by molecular resonance in gases have been obtained; but bandwidths are low, although it should soon be possible to increase them using solid-state devices. Reduction in gain with frequency will probably preclude application at longer wavelengths, but possibilities are offered in the millimeter and submillimeter ranges.

538.569.4:621.372.029.64 1734

Molecular-Beam Oscillator—N. G. Basov. (*Radiotekhnika i Elektronika*, vol. 1, pp. 752–757; June, 1956.) Brief description of a 23870-mc NH_3-beam oscillator. See also 3709 of 1956 (Basov and Prokhorov) and back references.

537.5 1735

Ionized Gases [Book Review]—A. von Engel. Clarendon Press, Oxford, England, 281 pp.; 1955. (*Brit. J. Appl. Phys.*, vol. 7, p. 455; December, 1956.) "... should be of real value to research workers ...."

538.56 1736

Electromagnetic Waves [Book Review]—G. Toraldo di Francia. Interscience, New York, N. Y. and London, England; 320 pp. (*Research, London*, vol. 9, p. 448; November, 1956.) A treatment of fundamentals is presented which deviates in some respects from standard theory.

GEOPHYSICAL AND EXTRATERRESTRIAL PHENOMENA

523.16 1737

Radio Astronomy—(*Telefunken Ztg*, vol. 29, pp. 143–198; September, 1956. English summaries, pp. 199–203.) A group of papers dealing with developments which led to the erection of the Stockert (West Germany) observatory and detailing its technical features and proposed research program. The issue includes the following papers:

Organization of the Technical Cooperation for the Construction of the Radio Telescope—H. B. Speicher (pp. 144–146).

Radio Engineering, the Atmosphere and the Universe—H. Rukop (pp. 146–147).

The Astronomical Research Program of the Bonn Radio Telescope—F. Becker (pp. 148–151).

The Radio Emission from Interstellar Gas and its Measurement—P. Mezger and W. Priester (pp. 152–156).

The Planning of the Construction of the Radio Observatory on the Stockert—T. Pederzani (pp. 157–166).

Driving and Tracking Problems of Radio-Astronomy Receiving Equipment on the Stockert—O. Mohr and H. Klessmann (pp. 166–173).

The Electrical System of Automatic Tracking Control—H. Klessmann (pp. 174–181).

The Resolving Power of the R.F. Receiving Equipment of the Radio Telescope—P. A. Mann and P. Mezger (pp. 182–191).

A Spectrometer for the 20-cm Band with Extremely High Resolution and Sensitivity—K. W. Grimm (pp. 191–198).

523.16 1738

The Radio Observatory Stockert—T. Pederzani. (*Elektrotech. Z., Ed. B*, vol. 8, pp. 357–361; October 21, 1956.) Brief description of the 21-cm-λ receiver system and control equipment for the 25-m diameter parabolic reflector used in the first radio telescope installed in West Germany. See also 1737 above.

523.16 1739

Photometric Paradox at Radio Frequencies—G. G. Getmantsev. (*Radiotekhnika i Elektronika*, vol. 1, pp. 838–839; June, 1956.) Conclusions based on data for metagalactic radio emission indicate that the photometric radius of the metagalaxy does not exceed 100 megaparsecs at radio frequencies. The problem of various "clipping mechanisms" in the radio emission from distant metagalactic sources is briefly discussed.

523.16 1740

Preliminary Results of the Measurement of the Polarization of Cosmic Radio Emission at a Wavelength of 1.45 m—V. A. Razin. (*Radiotekhnika i Elektronika*, vol. 1, pp. 846–851; June, 1956.) Weak (~4 per cent linear polarization of radiation from celestial regions outside the Milky Way was observed. The apparatus is briefly described.

523.16 1741

Parasitic Modulation—N. V. Karlov. (*Radiotekhnika i Elektronika*, vol. 1, pp. 852–860; June, 1956.) Parasitic modulation in modulation-type radiometers for radio-astronomical observations is considered and the use of ferrite attenuators is mentioned.

523.16 1742

Multichannel Radiospectrograph and First Results of Observations—V. V. Vitkevich, Z. I. Kameneva, and D. V. Kovalevski. (*Radiotekhnika i Elektronika*, vol. 1, pp. 864–868; June, 1956.) The apparatus is described with the aid of a block diagram. The frequency band of 80–120 mc is covered by eight receivers tuned to frequencies spaced at 5 mc with bandwidth 1 mc; the receiver noise factor is 5. Two parabolic reflectors with dimensions 18×8 m are used. Results of solar observations are also reported.

523.16 1743

Construction of Radiospectrograph NIZMIR—Ya. I. Khanin and A. K. Markeev. (*Radiotekhnika i Elektronika*, vol. 1, pp. 869–872; June, 1956.) Preliminary report on the construction of a radiospectrograph for the frequency band 45–90 mc at the Scientific Research Institute for Terrestrial Magnetism, the Ionosphere, and the Propagation of Radio Waves (N.I.Z.M.I.R.). Continuous tuning in this band is effected by ferrite variometers which are briefly described.

523.16:523.7 1744

Theory of Sporadic Radio Emission of the Sun—V. V. Zheleznyakov. (*Radiotekhnika i Elektronika*, vol. 1, pp. 840–845; June, 1956.) The transformation of plasma waves into em waves in an inhomogeneous plane-stratified medium is considered. The transformation coefficient, expressed as the square of the ratio of amplitudes of the em and plasma waves, is about 3×10^{-7} for the solar corona.

523.16:523.7 1745

Radio Emission of Corona Condensations—V. V. Vitkevich and M. I. Sigal. (*Radiotekhnika i Elektronika*, vol. 1, pp. 861–863; June, 1956.) Digest only. Results are presented of measurements at 10 and 50 cm λ, of the position of the center of solar emission. The movement of the center is explained by the presence of auxiliary sources which are connected with the 5303-Å green line emission from the corona.

523.5:621.396.11 1746

The Theoretical Length Distribution of Ionized Meteor Trails—V. R. Eshleman. (*J. Atmos. Terr. Phys.*, vol. 10, pp. 57–72; February, 1957.) The lengths are calculated from information on the production and radio detection of meteoric ionization, the mass distribution of shower and sporadic meteors, and the distribution of sporadic meteor radiants. The theory indicates that the length distribution of detected trails is independent of the sensitivity of the radar receiver and the power output of the transmitter.

523.5:621.396.11 1747

The Number Density Meteor Trails Observable by the Forward-Scattering of Radio Waves—R. E. Pugh. (*Canad. J. Phys.*, vol. 34, pp. 997–1004; October, 1956.) A mathematical expression is derived for the trail distribution as a function of the position of the celestial region relative to transmitter and receiver. "Observable" trails are those which produce pulses exceeding a given amplitude.

523.5:621.396.11 1748

The Spatial Distribution of Signal Sources in Meteoric Forward-Scattering—C. O. Hines and R. E. Pugh. (*Canad. J. Phys.*, vol. 34, pp. 1005–1015; October, 1956.) The contour charts of distribution obtained by a simplified method of analysis in which ellipsoids are replaced by cylinders [738 of 1956 (Hines)] are in good agreement with those computed by the more exact formulas given in *ibid.* pp. 997–1004 (Pugh). The influence of signal duration is examined and a comparison is also made with the earlier findings of Eshleman and Manning (1884 of 1954).

525.3:529.786 1749

The Atomic Clock and the Irregularity of the Earth's Rotation—Stoyko. (See 1846).

550.38:523.165 1750

Geomagnetic Variations in the Cosmic-Ray Disturbance of 23 February 1956—P. L. Marsden, J. G. Wilson, and D. C. Rose. (*J. Atmos. Terr. Phys.*, vol. 10, pp. 117–119; February, 1957.) The Leeds (England) data are compared with those from Ottawa, Durham (U.S.A.), and Chicago.

551.510.535 1751

Structure of the Lower Ionosphere and its Variations—E. A. Lauter. (*Ber. Dtsch. Wetterdienstes*, vol. 4, pp. 55–64; 1956.) The ionized region below the E-layer maximum at a height of about 100 km is discussed. 46 references.

551.510.535 1752

Remarks on the Meteorology of the Ionosphere—K. Rawer. (*Ber. Dtsch. Wetterdienstes*, vol. 4, pp. 83–84; 1956.) Brief remarks on: *a*) daily variation of the electron density distribution, *b*) horizontal movement, *c*) apparent vertical movements, and *d*) turbulence in the upper ionosphere (above 100 km).

551.510.535 1753

Diffusion in the Ionosphere—B. N. Gershman. (*Radiotekhnika i Elektronika*, vol. 1, pp. 720–731; June, 1956.) Diffusion of charged particles in a weakly ionized gas in the presence of molecules is considered, taking into account the presence of the geomagnetic field.

Generalized diffusion equations are derived and the ambipolar approximation is discussed. The results are used to determine the "lifetime" of inhomogeneities.

551.510.535 1754
Investigation of the Fine Structure of the Ionosphere by the Method of Frequency-Diversity Reception—V. D. Gusev and S. F. Mirkotan. (*Radiotekhnika i Elektronika*, vol. 1, pp. 743–746; June, 1956.) Results are presented of a theoretical and experimental investigation of the frequency distribution of amplitude fading of a single signal reflected by the ionosphere. The vertical dimension of small-scale inhomogeneities is estimated.

551.510.535 1755
Phase Method of Recording Large Ionospheric Inhomogeneities—V. D. Gusev and L. A. Drachev. (*Radiotekhnika i Elektronika*, vol. 1, pp. 747–751; June, 1956.) A vertical sounding method is described. Results for the F layer indicate a probable horizontal dimension of 135 km, assuming a constant velocity of 150 ms.

551.510.535 1756
The Calculation of Ionospheric Electron Density Distributions—J. M. Kelso. (*J. Atmos. Terr. Phys.*, vol. 10, pp. 103–109; February, 1957.) The method suggested includes the effect of the earth's magnetic field but is suitable for use when high-speed digital computers are unavailable or uneconomic.

551.510.535 1757
On the Determination of the Electron Density Distribution in the Ionospheric Regions from h'f Records—A. K. Saha. (*Indian J. Phys.*, vol. 30, pp. 464–479; September, 1956.) Various known methods for determining the height distribution of electrons are discussed; for routine work, Ratcliffe's method (1292 of 1952) is quickest, though other methods are more accurate under particular conditions. For latitudes around that of Calcutta, the errors resulting from neglecting the magnetic field do not exceed those involved in the actual height measurement, with the apparatus used.

551.510.535:523.72 1758
Relation between the Ionization of the Ionosphere E Layer and Solar R.F. Radiation—J. F. Denisse and M. R. Kundu. (*C.R. Acad. Sci., Paris*, vol. 244, pp. 45–47; January 2, 1957.) Analysis of observations indicates close correlation between the variations of the monthly mean values of f_0E and those of the solar radiation on 10.7 cm λ. The results suggest that the mechanisms of production of rf and X radiation from the sun are closely linked.

551.510.535:523.75:621.396.11.029.45 1759
Long-Path V.L.F.—Frequency Variations associated with the Solar Flare of 23 February 1956—Allan, Crombie, Penton. (See 1889.)

551.510.535:523.78 1760
Recombination in the Ionosphere during an Eclipse—D. R. Bates and M. R. C. McDowell. (*J. Atmos. Terr. Phys.*, vol. 10, pp. 96–102; February, 1957.) The change in electron density during a total eclipse is calculated on the assumption that there are two species of ion having different recombination coefficients. Various combinations of the coefficients and relative concentrations are investigated and the results are shown graphically.

551.510.535:621.396.11 1761
Note on a "QL-QT" Transition Level in the Ionosphere—B. Landmark and F. Lied. (*J. Atmos. Terr. Phys.*, vol. 10, pp. 114–116; February, 1957.) Experimental observations relating to Lepechinsky's hypothesis (see 3188 of 1956 and back reference) are discussed.

551.594.6:621.396.9 1762
Locating Atmospheric Disturbances by Synchronous Recording of Direction and Waveform—G. Skeib. (*Ber. Dtsch. Wetterdienstes*, vol. 4, pp. 146–147; 1956.) Note of equipment which has been operating in Potsdam since 1953. It comprises a cathode-ray direction finder of the type described by Adcock and Clarke (2779 of 1947) and an atmospherics waveform recorder used in an investigation by Schindelhauer, *et al.* (990 of 1952). Outputs from these two instruments are applied to a two-beam pulsed oscillograph displaying direction and waveform simultaneously.

523.16+551:621.396.96 1763
Les Applications du Radar à l'Astronomie et à la Météorologie [Book Review]—van Bladel. (See 1769.)

LOCATION AND AIDS TO NAVIGATION

621.396.932:621.396.63 1764
The Radio Call [System] for Ships in Distress—L. Chauveau. (*Rev. gén. Élect.*, vol. 65, pp. 561–568; October, 1956.) A survey of past and present automatic alarm systems.

621.396.96 1765
Choosing Radar Wavelengths—R. F. Hansford and R. T. H. Collis. (*Wireless World*, vol. 63, pp. 188–193; April, 1957.) The relative performances of 10- and 25-cm equipment for surveillance duties are discussed in relation to a medium-sized transport and a fighter aircraft. For the same antenna size, the 10-cm radar gives better coverage and discrimination but no advantage on ground clutter. Attenuation in rain is not significant for either wavelength but back-scatter is worse at 10 cm. No general preference appears possible.

621.396.96 1766
Marine Radar Equipment—Correction to 1085 of 1957: for 60 feet, please read 6 feet.

621.396.96:551.577/.578 1767
Radar Observations of Showers Suggesting a Coalescence Mechanism—P. J. Feteris and B. J. Mason. (*Quart. J.R. Met. Soc.*, vol. 82, pp. 446–451; October, 1956.) Observations using 3-cm and 10-cm equipment are reported and discussed.

621.396.963:621.397.3 1768
The P.P.I.-Television Image Converter of the S.F.R. [Société Française Radio-Électrique]—R. Asté. (*Onde élect.*, vol. 36, pp. 822–828; October, 1956.) Outline description of a tube for direct electronic conversion of a ppi radar image into a television signal.

621.396.96:[523.16+551 1769
Les Applications du Radar à l'Astronomie et à la Météorologie. [Book Review]—J. van Bladel. Gauthier-Villars, Paris, France, 147 pp.; 1955. (*Quart. J.R. Met. Soc.*, vol. 82, pp. 550–551; October, 1956.) The main emphasis is on meteors and precipitating clouds. References are given to nearly 200 papers dated between 1945 and 1954.

MATERIALS AND SUBSIDIARY TECHNIQUES

531.788.7:537.533 1770
The Measurement of Vary Low Gas and Vapour Pressures—F. Kirchner and H. Kirchner. (*Z. angew. Phys.*, vol. 8, pp. 478–481; October, 1956.) Technique is discussed for determining the pressure from the variation of the field emission of electrons from a clean W point as the point becomes coated with adsorbed gas molecules.

533.5 1771
Safety Assembly for Permanent-Vacuum Installations Connected to Pumps—J. Conard. (*C.R. Acad. Sci., Paris*, vol. 244, pp. 52–54; January 2, 1957.)

535.215 1772
The Influence of Boundary Layers on Photoconduction—F. Stöckmann. (*Z. Phys.*, vol. 146, pp. 407–422; October 16, 1956.) Grain-surface depletion layers produced by adsorption of foreign matter have a marked influence on currents forced to pass through them. The expression for the photocurrent is of the same form as for photoconduction in a homogeneous volume, but there is an additional dependence on the dark current. A mechanism explaining the photocurrents in ZnO is discussed.

535.215:537.311.33 1773
Review of Papers Presented at the Meetings of the "Photoelectric Phenomena in Semiconductors" Section [at the 8th All-Union Conference on Semiconductors, Leningrad, 14th–20th November, 1955]—S. M. Ryvkin. (*Uspekhi Fiz. Nauk*, vol. 60, pp. 225–248; October, 1956.)

535.215:537.311.33:539.23 1774
Theory of Photoconductivity in Semiconductor Films—R. L. Petritz. (*Phys. Rev.*, vol. 104, pp. 1508–1516; December 15, 1956.) A model for photoconductive films is analyzed in which it is assumed that the primary photoeffect is absorption of light and production of hole-electron pairs in the crystallites. The change in conductivity results from a change in majority-carrier density in the crystallites, and from reduction of intercrystalline potential barriers. The response to radiation, the noise, and the limit of sensitivity are analyzed and measurements necessary for the evaluation of the parameters involved are discussed.

535.215:546.289 1775
Pulse Method of Investigating the Photoelectric Properties of a *p-n* Junction in Germanium—Yu. I. Ukhanov. (C.R. *Acad. Sci. U.R.S.S.*, vol. 111, pp. 1238–1241; December 21, 1956. In Russian.) The dependence of the light-pulse modulation of a hf pulse on the current amplitude (up to 2A), carrier frequency (20 cps–20 kc), and probe position was investigated. Results are tabulated and presented graphically, together with oscillograms. Electroluminescence was observed in a Ge diode.

535.215:546.817.221 1776
Spectral Distribution of the Photoeffect in Lead Sulphide—H. U. Pfeiffer. (*Z. Naturf.*, vol. 11a, pp. 164–165; February, 1956.) Brief note on an experimental investigation of the effect of annealing conditions.

535.215.1:546.3 1777
The Effect of Mechanical Stresses on the Photoelectric Emission from Polycrystalline Metallic Substances—R. Bernard, C. Guillaud, and R. Goutte. (*J. Phys. Radium*, vol. 17, pp. 866–871; October, 1956.) Experimental investigations show that emission increases under stress. The effect is reversible within the elastic range and irreversible beyond it.

535.37 1778
Phase Equilibria and Fluorescence in the System Zinc-Oxide Boric-Oxide—D. E. Harrison and F. A. Hummel. (*J. Electrochem. Soc.*, vol. 103, pp. 491–498; September, 1956.) Detailed investigations were carried out on various forms of compounds. Experimental results are tabulated and discussed with reference to the findings of other authors.

535.376 1779
Secondary Waves of Electroluminescence—C. H. Haake. (*J. Appl. Phys.*, vol. 28, pp.

117–123, January, 1957.) A simple model for charge polarization is developed describing the behavior of secondary waves at varying temperature and frequency.

535.376:546.472.21 1780
The Electroluminescence of ZnS-Type Phosphors—P. Zalm. (*Philips Res. Rep.*, vol. 11, pp. 353–399; October; and pp. 417–451; December, 1956.) Photoluminescence theories, particularly those concerning the nature of the fluorescence centers in ZnS, and methods of preparing electroluminescent powders are outlined. A qualitative model has been drawn up to explain the mechanism of electroluminescence. Observations show that a distinction is necessary between phosphors where excitation by an alternating field causes activator ionization and those where this fails to occur. The electroluminescence mechanism of hexagonal, Cu-activated, single ZnS crystals is essentially the same as for powders, and a relation is established between the orientation of the barrier layers at which light emission occurs and that of the crystal axes. The voltage characteristic of the emittance is due to a Mott-Schottky-type barrier. The case of crystals embedded in a dielectric is particularly examined. Experiments are analyzed with regard to delayed light emission and temperature dependence of the emittance, and the energy efficiency of electroluminescent phosphors is studied. Sixty-two references.

535.376:546.472.21 1781
High-Frequency-Induced Electroluminescence in ZnS—G. G. Harman and R. L. Raybold. (*Phys. Rev.*, vol. 104, pp. 1498–1499; December 15, 1956.) Note on measurements made over a frequency range 1 cps–370 mc.

535.376:546.472.21 1782
The Green-2 Band in the Ultra-violet Luminescence of Zinc Sulphide—T. B. Tomlinson and E. A. D. White. (*J. Electronics*, vol. 2, pp. 404–405; January, 1957.) Experimental evidence suggests the green-2 band is not due to a new center.

537.226/.227 1783
Structure and Phase Transitions of Ferroelectric Sodium-Lead Niobates and of other Sodium Niobate Type Ceramics—M. H. Francombe and B. Lewis. (*J. Electronics*, vol. 2, pp. 387–403; January, 1957.) A structural and dielectric study shows that solid solutions of perovskite type are formed up to a limit of 35 per cent replacement of sodium atoms by lead atoms and vacancies. A new ferroelectric tetragonal phase is introduced immediately below the Curie temperature. Partial substitution of niobium by tantalum lowers the ferroelectric transition temperatures. Multiple-cell effects can be ascribed to puckering of the niobium-oxygen framework and depend primarily on lattice spacing and packing.

537.226:546.431.824-31 1784
Aging of the Dielectric Properties of Barium Titanate Ceramics—K. W. Plessner. (*Proc. Phys. Soc., London*, vol. 69, pp. 1261–1268; December 1, 1956.) The permittivity and power factor decrease linearly with log t over periods up to several years from the time of cooling the material through the Curie point. The results are explained in terms of a very wide distribution of the activation energies governing the motion of domain walls.

537.226:621.315.61 1785
The Universal Significance of Ion Adsorption in Insulating Materials—P. Böning. (*Z. angew. Phys.*, vol. 8, pp. 516–520; October, 1956.) A discussion illustrated by reference to mechanical, thermal, and electrical processes in insulating materials.

537.226:621.372 1786
Realizability of a Prescribed Frequency Variation of Dielectric Constant—R. J. Harrison. (PROC. IRE, vol. 45, p. 367; March, 1957.) Modified Kronig-Kramers theory is used to derive the minimum attainable loss in a dielectric having an inverse-square dependence on frequency of real permittivity. With a large bandwidth the loss tangent becomes large over most of that band, and may limit application to cases requiring a constant electrical length of waveguide.

537.227:546.431.824-31 1787
Thermodynamical Theory of Ferroelectric Properties of Barium Titanate—L. P. Kholodenko. (*Zh. Eksp. Teor. Fiz.*, vol. 31, pp. 244–253; August, 1956.) The nature of the phase transition from the nonferroelectric to the ferroelectric phase is discussed and the effect of an electric field on the temperature of the transition is considered. The change in the dielectric constant near the Curie point and the piezomoduli of the piezoelectric effect induced by an electric field at temperatures near the Curie point are discussed.

537.228.1:548.0].001.4(083.7) 1788
I.R.E. Standards on Piezoelectric Crystals—the Piezoelectric Vibrator: Definitions and Methods of Measurement, 1957 (PROC. IRE, vol. 45, pp. 353-358; March, 1957.) Standard 57 IRE 14.S1.

537.311.31 1789
Changes in the Electrical Conductivity of Metals on Fusion—G. Darmois. (*C.R. Acad. Sci., Paris*, vol. 244, pp. 174–176; January 7, 1957.)

537.311.31:538.632 1790
Electrical Resistivity and Hall Effect of Noble Metals at Very Low Temperatures—T. Fukuroi and T. Ikeda. (*Sci. Rep. Res. Inst. Tohoku Univ., Ser. A*, vol. 8, pp. 205–212; June, 1956.) Results are given of measurements on Au, Ag, and Cu covering a temperature range of 1°–20°K.

537.311.33+535.37 1791
Inapplicability of the Fermi-Dirac Distribution to Electrons of Impurity Centres in Semiconductors [and Crystal Phosphors—S. I. Pekar. (*Zh. Eksp. Teor. Fiz.*, vol. 31, pp. 351–353; August, 1956.)

537.311.33 1792
Theory of Semiconductors at the 8th All-Union Conference on Semiconductors [Leningrad, 14th–20th November, 1955]—V. L. Bonch-Bruevich. (*Uspekhi Fiz. Nauk*, vol. 60, pp. 213–224; October, 1956.) Survey of papers presented at the conference. Thirty-seven references.

537.311.33 1793
The Chemical Bond in Semiconductors—E. Mooser and W. B. Pearson. (*J. Electronics*, vol. 2, pp. 406–407; January, 1957.) A note on the transition from semiconducting to metallic behavior of group-V elements.

537.311.33 1794
A Method of Evaluating Surface State Parameters from Conductance Measurements on Semiconductors—G. G. E. Low. (*Proc. Phys. Soc., London*, vol. 69, pp. 1331–1334; December 1, 1956.) A theoretical treatment of the relationship between the various surface parameters involved in the determination of densities and cross sections for majority-carrier capture.

537.311.33 1795
The Statistics of Divalent Impurity Centres in a Semiconductor—C. H. Champness. (*Proc. Phys. Soc., London*, vol. 69, pp. 1335–1339; December 1, 1956.) The problem is treated by counting the states so as to allow for the double degeneracy due to spin, and applying the normal Fermi distribution function.

537.311.33 1796
Ionized Impurity Scattering in Nondegenerate Semiconductors—N. Sclar. (*Phys. Rev.*, vol. 104, pp. 1548–1558; December 15, 1956.) The problem is treated by the partial wave technique, using a square well for the attractive impurity and a square barrier for the repulsive impurity. For $ka \ll 1$, where k is the wave number of the charge carriers and a the range of the impurity potential, results for the variation of mobility with temperature and impurity concentration differ markedly from previous formulas, valid for $ka \gg 1$.

537.311.33 1797
Neutral Impurity Scattering in Semiconductors—N. Sclar. (*Phys. Rev.*, vol. 104, pp. 1559–1561; December 15, 1956.) A calculation by the partial wave technique is compared with that due to Erginsoy (*Phys. Rev.*, vol. 79, pp. 1013–1014; September 15, 1950) and with a Born-approximation treatment.

537.311.33 1798
Anisotropy of the Hot-Electron Problem in Semiconductors with Spheroidal Energy Surfaces—L. Gold. (*Phys. Rev.*, vol. 104, pp. 1580–1584; December 15, 1956.) The energy gain for electrons in many-valley semiconductors is determined for any orientation of electric field. In particular for germanium and silicon values are given of the directional accelerative masses for both isotropic ($T \to 0$°K) and nonisotropic scattering.

537.311.33 1799
Statistics of Electrons and Holes in a Homopolar Semiconductor taking Account of the Interaction with Lattice Oscillations—V. L. Bonch-Bruevich. (*Zh. Eksp. Teor. Fiz.*, vol. 31, pp. 254–260; August, 1956.) The stationary electron distribution is investigated, taking into account the electron-phonon interaction. The limiting cases of high and low temperatures are considered, and results indicate that, owing to the interaction, the electrical conductivity does not vanish at 0°K.

537.311.33 1800
Bipolar Diffusion of Current Carriers in the Presence of Deep Traps—K. V. Tolpygo and E. I. Rashba. (*Zh. Eksp. Teor. Fiz.*, vol. 31, pp. 273–277; August, 1956.) A theoretical study taking into account the dependence of the minority-carrier lifetime on the degree of occupation of the traps is presented; criteria for the validity of a linear recombination law are established. A formula is deduced for the minority-carrier concentration distribution for the case of a nonlinear recombination law.

537.311.33 1801
Fabrication of Multiple Junctions in Semiconductors by Surface Melt and Diffusion in the Solid State—K. Lehovec and A. Levitas. (*J. Appl. Phys.*, vol. 28, pp. 106–109; January, 1957.) Techniques are described suitable for preparation of structures with widths of intermediate layers accurately controlled over wide ranges. Close control is necessary over impurity concentration in preparing doubly doped crystals and in attachment of the base electrode contact.

537.311.33:537.533.9 1802
Measurement of Short Carrier Lifetimes—G. K. Wertheim and W. M. Augustyniak. (*Rev. Sci. Instr.*, vol. 27, pp. 1062–1064; December, 1956.) Semiconductor carrier lifetimes as short as 10^{-8}s have been measured by bombarding the specimen with short pulses of 700-kev electrons from a Van de Graaff accelerator.

537.311.33+537.311.31]:538.569.4 1803
Infrared Cyclotron Resonance in Bi, InSb, and InAs with High Pulsed Magnetic Fields—R. J. Keyes, S. Zwerdling, S. Foner, H. H. Kolm, and B. Lax. (*Phys. Rev.*, vol. 104, pp. 1804–1805; December 15, 1956.) Measurement of the increase in effective electron mass with magnetic field strengths up to 300,000 Gauss are reported.

537.311.33:538.69 1804
Magneto-band Effects in InAs and InSb in D.C. and High Pulsed Magnetic Fields—S. Zwerdling, R. J. Keyes, S. Foner, H. H. Kolm, and B. Lax. (*Phys. Rev.*, vol. 104, pp. 1805–1807; December 15, 1956.) Measurements of the increase in the energy gap with magnetic field strengths up to 250,000 Gauss are reported.

537.311.33:541.128 1805
Semiconductors as Catalysts for Chemical Reactions—F. F. Volkenshtein. (*Uspekhi Fiz. Nauk*, vol. 60, pp. 249–293; October, 1956.) A survey. Fifty-one references, mostly to Russian literature.

537.311.33:546.24 1806
Study of the Recombination Process in Tellurium—A. Pires de Carvalho. (*C.R. Acad. Sci., Paris*, vol. 244, pp. 461–462; January, 21 1957.) The lifetime of minority carriers was measured using a photomagnetoelectric method. The observed temperature dependence can be explained on the assumption that the Auger effect plays a predominant part in the recombination.

537.311.33:[546.28+546.289 1807
Density of States for Warped Spherical Energy Surfaces: Zeroth Order Solution for Holes in Silicon and Germanium—L. Gold. (*J. Electronics*, vol. 2, pp. 323–329; January, 1957.) No exact solution appears possible, but a zero-order calculation gives reasonable accuracy.

537.311.33:[546.28+546.289]:548.0 1808
Simplified Light Reflection Technique for Orientation of Germanium and Silicon Crystals—R. D. Hancock and S. Edelman. (*Rev. Sci. Instr.*, vol. 27, pp. 1082–1083; December, 1956.)

537.311.33:546.28:669.046 1809
Precise Heat for growing Silicon Crystals—E. T. Davis, W. B. Alden, and F. H. Wyeth. (*Electronics*, vol. 30, pp. 164–167; February 1, 1957.) Induction heating of a crucible is controlled automatically within 0.25°C by a thermopile.

537.311.33:546.289 1810
Dependence of Lifetime of Non-equilibrium Charge Carriers in Germanium on Temperature and Composition—E. I. Adirovich, G. M. Guro, and V. F. Kuleshov. (*Zh. Eksp. Teor. Fiz.*, vol. 31, pp. 261–272; August, 1956.) Approximate formulas are derived for a semiconductor with a low trap concentration.

537.311.33:546.289 1811
Etching Experiments on Germanium Crystals—H. A. Schell. (*Z. Metallkde*, vol. 47, pp. 614–620; September, 1956.) Etch patterns obtained with vertically pulled single crystals with various orientations are reproduced.

537.311.33:546.289 1812
The Isothermal Reverse Voltage/Current Characteristics of Small-Area Alloy Contacts on Germanium—E. G. S. Paige. (*J. Electronics*, vol. 2, pp. 378–386; January, 1957.) At high currents the characteristics become independent of the type of junction. The results verify Gunn's theory (1030 of 1953) for the resistance of a small-area contact. The relation of the results to observations on point contacts is discussed.

537.311.33:546.289 1813
Effects of Structural Defects in Germanium on the Diffusion and Acceptor Behavior of Copper—C. S. Fuller and J. A. Ditzenberger. (*J. Appl. Phys.*, vol. 28, pp. 40–48; January, 1957.) Experiments indicate the slow attainment of acceptor equilibrium especially in Ge having low concentrations of dislocation and the identification of dislocations as the initial loci of acceptor Cu in Ge. Ideas on the mechanism of diffusion of Cu need revision. See also 169 of 1957 (Tweet and Gallagher).

537.311.33:546.289 1814
Microdeterminations of Arsenic and Antimony in Metallic Germanium and Germanium Dioxide—H. Goto and Y. Kakita. (*Sci. Rep. Res. Inst. Tohoku Univ., Ser. A*, vol. 8, pp. 243–251; June, 1956.)

537.311.33:546.561-31 1815
Oxidation of Copper to Cu_2O and CuO (600°–1000°C and 0.026–20.4 atm Oxygen)—D. W. Bridges, J. P. Baur, G. S. Baur, and W. M. Fassell, Jr. (*J. Electrochem. Soc.*, vol. 103, pp. 475–478, September, 1956.) Summary and analysis of results of oxidation tests carried out on oxygen-free, high-conductivity copper under the above conditions. Eighteen references.

537.311.33:546.681.19 1816
Energy Bands in Gallium Arsenide—J. Callaway. (*J. Electronics*, vol. 2, pp. 330–340; January, 1957.) Electronic energy bands in GaAs are related to those of Ge by the use of second-order perturbation theory.

537.311.33:546.682.19 1817
Electrical Properties of *n*-Type InAs—T. C. Harman, H. L. Goering, and A. C. Beer. (*Phys. Rev.*, vol. 104, pp. 1562–1564; December 15, 1956.) Measurements of Hall coefficient and resistivity on uncompensated specimens are reported. The energy gap was found to be 0.32 ev and electron mobility 30,000 cm^2/v second at room temperature.

537.311.33:[546.682.86+546.682.19 1818
Determination of the Effective Masses in InSb and InAs by Measurement of the Differential Thermoelectric Force—H. Weiss. (*Z. Naturf.*, vol. 11a, pp. 131–138; February, 1956.) Results of measurements on three *p*-type and five *n*-type specimens of InAs and on two specimens of *p*-type InSb indicate the following values: for InAs in the temperature range 500–800°K, $m_n = 0.064\ m_o$, $m_p = 0.33\ m_o$; for InSb at 333°K, $m_n = 0.037\ m_o$, $m_p = 0.18\ m_o$. The effective electron mass in InSb increases with temperature and reaches $0.05\ m_o$ just below the melting point.

537.311.33:546.817.221 1819
Application of a Network Model to Semiconductors of the Lead Sulphide Type—T. K. Rebane. (*Zh. Eksp. Teor. Fiz.*, vol. 31, pp. 353–354; August, 1956.) Coulson's network model (*Proc. Phys. Soc., London*, vol. 67, pp. 608–614; July, 1954.) is applied to semiconductors of the type PbX, where X is S, Se, or Te.

537.311.33:548.0 1820
Deformation Twinning in Materials of the A4 (Diamond) Crystal Structure—A. T. Churchman, G. A. Geach, and J. Winton. (*Proc. Roy. Soc. A*, vol. 238, pp. 194–203; December 18, 1956.) Continuation of investigation reported by Franks, *et al.* (2321 of 1955). Deformation produced by hardness indentations in Si, Ge, InSb, GaSb, and zinc blende are studied.

537.311.33:621.314.632 1821
Hole Injection at Metal/Semiconductor Point Contact—D. Gerlich. (*Proc. Phys. Soc., London*, vol. 69, pp. 1350–1351; December 1, 1956.) An extension of the theory of Gunn (167 of 1955) to include the case of point contact with spherical geometry.

537.311.33:621.317.79:538.632 1822
A Pulse Method for Measurement of Hall Coefficient at Low Temperatures: Some Results on Indium Antimonide—Broom and Rose-Innes. (See 1862.)

537.533.8:546.3 1823
The Effect of Mechanical Stresses on the Secondary Electron Emission from Polycrystalline Metallic Substances—F. Davoine and R. Bernard. (*J. Phys. Radium*, vol. 17, pp. 859–865; October, 1956.) Experiments on strips and wires under tension show an increase of up to 20 per cent in the emission coefficient for Ni, Au, and Mo. After annealing the coefficient returns to its original value. See also 1777 above.

538.22 1824
Magnetic Susceptibility of Dilute Cu Alloys at Low Temperatures—F. T. Hedgcock. (*Phys. Rev.*, vol. 104, pp. 1564–1567; December 15, 1956.) Results of measurements between room temperature and 4.2°K indicate an anomalous paramagnetism near the temperature of the observed resistance minimum.

538.221 1825
The Significance of Dislocation Density in the Theory of the Coercive Force of Recrystallized Materials—M. Kersten. (*Z. angew. Phys.*, vol. 8, pp. 496–502; October, 1956.) Quantitative theory is based on the assumption that the domain walls are held fixed at dislocation sites but become curved on application of a magnetizing field (see also 501 of 1957). The coercive force represents the field strength at which the transition occurs from a reversible curvature of the walls to an irreversible Barkhausen jump. A simple formula is hence derived which gives values of the coercive force of magnetically soft recrystallized materials in good agreement with experimental values.

538.221 1826
Texture and Magnetization Curve of Silicon Iron—D. Ganz and R. Brenner. (*Z. angew. Phys.*, vol. 8, pp. 502–505; October, 1956.) The deleterious effects on the magnetization curve in nonuniformity of orientation of the crystal grains are indicated.

538.221 1827
The Effect of the Induced Uniaxial Anisotropy on the Domain-Wall Displacements and Magnetic Behaviour of Ferromagnetic Cubic Solutions—S. Taniguchi. (*Sci. Rep. Res. Inst. Tohoku Univ., Ser. A*, vol. 8, pp. 173–192; June, 1956.) The restoring force acting on domain walls is calculated as a function of wall displacement. The effects of domain-wall stabilization may account for certain properties of perminvars also commonly found in other cubic solid solutions. The properties of permalloys and the results of heat treatment are also discussed.

538.221 1828
The Density, Magnetic Properties, Young's Modulus, and ΔE-Effect, and their Changes due to Quenching in Ferromagnetic Iron-Aluminium Alloys: Part 2—Young's Modulus and the ΔE-Effect—M. Yamamoto and S. Taniguchi. (*Sci. Rep. Res. Inst. Tohoku Univ., Ser. A*, vol. 8, pp. 193–204; June, 1956.) Results of measurements by the method of magnetostrictive vibration are presented. Part 1: 195 of 1957.

538.221:621.3.042.14 1829
Magnetic Effects of Compressional Stress at Low Field Intensities—R. E. Fischell. (*Commun. & Electronics*, no. 24, pp. 148–151; May, 1956. Discussion, p. 151.) Further report of investigations on various magnetic materials in the form of clamped laminations. For results of earlier tests, see 182 of 1956.

538.221:621.318.134 1830
Low-Frequency Dispersion of ρ and ϵ in Ferrites—J. P. Suchet. (PROC. IRE, vol. 45, p. 360; March, 1957.) Note on the dependence of surface-layer thickness on firing conditions mentioned by Van Uitert (PROC. IRE, vol. 44, pp. 1294–1303; October, 1956.)

538.221:621.318.134 1831
Angles between Magnetic Spin Directions in Iron-Deficient Magnesium Manganese Ferrites–W. P. Osmond. (*Proc. Phys. Soc., London*, vol. 69, pp. 1319–1325; December 1, 1956.) The electrical and magnetic properties of thirteen square-loop ferrites are examined for evidence of the probable distribution of the various ions in the crystal lattice and of the relative strengths of their mutual interactions. See also, *Phil. Mag.*, vol. 1, pp. 1147–1156; December, 1956.

538.221:621.318.134:621.372.413 1832
Effects of Size on the Microwave Properties of Ferrite Rods, Disks, and Spheres—J. O. Artman. (*J. Appl. Phys.*, vol. 28, pp. 92–98; January, 1957.) Retardation effects associated with the propagation of em waves in the specimen are treated and results given for idealized cases of rods of infinite length and disks of infinite extent. An approximate solution for a sphere agrees qualitatively with experimental observations.

538.245:537.311.33 1833
Theory of Spontaneous Magnetization of Ferromagnetic Semiconductors in the Low-Temperature Region—E. I. Kondorski, A. S. Pakhomov, and T. Shiklosh. (*C.R. Acad. Sci. U.R.S.S.*, vol. 109, pp. 931–934; August 11, 1956. In Russian.)

538.569.4:538.222 1834
Relaxation in the Spin System of Paramagnetic Salts—L. J. Smits, H. E. Derksen, J. C. Verstelle, and C. J. Gorter. (*Physica*, vol. 22, pp. 773–784; September, 1956. In English.) Paramagnetic absorption due to relaxation within the spin system was studied in various salts at 20.4°K. Three distinguishable types of behavior were found and the results are discussed with reference to earlier theory.

539.23 1835
Electrical Resistances of Thin Metal Films before and after Artificial Aging by Heating—R. B. Belser. (*J. Appl. Phys.*, vol. 28, pp. 109–116; January, 1957.) Experimental results and comments.

549.514.51:621.372.412.029.45 1836
Flexural-Mode Quartz Crystals as A. F. Resonators—R. Bechmann and D. Hale. (*Electronic Ind. Tele-Tech*, vol. 15, pp. 52–53, 94; October, 1956.) New techniques for growing Y-bar quartz crystals are outlined. Details of dimensions and operating characteristics for YX- and YZ-cut bars are given.

621.315.611:537.529 1837
Time Lags in the Intrinsic Electric Breakdown of Solid Dielectrics—R. Cooper and D. T. Grossart. (*Proc. Phys. Soc., London*, vol. 69, pp. 1351–1353; December 1, 1956.) Measurements of time lag are described for various ionic crystals, polythene, and polystyrene.

537.226/.227 1838
Ferroelektrika. [Book Review]—H. Sachse. Springer, Berlin, Germany, 171 pp.; 1956. (*Z. Angew. Phys.*, vol. 8, p. 520; October, 1956.) A monograph including a detailed treatment of ferroelectric titanates. Conditions for the occurrence of ferroelectricity in solids are discussed. Applications of ferroelectric materials are indicated, manufacturers are listed, and patent literature is included in the bibliography.

MATHEMATICS

517.5 1839
Some Theorems on Fourier Transforms and on the Coefficients of Typically Real Functions—N. K. Artémiadis. (*C.R. Acad. Sci., Paris*, vol. 244, pp. 544–547; January 28, 1957.)

517.521.4 1840
Note on a Method for Computing Infinite Integrals of Oscillatory Functions—I. M. Longman. (*Proc. Camb. Phil. Soc.*, vol. 52, pp. 764–768; October, 1956.) The method is based on Euler's transformation of slowly convergent alternating series.

517.566:621.396.812.3 1841
Properties of Random Functions—D. S. Palmer. (*Proc. Camb. Phil. Soc.*, vol. 52, pp. 672–686; October, 1956.) The relationships of the maxima, minima, and zeros of two random functions of known correlations are investigated. Reference is made to the analyses of ionospheric reflection by Ratcliffe (3216 of 1954) and Briggs and Spencer (2945 of 1954). The frequency distributions of intervals between successive zeros and maxima, and of the lengths of intercepts by a horizontal line are considered; this has applications to the study of long-wave signal fading.

517.7 1842
Perturbation Solutions of the Ellipsoidal Wave Equation—F. M. Arscott. (*Quart. J. Math.*, vol. 7, pp. 161–174; September, 1956.)

517.942:621.3.015.3 1843
Approximation to Transients by means of Laguerre Series—J. W. Head. (*Proc. Camb. Phil. Soc.*, vol. 52, pp. 640–651; October, 1956.) Tricomi's method as discussed by Ward (2163 of 1954) is investigated with special reference to conditions for convergence. The wider applications of Lin's iteration process for determining quadratic factors of polynomials is outlined.

518.61 1844
A Note on the Approximate Solution of the Equations of Poisson and Laplace by Finite-Difference Methods—J. Eve and H. I. Scoins. (*Quart. J. Math.*, vol. 7, pp. 217–223; September, 1956.)

519.24:621.396.822 1845
The Statistical Description of Fluctuating Electrical Quantities—G. Francini. (*Ricerca sci.*, vol. 26, pp. 2973–3004; October, 1956.) The principal methods of statistical analysis of frequency and amplitude distribution restricted to a single parameter are discussed. Problems of measurement are examined.

MEASUREMENTS AND TEST GEAR

529.786:525.3 1846
The Atomic Clock and the Irregularity of the Earth's Rotation—N. Stoyko. (*C.R. Acad. Sci., Paris*, vol. 244, pp. 43–45; January 2, 1957.) The frequency deviations of standard-frequency transmissions based on the Cs resonator at the National Physical Laboratory are compared with figures derived on an astronomical basis in France. The results clearly indicate a seasonal variation of the rate of rotation of the earth.

539.32.082.4 1847
An Instrument for the Measurement of Elastic Moduli of Crystals—K. S. Aleksandrov and O. V. Nosikov. (*Akust. Z.*, vol. 2, pp. 244–247; July–September, 1956.) The principles are outlined of an instrument for the determination of the moduli by measurement of the velocity of propagation of longitudinal and transverse vibrations excited by ultrasonic pulses.

621.3.08+621–52 1848
Some Principles of Measurement and Control—J. F. Coales. (*J. Sci. Instr.*, vol. 33, pp. 457–464; December, 1956.) The principles of the design of measuring systems are discussed in relation to the limitations imposed by inertia, damping, and the disturbing effects on the measured quantities. The simple theory of linear control systems is developed and it is shown that they differ from measuring systems only in the magnitude of the required output.

621.3.08:621.3.018.78:534.86 1849
Correlation Method of Measuring the Distortion Coefficient of Transmitted Signals—M. A. Sapozhkov. (*Akust. Z.*, vol. 2, pp. 279–284; July–September, 1956.) The method of measuring the generalized coefficient of distortion and interference is based on the determination of the input-output correlation.

621.3.083.4:621.317.72 1850
Transistor Null Detector has High Sensitivity—C. D. Todd. (*Electronics*, vol. 30, pp. 184–185; February 1, 1957.) A four-stage af amplifier and detector are built into a compact case with a microammeter. Sensitivities from 20 μv to 2 v are achieved.

621.317.32 1851
The Measurement of Periodic High Voltages by Capacitor Currents—J. Lagasse and G. Giralt. (*C.R. Acad. Sci., Paris*, vol. 244, pp. 442–444; January 21, 1957.) The method of determining peak voltage values by measuring the rectified current through a standard capacitor is discussed; typical values of the currents to be rectified are between 10 and 50 μa. An arrangement using a pair of Si rectifiers in parallel opposition can be designed to give very low errors.

621.317.32.029.4 1852
Modulation Method of Measuring Small Electric Voltages in the Audio Frequency Region—D. K. Balabukha, L. L. Myasnikov, and E. N. Plotnikova. (*Akust. Z.*, vol. 2, pp. 248–254; July–Sept., 1956.) The principles of an instrument for the measurement of af voltages of the order of a few microvolts in the frequency range 200 cps–20 kc are discussed and some practical details are given. The af voltage was modulated at 24 cps by a periodically varying capacitance in the input stage of an af amplifier. Various detectors were used.

621.317.342.012 1853
An Instrument for the Static Measurement and Oscillographic Representation of Phase [-angle] or Phase-Delay Curves—H. Schönfelder. (*Frequenz*, vol. 10, pp. 309–318; October, 1956.) A comparison of methods of measurement and their application shows that group-delay indication is the most useful in the majority of cases. A circuit is described which is suitable for measuring phase angle, phase delay, and signal amplitude, their variation with frequency being shown in the form of oscillograms.

621.317.361.029.64:621.373 1854
Measurement of the Spectral Line Width of a Klystron Oscillator at a Wavelength of 3.2 cm—V. S. Troitski and V. V. Khrulev. (*Radiotekhnika i Elektronika*, vol. 1, pp. 831–837; June, 1956.) Bershtein's method (see 1696 above) was used. The fundamental line width was 0.3–0.8 cps. The amplitude and frequency fluctuation spectra in the 2–25-mc band were also investigated.

621.317.444 1855
Magnetic Fluxmeter for Measuring in Three Dimensions—M. Müller. (*Elect. Com-*

mun., vol. 33, pp. 220–223; September, 1956.) A rotating-probe instrument is described capable of measuring the three components of narrow cylindrical magnetic fields required for the focusing of electron beams.

621.317.7:621.374.3:621.397.62 1856
A Spot and Graticule [pattern] Generator for Laboratory Use—E. E. Hücking. (*Elektronische Rundschau*, vol. 10, pp. 270–274; October, 1956.) The instrument described generates pulses of 0.1-μs duration which are used to form either a spot or a graticule raster for television testing.

621.317.725:621.313.32.001.4 1857
A Valve Voltmeter for Synchro Testing—D. L. Davies. (*Electronic Eng.*, vol. 29, pp. 52–57; February, 1957.) The apparatus detects synchro null positions and measures total residue signal, separating quadrature fundamental from harmonics and noise. Circuit diagrams are given.

621.317.725:621.385 1858
A Phase-Sensitive Valve Voltmeter—R. Kitai. (*Electronic Radio Eng.*, vol. 34, pp. 124–128; April, 1957.) Details of its design and characteristics.

621.317.733 1859
A Simple Method for the Measurement of High Resistance Values—A. E. Hawkins. (*J. Sci. Instr.*, vol. 33, p. 486; December, 1956.) A modified Wheatstone-bridge network is described for resistance measurement up to 10^9 Ω. Accuracy is within ±2 per cent.

621.317.733:621.316.86 1860
A Simple Direct-Reading Thermistor Bridge—J. Swift. (*Proc. IRE, Australia*, vol. 17, pp. 341–345; October, 1956. *J. Brit. IRE*, vol. 7, pp. 155–159; March, 1957.) The bridge described is suitable for accurate rf power measurements in the range approximately 10 μw-1 mw. Ambient temperature compensation and facilities for battery operation are provided.

621.317.733.029.3 1861
An A.C. Kelvin Bridge for the Audio-Frequency Range—B. L. Dunfee. (*Commun. & Electronics*, no. 24, pp. 123–127; May, 1956; Discussion, pp. 127–128.) Details are given of a four-terminal resistor adjustable from 0.1 to 0.05 Ω designed for use as an ac reference standard with the Kelvin bridge described.

621.317.79:538.632:537.311.33 1862
A Pulse Method for Measurement of Hall Coefficient at Low Temperatures: some Results on Indium Antimonide—R. F. Broom and A. C. Rose-Innes. (*Proc. Phys. Soc., London*, vol. 69, pp. 1269–1275, plate; December 1, 1956.) A description of a method suitable for use at liquid-helium temperatures with high-resistance semiconductors having a Hall mobility not less than 2 cm^2/v sec. The activation energy is calculated from the variation of Hall coefficient with temperature. The results are in agreement with the equation proposed by Pearson and Bardeen (*Phys. Rev.*, vol. 75, pp. 865–883; March 1, 1949) relating activation energy with impurity concentration.

621.317.794:621.396.822 1863
Stability Requirements and Calibration of Radiometers when Measuring Small Noise Powers—J. C. Greene. (PROC. IRE, vol. 45, pp. 359–360; March, 1957.) Note on a modification of Dicke's system (475 of 1947).

621.317.794:621.396.822 1864
A Comparison of Two Radiometer Circuits—D. G. Tucker, M. H. Graham, and S. J. Goldstein, Jr. (PROC. IRE, vol. 45, pp. 365–366; March, 1957.) Comments on 535 of 1956 (Goldstein) and author's reply.

OTHER APPLICATIONS OF RADIO AND ELECTRONICS

531.77:621.383.4:621.314.7 1865
A Simple Direction-Sensitive Phototransistor Circuit for Use in Optical Pulse-Counting Systems—W. T. Bane and D. L. A. Barber. (*J. Sci. Inst.*, vol. 33, pp. 483–486; December, 1956.) An output pulse is directed to one of two lines according to the direction of rotation of a serrated disk interrupting a beam of light falling on two photocells.

534.1:8:620.179.1 1866
Step Function Pulse Technique for Ultrasonic Measurement—(*Electronic Eng.*, vol. 29, p. 77; February, 1957.) A basically new technique for thickness measurement and flaw detection whereby sections between 0.10 inch and 0.25 inch can be directly inspected.

621–52:681.142 1867
Systems of Automatic Regulation Involving Digital Computers—Ya. Z. Tsypkin. (*Avtomatica i Telemekhanika*, vol. 17, pp. 665–679; August, 1956.) A review.

621.317.39:531.7:621.374.32 1868
The Automatic Measurement and Recording of Quasi-static Expansions by means of String Extensometers and Electronic Counters used as Frequency and Time-Interval Meters—C. Rohrbach. (*Z. Ver. Dtsch. Ing.*, vol. 98, pp. 1541–1548; September 11, 1956.)

621.362:621.385.2 1869
Thermionic Diodes as Energy Converters—Moss. (See 1983.)

621.383:621.373.5:616–1 1870
Sensory Aid Defines Lights and Marks—C. R. Hurtig. (*Electronics*, vol. 30, pp. 162–163; February 1, 1957.) A miniature device which enables the blind to locate a meter needle or other light or dark object. An audible note produced by a transistor relaxation oscillator is varied by a photocell.

621.384 1871
A Thermal-Ion Source with Extremely Low Consumption of Material—H. Hintenberger and C. Lang. (*Z. Naturf.*, vol. 11a, pp. 167–168; February, 1956.) The construction of an ionization source is described.

621.384.6 1872
Particle Accelerators and Their Applications—D. R. Chick and C. W. Miller. (*Brit. Commun. Electronics*, vol. 3, pp. 539–545; October, and pp. 596–601; November, 1956.) A survey of existing types and an outline of present and future applications. Thirty-three references.

621.384.6 1873
All-Union Conference on Physics of High-Energy Particles [Moscow, 14th–22nd May, 1956] (Second Section)—P. O. Chechik. (*Radiotekhnika i Elektronika*, vol. 1, pp. 1014–1023; July, 1956.) Abstracts and references of papers presented at the conference. Texts of the following ten papers are printed in full (*ibid.*, pp. 893–1013):

Some Properties and Basic Data of the High-Frequency System of the 6-Metre Phasotron—A. L. Mints, I. Kh. Nevyazhski, and B. I. Polyakov (pp. 893–902).

Transverse Oscillations in the Dee System of the Phasotron—A. D. Vlasov (pp. 903–909).

System Linking the Frequency of the Accelerating Field with the Field Strength of the Magnetic Field of the 10^9-eV Synchrophasotron—A. L. Mints, S. M. Rubchinski, M. M. Veisbein, F. A. Vodop'yanov, A. A. Kuz'min, and V. A. Uvarov (pp. 910–927).

Primary Oscillator in System Linking the Frequency of the Accelerating Field with the Field Strength of the Magnetic Field of the 10^9-eV Synchrophasotron—V. A. Vodop'yanov (pp. 928–939).

Accelerating Elements of Synchrophasotrons and Fundamental Problems of Supplying Them with High-Frequency Voltage—Yu. M. Lebedev-Krasin (pp. 940–953).

Application of Ferrite-Cored Inductors in the High-Power High-Frequency Stages of the Synchrophasotron—I. Kh. Nevyazhski, G. M. Drabkin, V. F. Trubetskoi, and A. S. Temkin (pp. 954–964).

Automatic Tuning of the Final Stage of the High-Frequency Oscillator in the 10^9-eV Synchrophasotron—G. M. Drabkin, L. M. Gurevich, B. M. Gutner, and N. K. Kaminski (pp. 965–973).

Control Systems for the Injection and Particle Acceleration Processes in the Synchrophasotron—A. L. Mints, S. M. Rubchinski, M. M. Veisbein, and A. A. Vasil'ev (pp. 947–985).

Measurement of the Instantaneous Frequency of the Frequency-Modulated Oscillations—S. M. Rubchinski, A. A. Vasil'ev, V. F. Kuz'min, and N. I. Fedorenko (pp. 986–1000).

Measurement of the Instantaneous Values of the Intensity of the Varying Magnetic Fields—S. M. Rubchinski, M. P. Zel'dovich, and S. S. Kurochkin (pp. 1001–1013).

621.384.6 1874
Gyroscopic Analogies for Circular Accelerators—F. Fer. (*C.R. Acad. Sci., Paris*, vol. 244, pp. 566–568; January 28, 1957.) Analog techniques for investigating the trajectories of particles in a circular accelerator are discussed.

621.384.6 1875
Fixed-Field Alternating-Gradient Accelerators—L. J. Laslett. (*Science*, vol. 124, pp. 781–787; October 26, 1956.) Structures of two types are surveyed, one using radial and the other spiral sectors. Twenty-three references.

621.385.833 1876
A Mathematical Field Model for a Permanent-Magnet Unipotential [electron] Lens—F. Lenz. (*Z. angew. Phys.*, vol. 8, pp. 492–496; October, 1956.) The magnetic "unipotential" lens is defined, by analogy with the es unipotential lens, as one in which the integral of the magnetic induction along the axis is zero. Analysis is presented for rotationally symmetrical arrangements. An expression is given for the field distribution which permits a solution in closed form to be obtained for the differential equation for the paraxial electron trajectories.

621.385.833.032.2:621.319.47 1877
Potential in Doubly Curved Condensers—R. Albrecht. (*Z. Naturf.*, vol. 11a, pp. 156–163; February, 1956.) The potential distribution between a pair of doubly curved electrodes for use in an electron-optical system is calculated; the converse problem of calculating the constants of the electrodes when the field is given, is also considered.

621.397.3:681.142 1878
Reading by Electronics—(*Wireless World*, vol. 63, pp. 173–175; April, 1957.) A note on automatic character recognition using logical gate circuits, and an outline description of a machine with a recognition rate of 120 characters per second.

77:537.2 1879
Xerography—W. D. Oliphant. (*Research, London*, vol. 9, pp. 436–442; November, 1956.) "Xerography is a photographic process in which image reproduction is controlled by electrostatic and triboelectric phenomena. The fundamentals of the technique are outlined here and its applications discussed."

PROPAGATION OF WAVES

538.566:537.56 1880
Propagation of Strong Electromagnetic Waves in Plasma—A. V. Gurevich. (*Radiotekhnika i Elektronika*, vol. 1, pp. 704–719; June, 1956.) The effects of the change in the energy of electrons in the plasma (ionosphere) produced by an em wave are considered theoretically. Expressions are derived, and analyzed, for the absorption and the phase change of the wave in the plasma.

538.56:537.56 1881
Wave Propagation in the Plasma between Two Perfectly Conducting Planes in the Direction of an Applied Magnetic Field—W. O. Schumann. (*Z. angew. Phys.*, vol. 8, pp. 482–485; October, 1956.) Extension of analysis presented previously (*e.g.*, 717 of 1951). In general, for the system discussed, there are three frequency ranges for which the propagation constant is imaginary. When the plasma moves in the direction of the magnetic field, growing em waves are possible in these ranges.

538.566:537.56 1882
The Influence of a Constant Magnetic Field on the Resonance Effect, Observed at the Reflection of an Electromagnetic Wave by an Inhomogeneous Plasma—N. G. Denisov. (*Radiotekhnika i Elektronika*, vol. 1, pp. 732–738; June, 1956.) Theoretical paper. Results indicate that for ionospheric conditions the effect of the resonance region on the reflection of radio waves is negligible. The influence of plasma waves is also considered.

538.566.2 1883
Propagation of Modulated Waves in a Medium with Pronounced Dispersion—S. I. Averkov and V. Ya. Ryadov. (*Radiotekhnika i Elektronika*, vol. 1, pp. 739–742; June, 1956.) Brief description of apparatus and results of an experimental investigation of the conversion of a periodic amplitude modulation into frequency modulation due to the propagation of an em wave through a dispersive medium.

538.566.2 1884
Theory of Scattering of Radio Waves at Moving Inhomogeneities—G. S. Gorelik. (*Radiotekhnika i Elektronika*, vol. 1, pp. 695–703; June, 1956.) Discussion on the basis of the turbulent diffusion theory is presented. The time function of auto-correlation of the scattered field is related to the statistical characteristics of the motion of the inhomogeneities.

538.56 1885
Multiple Small-Angle Scattering of Waves by an Inhomogeneous Medium—P. Gosar. (*Nuovo Cim.*, vol. 4, pp. 688–702; October 1, 1956. In English.) Theory is presented for propagation in a medium with very small fluctuations of the refractive index; *e.g.*, radio propagation in a turbulent atmosphere. The analysis starts from the scalar wave equation and makes use of an autocorrelation function.

621.396.11 1886
British Research into Radio Propagation by Tropospheric Scatter—*Engineer, London*, vol. 202, p. 595; October 26, 1956.) Experiments have been made using a 30-foot-diameter fixed radiator fed by a horn mounted on a trailer carrying a 500-w transmitter operating at a frequency of 858 mc. Plans for further tests on a multichannel link between London and Newcastle are briefly indicated; a transmitter power of 10 kw is to be used.

621.396.11:551.510.535 1887
Note on a 'QL-QT' Transition Level in the Ionosphere—Landmark and Lied. (See 1761.)

621.396.11:551.510.535:621.317.328 1888
The Measurement of the Scattering Coefficient in the Back-Scattering of Short-Wave Telegraphy Signals—B. Beckmann and L. Vogt (*Nachrichtentech. Z.*, vol. 9, pp. 441–448; October, 1956.) The influence of antenna radiation patterns on the values of field strength near the transmitter and the receiver is investigated. The correlation between these values is established by determining the scattering coefficient from measurements of the elevation angle for the maximum back-scatter signal. The method of indication was that adopted in previous tests (896 of 1956).

621.396.11.029.45:551.510.535:523.75 1889
Long-Path V.L.F.-Frequency Variations associated with the Solar Flare of 23 February 1956—A. H. Allan, D. D. Crombie, and W. A. Penton. (*J. Atmos. Terr. Phys.*, vol. 10, pp. 110–113; February, 1957.) The frequency and phase variations of Rugby (16 kc) received in New Zealand during the great solar flare are compared with the changes during a normal flare. The difference is attributed to the cosmic-ray increase which accompanied the great flare.

621.396.11.029.6 1890
Propagation Tests at Frequencies of 250, 500 and 1000 Mc/s—F. Carassa. (*Alta Frequenza*, vol. 25, pp. 378–390; October, 1956.) Summary and analysis of results obtained during the period 1951–1952 over the 189-km path in Northern Italy for which 1-kmc tests had earlier been reported [see 3522 of 1956 (Vecchiacchi)].

621.396.11.029.6:[621.396.41.+621.397.26 1891
Television and Telephone Radio Relay System in Denmark—Nielsen, Christensen, Sterndorff, and Gudmandsen. (See 1908.)

RECEPTION

621.396.62 1892
Modern Means of Radio Reception—C. Reuber. (*Elektrotech. Z., Ed. B*, vol. 8, pp. 361–366; October 21, 1956.) A description of the receiving and af distribution equipment used for the monitoring services of the German Federal Government Information Department.

621.396.62:621.314.7 1893
A Passive Transistor Receiver—H. E. Hollmann. (*Frequenz*, vol. 10, pp. 329–331; October, 1956.) The circuit outlined draws its power from the rf energy of a local transmitter and is capable of driving a loudspeaker.

621.396.62:621.376.3 1894
A Stable F.M. Receiver with Preset Tuning—G. S. Robinson. (*Electronic Eng.*, vol. 29, pp. 88–91; February, 1957.) A detailed description of circuits and construction. A crystal-controlled local oscillator is used.

621.396.621:621.398 1895
Remote-Control Receiver—E. Bohr. (*Electronics*, vol. 30, p. 149; February 1, 1957.) Description of the circuit of a light-weight two-transistor receiver operating on 27 mc, the output of which operates a conventional relay.

621.396.621.54:621.314.7 1896
The Application of Transistors to A.M. Broadcast Receivers—B. F. C. Cooper. (*Proc. IRE, Australia*, vol. 17, pp. 331–340; October, 1956. *J. Brit. IRE*, vol. 17, pp. 95–106; February, 1957.) An experimental superheterodyne receiver using five *n-p-n* transistors is described and the performance analyzed against that of a conventional four-tube portable receiver as a target.

621.396.621.54:621.372.54 1897
Some Aspects of Intermediate-Frequency Filtering in a Receiver—Carteron. (See 1691.)

621.396.82:621.376.2 1898
Some Aspects of Detection from the Point of View of Information—J. Cauchois. (*Ann. Radioélect.*, vol. 11, pp. 308–316; October, 1956.) Brief survey of detection theory applicable to AM, with particular reference to synchronous methods. Twenty-four references.

621.396.822:621.317.794 1899
Stability Requirements and Calibration of Radiometers when Measuring Small Noise Powers—Greene. (See 1863.)

621.396.822:621.317.794 1900
A Comparison of Two Radiometer Circuits—Tucker, Graham, Goldstein. (See 1864.)

STATIONS AND COMMUNICATION SYSTEMS

621.376.22.029.64:621.372.8 1901
Amplitude Modulation of Microwaves by Tunable Transmission Waveguide Filters—Potok and Barbour. (See 1652.)

621.39.001.11 1902
Hearing and Seeing—C. Cherry. (*Wireless World*, vol. 63, pp. 164–168; April, 1957.) The reduction of redundancy in information channels becomes increasingly important. To achieve this without increasing the probability of errors, it is necessary to have a more complete understanding of the fundamental problems of human perception.

621.396.2:621.376.2 1903
Reception of a Doubly Modulated Signal—M. Anastassiadés. (*C.R. Acad. Sci., Paris*, vol. 244, pp. 183–184; January 7, 1957.) A radio system is proposed in which the carrier (*e.g.*, 50 mc) is modulated by an IF (*e.g.*, 1 mc) as well as by the af signal. No frequency changer is needed at the receiver, a Si diode is used as a simple detector, its slope being about twice the conversion slope when used as a mixer, the comparison being made on the basis of calculations presented by Herold and Malter (797 of 1944). The IF strength would be comparatively low, because of the absence of the local oscillator. Bandwidth considerations indicate that such a system would not be practical at frequencies below uhf.

621.396.41 1904
A 72-Channel Radio System for Toll Telephone Service—M. C. Harp and M. H. Kebby. (*Commun. & Electronics*, no. 24, pp. 113–119; May, 1956. Discussion, p. 119.) Description of the Type-72B system for operation in the 900-mc band.

621.396.41 1905
Description and Technical Details of the Semi-fixed Pulse-Multiplex Installation Type MX. 620 for 12 or 24 [telephone] Channels—R. Casse and L. Masliah. (*Ann. Radioelect.*, vol. 11, pp. 339–358; October, 1956.)

621.396.41:621.317.34 1906
Crosstalk Measuring Equipment for [f.m.] Multichannel Radio Links—G. De Lotto. (*Alta Frequenza*, vol. 25, pp. 411–425; October, 1956.) The equipment described produces white-noise modulation, and measurements are directly applicable to operational conditions as covered by CCIF recommendations.

621.396.41:621.374.4 1907
Reference Generator for S.S.B. Systems—Jacob. (See 1705.)

621.396.41.+621.397.26]:621.396.11.029.6 1908
Television and Telephone Radio Relay System in Denmark—B. Nielsen, P. Christensen, P. Sterndorff, and P. Gudmandsen. (*Teleteknik, Copenhagen*, vol. 7, pp. 113–156; October, 1956.) A detailed description is given of the network, the station installations, and the operating facilities. Several unattended stations are operated by remote control from two attended stations. Preparatory measurements on two oversea paths of lengths 54 and 82 km

respectively are reported; wavelengths of 6.4 and 17.0 cm were used simultaneously.

621.396.41.029.6:621.396.822.1 1909
The Problem of Cross talk in Frequency-Modulated Radio Relay Equipment for Small Numbers of Channels—I. Wigdorovits. (*Brown Boveri Rev.*, vol. 43, pp. 384–393; September, 1956.) A combined graphical and numerical method of calculating the crosstalk noise at the output terminals of a frequency-division multiplex link is described with the aid of an example.

621.396.5:534.78 1910
Instantaneous Speech Compressor—Rutherford. (See 1632.)

621.396.65:621.376.3:621.397.8 1911
The Effect of Group Delay Variations on the Video Pass Band of a Radio Link—I. S. Stojanović. (*Ann. Radioélect.*, vol. 11, pp. 293–301; October, 1956.) The distortions introduced by time delay variations are analyzed to obtain a general formula for calculating the signal amplitude.

621.396.712.2:621.396.664 1912
Automatic Programming in Small A.M. Stations—E. C. Miller. (*Electronics*, vol. 30, pp. 146–148; February 1, 1957.) 20 cps tone superimposed on a magnetic tape recording controls the operation of the reproducer and associated record player.

SUBSIDIARY APPARATUS

621-52+621.3.08 1913
Some Principles of Measurement and Control—Coales. (See 1848.)

621.3.087.6 1914
Pen Motor for Rectilinear Recording—F. Massa and E. A. Massa. (*Electronics*, vol. 30, pp. 159–161; February 1, 1957.) Describes a recorder-pen driven by a moving coil through a mechanical linkage. Critical damping, and freedom from ink-spattering and pen-whip at writing speeds up to 200 cps are achieved.

621.316.722.1 1915
Barretter-Bridge-Circuit Voltage Stabilizer—G. Szabó. (*Z. angew. Phys.*, vol. 8, pp. 512–516; October, 1956.) Conditions for optimum power consumption, temperature compensation, and stability are investigated for a bridge comprising two ohmic resistances and two tungsten-filament lamps.

621.35:539.169 1916
Nuclear Batteries—J. R. Milliron. (*Elec. Mfg.*, vol. 56, pp. 125–131; November, 1955.) The principles of operation of the contact-potential, solid-dielectric, and solid-state types of cell are described and details of some commercial products, including the solar battery, are given.

TELEVISION AND PHOTOTELEGRAPHY

621.397.24:[621.372.54+621.372.553 1917
Filters and Delay Equalizers for Television Transmission on Cables—H. Keil. (*Nachrichtentech. Z.*, vol. 9, pp. 469–475; October, 1956.) The solution of network design problems arising from ssb television transmissions on coaxial cables is discussed.

621.397.3:621.396.963 1918
The P.P.I./Television Image Converter of the S.F.R. [Société Française Radio-Électrique]—Asté. (See 1768.)

621.397.5:535.623 1919
Perceptions of Colours in Projected and Televised Pictures—D. A. MacAdam. (*J. Soc. Mot. Pict. Telev. Eng.*, vol. 65, pp. 455–469; September, 1956. Discussion, p. 469.) A special colorimetric method was used to investigate the chromatic adaptation of the eye to artificial and daylight illumination. The test results are analyzed in detail and their relevance to satisfactory reproduction of color television is discussed. Twenty-three references.

621.397.5:535.623:621.395.625.3 1920
Colour TV on Tape—H. R. L. Lamont. (*Wireless World*, vol. 63, pp. 183–187; April, 1957.) Description of a RCA video recorder. See 1592 of 1957 (Olson, *et al.*).

621.397.5:778.5 1921
A New Telerecording Equipment. (*Electronic Eng.*, vol. 29, p. 70; February, 1957.) Features of the Marconi Type-BD679 equipment are briefly described with a photograph.

621.397.6:535.623 1922
Some Problems in a Band-Sharing Color Television System—A. V. Lord. (*J. Telev. Soc.*, vol. 8, pp. 130–141; October/December, 1956.) The discussion of distortion effects and remedies is restricted to the NTSC type of system.

621.397.61 1923
Vision Transmitter Design—V. J. Cooper. (*J. Telev. Soc.*, vol. 8, pp. 149–162; October/December, 1956.) The techniques described refer particularly to bands III and IV and to color-television requirements.

621.397.61 1924
Implications of Phase Precompensation in a Television Transmitter on the Shape of the Radiated Signal—A. van Weel. (*J. Brit. IRE*, vol. 17, pp. 129–134; February, 1957.) Phase errors in the receiver which produce smears following black-to-white transitions can be compensated by an overshoot introduced by a phase-precompensating network in the video-frequency section of the transmitter, provided that the modulation characteristic is linear. Some loss of signal power may result.

621.397.61 1925
Portable TV Station for Remote Pickups—L. E. Flory, G. W. Gray, J. M. Morgan, and W. S. Pike. (*Electronics*, vol. 30, pp. 170–177; February 1, 1957.) Describes a complete television outside broadcasting unit for carriage on a man's back. The equipment, using transistors, has a range of 1 mile and includes monitoring facilities and power supplies. See also, 1599 of 1957.

621.397.61:535.623 1926
Color TV System uses Flying-Spot Scan—H. Mate. (*Electronics*, vol. 30, pp. 138–142; February 1, 1957.) Light is projected on to the scene to be televised from a raster on a cr tube in a conventional television-camera housing. Reflected light is picked up by color-sensitive photoelectric cells.

621.397.61:621.397.7(43) 1927
Südwestfunk Television Transmitter Technique—(*Tech. Hausmitt. NordwDtsch. Rdfunks*, vol. 8, pp. 41–89; 1956.) Eight papers give details of antenna and transmitter installations including frequency-conversion relay stations. The use of helicopters in measuring field strengths and in selecting antenna location and height is described. For details of Südwestfunk studios, see 2895 of 1956.

621.397.61:621.397.7:535.623 1928
Compact Plug-In Colour Video Equipment—W. B. Whalley. (*J. Soc. Mot. Pict. Telev. Engrs.*, vol. 65, pp. 488–492; September, 1956.) Design details and operating characteristics are given of newly developed studio equipment, which includes distribution and correcting amplifiers, a relay switching unit, and regulated power supplies.

621.397.62:535.623:621.385.832 1929
A New Flat Picture Tube—D. Gabor. (*J. Telev. Soc.*, vol. 8, pp. 142–145; October/December, 1956.) See 588 of 1957.

621.397.62:621.317.7:621.374.44 1930
A Spot and Graticule [Pattern] Generator for Laboratory Use—Hücking. (See 1856.)

621.397.62:621.373.43 1931
Television Sweep Generation with Resonant Networks and Lines—T. C. G. Wagner; W. D. White; K. Schlesinger. (Proc. IRE, vol. 45, pp. 362–364; March, 1957.) Discussion on 2893 of 1956 (Schlesinger) and author's reply.

TUBES AND THERMIONICS

621.314.63:[546.28+546.289 1932
Excess Surface Currents on Germanium and Silicon Diodes—W. T. Eriksen, H. Statz, and G. A. de Mars. (*J. Appl. Phys.*, vol. 28, pp. 133–139; January, 1957.) Excess current is associated with an anomalous surface inductance as a function of bias voltage. Conduction in outer surface states can explain observed data.

621.314.63:546.289 1933
Slow Relaxation Phenomena in Junction Diodes—T. B. Watkins. (*Proc. Phys. Soc., London*, vol. 69, pp. 1353–1355; December 1, 1956.) The relaxation effect is demonstrated by measurements of the reverse current in a Ge junction diode, for various ambient atmospheres.

621.314.63:546.289 1934
Measurements of H.F.-Diode Impedance as a Function of Bias Voltage—H. Flietner and G. Hesse. (*Hochfreq. und Elektroak.*, vol. 65, pp. 41–46; September, 1956.) Description of a method for determining the impedance bias characteristic of Ge point-contact rectifiers. The effect of bias voltage on the real part of the barrier-layer impedance is discussed with reference to the rectifier equivalent circuit.

621.314.632:537.311.33 1935
Frequency Characteristics of Germanium Junction Diodes at a Small Alternating Voltage—S. G. Kalashnikov, N. A. Penin, and K. V. Yakunina. (*Radiotekhnika i Elektronika*, vol. 1, pp. 1058–1070; August, 1956.) An experimental investigation of Ge-In alloy diodes is reported. Results, which are presented graphically, are in agreement with calculated characteristics based on theoretical work by Kalashnikov and Penin (1889 of 1956). The measurements reported were carried out at frequencies between 1 kc and 100 mc.

621.314.632:537.311.33 1936
Properties of Germanium Detectors with Welded Junction at Ultra-high Frequencies—N. A. Penin and N. E. Skvortsova. (*Radiotekhnika i Elektronika*, vol. 1, pp. 1071–1079; August, 1956.) The capacitance and impedance of the barrier layer was experimentally determined in the frequency range 1–6 kmc for several values of positive bias current. The capacitance was inversely proportional to the square root of frequency and both the capacitance and resistance varied linearly with the bias current. The results are in agreement with the diffusion theory of electron-hole junctions taking into account the effect of injection of nonequilibrium charge carriers.

621.314.632:537.311.33 1937
Investigation of Breakdown of Germanium Junction Diodes—B. M. Vul and A. P. Shotov. (*Radiotekhnika i Elektronika*, vol. 1, pp. 1080–1085; August, 1956.) Application of voltage pulses lead to breakdown due to shock ionization; breakdown by constant voltages depended on the structure of the p-n junction and on heat-transfer conditions.

621.314.632:537.311.33 1938
Investigation of Rectification Properties of Point-Contact Germanium Diodes—K. B. Tolpygo and V. A. Fomenko. (*Radiotekhnika i Elektronika*, vol. 1, pp. 1093–1105; August, 1956.) Report on theoretical and experimental investigations. The experimental results indicate that at small voltages point contact diodes made of low-resistivity (2–4-Ω cm) Ge with weak forming (forming current = 0.2A) possess a superior forward characteristic and higher detection-efficiency than those using 20–25-Ω cm Ge and strong forming.

621.314.632:537.311.33 1939
Electrochemical Method for Improving the Quality of the Electron-Hole Transition Region in a Selenium Rectifying Element—L. Yu. Belenkova, I. Kh. Geller, D. N. Nasledov, and F. M. Tartakovskaya. (*Radiotekhnika i Elektronika*, vol. 1, pp. 1121–1126; August, 1956.)

621.314.7 1940
Bibliography of Literature on Semiconductor Triodes (1948–1956)—V. V. Pavlov. (*Avtomatika i Telemekhanika*, vol. 17, pp. 946–952; October, 1956.) About 150 references including some to Russian literature.

621.314.7 1941
Parameters and Construction of Semiconductor Amplifying Devices of Home [U.S.S.R.] Manufacture—A. V. Krasilov. (*Radiotekhnika i Elektronika*, vol. 1, pp. 1113–1120; August, 1956.) Tables of characteristics and section drawings of Russian transistors.

621.314.7 1942
Transistor Graphical Symbols—(*Wireless World*, vol. 63, pp. 194–198; April, 1957.) A critical analysis of existing ideas and conventions.

621.314.7 1943
Some Aspects of Transistor Progress—H. W. Loeb. (*J. Brit. IRE*, vol. 17, pp. 125–128; February, 1957.) Discussion of 295 of 1957 and author's reply, stressing that developments have reached a stage where, for a considerable number of important fields of application of several types of structure have been proved feasible. Temperature limitations in power transistors were due to mechanical changes or alteration of parameters, and satisfactory operation of Ge alloyed-junction types was possible over temperatures ranging from −55°C to +85°C. Reliability was very high, even for point-contact types. The outputs of junction photocells were at present an order of magnitude higher than those of vacuum photocells.

621.314.7 1944
Transistor Impedance Matching—H. P. Williams. (*Electronic Radio Eng.*, vol. 34, pp. 128–129; April, 1957.) Simplified matching formulas applicable to junction transistors are presented and attention is drawn to the property that the product of the input and output impedances is, for practical purposes, the same for all three configurations.

621.314.7 1945
The Dependence of Junction-Transistor Current Amplification on the Emitter Current—E. R. Hauri. (*Tech. Mitt. schweiz. Telegr.-Teleph Verw.*, vol. 34, pp. 441–451; November 1, 1956.) A theoretical investigation of the α characteristics at high frequencies and large emitter currents is reported. Results indicate that the formulas derived by Webster (2798 of 1954) need to be modified. Calculated characteristics of commercial transistors are in good agreement with experimental results.

621.314.7 1946
Measurements on Alloy-Type Transistors with Varying Collector Voltage—D. M. Evans. (*Brit. J. Appl. Phys.*, vol. 8, pp. 44–45; January, 1957.) Dependence of the effective base width and α cutoff frequency on collector voltage.

621.314.7 1947
The Spacistor, a New Class of High-Frequency Semiconductor Devices—H. Statz and R. A. Pucel. (PROC. IRE, vol. 45, pp. 317–324; March, 1957.) New devices are considered in which electrons or holes are injected directly into space-charge regions of reverse-biased junctions, avoiding the diffusion of carriers through field-free regions. In the "spacistor" the junction is biased at a voltage such that the injected carriers are multiplied by the avalanche process. Difficulties with the accumulation of generated carriers in front of the emitting contact are discussed, and applications are considered.

621.383:546.289 1948
Efficiency and Characteristics of a Germanium Photocell with an Electron-Hole Junction—V. S. Vavilov and L. S. Smirnov. (*Radiotekhnika i Elektronika*, vol. 1, pp. 1147–1154; August, 1956.)

621.383.27 1949
On the Reduction of the Dark Current of Photomultipliers—Zs. Náray. (*J. Sci. Instr.*, vol. 33, pp. 476–478; December, 1956.) Two methods are suggested: *a*) effectively reducing the sensitive area of the photo-cathode by defocusing the electrons from the unilluminated portion; *b*) the application of a suitable shield potential to a conducting layer on the outer surface of the photomultiplier envelope. The reduction obtained is equivalent to cooling by about 100°C.

621.383.4:535.37:621.318.57 1950
Principles of the Light-Amplifier and Allied Devices—T. B. Tomlinson. (*J. Brit. IRE*, vol. 17, pp. 141–154; March, 1957.) The topics surveyed and discussed are light-amplifier systems, electroluminescent panels, photoconductive materials, and electro-optical switching devices.

621.385:621.395.64 1951
Electron Tubes for the Transatlantic Cable System—J. O. McNally, G. H. Metson, E. A. Veazie, and M. F. Holmes. (*Bell Sys. Tech. J.*, vol. 36, pp. 163–188; January, 1957.) The design considerations governing the development of the tube Type 6P12 by the General Post Office and the tube Type 175HQ by the Bell Telephone Laboratories are discussed together with problems arising in manufacture and selection. Electrical characteristics and life-test data are given.

621.385:621.396.822 1952
Noise and its "Spectrum"—F. N. H. Robinson. (*J. Brit. IRE*, vol. 17, pp. 115–119; February, 1957.) The physical ideas underlying the familiar equation for shot noise in a temperature limited current are explained. The mathematical analysis is based on Campbell's theorem, which is proved, and some consideration is given to the meaning of the averages which appear in expressions describing noise.

621.385.029.6 1953
Elektron Tubes for Microwave Applications—a Survey of Available Types—P. K. Worsley. (*Brit. Commun. Electronics*, vol. 3, pp. 606–609 and 668–669; November and December, 1956.) A tabulation of the principal characteristics of British commercial types.

621.385.029.6 1954
Stability of Periodic-Field Beam Focusing—K. K. N. Chang. (*J. Appl. Phys.*, vol. 27, pp. 1527–1532; December, 1956.) An analytical solution for beam focusing with a sinusoidal field is found and from it a stability criterion is derived.

621.385.029.6 1955
Formation of High-Density Electron Beams—G. R. Brewer. (*J. Appl. Phys.*, vol. 28, pp. 7–15; January, 1957.) Physical principles underlying the design and characteristics of electron guns for high-perveance beams are considered, with a description of experimental techniques and results of studies of gun and beam performance.

621.385.029.6 1956
On the Effect of the Transition Region upon an Electron Beam Constrained by Brillouin Flow—B. W. Manley. (*J. Electronics*, vol. 2, pp. 241–246; November, 1956.) Analysis indicates that Müller's result (2827 of 1953) is not valid. The position of the beam throat will depend on the extent of the transition region and the strength of the magnetic field. Design data are given for a range of beam parameters.

621.385.029.6 1957
Synchronization of a Reflex Klystron—I. I. Minakova and N. V. Stepanova. (*Radiotekhnika i Elektronika*, vol. 1, pp. 805–808; June, 1956.) Synchronization by a small sinusoidal emf of frequency near the natural resonance of the klystron is discussed.

621.385.029.6 1958
One Mode of Self-Oscillation of the Space Charge in a Nonslotted Magnetron—M. I. Kuznetsov. (*Radiotekhnika i Elektronika*, vol. 1, pp. 785–793; June, 1956.)

621.385.029.6 1959
Contribution to the Large-Signal Theory of Travelling-Wave Valves—G. Mourier. (*Ann. Radioélect.*, vol. 11, pp. 271–280; October, 1956.) The saturation condition arising in O-type traveling-wave tubes when electron and wave velocities are equal is investigated. See also 2571 of 1956 (Tien).

621.385.029.6 1960
Plasma Wavelength and Low-Noise Travelling-Wave Valve—J. Labus and R. Liebscher. (*Arch. elekt. Übertragung*, vol. 10, pp. 421–423; October, 1956.) The calculation of the plasma wavelength in an electron beam is usually based on the assumption that the electrons do not rotate round the axis. With a finite space charge, this condition can occur only if the magnetic focusing field is infinite. The dependence of the reduction factor on the distribution of magnetic flux along the beam is determined, and the theory is applied to the design of the drift region to give low noise in a traveling-wave tube.

621.385.029.6 1961
Conditions for the Minimum Noise Figure of Travelling-Wave Valves—J. Labus, R. Liebscher, and K. Pöschl. (*Arch. elekt Übertragung*, vol. 10, pp. 486–490; November, 1956.) The length of the drift space and the potential distribution between cathode and drift space are considered.

621.385.029.6 1962
Experimental Investigation of a Backward-Wave Valve with Bifilar Helix—V. P. Kiryushin. (*Radiotekhnika i Elektronika*, vol. 1, pp. 798–804; June, 1956.) The tube investigated oscillated in the continuous waveband 4.08–39.5 at voltages from 3400 to 20 v, with a power output of 80 mw, at an efficiency of up to 2 per cent.

621.385.029.6:537.533 1963
Excitation of Space-Charge Waves in Drift Tubes—A. H. Beck. (*J. Appl. Phys.*, vol. 28, pp. 140–141; January, 1957.) Comment on 2812 of 1956 (Scotto and Parzen).

621.385.029.6:621.3.083 1964
A Sensitive Method of Measuring the Reflections and Stability in High-Gain Travelling-Wave Valves—W. Klein. (*Arch. elekt. Über-*

tragung, vol. 10, pp. 477–482; November, 1956.) The method described permits the separation of internal and external reflections and the location of the disturbances. It can be used to check tube stability and the quality of the complete amplifier.

621.385.029.6:621.372.2 1965
Measurement of the Coupling Impedances of Delay Lines [in travelling-wave valves]—R. Müller. (*Arch. elekt. Übertragung*, vol. 10, pp. 424–428; October, 1956.) Two previously described experimental methods [2061 of 1950 (Lapostolle) and 3155 of 1955 (Aikin)] are compared, with particular reference to the investigation of lines with band-pass characteristics.

621.385.029.6+621.56.029.6]:621.396.41 1966
Ultra-high-Frequency Valves for a Wide-Band Radio-Link System—W. Kleen. (*Arch. elekt. Übertragung*, vol. 10, pp. 415–420; October, 1956.) A fm radio-link system inaugurated in Denmark in the summer of 1956 is discussed. Operation is in the frequency band 3.8–4.2 kmc, the channel width being 30 mc, and accommodating 600 speech channels or one television channel. A Type-RW3 traveling-wave tube with saturation power of 9w is used as transmitting tube; it has permanent-magnet focusing designed to reduce stray magnetic fields. A Type-RK25 reflex klystron with L cathode is used as modulator. The output of the traveling-wave tube is isolated from the antenna line by means of a unidirectional attenuator comprising a helix embedded in a ferrite cylinder.

621.385.029.6:621.396.822 1967
The Transformation of [noise] Power Spectra in Electron Beams—H. Pötzl. (*Arch. elekt. Übertragung*, vol. 10, pp. 376–382; September, 1956.) From the transformation equations given by Haus (3123 of 1955) a simple expression is derived for the determination of coherence conditions between current and potential fluctuations. The influence of coherence and the effect of lossy networks on the minimum noise figure of amplifiers are investigated. The analysis of a loss-free six-terminal network leads to a generalization of the results obtained by König (1277 of 1957).

621.385.029.63 1968
Micro-miniature [triode] Tube for U.H.F. and High Temperature—(*Elec. Mfg.*, vol. 56, pp. 154–155; November, 1955.) The tube Type 6BY4 described has a ceramic envelope and electrodes consisting mainly of titanium. Its dimensions are $\frac{3}{16}$ inch diameter by $\frac{5}{8}$ inch long; it operates at frequencies up to 900 mc and can withstand a temperature of 500°C.

621.385.029.64 1969
A Twin-Helix Travelling-Wave Power Valve with 50-dB Gain at 4 kMc—W. Klein and W. Friz. (*Nachrichtentech. Z.*, vol. 9, pp. 476–482; October, 1956.) The tube Type LW53-V described is intended for high-gain applications over the range 3.6–4.2 kmc. Design problems arising from high-gain requirements are discussed.

621.385.029.64 1970
A Low-Noise Traveling-Wave-Tube Amplifier for the 4000-Mcs Communications Band—D. H. O. Allen and J. M. Winwood. (*J. Brit. IRE*, vol. 17, pp. 75–85; January, 1957.) "The factors which influence the performance of a low-noise traveling-wave tube are discussed and design data are developed for a particular tube. The mechanical design is considered and some performance curves presented."

621.385.029.64 1971
A Medium-Power Travelling-Wave Tube for 6000-Mcs Radio Relay—J. P. Laico, H. L. McDowell and C. R. Moster. (*Bell Sys. Tech. J.*, vol. 35, pp. 1285–1346; November, 1956.) Discussion of a traveling-wave amplifier which gives 30-db gain at 5-w output in the 5 925–6 425-mc common-carrier band. A description of the tube and detailed performance data are given.

621.385.032.21 1972
Mixed Monolayers of Barium and Calcium on Tungsten—I. Brodie and R. O. Jenkins. (*Proc. Phys. Soc., London*, vol. 69, pp. 1343–1344; December 1, 1956.) The saturated thermionic emission from tungsten wire at a constant temperature was measured as a function of the time for which the wire was exposed to the mixed vapor. Maximum emission was found for a monolayer with 25 per cent calcium.

621.385.032.21:621.396.822 1973
An Anomalous Periodic Flicker Effect—O. M. White and K. G. Emeleus. (*J. Electronics*, vol. 2, pp. 358–367; January, 1957.) Low-Frequency oscillations are observed in cylindrical-anode diodes when high cathode heating currents are used. A model of an oscillating space charge with stationary transverse wave patterns is discussed.

621.385.032.216 1974
The Nature of the Emitting Surface of Barium Dispenser Cathodes—L. Brodie and R. O. Jenkins. (*Brit. J. Appl. Phys.*, vol. 8, pp. 27–29; January, 1957.) It is deduced from data examined that the tungsten surface of an L-type cathode must be covered with a layer of oxygen on which the barium is adsorbed. Emission from cathodes impregnated with barium aluminate results mainly from a similar layer on the tungsten, but with barium-calcium-aluminate the enhanced emission is mostly derived from the impregnant itself, the emitting surface being probably a thin layer of calcium oxide activated by barium.

621.385.032.216 1975
An Engineering Study of Oxide-Coated Cathode—K. Amakasu. (*Rep. Elect. Commun. Lab., Japan*, vol. 4, pp. 8–27: September, 1956.) Results of investigations of initial decay and noise are summarized for various types of cathodes. The relation between crystal shape and emission and the effects of impurities, electron bombardment, gas etc. are shown in tables and graphs, and methods of improvement are suggested.

621.385.032.216 1976
On the Initial Decay of Thermionic Emission from Oxide-Coated Cathodes—K. Ishikawa. (*Sci. Rep. Res. Inst. Tohoku Univ., Ser. A*, vol. 8, pp. 421–440; October, 1956.) Report of detailed investigations originally outlined in 868 of 1952 (Hibi and Ishikawa).

621.385.032.216 1977
Influence of the Cathode Base on the Chemical Activation of Oxide Cathodes—R. W. Peterson, D. E. Anderson, and W. G. Shepherd. (*J. Appl. Phys.*, vol. 28, pp. 22–23; January, 1957.) Radioactive tracer techniques show that strontium evaporation from an oxide-coated cathode indicates the rate of reduction of the coating by reducing agents in the base metal. The cathode activity without current drain correlates experimentally and qualitatively on a theoretical basis, with rates of coating reduction.

621.385.032.216 1978
Donor Concentration Changes in Oxide-Coated Cathodes resulting from Changes in Electric Field—H. J. Krusemeyer and M. V. Pursley. (*J. Appl. Phys.*, vol. 27, pp. 1537–1545; December, 1956.) Sudden changes in dc drawn from, or to, the coating produce large changes in work function characterized by two, sometimes three, time constants.

621.385.032.216:546.841.4-31 1979
Some Physical Properties of High-Density Thorium Dioxide—S. M. Lang and F. P. Knudsen. (*J. Amer. Ceram. Soc.*, vol. 39, pp. 415–424; December, 1956.) Data are tabulated of the mechanical properties of specimens of ThO_2 and ThO_2+CaO solid solutions of 99 per cent of theoretical density.

621.385.032.216.1:546.841.4-31 1980
The Thermionic Emission of Thoria Cathodes under Pulse Conditions—G. Déjardin, G. Mesnard, and R. Uzan. (*Can. J. Phys.*, vol. 10, pp. 1–21; October, 1956.) Report of measurements on thoriated tungsten cathodes subjected to millisecond voltage pulses to reach temperatures in the range 1400–1900°K. The amplitude and speed of decay of the emission were investigated as a function of temperature and activation and the results were used to derive the equation of the decay curve. For tests under static conditions, see 2840 of 1953 (Mesnard).

621.385.1 1981
A New Method of Investigating the Microphony of Valves: Part 1—I. P. Valkó. (*Hochfreq. und Elektroak.*, vol. 65, pp. 59–65; September, 1956.) In the equipment described tubes are vibrated by an electrodynamic transducer which is controlled by a white-noise generator. The advantages and limitations of the method are discussed; repeated tests gave consistent results.

621.385.14-713 1982
"Duct Cooling" (Kanalkühlung), a Method of Evaporation Cooling for High-Power High-Frequency Oscillator and Transmitter Valves—C. Protze. (*Telefunken Ztg.*, vol. 29, pp. 87–92; June, 1956. English summary, pp. 132–133.) In the tubes Type RS822 and Type RS826 heat from thick-walled cylindrical anodes is efficiently extracted by water evaporation. The walls are perforated by small-diameter ducts parallel to the cylinder axis, and, with the anode partly submerged in a water container, the upward surge of steam bubbles in the ducts ensures rapid circulation without pumps. Advantages include freedom from vibration, great overload capacity and the possibility of downward steam extraction convenient in sw transmitters. A dissipation of over 450 w/cm² can be obtained from the energized anode surface.

621.385.2:621.362 1983
Thermionic Diodes as Energy Converters—H. Moss. (*J. Electronics*, vol. 2, pp. 305–322; January, 1957.) An analysis of the conversion phenomena in a plan or system relating power output to various diode parameters. The exact diode characteristic solution is compared with the Langmuir approximate expansion formula.

621.385.2/.3].029.63 1984
Investigation of Electronic Conductances of Planar Valves—A. I. Kostienko. (*Radiotekhnika i Elektronika*, vol. 1, pp. 809–813; June, 1956.) Results are presented of measurements of the input admittances of diodes and lighthouse triodes in the 10-cm-λ band. The results are compared with theory.

621.385.3 1985
Triode Amplification Factor—P. Hammond. (*Electronic Radio Eng.*, vol. 34, pp. 135–137; April, 1957.) Re-examination of current theory with reference to Moullin's analysis (*Proc. IEE*, Part C, vol. 104, pp. 222–232; March, 1957).

621.385.4.032.25:537.533 1986
The Suppression of Screen-Grid Emission by Carbon—J. A. Champion. (*Brit. J. Appl. Phys.*, vol. 7, pp. 395–399; November, 1956.) The emission from an unsuppressed screen grid is shown to be of the same magnitude as that from a thin activated layer of barium oxide. The effect of carbon coating is to increase with

time the emission at temperatures below 900°C; at temperatures above 950°C the emission decays to a negligibly small value in a few minutes. The mechanism of the suppression is the chemical reduction of the deposited barium oxide to barium which evaporates.

621.385.83 1987

Focusing Low-Energy Electron Beams—W. W. H. Clarke and L. Jacob. (*J. Appl. Phys.*, vol. 27, pp. 1519–1524; December, 1956.) The distributions of the electrons in beams of energies 30–70 v were studied using a system of concentric collectors in a cr tube.

621.385.832 1988

The Picture Quality of a Modern Oscillograph Tube—(*Telefunken Ztg.*, vol. 29, pp. 124–126; June, 1956. English summary, p. 135.) A raster photograph illustrates the high degree of resolution and linearity of the electrostatically focused cr tube Type DG 13-54. The raster 87 mm high consists of 260 lines 55 mm long and about 0.2 mm thick.

621.385.832 1989

Method of Measuring Spot Size of Cathode-Ray Tube—R. B. Kuhn and D. Levine. (*Commun. & Electronics*, no. 25, pp. 357–359; July, 1956. Discussion, p. 359.) An objective method is described in which a slit mask and photocell are used. Gaussian distribution of light flux density is assumed.

621.385.832:535.371.07 1990

Cathode-Ray-Tube-Screen Charging and Conditions Leading to Positive-Ion Deterioration—A. B. Laponsky, M. J. Ozeroff, W. A. Thornton, and J. R. Young. (*J. Electrochem. Soc.*, vol. 103, pp. 498–507; September, 1956.) The relation of screen charging effects to gas pressure and screen surface conditions and dimensions is discussed on the basis of existing literature, some previously unpublished, and experiments. The influence of tube and raster geometry on observed deterioration patterns is examined and results are summarized regarding the effects of anode coating material and screen potentials leading to burn patterns in the form of a cross.

621.385.832:621.397.62:535.623 1991

A New Flat Picture Tube—D. Gabor. (*J. Telev. Soc.*, vol. 8, pp. 142–145; October/December, 1956.) See 588 of 1957.

621.385.832.032 1992

The Technology of Electrostatic-Storage Cathode-Ray Tubes—P. Choffart. (*Onde élect.*, vol. 36, pp. 815–821; October, 1956.) An outline of some of the manufacturing problems.

MISCELLANEOUS

621-52 1993

Man as a Link in Complex Machine Systems—G. H. Mowbray. (*Sci. Mon.*, vol. 83, pp. 269–276; December, 1956.) The performance, particularly the speed of response, of man as a series or parallel link in a control system is discussed. Instrument dials, providing the input to the link, and control devices receiving its output should be designed to facilitate rapid reading and operation respectively.

621.396:061.3 1994

Documents and Papers Read at the Scientific Conference of the [U.S.S.R.] Ministry of Higher Education on Radioelectronics (Gorki, January 1956)—(*Radiotekhnika i Elektronika*, vol. 1, pp. 878–887; June, 1956.) Abstracts and references to sixty-six papers presented at the conference. The principal topics were: *a*) radio astronomy, *b*) propagation of radio waves, and *c*) physics of ultra high frequencies.